NIST GCR 12-917-20

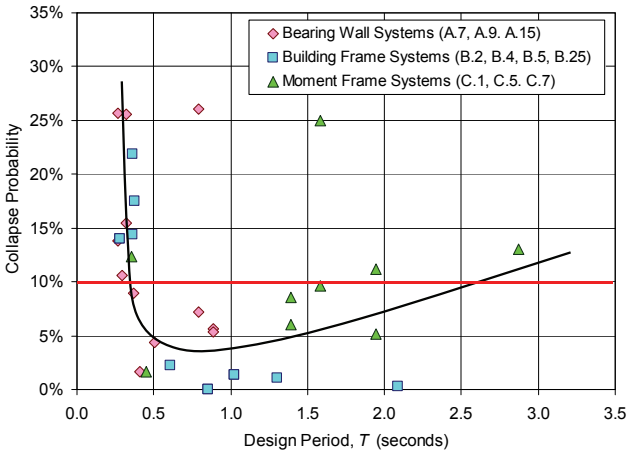

Tentative Framework for Development of Advanced Seismic Design Criteria for New Buildings

NEHRP Consultants Joint Venture
A partnership of the Applied Technology Council and the Consortium of Universities for Research in Earthquake Engineering

National Institute of Standards and Technology
U.S. Department of Commerce

Disclaimers

This report was prepared for the Engineering Laboratory of the National Institute of Standards and Technology (NIST) under the National Earthquake Hazards Reduction Program (NEHRP) Earthquake Structural and Engineering Research Contract SB134107CQ0019, Task Order 69226. The contents of this publication do not necessarily reflect the views and policies of NIST or the U.S. Government.

This report was produced by the NEHRP Consultants Joint Venture, a joint venture of the Applied Technology Council (ATC) and the Consortium of Universities for Research in Earthquake Engineering (CUREE). While endeavoring to provide practical and accurate information, the NEHRP Consultants Joint Venture, the authors, and the reviewers assume no liability for, nor express or imply any warranty with regard to, the information contained herein. Users of information contained in this report assume all liability arising from such use.

Unless otherwise noted, photos, figures, and data presented in this report have been developed or provided by NEHRP Consultants Joint Venture staff or consultants engaged under contract to provide information as works for hire. Any similarity with other published information is coincidental. Photos and figures cited from outside sources have been reproduced in this report with permission. Any other use requires additional permission from the copyright holders.

Certain commercial software, equipment, instruments, or materials may have been used in the preparation of information contributing to this report. Identification in this report is not intended to imply recommendation or endorsement by NIST, nor is it intended to imply that such software, equipment, instruments, or materials are necessarily the best available for the purpose.

NIST policy is to use the International System of Units (metric units) in all its publications. In this report, however, information is presented in U.S. Customary Units (inch-pound), as this is the preferred system of units in the U.S. earthquake engineering industry.

Cover image – Plot showing the trend in the probability of collapse of selected systems as a function of design period (data adopted from FEMA, 2009 and NIST, 2010).

NIST GCR 12-917-20

Tentative Framework for Development of Advanced Seismic Design Criteria for New Buildings

Prepared for
U.S. Department of Commerce
National Institute of Standards and Technology
Engineering Laboratory
Gaithersburg, MD 20899

By
NEHRP Consultants Joint Venture
A partnership of the Applied Technology Council and the Consortium of Universities for Research in Earthquake Engineering

November 2012

U.S. Department of Commerce
Rebecca M. Blank, Acting Secretary

National Institute of Standards and Technology
Patrick D. Gallagher, Under Secretary of Commerce for Standards and Technology and Director

Participants

National Institute of Standards and Technology

John (Jack) R. Hayes, Jr., Director, National Earthquake Hazards Reduction Program
Steven L. McCabe, Deputy Director, National Earthquake Hazards Reduction Program
John (Jay) L. Harris III, Project Manager

NEHRP Consultants Joint Venture

Applied Technology Council
201 Redwood Shores Parkway, Suite 240
Redwood City, California 94065
www.ATCouncil.org

Consortium of Universities for
Research in Earthquake Engineering
1301 S. 46th Street, Building 420
Richmond, California 94804
www.CUREE.org

Joint Venture Management Committee

James R. Harris
Robert Reitherman
Christopher Rojahn
Andrew Whittaker

Joint Venture Program Committee

Jon A. Heintz (Program Manager)
Michael Constantinou
C.B. Crouse
James R. Harris
William T. Holmes
Jack P. Moehle
Andrew Whittaker

Project Technical Committee

Charles A. Kircher (Project Director)
Finley A. Charney
Gregory G. Deierlein
James R. Harris
William T. Holmes
John D. Hooper
Laura N. Lowes

Working Group Members

Henry Burton
Scott Darling
Matthew R. Eatherton
Jennifer Foschaar
Andrew Hardyniec
Curt B. Haselton
Joshua Pugh

Project Manager

Ayse Hortacsu

Project Review Panel

Robert E Bachman
David R. Bonneville
Kelly E. Cobeen
Ronald O. Hamburger
Greg Kingsley
Richard E. Klingner
Philip Line
James O. Malley
Bonnie E. Manley
Jack P. Moehle
Laurence Novak
Charles W. Roeder
Kurt Stochlia

FEMA Representative

Robert D. Hanson

Preface

The NEHRP Consultants Joint Venture is a partnership between the Applied Technology Council (ATC) and the Consortium of Universities for Research in Earthquake Engineering (CUREE). In 2007, the National Institute of Standards and Technology (NIST) awarded a National Earthquake Hazards Reduction Program (NEHRP) "Earthquake Structural and Engineering Research" contract (SB1341-07-CQ-0019) to the NEHRP Consultants Joint Venture to conduct a variety of tasks, including Task Order 69226 entitled "Improved Structural Response Modification Factors for Seismic Design of New Buildings: Phase I."

During the conduct of the ATC-63 Project, which was funded by the Federal Emergency Management Agency (FEMA) and resulted in the publication of the FEMA P-695 report, *Quantification of Building Seismic Performance Factors*, (FEMA, 2009), it became apparent that the current "formulation" of seismic design parameters, including the response modification coefficient (R factor), the system overstrength factor (Ω_O), and deflection amplification factor (C_d), did not fully address the potential variation in collapse performance of buildings due to differences in building period, inelastic response capacity, and seismic design loading. Results from beta testing of the FEMA P-695 Methodology, documented in the NIST GCR 10-917-8 report, *Evaluation of the FEMA P-695 Methodology for Quantification of Building Seismic Performance Factors*, (NIST, 2010), also supported the notion that the observed variation in collapse performance was important, and that alternative formulations of seismic design parameters were needed to ensure a uniform level of collapse risk for all building systems.

In deciding on a recommended path forward, the project team first developed a list of preliminary reformulation concepts and related areas of needed technical investigation. This list was prioritized based on relative importance and relative potential for changing the way that design parameters relate to system collapse behavior. The following topics were chosen for study: (1) short-period systems; (2) overstrength; and (3) long-period systems. A conceptual framework for reformulation of seismic design parameters was developed using the findings from problem-focused studies and additional conceptual ideas from the project team.

The NEHRP Consultants Joint Venture is indebted to the leadership of Charlie Kircher, Project Director, and to the members of the project team for their efforts in developing this report. The Project Technical Committee, consisting of Finley

Charney, Greg Deierlein, Jim Harris, Bill Holmes, John Hooper, and Laura Lowes, performed, monitored, and guided the technical work on the project. The Working Groups, including Henry Burton, Scott Darling, Matthew Eatherton, Jen Foschaar, Andy Hardyniec, Curt Haselton, and Joshua Pugh, conducted problem-focused analytical studies. The Project Review Panel, consisting of Bob Bachman, David Bonneville, Kelly Cobeen, Ron Hamburger, Greg Kingsley, Richard Klingner, Philip Line, Jim Malley, Bonnie Manley, Jack Moehle, Laurence Novak, Charles Roeder, and Kurt Stochlia, provided technical review, advice, and consultation at key stages of the work. A workshop of invited experts was convened to obtain feedback on the focused study results and preliminary recommendations, and input from this group was instrumental in shaping the final report. The names and affiliations of all who contributed to this report are provided in the list of Project Participants.

The NEHRP Consultants Joint Venture also gratefully acknowledges Jack Hayes (NEHRP Director), Steven McCabe (NEHRP Deputy Director), Jay Harris (NIST Project Manager), and Robert Hanson (FEMA Technical Monitor) for their input and guidance in the preparation of this report, Ayse Hortacsu for ATC project management, and Peter N. Mork for ATC report production services.

Jon A. Heintz
Program Manager

Table of Contents

List of Figures

List of Tables

Chapter 1
Introduction

1.1 Background and Purpose

The seismic performance factors (R, C_d, Ω_O) were first introduced in the ATC-3-06 report, *Tentative Provisions for the Development of Seismic Regulations for Buildings* (ATC, 1978), and implemented in the *NEHRP Recommended Provisions for the Development of Seismic Regulations for New Buildings* (FEMA, 1985). These factors were also historically called response modification factors (or coefficients). Initial values were formulated by committee consensus and calibration with building code parameters then in use in California. Since then, such factors have become fundamentally critical in the specification of seismic loading in the design of new buildings.

Over time, the number of systems with given values of seismic performance factors found in consensus documents have grown from the original 21 systems of ATC-3-06 to the 84 systems of ASCE/SEI 7-10, *Minimum Design Loads for Buildings and Other Structures* (ASCE, 2010), based largely on the qualitative judgment of seismic code committees.

The ATC-19 report, *Structural Response Modification Factors* (ATC, 1995), investigated the basis of the values of R and concluded that: (1) there is no mathematical basis for the R factors tabulated in modern seismic codes in the United States; (2) the current R factors investigated (as of 1995) will probably not result in uniform levels of risk for all buildings; and (3) a reformulation of the R factor including systematic and coordinated studies is recommended.

The FEMA P-695 report, *Quantification of Building Seismic Performance Factors* (FEMA, 2009), provides a rational quantitative basis for establishing global seismic performance factors of new seismic force-resisting systems proposed for inclusion in national model building codes and standards. This Methodology is intended for use in the development of model building codes and reference standards to set minimum acceptable criteria for new seismic force-resisting systems proposed for inclusion as a standard code-approved system. The acceptance criteria of the FEMA P-695 Methodology limit the probability of total or partial collapse for a new seismic force-resisting system to 10% given the occurrence of Maximum Considered Earthquake (MCE) ground motions.

In parallel to the development of the FEMA P-695 Methodology, the 2009 NEHRP Provisions Update Committee adopted a risk-targeted design philosophy, which was subsequently adopted by ASCE/SEI 7-10. The intent of the risk-targeted approach is to shift from a uniform hazard design basis to a uniform risk design basis. In the risk-targeted approach, the acceptance criteria used in FEMA P-695 Methodology, 10% collapse probability given an MCE event, was implemented. Risk-based design criteria necessarily combine performance objectives with seismic hazard (ground motion intensity). For life-safety objectives, ASCE/SEI 7-10 defines MCE ground motion intensity (denoted as MCE_R) as ground motions having a 1% probability of causing structural collapse in 50 years.

FEMA P-695 also provides a basis for evaluation of criteria for current code-approved systems, and for improving current design requirements to better achieve the seismic performance objectives intended by current seismic design provisions. It is important to note certain, subtle differences between the FEMA P-695 Methodology and the current design methodology of ASCE/SEI 7-10, such as basing the amplification factor, C_d, on the acceptable value of the response modification factor, R. During the development of the FEMA P-695 Methodology, it became apparent that the current values of the seismic design parameters for specific system types in ASCE/SEI 7-05 do not properly address variation in collapse performance due to differences in building period, inelastic response capacity, and seismic design loading, i.e., seismic design category.

Further, results of beta testing of the FEMA P-695 Methodology documented in the NIST GCR 10-917-8 report, *Evaluation of the FEMA P-695 Methodology for Quantification of Building Seismic Performance Factors* (NIST, 2010), support the notion that observed differences in collapse performance are important, and that in order to be consistent with the risk-targeted design approach, alternative formulations of seismic design parameters are needed to ensure a uniform level of collapse risk for all building systems.

1.2 Project Objectives

Updating the values of the seismic performance factors for existing seismic force-resisting systems also requires consideration of changes to the formulation of the seismic design parameters to be most effective in achieving uniform collapse risk for buildings across categories with different periods, inelastic response capacities, or seismic design loads.

The primary objective of this project was to develop a conceptual framework for revised formulations of seismic performance factors and other design criteria that consider the interdependency of period, ductility, overstrength, and other factors influencing seismic performance. All reformulation recommendations were anchored

to ASCE/SEI 7-10, which uses MCE_R ground motions, rather than ASCE/SEI 7-05, which uses the uniform hazard-based definition of MCE ground motions. Thus, this effort will join the parallel paths of the risk-targeted design approach of ASCE/SEI 7 and the FEMA P-695 Methodology in a consistent manner. That is, structures designed with improved values of design parameters should more uniformly achieve the safety objective of 10% probability of collapse given MCE_R ground motions occur.

This report addresses reformulation by creating a new framework for earthquake design loads and based on revised formulations of seismic design parameters. Analytical studies on key issues were carried out to further improve reformulation to facilitate uniform collapse risk were also identified.

The conceptual reformulation presented in this report also includes refining the characterization of earthquake ground motions with the use of multi-period, site-specific design spectra and expanding the risk-targeted concept to address economic and functional risk objectives, as well as life-safety risk objectives. The latter topic is of particular relevance to seismic code development because it provides concepts for transforming quantitative risk criteria into seismic design criteria for meeting other specific performance objectives. Collectively, the recommendations of this report create a new framework for advancing seismic design criteria to more reliably achieve uniform risk objectives at multiple performance levels. It is envisioned that future studies will utilize this new framework to review and revise design requirements in the *NEHRP Recommended Provisions*, ASCE/SEI 7, model building codes, and other reference standards to improve the reliability and predictability of current seismic design criteria.

1.3 Identification and Prioritization of Study Topics

As a first step, the project developed a list of preliminary reformulation concepts and related areas of technical investigation. Twenty-one topics of potential study, many with multiple areas of interest, were identified. Sources of information on alternative formulations and related issues include the findings from studies reported in the FEMA P-695 and NIST CGR 10-917-8 reports, as well as input from the project team.

Topics were categorized in terms of their relative importance to the reformulation effort. Concepts and related issues were sorted, grouped, and prioritized in terms of their potential to provide benefit to reformulation of seismic performance parameters and related design criteria. Study topics were assigned to one of the following four priority classes and listed in Table 1-1 through Table 1-4:

- **Highest priority.** Very important topics that should be investigated as a research-driven problem-focused study of this project.

- **High priority.** Very important topics beyond the scope of this project that should be investigated in near-term problem-focused studies.
- **Moderate priority**. Important topics that should be considered for future studies.
- **Low priority.** Topics of lesser importance (to reformulation) that need not be considered for future studies.

Initial investigations of reformulation began with the identification of topics of interest that greatly exceeded the number that could be investigated in this project. Certain topics were conceptual in nature that require serious consideration before adoption, but would not benefit from analytical study. Other topics of interest that would benefit from analytical study (using the FEMA P-695 Methodology) were ranked and the three most promising areas of study with respect to reformulation were identified as topics related to the following: (1) short-period systems; (2) overstrength; and (3) long-period systems. Highest priority study topics identified in Table 1-1 were grouped into one of the following areas:

- Topics related to reformulation of terms, which do not require analytical investigation.
- Technical topics primarily related to design and performance of short-period structures.
- Technical topics primarily related to design and performance of structures considering overstrength.
- Technical topics primarily related to design and performance of long-period structures.

Table 1-1 Highest Priority Study Topics

	Description
Conceptual Reformulation	
Components of *R* factor	Separate *R* factor into ductility and overstrength components
Basis for *R* factors	Change basis for *R* factors to MCE_R rather than design earthquake ground motions
R values < 1.0	Consider *R* factors less than 1.0
Simplify *R* table	Develop set of "standardized" *R* factors
Short-Period Systems	
Short-period modification factor	Develop concept for reducing effective value of the *R* factor at short periods to offset collapse risk
Overstrength	
Overstrength factor	Develop concept/values/reformulation of the overstrength factor
Implementation of design rules	Investigate overstrength and implementation of design rules
Capacity design	Study influence of capacity design on performance and overstrength requirements as part of system design requirements
Long-Period Systems	
Risk-based drift limits	Develop concept and values of drift limits that achieve uniform collapse risk of taller systems; considering $C_d = R$; consider stability issues, long-period *R* factors, and minimum base shear requirements
Stability criteria	Develop concept of a stability check that achieves uniform collapse risk

Table 1-2 High Priority Study Topics

	Description
Essential facility (*I* factor) criteria	Develop concept and values of the *I* factor that achieve uniform collapse risk for systems in Seismic Design Categories (SDC)C D, E, and F. Develop values of the *I* factor that achieve uniform collapse risk for values of probability of collapse given MCE_R that are less than the 10 % criterion of non-essential facilities
Strong column weak beam (SCWB)	Conduct studies to establish methods for building archetypes with SCWB
Shear-flexure behavior of walls	Consider aspect-ratio dependent *R* factors (tall skinny vs. short squat walls with the same *R*)
Near-field effects	Consider near-field effects and changes in design rules and associated change in collapse risk with a possible link to topic regarding essential facilities

Table 1-3 Moderate Priority Study Topics

	Description
Analysis method	Consider different methods of analysis (ELF, RSA, LRHA), adjusted as required to achieve uniform collapse risk
Limits of equivalent lateral force (ELF) procedure	Identify systems for which ELF is not an appropriate method of analysis
Irregularity requirements	Investigate effects of irregularity requirements on collapse performance, e.g., evaluate archetypes with and without irregularities; also consider redundancy
Three-dimensional effects	Consider three-dimensional effects on components of the seismic force-resisting system
Inelastic deformation capacity	Investigate "generic" detailing requirements (specifics to be investigated by material standards groups)
Height limits	Investigate the need (or lack of need) for height limits
Trade strength for ductility	Consider trading strength (smaller *R*) for less ductility (relaxed detailing requirements) in regions of lower seismicity, with a possible link to topic regarding essential facilities
Shaking duration	Consider ground motion duration effects on collapse performance (e.g., in the Pacific Northwest); with a possible link to topic regarding near field effects
Gravity framing	Consider effects of gravity framing on collapse performance (especially in lower seismic regions)
Finish materials	Consider influence of finish materials on collapse performance
R factors for diaphragms	Study collapse behavior based on diaphragm behavior

Table 1-4 Low Priority Study Topics

	Description
Soil-structure interaction (SSI) effects	Consider SSI effects on short-period period response (*R* factors)
Nonstructural performance	Investigate issues pertaining to nonstructural performance
Risk-targeted ground motions	Explain the effects of using risk-targeted ground motions
Material requirements	Adjust material requirements that do not adequately control ductility and consequently affect collapse performance
Unintended bracing	Consider effects of unintended bracing (e.g., stairs) on collapse performance
Evaluate methodology	Conduct further evaluation of the FEMA P-695 Methodology

1.4 Project Scope

Conceptual reformulation topics identified in Table 1-1 include fundamental changes to the approach, methods, or terms, such as redefining the *R* factor as the product of a ductility component, R_d, and an overstrength component, R_O. This topic does not require analytical investigation, but relies on the findings of the other three topical areas of study.

Working groups were formed to conduct problem-focused studies on the remaining topical groups identified in Table 1-1. Existing analytical models developed for work in the FEMA P-695 and NIST GCR 10-917-8 reports were used for these studies, augmented with new analytical models developed specifically for the topic of interest. When possible, analytical models and results were shared between working groups.

The analytically intensive nature of the problem-focused studies resulted in the need to expedite modeling and associated pre- and post-processing of related data. To this end, a computer program capable of performing FEMA P-695 collapse evaluations with OpenSees models was developed, herein referred to as the analysis Toolkit. The Toolkit was used by the working groups to more efficiently perform FEMA P-695 collapse evaluations as part of the problem-focused studies (see Appendix E).

1.4.1 Study of Short-Period Systems

Short-period systems were investigated for trends in collapse performance of short-period archetypes (i.e., archetypes with periods less than about 0.5 seconds) as a function of archetype period for systems commonly used for shorter buildings. Based on observed trends, recommendations for revising the formulation of design parameters to better achieve uniform collapse risk at short periods (i.e., 10% probability of collapse given MCE_R ground motions) were developed.

1.4.2 Study of Overstrength

The overstrength studies investigated the basis and formulation of the overstrength component of the *R* factor, R_O, and the basis and formulation of the overstrength factor, Ω_O, used in special load combinations for design of capacity-controlled elements. Based on findings from these studies, recommendations for revising values, or reformulating overstrength to better achieve uniform collapse risk (i.e., 10% probability of collapse given MCE_R ground motions) were developed.

1.4.3 Study of Long-Period Systems

Long-period systems were investigated for trends in collapse performance of long-period archetypes (i.e., archetypes with periods greater than about 1.5 seconds) as a function of archetype period for systems commonly used for taller buildings. Based on observed trends, recommendations for revising the formulation of design

parameters to better achieve uniform collapse risk of long-period structures (i.e., 10% probability of collapse given MCE_R ground motions) were developed.

1.5 Report Content and Organization

This report summarizes investigations of the current formulation of the seismic performance factors and other design parameters and presents a reformulation of these parameters. It is organized to present findings of prior studies and problem-focused studies, followed by the presentation of the reformulation.

Chapter 2 provides a summary of the seismic force-resisting systems, archetype models, and analysis results used in previous FEMA P-695 collapse evaluations. Collapse results are collectively evaluated for trends in the collapse margin ratio as a function of system period.

Chapters 3 provides an overview of each of the three topical studies summarizing the approach, key findings, results pertinent to reformulation for each study. Conclusions and recommendations for future topical research studies are also provided in this chapter.

Chapter 4 describes a conceptual framework for reformulation of seismic performance factors and related design criteria, incorporating relevant findings of the problem-focused studies and prior studies.

Chapter 5 summarizes project investigations and provides recommendations for reformulation of seismic performance factors and related design requirements using the conceptual framework of Chapter 4.

Appendix A provides a compilation of design properties, nonlinear analysis results, and collapse evaluation parameters of previously evaluated seismic force-resisting systems.

Appendix B through Appendix D provide background information supporting the problem-focused studies undertaken in this project.

Appendix E provides an overview of the analysis Toolkit developed to automate the implementation of the FEMA P-695 Methodology.

References cited and a list of all project participants are provided at the end of this report.

Chapter 2

Summary of Prior Collapse Evaluation Studies

This chapter summarizes two prior studies that evaluated collapse performance of ten seismic force-resisting systems using the FEMA P-695 Methodology. These studies include the example applications in the FEMA P-695 report, *Quantification of Building Seismic Performance Factors* (FEMA, 2009) and the trial beta test applications in NIST GCR 10-917-8 Report, *Evaluation of the FEMA P-695 Methodology for Quantification of Building Seismic Performance Factors* (NIST, 2010).

These prior studies provide a wealth of data on the collapse performance of a wide range of different seismic force-resisting systems for Maximum Considered Earthquake (MCE) ground motions. Although collapse performance was found to be different for each system, certain trends in performance were identified, including trends in collapse performance with regard to building period, which are examined in this chapter.

2.1 Overview of Prior Studies

Prior studies were performed as part of the development of the FEMA P-695 Methodology and in a subsequent effort to evaluate (beta test) the Methodology. Several different seismic force-resisting systems were selected across the range of seismic force-resisting systems in Table 12.2-1 of ASCE/SEI 7-10, *Minimum Design Loads for Buildings and Other Structures* (ASCE, 2010). The ten systems summarized in this chapter include three bearing wall systems, four building frame systems, and three moment frame systems that are commonly used in practice.

Prior studies did not investigate all performance groups or model all of the archetypes required in a full application of the FEMA P-695 Methodology for full evaluation of a hypothetical new seismic force-resisting system, but a sufficiently large number of performance groups (over 35) and individual archetypes (about 200) have been evaluated so that trends in behavior and collapse performance can be identified.

2.1.1 Studies in the FEMA P-695 Report

During the development of the FEMA P-695 Methodology, a number of seismic force-resisting systems were investigated to test and refine the procedures as they were being developed, and to illustrate applications of the Methodology in the final

report. Example applications investigated the following seismic force-resisting systems:

- Special reinforced concrete moment frames (special RCMF),
- Ordinary reinforced concrete moment frames (ordinary RCMF), and
- Wood light-frame shear walls (WLFSW).

ASCE/SEI 7-05 (ASCE, 2006), including Supplement No. 1, was in effect at the time that the FEMA P-695 Methodology was developed. Archetypes of the example applications were designed to meet the requirements of ASCE/SEI 7-05 according to FEMA P-695 Methodology requirements, such as $C_d = R$, for new systems, but values of properties and results reported in FEMA P-695 would not have been substantially different if ASCE/SEI 7-10 had been used for design rather than ASCE/SEI 7-05. Also, ASCE/SEI 7-05 used MCE ground motions, but in this report, MCE is assumed to equal MCE_R because study results would not be affected.

However, as a notable exception to the above, while not permitted in Table 12.2-1 of ASCE/SEI 7-05, in one case, ordinary RCMFs were designed for Seismic Design Category (SDC) C seismic loads (as well as for SDC B seismic loads) to investigate collapse performance of a system with ordinary detailing when located in a region of higher seismicity.

Since the three example applications were completed in parallel with the creation of the FEMA P-695 Methodology, in some cases, portions of the examples are not complete with respect to the final requirements of the Methodology. This lack of example application completeness, however, does not affect the values of properties and results reported.

2.1.2 Studies in the NIST GCR 10-917-8 Report

The trial beta test applications in the NIST GCR 10-917-8 report test the FEMA P-695 Methodology on additional seismic force-resisting systems to evaluate the collapse performance of each and to develop recommendations for improving the methodology, if needed. Also, in order to verify the accuracy and reliability of the FEMA P-695 Methodology to material industry groups and model building codes and standards organizations, additional testing and evaluation of the Methodology was performed.

The scope of the beta testing effort was structured to cover a broad cross-section of building types, response characteristics, and seismic detailing requirements. Additional considerations included the availability of reliable test data on component and system performance, as well as the ability to simulate significant failure modes and component degrading behavior in analytical models. Trial applications were investigated for the following seismic force-resisting systems:

- Special reinforced masonry shear walls (special RMSW),
- Ordinary reinforced masonry shear walls (ordinary RMSW),
- Special reinforced concrete shear walls (special RCSW),
- Ordinary reinforced concrete shear walls (ordinary RCSW),
- Special steel concentrically braced frames (special SCBF),
- Steel buckling-restrained braced frames (BRBF), and
- Special steel moment frames (special SMF) designed by the equivalent lateral force (ELF) procedure, and the modal response spectrum analysis (RSA) procedure.

The archetypes in NIST GCR 10-917-8 were designed to meet the requirements of ASCE/SEI 7-05 (including Supplement No. 1), assuming philosophically that MCE = MCE_R, but current versions of material codes (e.g., ACI 318-08, *Building Code Requirements for Structural Concrete and Commentary* (ACI, 2008), for reinforced concrete and TMS 402-08/ACI 530-08/ASCE 5-08, *Building Code Requirements for Masonry Structures* (TMS, 2008), for reinforced masonry) were used in lieu of those referenced by ASCE/SEI 7-05. Values of properties and results reported in NIST GCR 10-917-8 would not have been substantially different if ASCE/SEI 7-10 had been used for design rather than ASCE/SEI 7-05.

Although system performance was evaluated using a large number of archetypes (total of 128 archetypes for all seven systems), full implementation of the FEMA P-695 Methodology would have required an even larger number of archetypes and performance groups. For the purpose of beta testing the FEMA P-695 Methodology, it was considered more useful to evaluate a large number of systems with a carefully selected, but limited, number of archetypes for each system, rather than to evaluate fewer systems using a larger number of archetypes for each system.

Additional archetypes would be required to meet the minimum number of three archetypes per performance group, and additional performance groups would be required to evaluate system performance for other combinations of design loads (i.e., seismic loads corresponding to other seismic design categories).

The number of short- or long-period archetypes in some performance groups was less than the prescribed minimum. Also, the number of different system configurations (e.g., different brace configurations for braced frame systems or different wall configurations for shear wall systems) was limited.

2.2 Findings from Prior Studies

Section 11.2.1 of the FEMA P-695 report describes generic findings of that study, including observations of relatively poor collapse performance of short-period systems and generally better collapse performance of systems with larger amounts of overstrength. These are not new findings, rather confirmation of long-standing results of previous research. Section 8.3 of the NIST GCR 10-917-8 report describes system-related findings that include similar observations to those of FEMA P-695 (e.g., relatively poor collapse performance of short-period systems), as well as new findings regarding the influence of drift and stability requirements on the collapse performance of taller, flexible systems.

Table 2-1 provides an overview of the 35 performance groups representing the seismic force-resisting systems previously evaluated and selected for further investigation. For each performance group, the table identifies the seismic force-resisting system, characteristics used to group archetypes, and the number of archetypes designed for maximum and minimum seismic criteria (e.g., N_{Dmax}/N_{Dmin}). The ELF procedure was used for design of all archetypes, except for the archetypes of two special SMF performance groups (C.1.RSA.S and C.1.RSA.L), which were designed using the RSA procedure. Seismic design criteria, design properties, and nonlinear analysis results for each archetype of each of the performance groups are presented in Appendix A and keyed to the Performance Group Reference Number.

Table 2-2 summarizes collapse evaluation results for each of the 35 performance groups selected for investigation. The collapse evaluation results in this table are representative of the archetypes of the performance group of interest (i.e., values given in the table are the average of individual archetype values of the performance group of interest). The table displays values of acceptable values of adjusted collapse margin ratio, $ACMR_{10\%}$ and $ACMR_{20\%}$, based on the total system collapse uncertainty and values of acceptable collapse probability, taken as 10% and 20%, respectively. The concept of the10% adjusted collapse margin ratio is described in the FEMA P-695 report. Achieving 10% probability of collapse given MCE_R ground motions occur has been adopted by ASCE/SEI 7-10 as the collapse objective of for Risk Category II structures.

In Table 2-2, performance groups that fail both criteria (more than 20% probability of collapse, on average) are indicated by dark grey shading, performance groups that fail only the $ACMR_{10\%}$ (more than 10%, but less than 20% probability of collapse) by medium grey shading, performance groups that pass both criteria but with more than 2% but less than 10% probability of collapse by light grey shading, and systems with 2%, or less, probability of collapse by no shading.

Figure 2-1 is a plot of the collapse probabilities for the 35 performance groups of Table 2-2 as a function of the fundamental design period, T, i.e., $T = C_u T_a$, upper

Table 2-1 Overview of Selected Performance Groups of Previously Evaluated Systems

Performance Group Reference Number	Seismic Force-Resisting System Performance Groups						
	Seismic Force-Resisting System		Grouping Criteria				No. of Arche-types
			Basic Configuration	Design Level		Period Domain	
	Type	Detailing		Gravity	Seismic		
Bearing Wall Systems							
A.7.H.S	RMSW	Special	Cantilevered Walls	High	SDC D	Short	3/2
A.7.H.L						Long	2/3
A.7.L.S				Low		Short	2/3
A.7.L.L						Long	3/2
A.9.H.S	RMSW	Ordinary	Cantilevered Walls	High	SDC C	Short	2/2
A.9.H.L						Long	3/3
A.9.L.S				Low		Short	2/2
A.9.L.L						Long	3/3
A.15.L.S	WLFSW		Low Aspect Ratio Walls	Nominal	SDC D	Short	3/0
A.15.L.L						Long	0/1
A.15.H.S			High Aspect Ratio Walls			Short	5/4
A.15.H.L						Long	0/3
Building Frame Systems							
B.2.2X.S	SCBF	Special	2-Story X-Bracing	Typical	SDC D	Short	2/2
B.2.2X.L						Long	3/3
B.4.H.S	RCSW	Special	Cantilevered Walls	High	SDC D	Short	3/2
B.4.H.L						Long	2/3
B.4.L.S				Low		Short	3/2
B.4.L.L						Long	2/3
B.5.H.S	RCSW	Ordinary	Cantilevered Walls	High	SDC C	Short	2/3
B.5.H.L						Long	3/2
B.5.L.S				Low		Short	2/3
B.5.L.L						Long	3/2
B.25.S	BRBF		2-Story X-Bracing	Typical	SDC D	Short	2/2
B.25.L						Long	3/3
Moment Frame Systems							
C.1.ESA.S	SMF	Special	Perimeter Frame with Reduced Beam Section (RBS) Connections	Typical (Low)	SDC D	Short	2/1
C.1.ESA.L						Long	2/3
C.1.RSA.S						Short	2/1
C.1.RSA.L						Long	4/5
C.5.P.S	RCMF	Special	Perimeter Frame (20ft bays)	Typical (Low)	SDC D	Short	2/0
C.5.P.05.L						Long	4/3
C.5.P.L						Long	4/3
C.7.S.L	RCMF	Ordinary	Space (30ft)	High	SDC B	Long	4/4
C.7.P.L			Perimeter (30ft)	Low		Long	4/4
C.7.S.L (C)			Space (30ft)	High	SDC C (C_{max})	Long	2/(4)
C.7.P.L (C)			Perimeter (30ft)	Low		Long	2/(4)

Table 2-2 Representative Collapse Evaluation Results of Selected Performance Groups of Previously Evaluated Systems

Performance Group Reference Number	Collapse Evaluation (average of individual archetype values)						
	Quality Rating			*Acceptable ACMR*			
	Design Req'ts.	Test Data	Models	*20%*	*10%*	*ACMR*	Collapse Probability
Bearing Wall Systems							
A.7.H.S	B	B	B	1.56	1.96	1.41	26%
A.7.H.L	B	B	B	1.56	1.96	2.30	6%
A.7.L.S	B	B	B	1.56	1.96	1.71	15%
A.7.L.L	B	B	B	1.56	1.96	2.33	5%
A.9.H.S	C	C	B	1.68	2.23	1.51	26%
A.9.H.L	C	C	B	1.74	2.38	1.54	26%
A.9.L.S	C	C	B	1.68	2.23	1.98	14%
A.9.L.L	C	C	B	1.73	2.38	2.69	7%
A.15.L.S	A	A	B	1.52	1.92	1.89	11%
A.15.L.L	A	A	B	1.52	1.92	2.98	2%
A.15.H.S	A	A	D	1.76	2.38	2.48	9%
A.15.H.L	A	A	D	1.76	2.38	3.18	4%
Building Frame Systems							
B.2.2X.S	B	B	B	1.56	1.96	1.64	17%
B.2.2X.L	B	B	B	1.53	1.96	3.37	1%
B.4.H.S	B	B	B	1.56	1.96	1.50	22%
B.4.H.L	B	B	B	1.56	1.96	3.18	1%
B.4.L.S	B	B	B	1.56	1.96	1.75	14%
B.4.L.L	B	B	B	1.56	1.96	3.20	1%
B.5.H.S	B	B	B	1.56	1.96	1.77	14%
B.5.H.L	B	B	B	1.56	1.96	5.87	0%
B.5.L.S	B	B	B	1.56	1.96	1.77	14%
B.5.L.L	B	B	B	1.56	1.96	6.42	0%
B.25.S	B	B	B	1.56	1.96	2.87	2%
B.25.L	B	B	B	1.53	1.96	4.20	0%
Moment Frame Systems							
C.1.ESA.S	A	B	B	1.52	1.90	2.97	1%
C.1.ESA.L	A	B	B	1.44	1.75	1.94	0%
C.1.RSA.S	A	B	B	1.52	1.90	2.91	2%
C.1.RSA.L	A	B	B	1.52	1.90	1.76	13%
C.5.P.S	A	B	B	1.52	1.90	1.79	12%
C.5.P.05.L	A	B	B	1.52	1.90	1.84	11%
C.5.P.L	A	B	B	1.52	1.90	2.27	5%
C.7.S.L	A	B	C	1.62	2.09	2.44	6%
C.7.P.L	A	B	C	1.62	2.09	2.20	9%
C.7.S.L (C)	A	B	C	1.62	2.09	2.12	10%
C.7.P.L (C)	A	B	C	1.62	2.09	1.48	25%

limit calculated value of the approximate fundamental period per Section 12.8.2.1 of ASCE/SEI 7-10). Symbols distinguish among bearing wall systems (A.7, A.9, A.15), building frame systems (B. 2, B.4, B.5, B.25), and moment frame systems (C.1, C.5, C.7), where the designators in parentheses refer to the specific seismic force-resisting systems of Table 12.2-1 of ASCE/SEI 7-10, and denote average of individual archetype values of the performance group of interest.

Based on this figure, the most significant overall observation is that probability of collapse varies greatly as a function of period, but shows a common trend regardless of the type of system. This trend includes the observation of relatively poor performance for short-period systems, relatively good performance in the mid-period range, and potentially inferior performance for systems with very long periods.

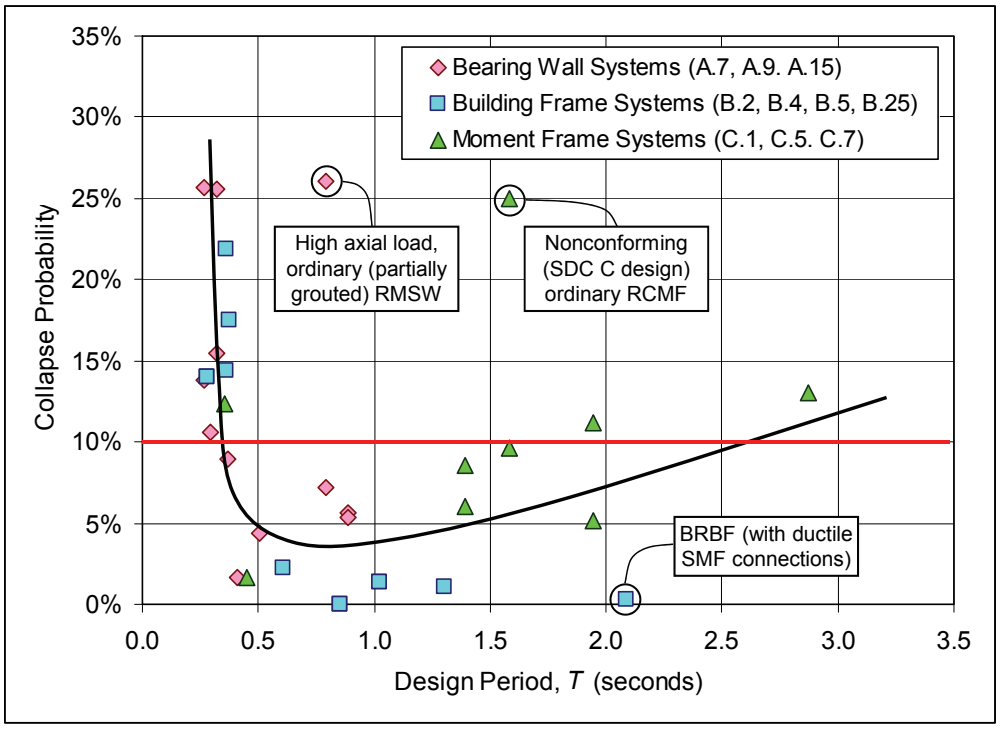

Figure 2-1 Plot showing the trend (and three circled outliers) in the probability of collapse of selected systems as a function of design period MCE_R ground motions. Data shown in this figure are based on results of prior studies of FEMA P-695 and NIST GCR 10-917-8.

Figure 2-1 identifies data points as "outliers" (circled) from the general trend, based on the characteristics of the archetypes of these groups. The identified systems are the following:

- **Partially grouted ordinary RMSW.** Although partial grouting of RMSWs is permitted by current design codes, the studies in NIST GCR 10-917-8 report found that full grouting was essential for proper collapse performance of RMSWs, particularly under high axial loads.

- **Nonconforming ordinary RCMF.** Ordinary RCMFs are not permitted by ASCE/SEI 7-10 for use as a SDC C system and thus the performance group reflected a very high collapse probability due to poor performance of the low ductility system subjected to moderately high (SDC C) seismic demand.
- **BRBF with ductile SMF connections.** This performance group represents superior collapse performance of BRBFs assumed to be part of a ductile steel moment frame. That is, after initial brace failure, the remaining frame of the archetype model sustained large story drifts without connection failure. If the frame behaves in this manner, then the low value of collapse probability is valid but may not represent typical performance of braced frame systems, even those with BRBFs.

2.3 Uniform Collapse Probability Inferred from Results of Prior Studies

The FEMA P-695 Methodology evaluates collapse performance of archetype models designed for an assumed value of the *R* factor (and $C_d = R$). In the studies documented in the FEMA P-695 and NIST GCR 10-917-8 reports, trial values of the *R* factor were taken from Table 12.2-1 of ASCE/SEI 7-05 (the values of the *R* factor are the same in ASCE/SEI 7-10) for the seismic force-resisting system of interest.

As indicated by the representative results of Table 2-2, the average collapse probability of a performance group of interest was typically less than the 10% limit of the FEMA P-695 Methodology but was seldom very close to this limit and tended to vary greatly as a function of design period and other factors. Thus, the results of these studies do not, in general, provide values of the *R* factor that correspond to a uniform 10% probability of collapse (given MCE_R ground motions) over the range of design periods (building height) and seismic design levels of the system of interest, as intended by ASCE/SEI 7-10. Understanding the trends in the values of the *R* factor that correspond to a uniform 10% collapse probability over the range of all contributing factors is of interest to the reformulation of the *R* factor and other seismic performance factors.

The value of a uniform risk factor, $R_{UR10\%}$, corresponding to a uniform 10% collapse probability, may be approximated from the design properties and collapse results of archetypes from prior studies, as follows:

$$R_{UR10\%} = \left(\frac{S_{MT} / 1.5}{V / W} \right) \left(\frac{ACMR}{ACMR_{10\%}} \right) \tag{2-1}$$

where:

$R_{UR10\%}$ = value of the *R* factor of the archetype model of interest that corresponds approximately to a 10% probability of collapse,

S_{MT} = MCE_R response spectral acceleration at archetype period, T (i.e., $C_u T_a$)

V/W = normalized base shear (C_s coefficient) used for archetype design,

$ACMR$ = adjusted collapse margin ratio of archetype model of interest, and

$ACMR_{10\%}$ = acceptable value of $ACMR$ (based on total uncertainty of collapse fragility).

Since the value of the design base shear, V/W, is not changed, the second term of Equation 2-1 implicitly modifies the effective level of MCE_R ground motions, S_{MT}, corresponding to the calculated value of $R_{UR10\%}$. Prior studies have shown that collapse performance is influenced by the level of MCE_R ground motions. Hence, the value of $R_{UR10\%}$ must be considered approximate. However, if value of the $ACMR$ is close to the value of $ACMR_{10\%}$, then the approximation is quite good. Conversely, for systems in which the collapse performance changes significantly with seismic design level or which have a value of the $ACMR$ substantially different from the acceptable $ACMR_{10\%}$ value, the approximation may be poor.

The first term in Equation 2-1 represents the effective value of R used for design of the archetype. This term equals either the value of the R factor given in Table 12.2-1 of ASCE/SEI 7-10 for the system of interest, or the effective value of the R factor for systems with very long periods whose design base shear is governed by the minimum base shear requirement of Equation 12.8-5 of ASCE/SEI 7-10. The second term represents an adjustment that effectively shifts extra margin into the R factor when the value of the $ACMR$ is greater than the acceptable value of $ACMR_{10\%}$ or conversely pulls margin out of the R factor when the value of the $ACMR$ is less than the acceptable value of $ACMR_{10\%}$, thus lowering the value of the R factor for those systems found to have less than 10% probability of collapse.

An example calculation of uniform risk is shown in Figure 2-2, which compares values of $R_{UR10\%}$ for the following two sets of long-period seismic force-resisting systems:

1. 8-, 12-, and 20-story special RCMF archetypes designed without minimum base shear requirements, and
2. 8-, 12-, and 20-story special RCMF archetypes designed with the minimum base shear requirements of Equation 12.8-5 of ASCE/SEI 7-10.

This example utilizes the archetype design properties and collapse results from the special RCMF example application of Section 9.2 of FEMA P-695 Report, which includes investigation of the effects of the minimum base shear requirement (e.g., Equation 12.8-5 of ASCE/SEI 7-10) on the collapse performance of tall, long-period archetypes. The minimum base shear requirement of interest had been removed from the original version of ASCE/SEI 7-05 but then reinstated by Supplement No. 1, after

it was found (by FEMA P-695 studies) to be essential for adequate collapse performance of tall buildings.

The 8-story archetypes have a design period, $T = 1.49$ seconds, which, in this case, is too short to trigger the minimum base shear requirement. Hence, the two 8-story archetypes have the same design base shear and other properties, and Figure 2-2 shows the same value of $R_{UR10\%}$ for the 8-story archetype designed with minimum base shear requirement as the 8-story archetype designed without minimum base shear requirement. In this comparison, the values of $R_{UR10\%}$ are just slightly greater than the ASCE/SEI 7-10 value of $R = 8$, indicating that an 8-story special RCMF system is expected to have collapse performance close to, but slightly better than the 10% collapse goal of FEMA P-695.

Both the 12-story and 20-story archetypes have design periods long enough to trigger the minimum base shear requirement. The 12-story archetypes have a design period, $T = 2.13$ seconds, which requires a modest (25%) change in the design base shear (from $V/W = 0.035$ to $V/W = 0.044$) to meet the minimum base shear requirement. The 20-story archetypes have a design period, $T = 3.35$ seconds, which requires a significant (100%) change in the design base shear (from $V/W = 0.022$ to $V/W = 0.044$) to meet the minimum base shear requirement.

In Figure 2-2, values of the $R_{UR10\%}$ factor for the 12-story archetypes are at or near the ASCE/SEI 7-10 design value of $R = 8$, indicating that $R = 8$ is appropriate for design of 12-story ($T = 2.13$ seconds) special RCMF systems to achieve a 10% probability of collapse (for MCE_R ground motions). In contrast, Figure 2-2 suggests that values of about $R = 5$ would be required for design of 20-story ($T = 3.35$ seconds) special RCMF systems to achieve the same level of collapse safety.

Figure 2-2 illustrates how period-dependent values of the R factor (i.e., R based on $R_{UR10\%}$) could be developed for design of taller, long-period systems to achieve the 10% probability of collapse objective of FEMA P-695 and ASCE/SEI 7-10 for Risk Category II structures.

Figure 2-2 also shows that values of $R_{UR10\%}$ are determined equally well by applying Equation 2-1 to the results of either 12- and 20-story archetypes designed for minimum base shear, or 12- and 20-story archetypes designed without minimum base shear. In this example, Equation 2-1 is relatively insensitive to the value of base shear used for design of the archetype. Conversely, Equation 2-1 does not (cannot) account for additional archetype capacity of designs governed by drift limits, and values of $R_{UR10\%}$ based on results of prior studies of archetypes designed for drift (e.g., special SMF archetypes) should be used with caution.

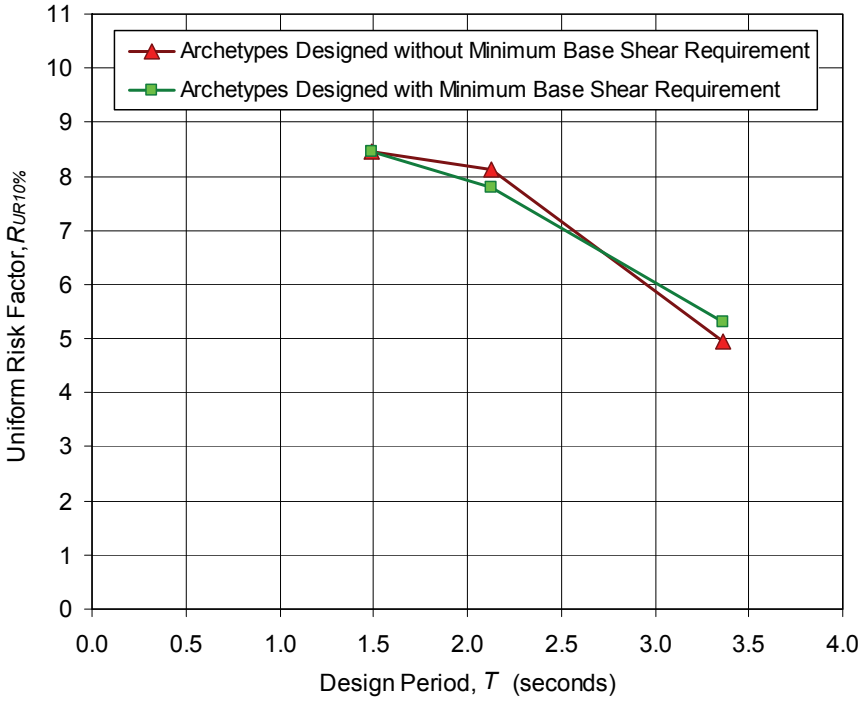

Figure 2-2 Comparison of uniform-risk factors, $R_{UR10\%}$, for 8-story (T = 1.49s), 12-story (T = 2.13s), and 20 story (T = 3.35s) special RCMF archetypes designed with and without the minimum base shear requirement of Equation 12.8-5 of ASCE/SEI 7-10.

If the R factor is formulated as the product of an overstrength component, R_O, and ductility component, R_d, as recommended in Chapter 4:

$$R = R_O \, R_d \tag{2-2}$$

then it follows that a uniform-risk-based value of the R_d factor may be calculated for each archetype (or performance group) as follows:

$$R_{d10\%} = \frac{R_{UR10\%}}{\Omega} \tag{2-3}$$

where:

$R_{d10\%}$ = uniform risk ductility factor, value of the R_d factor of the archetype of interest that corresponds approximately to a 10% probability of collapse,

$R_{UR10\%}$ = uniform risk factor, value of the R factor of the archetype of interest that corresponds approximately to a 10% probability of collapse, defined by Equation 2-1, and

Ω = value of archetype overstrength as determined by pushover analysis (FEMA P-695).

The purpose of normalizing the uniform risk factor, $R_{UR10\%}$, by overstrength, Ω, is to remove the influence of overstrength, if any, on trends in collapse performance, including the influence of drift limits to the extent that drift-based design adds strength to the archetype.

Table 2-3 summarizes representative design properties, results, and values of uniform collapse risk parameters, $R_{UR10\%}$ and $R_{d10\%}$, of governing performance groups of systems previously evaluated as part of either FEMA P-695 or NIST GCR 10-917-8 studies.

Table 2-3 includes the same ten seismic force-resisting systems and associated performance groups as those listed and described in Table 2-2. As in that table, a single "representative" value of the parameter of interest is given in Table 2-3 for each performance group (e.g., based on the average value of the parameter of the archetypes of the performance group).

Similar to Table 2-2, in Table 2-3, performance groups with more than 20% probability of collapse, on average, are indicated by dark grey shading, performance groups with more than 10%, but less than 20% probability of collapse by medium grey shading, performance groups with more than 2% but less than 10% probability of collapse by light grey shading, and systems with 2%, or less, probability of collapse by no shading.

Figure 2-3 is a plot of values of the uniform risk factor, $R_{UR10\%}$, and Figure 2-4 is a plot of values of the uniform risk ductility factor, $R_{d10\%}$, as function of design period for seismic force-resisting systems of Table 2-2, selected to be more ductile and have similar values of the R factor (between 6 and 8). These systems are commonly used in practice and are expected to perform well in strong ground motions as reflected in the relatively large design values of their respective R factors. These five systems are wood light-framed shear walls (R = 6.5), special steel concentrically braced frames (R = 6), special reinforced concrete shear walls (R = 6), special steel moment frames (R = 8) designed using the RSA method, and special reinforced concrete moment frames (R = 8).

In Figure 2-3 and Figure 2-4, uniform collapse risk factors of individual archetypes (taken from Appendix A data), which provide a more complete picture of the trends in values of $R_{UR10\%}$ and $R_{d10\%}$ with design period, are shown with open symbols. Data from Table 2-3 representing governing performance groups of the five seismic force-resisting systems are shown in these figures by closed symbols. Figure 2-3 includes horizontal lines corresponding to the (single) ASCE/SEI 7-10 value of the R factor for each system.

The design period, T, is used in these plots rather than the calculated modal period, T_1, since the design period is the basis for values, such as S_{MT}. In the case of special SMF

systems designed using the RSA method, the design period was taken as equal to the modal period for long-period archetypes to better reflect the use of RSA for design.

Table 2-3 Representative Design Properties, Results, and Uniform Collapse Risk Parameters of Selected Performance Groups of Previously Evaluated Systems

Performance Group Reference Number	Representative Value of Governing Performance Group						Approximate Uniform Collapse Risk	
	Archetype Design or Analysis Property					*Acceptable ACMR*		
	T (sec.)	*V/W*	Ω	$S_{MT}(T)$ (g)	*ACMR*	$ACMR_{10\%}$	$R_{UR10\%}$	$R_{d10\%}$
Bearing Wall Systems								
A.7.H.S	0.32	0.20	2.00	1.50	1.41	1.96	3.6	1.8
A.7.H.L	0.89	0.14	1.75	1.05	2.30	1.96	5.9	3.4
A.7.L.S	0.32	0.20	1.80	1.50	1.71	1.96	4.4	2.4
A.7.L.L	0.89	0.14	1.53	1.05	2.33	1.96	6.0	3.9
A.9.H.S	0.27	0.25	1.89	0.75	1.51	2.23	1.3	0.7
A.9.H.L	0.79	0.14	2.08	0.43	1.54	2.38	1.3	0.6
A.9.L.S	0.27	0.25	1.91	0.75	1.98	2.23	1.8	0.9
A.9.L.L	0.79	0.14	1.67	0.43	2.69	2.38	2.3	1.4
A.15.L.S	0.29	0.17	2.17	1.50	1.89	1.92	5.9	2.7
A.15.L.L	0.41	0.06	2.10	0.75	2.98	1.92	12.3	5.9
A.15.H.S	0.37	0.17	3.42	1.50	2.48	2.38	6.2	1.8
A.15.H.L	0.51	0.06	3.57	0.75	3.18	2.38	10.6	3.0
Building Frame Systems								
B.2.2X.S	0.38	0.17	1.43	1.50	1.64	1.96	5.0	3.5
B.2.2X.L	1.30	0.08	1.66	0.76	3.37	1.96	10.3	6.2
B.4.H.S	0.36	0.17	1.98	1.50	1.50	1.96	4.5	2.3
B.4.H.L	1.02	0.11	1.54	0.90	3.18	1.96	9.3	6.0
B.4.L.S	0.36	0.17	2.08	1.50	1.75	1.96	5.3	2.5
B.4.L.L	1.02	0.11	1.70	0.90	3.20	1.96	9.3	5.5
B.5.H.S	0.28	0.10	2.85	0.75	1.77	1.96	4.5	1.6
B.5.H.L	0.85	0.05	3.43	0.39	5.87	1.96	14.7	4.3
B.5.L.S	0.28	0.10	2.85	0.75	1.77	1.96	4.5	1.6
B.5.L.L	0.85	0.05	2.36	0.39	6.42	1.96	16.1	6.8
B.25.S	0.61	0.05	1.78	0.54	2.87	1.96	11.6	6.5
B.25.L	2.09	0.02	1.29	0.16	4.20	1.96	10.4	8.0
Moment-Resisting Frame Systems								
C.1.ESA.S	0.45	0.13	4.16	1.50	2.97	1.90	12.5	3.0
C.1.ESA.L	2.16	0.06	3.67	0.61	1.94	1.75	7.6	2.1
C.1.RSA.S	0.45	0.11	4.70	1.50	2.91	1.90	14.4	3.1
C.1.RSA.L	2.88	0.05	2.61	0.54	1.76	1.90	7.4	2.9
C.5.P.S	0.36	0.13	1.70	1.50	1.79	1.90	7.5	4.4
C.5.P.05.L	1.95	0.05	1.88	0.60	1.84	1.90	7.8	4.2
C.5.P.L	1.95	0.06	1.63	0.60	2.27	1.90	8.3	5.1
C.7.S.L	1.40	0.04	3.20	0.20	2.44	2.09	3.5	1.1
C.7.P.L	1.40	0.04	1.60	0.20	2.20	2.09	3.2	2.0
C.7.S.L (C)	1.58	0.05	2.40	0.24	2.12	2.09	3.0	1.2
C.7.P.L (C)	1.58	0.05	1.45	0.24	1.48	2.09	2.1	1.4

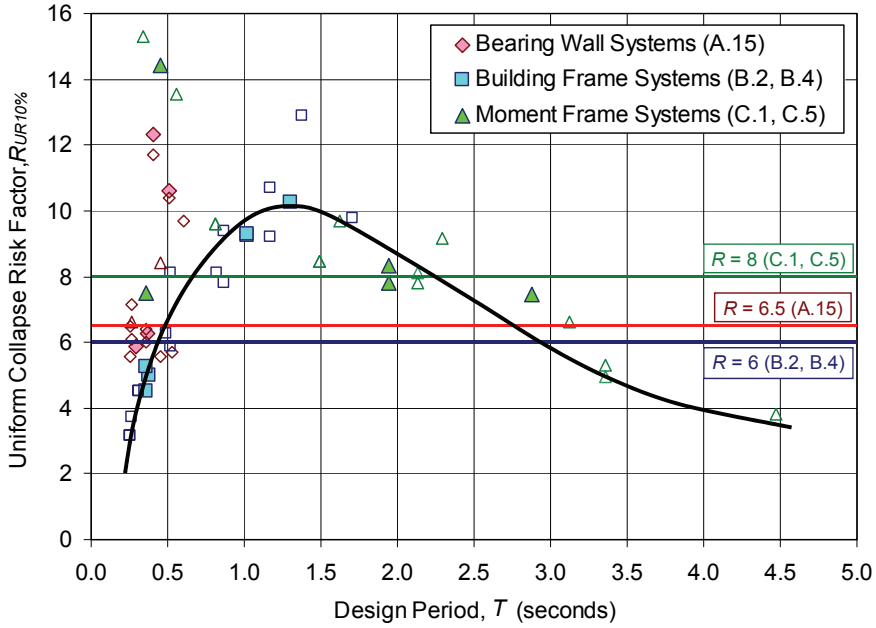

Figure 2-3 Plot showing the trend in the $R_{UR10\%}$ factor required to achieve uniform collapse risk for selected systems as a function of design period.

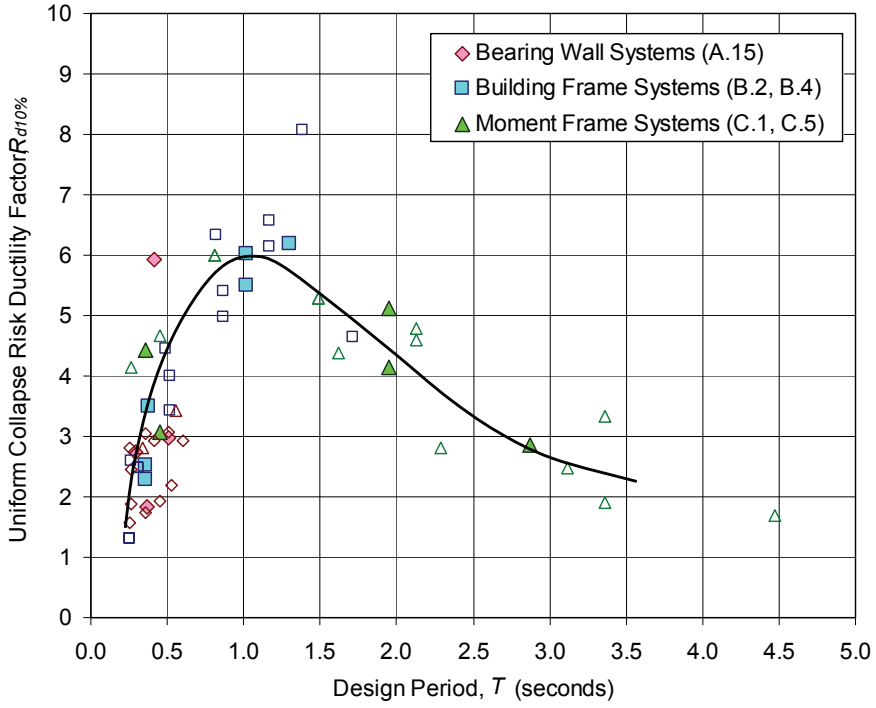

Figure 2-4 Plot showing the trend in the $R_{d10\%}$ factor required to achieve uniform collapse risk for selected systems as a function of design period.

Figure 2-3 and Figure 2-4 show clear trends in uniform risk factors, $R_{UR10\%}$ and $R_{d10\%}$, that are similar for each of the five systems. Consistent with the findings of previous studies, archetypes with short periods (periods less than about 0.5 seconds) typically

require reduced values of the R factor to achieve the collapse safety objective. Similarly, archetypes with long periods (periods greater than 2 to 3 seconds) require reduced values of the R factor (or other design criteria) to meet the collapse safety objective.

Although there are distinct differences between systems, trends in the uniform risk factors are generally very consistent for each of the five systems. A very large range of R factor values would be required to achieve uniform risk over the broad period range of interest. While a single value of the R factor is both desirable (for simplicity) and consistent with current seismic code criteria, such as those of the consensus standard ASCE/SEI 7-10, a single R factor value would either be very unconservative at certain periods, overly conservative at others, or both. The trend in the uniform risk ductility factor, $R_{d10\%}$, shown in Figure 2-4 is very similar to the trend in the $R_{UR10\%}$ factor, shown in Figure 2-3. However, removal of archetype overstrength from $R_{UR10\%}$ has reduced the dispersion around the trend. Reduced dispersion suggests that the $R_{d10\%}$ factor, rather than the $R_{UR10\%}$ factor, would be a more suitable parameter for measuring inelastic (ductile) performance of seismic force-resisting systems.

While each of the five systems is expected to perform well inelastically, as demonstrated by design values of R ranging from 6 to 8, they are not considered equal, because they do not have the same design value of R. Yet, the values of $R_{d10\%}$ shown in Figure 2-4 are not able to make such fine distinctions. If anything, the values of $R_{d10\%}$ for building frame systems (B.2 and B.4), whose design value of R is 6, seem to indicate slightly better performance than other systems with larger design values of $R = 8$. Of course, these data are based on limited studies of each system, but suggest caution in attempting to fine tune the R factor and other seismic performance factors and design requirements.

Figure 2-5 is a plot of $R_{d10\%}$ as a function of $R_{UR10\%}$ for each performance group and individual archetype of the five seismic force-resisting systems. If the value of overstrength factor, Ω, was the same for each archetype of a given system, then the plotted data would simply be a line from the origin with slope equal to $1/\Omega$. While not always the case, straight line trends can be seen for many of the data plotted in Figure 2-5, and differences in overstrength can be clearly seen for the different systems.

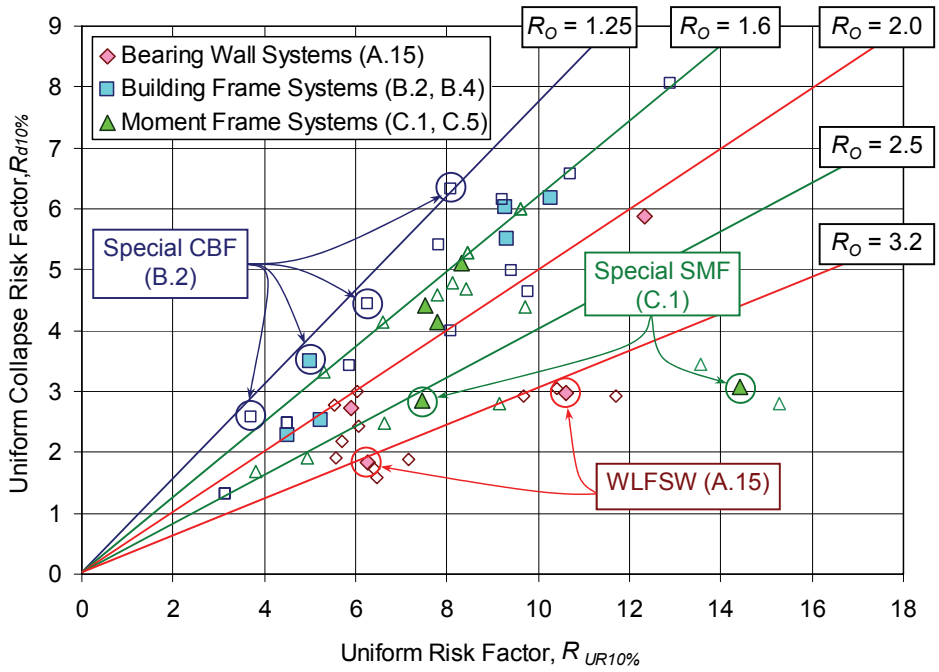

Figure 2-5 Plot showing trends in the $R_{d10\%}$ factor as a function of the $R_{UR10\%}$ factor for selected systems.

Figure 2-5 also illustrates a method of selecting reasonable "lower-bound" values of the R_O factor for each system. For example, in Figure 2-5 lines of constant overstrength show reasonable bounds on each system (or subsets thereof), suggesting lower-bound values of R_O as follows:

- Bearing wall systems:
  - WLFSW (A.15): $R_O = 2.0$ (low aspect ratio walls)
  - WLFSW (A.15): $R_O = 3.2$ (high aspect ratio walls)
- Building frame systems:
  - Special SCBF (B.2): $R_O = 1.25$
  - Special RCSW (B.4): $R_O = 1.6$
- Moment frame systems:
  - Special SMF (C.1): $R_O = 2.5$
  - Special RCMF (C.5): $R_O = 1.6$

As noted before, these data are based on limited studies of each system, but suggest a method that could be used to establish a "lower-bound" value of the overstrength component, R_O, of the R factor for each seismic force-resisting system. The overstrength component of the R factor, R_o, is not the same parameter, nor

appropriate for use, as the overstrength factor, Ω_O, of Table 12.2-1 of ASCE/SEI 7-10.

The notion here is that seismic design loads for ELF design would be based on reduced forces using a generic, conservative "lower-bound" value of overstrength, but that specific designs shown to have additional overstrength (e.g., by nonlinear static analysis) could be permitted to increase the value of the R_O factor (and hence the effective value of R factor), accordingly.

Chapter 3
Overview of Problem-Focused Studies

This chapter provides an overview, a summary of key findings, and discussion of results pertinent to reformulation topics of each of the three problem-focused studies of this report. The FEMA P-695 Methodology was used to investigate reformulation topics related to short-period systems, overstrength, and long-period systems as related to collapse assessment. These topics were selected based on their importance to the reformulation effort, as explained in Chapter 1. Chapter 5 includes recommendations for additional research resulting from these studies, and appendix material more completely describes each study's analyses.

The problem-focused studies provide additional data on the collapse performance of different seismic-force-resisting systems, augmenting the results and findings of the prior studies described in Chapter 2. Results of the problem-focused studies are intended to address certain specific reformulation topics of Chapter 4.

3.1 Study of Short-Period Systems

Prior studies using the FEMA P-695 Methodology (summarized in Chapter 2) found that short-period systems (structures with fundamental periods of vibration, T_1, smaller than or equal to 0.6 seconds) were likely to have a lower margin against collapse than structures with longer periods of the same basic structural material, configuration, and seismic design criteria. Although none of the short-period systems studied in the FEMA P-695 report (FEMA, 2009) failed the acceptance criteria, these systems tended to have the lowest ratio of computed Adjusted Collapse Margin Ratio (*ACMR*) to the acceptable *ACMR* for individual archetypes ($ACMR_{20\%}$) of a given performance group. Problems with short-period systems were particularly evident in the special reinforced masonry shear wall (special RMSW) and special reinforced concrete shear wall (special RCSW) systems evaluated in the NIST GCR 10-917-8 report (NIST, 2010), where several of the short-period system archetypes failed or came close to failing the acceptance criterion.

Short-period systems do not follow the equal displacement rule between inelastic (nonlinear) and elastic (linear) displacements. A number of previous analytical studies (Qui and Moehle, 1991; Krawinkler and Nasser, 1992; Miranda and Bertero, 1994; Miranda, 2000; Ruiz-Garcia and Miranda, 2003 and 2004; Chopra and Chintanapakdee, 2004) show that inelastic displacements are larger than elastic

displacements for the same dynamic demand starting at calculated fundamental periods of about 0.6 seconds, and the difference increases significantly as the period decreases. For very stiff systems (e.g., systems with periods of approximately 0.1 seconds), inelastic displacements predicted from nonlinear response history analysis may be more than an order of magnitude greater than those computed using a linear elastic model. The results of prior FEMA P-695 analyses, which are based on designs using a constant response modification coefficient, *R* factor, for a given system manifest this phenomenon. A variety of approaches have been proposed for dealing with this apparent problem.

The first, and most common, of the recommended approaches is to reduce the value of *R* factor as periods decrease below 0.6 seconds while maintaining the detailing requirements that would be associated with a higher *R* factor.

A related problem for short-period systems is the use of a constant (period independent) deflection amplification factor, C_d, equal to or slightly less than *R*, to adjust computed elastic design level displacements to represent unreduced inelastic displacements. This adjustment, which is based on the equal-displacement concept, is theoretically applicable only to systems with longer periods and may be unconservative for short-period systems. Thus, adjustments (reductions) to the *R* factor for short-period systems may need to be accompanied by increased values of C_d (or multipliers on C_d). Chapter 4, which covers reformulation, proposes the new term, C_{ds}, as the short-period displacement multiplier.

A second approach that has been recommended for improving short-period system performance is to increase the ductility capacity of short-period systems as the fundamental period reduces.

In both of the above approaches, the solution attempts to force short-period systems to be designed on the basis of assumptions that perhaps can only be successfully applied to systems with longer periods, such as models that respond to masses lumped at floor levels, bases that are fixed against sliding and rotation, and rigid diaphragms.

Thus, a third way to resolve the short-period problem is to recognize that the traditional approach of dissipating energy entirely through inelastic material behavior is not viable for systems with very short periods. Instead, these systems could be evaluated by a completely different set of rules, not yet developed. These new set of rules would provide improved methods to account for sliding, rocking, and soil-structure interaction that has been observed to occur at the base of low-period reinforced concrete and reinforced masonry walls. The development of such rules, if ultimately found to be necessary, are not included in the reformulation concepts presented in this report.

A final possible approach is to make no modifications to design rules or system behavior and ignore the apparent increase in the probability of collapse on the basis that there is little experimental or post-earthquake evidence that the short-period problem exists outside of the theoretical arena. The "make no modification" approach may be made on the basis that the analytical models and non-simulated collapse metrics used in the FEMA P-695 analyses of previous studies were necessarily limited and overly conservative for short-period systems. For example, analytical models of previous studies did not explicitly incorporate diaphragms, the foundation interface, or other sources of system flexibility which would tend to lengthen the period of building response, dissipate additional energy and reduce demands on primary elements of the lateral system (e.g., walls). In the case of stiff shear wall systems, non-simulated collapse metrics have effectively assumed that a complete loss of the structure, including the gravity system, would occur at relatively small lateral displacements not representative of actual building collapse.

3.1.1 Overview of Study

In this study, presented in detail in Appendix B, first, several prior studies documented in the FEMA P-695 and NIST GCR 10-917-8 reports were rerun with simple single-degree-of-freedom (SDOF) models. These studies developed data to help set the stage for detailed and systematic FEMA P-695 evaluation of short-period archetypes of special reinforced masonry shear walls (special RMSW) and buckling-restrained braced frame (BRBF) systems to develop relationships specifically applicable to potential code reformulation issues.

Study of Single-Degree-of-Freedom Models

In the SDOF study, a design space of simple bilinear systems was designed with *R* factor values ranging from 1 to 10, and with periods ranging from 0.1 seconds to 1.0 second in 0.1 second intervals. Other variables include strain hardening stiffness (in terms of initial stiffness), and the ductility demand at which collapse was defined. Quality ratings of design, modeling, and test uncertainties were all assumed to be B (Good), according to the FEMA P-695 Methodology. Each archetype model in the design space was evaluated with *ACMR*s and probabilities of collapse were reported for each model. Also reported in the SDOF study was the ratio of the median maximum computed inelastic displacement to the median maximum elastic displacement for each model.

A typical set of results from the SDOF study is illustrated in Figure 3-1. The figure shows the results for systems with 10% post-yield strain hardening (alpha = 0.1), a collapse ductility demand of 10, and no consideration for P-delta effects (alphaPD = 0). Part (a) of Figure 3-1 shows the probability of collapse on the vertical axis and the period of vibration on the horizontal axis. Results are collected in terms of *R* values, with one curve being plotted for each *R* value. Only the *R* = 1 system

has a probability of collapse of less than 0.1 at a period of 0.1 seconds, and systems with $R > 4$ have a probability of collapse greater than 0.1 even at periods beyond 0.6 seconds (i.e., even if short-period results are ignored, the FEMA P-695 Methodology would limit the system, as modeled, to about $R = 4$).

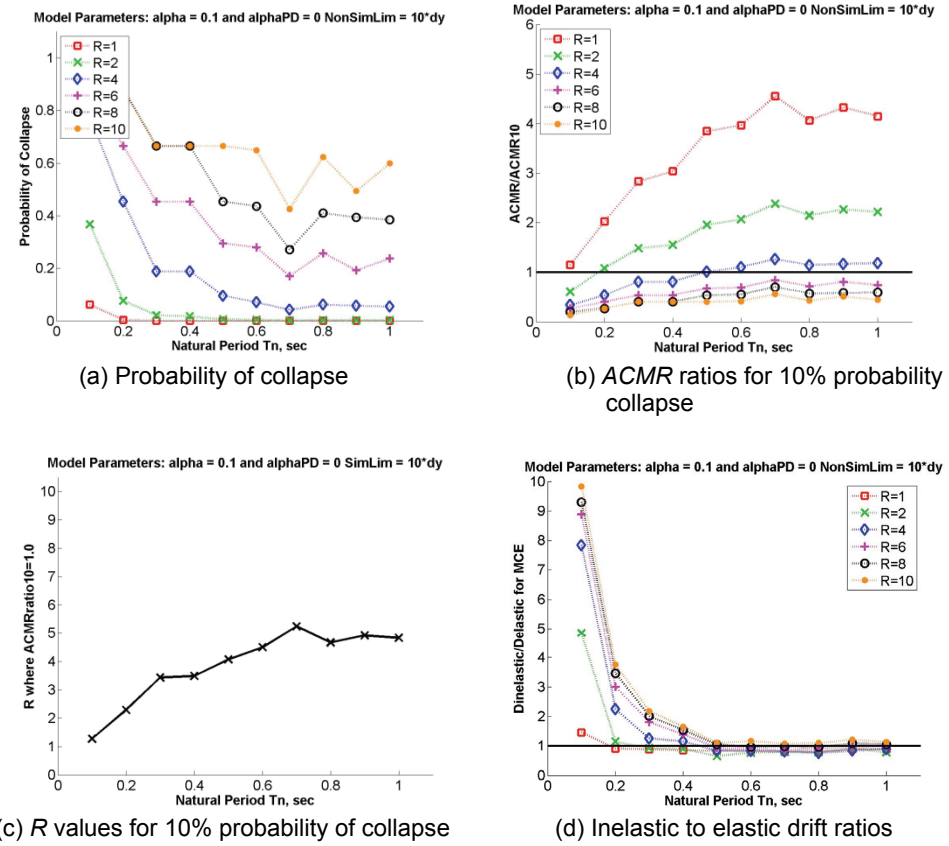

(a) Probability of collapse

(b) *ACMR* ratios for 10% probability of collapse

(c) *R* values for 10% probability of collapse

(d) Inelastic to elastic drift ratios

Figure 3-1 Results for SDOF systems with 10% post-yield strain hardening and collapse ductility demand of 10.

Figure 3-1b shows the ratio of *ACMR* to the acceptable collapse margin ratio for 10% collapse probability, $ACMR_{10\%}$, plotted against the period, with one curve for each *R* value. Ratios less than 1.0 indicate a greater than 10% probability of collapse, and hence, a failure to meet the FEMA P-695 acceptance criterion for a given performance group. The system with $R = 1$ passes for all period values, and systems with *R* values of 6, 8, and 10 fail for all period values.

The curves in Figure 3-1b can be used to interpolate the value of *R* at which the *ACMR* ratio is exactly 1.0 for each period analyzed. The resulting interpolated curve, shown in Figure 3-1c, indicates that the value of *R* required to meet the FEMA P-695 criterion is approximately 1 for systems with a period of 0.1 seconds and could be as high as 4 for systems with periods greater than 0.6 seconds. If desired, such a curve could be used to establish a period-dependent formula for *R*.

The resulting low R factor ($R = 4$) for models with longer periods (greater than 0.6 seconds) is because of the assumption that the structure yields at the elastic design level effectively eliminating the overstrength component of the R factor (i.e., $R_O = 1.0$ for an elastic-plastic system).

Figure 3-1d shows computed ratios of inelastic displacement to elastic displacement for different systems. This ratio is approximately 1.0 for systems with periods greater than 0.6 seconds but increases exponentially as the period decreases from 0.6 seconds to 0.1 seconds. Note the very high ratios for the larger R value systems with a period of 0.1 seconds.

Study of Reinforced Masonry Shear Wall and Buckling-Restrained Braced Frame Archetypes

The results of the detailed and systematic FEMA P-695 studies of reinforced masonry archetypes followed trends similar to that shown above for the SDOF systems. The analytical modeling approach and the non-simulated collapse criteria used in the study were essentially the same as utilized in the NIST GCR 10-917-8 report.

In this study, 1-, 2-, and 4-story archetypes, subjected to heavy gravity load and Seismic Design Category (SDC) D_{min} and D_{max} shaking, were redesigned using R values of 1, 2, 4, 6, and 8 and analyzed using the FEMA P-695 Methodology to determine how the collapse margin ratios and probability of collapse vary with design R values. Also computed were the ratios of the peak computed inelastic displacement to the peak elastic displacement.

Short-period steel buckling-restrained braced frames were also studied. The design space consisted of one- and two-story systems designed for SDC D_{max} and D_{min} ground motions and for $R = 2$, 4, 6, and 8. Individual archetypes were similar to those developed in Chapter 7 of the NIST GCR 10-917-8 report. Although none of these systems failed the FEMA P-695 criteria, general trends in the results show that systems with lower periods had a higher probability of collapse than systems with longer periods and that the ratio of inelastic to elastic displacement was also somewhat higher for systems with shorter periods. Detailed results of these studies are presented in Appendix B.

3.1.2 Summary of Key Findings

The study of SDOF systems and reinforced masonry shear wall archetypes demonstrated consistent behavior as follows:

- If it is desired to maintain a probability of collapse of 10% under Maximum Considered Earthquake (MCE_R) ground motions, the design R values should range from about 1 for systems with periods of about 0.1 seconds to the maximum value for systems with periods of about 0.6 seconds. The probability

of collapse is not strongly sensitive to the *R* value for periods from 0.6 seconds to 1.0 seconds.

- The ratio of computed inelastic displacement to computed elastic displacement is about 1.0 for systems with periods ranging from 0.6 seconds to 1.0 seconds but increases exponentially as the period decreases from about 0.6 seconds to 0.1 seconds. In the period range of 0.1 to 0.2 seconds, the computed ratios of inelastic to elastic displacement far exceed those predicted using the equal energy concept, because of the accumulation of residual displacement.

The study of buckling-restrained braced frame systems shows a clear trend of increase in probability of collapse as the system period decreases, and the ratios of inelastic to elastic displacement tend to increase as the design period decreases. However, none of the BRBF archetypes failed the FEMA P-695 acceptance criteria, and the ratios of inelastic to elastic displacement never exceeded 1.1, even for the system with the shortest period. This is due to the periods of the archetypes of the BRBF system being in excess of 0.45 seconds (see Table B-21), and approaching the transition between short- and long-period systems.

If it is desired to maintain a 10% probability of collapse under MCE_R shaking across all periods less than about 0.6 seconds (given a constant collapse metric, such as a limiting strain in shear wall reinforcement), it is theoretically necessary to reduce the design *R* value as the period decreases, with a limiting value of $R = 1$ being required when the period is less than about 0.1 seconds (and the system has little or no overstrength). However, the reduction in *R* towards the limiting value of 1.0 is needed because the ratio of inelastic displacement to elastic displacement increases exponentially as the period decreases. For systems with very short periods, providing sufficient ductility to accommodate this behavior is possible, so a design *R* value of 1.0 would be needed.

As noted in NIST GCR 10-917-8, it is doubtful that exceeding the collapse metric for the reinforced masonry and reinforced concrete shear walls systems would lead to a true collapse of the system, where collapse in this sense would include the loss of the gravity load-resisting capacity. If, for example, the wall reaches its strain-based collapse at a story drift of 1.0% of the story height, and the system loses its gravity load-resisting capacity at a story drift of 2.5% of the story height, there is a range of 1.5% drift in which the wall must be able to continuously rotate or slide after the strain limit is reached. If the wall is detailed to accommodate that additional deformation, the system will not collapse as long as the 2.5% drift limit is not exceeded. If the collapse metric were adjusted to represent the full system failure and not the wall failure, then a more appropriate measure of the probability of collapse could be determined.

3.1.3 Discussion of Results Pertinent to Reformulation of Seismic Design Parameters

The possible changes made to values of the R factor at short periods are presented on the basis of the reformulation presented in Chapter 4 of this report, wherein an MCE_R based value of R, designated as R_M, is used. R_M consists of the product of ductility and overstrength components, as follows:

$$R_M = R_{Md} R_O \tag{3-1}$$

The short-period adjustment would be placed on the full value of R_{Md}, because the studies for the masonry systems indicate that a design value of $R = 1$ is required for systems with periods less than about $T_1 = 0.1$ seconds. As previously discussed, models of masonry (and other) short-period systems of this and previous studies were necessarily limited and had conservative collapse acceptance criteria. More refined models and appropriate collapse acceptance criteria would likely change current criteria, but not necessarily eliminate the need to adjust the value of the R_{Md} factor at short periods to achieve uniform probability of collapse. Thus, the following formulations for adjustment are generalized and would require additional study of short-period systems (presumably with improved models and acceptance criteria) before implementation.

If it is desired to have a uniform probability of collapse across all periods, the relationship between R_{Md} and period would look like Line E on Figure 3-2. Line A on the same figure represents the current approach wherein the same reduction value is used for all periods and where the probability of collapse increases significantly at very short periods. Each line on Figure 3-2 is defined mathematically as follows:

For $T \le T_{min}$ $\qquad R = R_{Md,\,min}$ (3-2a)

For $T_{min} < T < T_{max}$ $\qquad R_{Md} = R_{Md,\,min} + \left[R_{Md,\,max} - R_{Md,\,min} \right] \dfrac{T - T_{min}}{T_{max} - T_{min}}$ (3-2b)

$T \ge T_{max}$ $\qquad R_{Md} = R_{Md,\,max}$ (3-2c)

In Figure 3-2, example values of R_{Md} are based on assumed values of $T_{min} = 0.2$ seconds and $T_{max} = 0.6$ seconds, $R_{Md,min} = 1.0$, and $R_{Md,max} = 5.0$, and the expression for the sloping part of Line E is:

$$R_{Md} = 1 + 10\left(T - 0.2\right) \tag{3-3}$$

For a system designed using Line E in Figure 3-2, the value of the short period displacement magnification factor, C_{ds}, would be 1.0 for all periods. The reason is that for low periods ($T < 0.2$s) the system is responding elastically ($C_{ds} = 1$), and for

periods greater than 0.6 seconds, the value of C_{ds} is also 1.0. There is no basis for varying the value of C_{ds} above 1.0 in the intermediate period range.

However, if the value for R_{Md} is not period dependent (the probability of collapse of greater than 10% for a performance group is accepted), it is theoretically necessary to provide a short-period displacement amplifier in the very short-period range ($T < T_{min}$), and to transition this multiplier to 1.0 for periods greater than T_{max}. Such a transition is provided graphically by Line A on Figure 3-3. In this example, the maximum short-period deflection amplification factor is 5.0 for very low periods. This value is in the general range of inelastic to elastic deflection ratios determined from the analysis of SDOF systems. Note that Line E on Figure 3-3 corresponds to the case where R_{Md} is modified to produce a constant probability of collapse across all periods. A general expression for the short-period multiplier is provided in the following equations:

For $T \le T_{min}$ $$C_{ds} = C_{ds,\,max} \tag{3-4a}$$

For $T_{min} < T < T_{max}$ $$C_{ds} = C_{ds,\,max} - \left[C_{ds,\,max} - C_{ds,\,min} \right] \frac{T - T_{min}}{T_{max} - T_{min}} \tag{3-4b}$$

$T \ge T_{max}$ $$C_{ds} = C_{ds,\,min} \tag{3-4c}$$

The sloping part of Line A in Figure 3-3 would have the following expression:

$$C_{ds} = 5 - 10\left(T - 0.2\right) \tag{3-5}$$

Lines B, C, or D on Figures 3-2 and 3-3 could be used for an intermediate design. However, the same alphabetically designated line would be used from each figure (for example, one would use Line D from each figure and not Line D from Figure 3-2 and Line B from Figure 3-3).

The use of Line E would impact the required strength of structures, and may not be economically justifiable given the limitations of the modeling used in the analysis, the conservative collapse criterion assumed in the analysis, and the scarcity of evidence that short-period systems are problematic. The use of Line A, which increases displacements at short periods, may not be as severe a penalty because short-period systems are rarely drift controlled. In all cases, significant research would be required to determine the appropriate period bounds and upper and lower limits on R_{Md} and C_{ds} in Figure 3-2 and Figure 3-3. Another factor in the research is whether the period limits should be based on empirical or computed periods of vibration. The use of expressions as illustrated in Figure 3-2 and Figure 3-3 could be system dependent, and in some cases, such as steel moment frames, the figures would

probably not be needed because even 1-story systems often have periods exceeding 0.4 seconds.

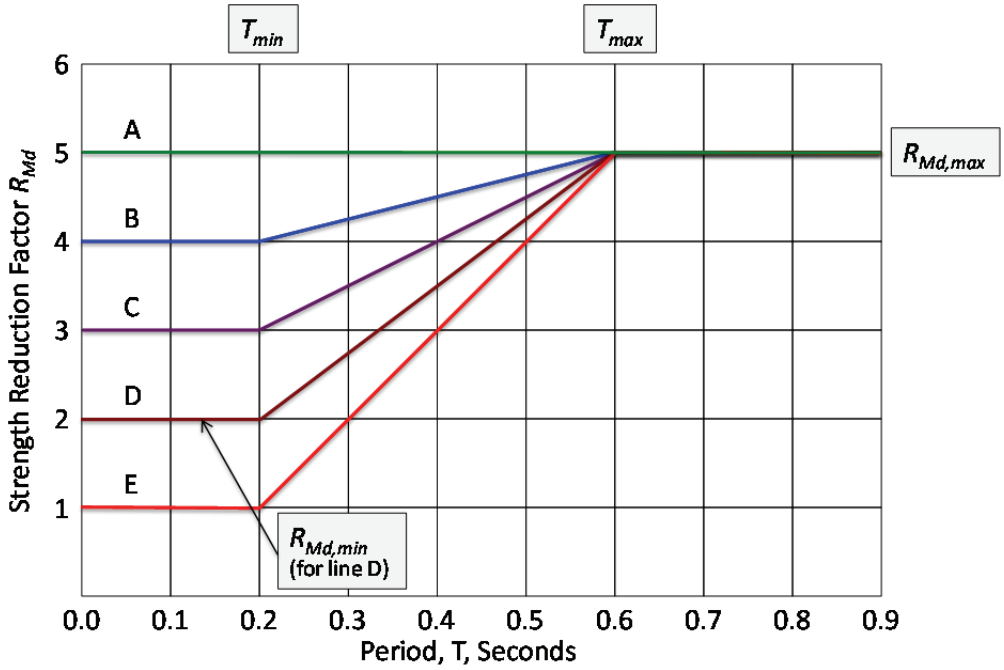

Figure 3-2 Variation in R_{Md} with period of vibration.

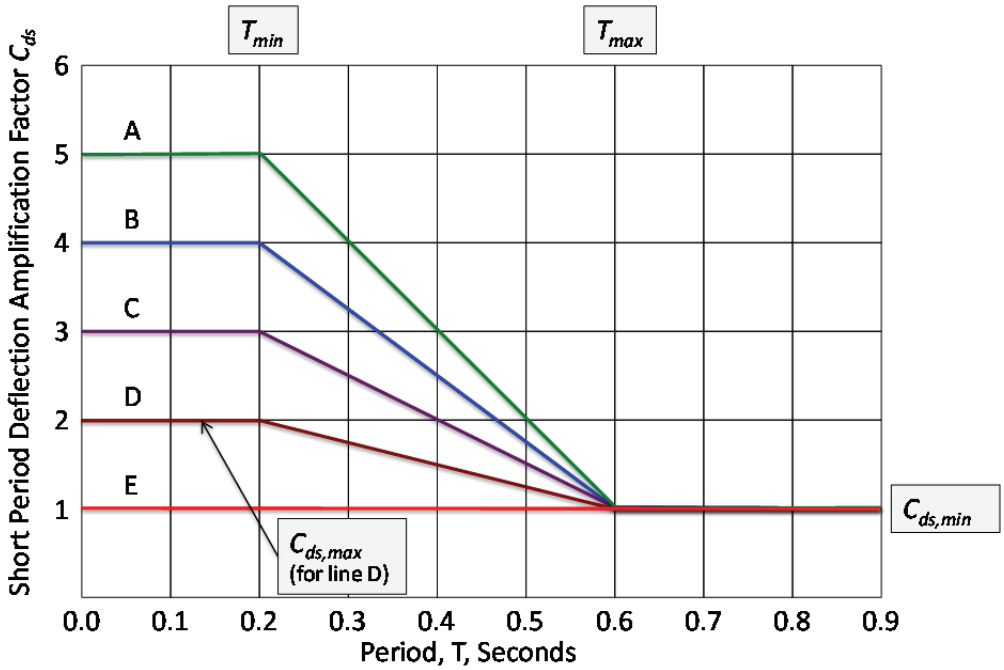

Figure 3-3 Variation in C_{ds} with period of vibration.

Because of the lack of clear evidence that short-period systems are problematic outside of the computational arena, it seems unwise to proceed with a recommendation to make significant adjustments to R_{Md} for short-period systems

without additional study. However, adjustments to the computed deflection of short period systems might be warranted**.** Thus, the principal preliminary recommendation from the work completed to date is to make no modification to R_{Md}, but to further develop a period-dependent relationship for C_{ds}.

Any final recommendation to provide period-dependent expressions for C_d (or for R_{Md}) must come only if additional studies on short-period systems indicate that this is necessary and that such formulas represent the best approach for solving the short-period problem. Key features of such studies should include improved modeling of material behavior, improved component modeling, improved system modeling, consideration of diaphragm and other sources of flexibility, refined definitions and metrics for collapse, and rethinking of the pure ductility-based design paradigm for structures with very short periods (in which post-yielding loss of strength accompanied by limited sliding and rocking does not necessarily indicate collapse.)

3.1.4 Conclusions

Studies described in this summary, and in more detail in Appendix B, show that one- and two-story reinforced masonry and reinforced concrete shear wall archetypes with short periods are likely to have conditional probabilities of collapse in excess of 10%, whereas taller systems of the same basic material, configuration, and design have less than a 10% probability of collapse. The poor behavior of the short-period systems is attributable to a low inherent ductility supply for these systems and to relatively large residual deformations that tend to dominate the dynamic behavior. Associated with the large residual deformations is the observation that inelastic displacements that are computed for systems with very short periods far exceed the elastic displacements computed for the same system. This phenomenon is in conflict with the equal displacement concept on which the parameters R and C_d are founded.

Although it is possible to overcome this problem by providing period-dependent values of R and C_d, such modifications are premature because the observations from the analytical studies appear to be at odds with observed behavior of short-period systems during real earthquakes. The disconnect between clear trends in the computational behavior and field observations is likely related to the use of oversimplified analytical models and to the use of unrealistic and overly conservative collapse metrics.

3.1.5 Recommendations for Future Studies

It is recommended that additional analysis be performed using improved mathematical models. For example, such models should include a more realistic representation of the inelastic axial-flexural-shear behavior of masonry and concrete systems, foundation flexibility, three-dimensional diaphragm behavior, and, in some instances, controlled sliding at the base of the walls. Collapse metrics should be

based on system collapse (including the gravity system) and should not be based simply on loss of strength of the masonry or concrete wall systems.

3.2 Study of Overstrength

Structural overstrength has two related but distinct influences on seismic design. One effect is the contribution of overstrength to the seismic response modification coefficient, *R* factor, which can be considered as the product of static overstrength, R_o, and a dynamic ductility response factor, R_d. In this regard, the overstrength provides a beneficial effect to the system, where for a given ductility the overstrength increases the available *R* factor (i.e., $R = R_O R_d$), or alternatively, for a given *R* factor, the overstrength reduces the required ductility (i.e., $R_d = R/ R_O$). This concept of overstrength is not changed by the reformulation of the overall *R* from design at two-thirds of the MCE_R using *R* (= $R_O R_d$) to design at the full MCE_R using R_M (= $R_{dM} R_O$); the R_O is the same for both methods. The other impact of overstrength is to increase the force demands on so-called force-controlled components, which are subject to design forces amplified by Ω_O typically designed using some type of capacity design requirement. The overstrength used for capacity design is quantified as the Ω_O factor, which is specified in ASCE/SEI 7-10, *Minimum Design Loads for Buildings and other Structures* (ASCE, 2010) for use in the amplified seismic force demand calculation.

This study of overstrength is concerned primarily with the second of these effects, i.e., the role of overstrength in establishing capacity design requirements for force-controlled components. The study is motivated by the following considerations:

- Prior studies of system archetypes, as summarized in Chapter 2, indicate that overstrength values, calculated using static pushover analyses, can vary considerably from the specified values of Ω_O in ASCE/SEI 7-10. As a practical measure, the FEMA P-695 Methodology for defining Ω_O limits the maximum value to 3, regardless of the calculated overstrengths from pushover analyses of the archetype configurations; however, there is no theoretical justification for this limit.
- In addition to the large variability in overstrength values calculated by static pushover analysis, there are basic questions as to whether the overstrength, as determined by this method, is an accurate measure of force demands that can develop in force-controlled components during earthquake shaking and whether a single factor for a generic system can, in fact, be a reasonably safe and economical protection against premature failure of the system.
- While material-specific design specifications, notably ANSI/AISC 341-10, *Seismic Provisions for Structural Steel Buildings* (AISC, 2010), and ACI 318-11, *Building Code Requirements for Structural Concrete and Commentary* (ACI,

2011), include requirements for capacity-based design of force-controlled components, they rely less on the system overstrength factor and more on design provisions that are directly based on the expected strength of deformation-controlled (yielding) elements. This suggests that rather than focusing on refinement of a single system overstrength factor, it would be more appropriate to revisit the needs for capacity design and to develop component specific overstrength requirements for design.

3.2.1 Overview of Study

While the original motivation of the overstrength study was to assess the Ω_O values specified in ASCE/SEI 7-10, it was expanded to more broadly consider capacity design requirements for force-controlled components of seismic systems and how well the force demands are calculated by the system overstrength factor or other methods. Thus in this study, force demands were calculated by nonlinear analyses of structural archetypes for special steel concentrically braced frame (SCBF) and special reinforced concrete moment frame (RCMF) systems. Complete details of this study, including a review of current design provisions for overstrength and related research, are provided in Appendix C.

The special SCBF study includes analyses of 3-, 6-, and 12-story single bay frames, whose designs where developed and evaluated for the NIST GCR 10-917-8 report. The special RCMF study included 4-, 12-, and 20-story perimeter concrete frame archetypes, which were previously designed as part of the FEMA P-695 study.

In contrast to the other problem-focused studies where the primary goal is to assess collapse capacity, the overstrength analyses focused primarily on assessing the force demands in force-controlled components. The steel braced frame and reinforced concrete moment frame archetypes were modeled and analyzed using OpenSees (http://opensees.berkeley.edu/) to capture all significant contributions to nonlinear strength and stiffness degradation, including geometric nonlinear effects. The special SCBF models captured brace yielding, buckling and fracture along with flexural hinging and degradation to the beams and columns. The special RCMF models captured flexural hinging and degradation to the beams and columns.

The structural archetype models were analyzed by nonlinear static (pushover) and nonlinear dynamic (response-history) analyses, where the latter were performed using the ground motion set and scaling procedures set forth in the FEMA P-695 report. Force demands for selected components were evaluated at varying levels of ground motion intensities, where the demands were characterized in terms of median values from nonlinear dynamic analyses under the forty-four ground motions of the FEMA P-695 far-field record set. In the special SCBFs, forces were monitored to establish the following force demands: axial forces on brace connections, axial forces on columns, and inertial forces on collectors. In special RCMFs, the following force

demands were recorded: beam shear forces, column shear forces, column axial forces, and inertial forces on collectors. All of the archetype models were two-dimensional frames, where collector forces were determined assuming rigid diaphragm behavior, where the collector forces are calculated as the difference in the resultant building shear forces above and below the floor level. The resulting data provide information on: (1) how the component forces increase with respect to ground motion intensity, including whether or not the force demands saturate at some ground motion intensity; and (2) medians and variability in these particular force demands at selected ground motion intensities.

3.2.2 Summary of Key Findings

The following is a summary of observations and findings from the review of overstrength design requirements and supporting studies:

- Current material design standards, such as ANSI/AISC 341-10 and ACI 318-11, make limited reference to the overstrength factor, Ω_O. Instead, where overstrength and capacity design are deemed important, current material standards tend to rely more on explicit capacity design checks, where the required strengths are based on force demands calculated using the expected strengths of yielding components. However, these approaches can be limited due their focus on either first mode behavior or the assumption of all designated elements yielding simultaneously. Moreover, whereas the commentary to ASCE/SEI 7-10 implies that capacity design approaches can be applied to limit the required strengths to a value less than that calculated by Ω_O (implying that Ω_O will tend to envelope the force demands), material design standards often specify the Ω_O amplifier (or another similar, but usually smaller, number) as an exception to relieve the forces that would otherwise be required by a strict capacity design requirement. Thus, the rationale behind the entire concept of using overstrength as a protection of vulnerable limit states is sometimes inconsistent with its formulation and how it is applied.
- The designation of force-controlled components and the use of capacity-based design concepts to proportion force-controlled components are highly variable across different system types and materials. Whereas some provisions, notably those for steel-framed structures, make fairly extensive use of capacity-based design concepts, other provisions (e.g., for wood framed structures) make relatively little use of capacity design requirements, other than the general requirements imposed by ASCE/SEI 7-10. Moreover, some wood systems are granted exemptions from some of the general requirements in ASCE/SEI 7-10. Accordingly, the use and design relevance of Ω_O is quite varied across systems and materials.

- Whereas the FEMA P-695 collapse analysis procedures were originally conceived to assess overall system collapse that is dominated by inelastic behavior associated with first-mode response, the FEMA P-695 procedures are less effective at assessing other effects, such as variability of force demands in force-controlled components and their influence on collapse safety. For example, this study of collectors revealed their force demands to be heavily influenced by short-period higher-mode response, which can be significantly overestimated using the first-mode period scaling procedures of FEMA P-695. In addition, the use of median model parameters in the FEMA P-695 analyses precludes the direct assessment of how variability in design requirements, actual strengths of yielding mechanisms, and behavior of force-controlled components influences structural collapse.
- The static strength is not necessarily an accurate measure of the maximum forces that can develop in the various force-controlled components of the structure. This is particularly true where higher mode or transient pulse-like effects are present. For example, in slender concrete walls where higher modes are significant, the maximum shear that develops in walls is not necessarily limited by hinging at the base of the wall. Therefore, the shear demands calculated from a static nonlinear (pushover) analysis may be much lower than shears that can develop during dynamic loading. Similarly, in braced frames, the localization of inelastic deformations in one or two stories, which are typically observed in pushover analyses, do not necessarily reflect the maximum story shear and overturning forces that can develop under dynamic loading. And, finally, the collector forces in the lower stories of a building are often considerably larger than those inferred by first-mode pushover behavior and the associated equations in ASCE/SEI 7-10 that are based on the equivalent lateral force (ELF) procedure.
- In comparisons between forces calculated using system overstrength factors versus yielding element-based capacity design factors, the element-based factors are usually more accurate at assessing the force demands – particularly where the forces of interest are governed by local behavior adjacent to yielding elements (e.g., shear in beams with flexural hinges, connections in yielding braces). Where force demands are controlled by yielding of adjacent elements, the capacity design provisions of AISC *Seismic Provisions for Structural Steel Buildings* and ACI *Building Code Requirements for Structural Concrete and Commentary* tend to work well, in that the median force demands can be reliably calculated and the variability in the maximum force due to ground motion variability is fairly constrained. For example, brace connection forces and beam shear forces in optimally designed systems had well-controlled median values and coefficients of variation (COV) less than about 10%. On the other hand, for force-controlled components whose response depends more on overall system behavior, the medians are more difficult to predict and the variability is higher.

For example, the median values of axial column force demands were not well-predicted and had COVs of up to 30%. The observed variability in the force demands is largest for the diaphragm collector forces for lower stories in tall buildings, where the demands reflect the high frequency characteristics of the ground motion input. In the 20-story frame building, the calculated median values appeared to have little relationship to the yield strength of the frame and COVs of up to 50% were observed in the collector forces. In the lower floors of buildings, the collector forces are better predicted by the peak ground accelerations and are not influenced much by the structural systems strength.

- The force demands in components with well-controlled mechanisms had low variability and tended to increase and saturate rapidly at low ground motion intensities, sometimes reaching their full force demands at ground motion intensities of about 20% to 30% of the MCE_R intensity. While small variability with respect to system reliability is good, the rapid increase in forces at low ground motion intensities can have negative effects on system reliability. This is because these force-controlled components will experience their maximum demands much more frequently (smaller return periods), as compared to the frequency that deformation-controlled components will experience their maximum deformation demands. Thus, while MCE_R level force demands provide a reasonable measure of the maximum force demands on force-controlled components, their frequency of occurrence is typically much higher than implied by MCE_R intensity checks.
- ASCE/SEI 7-10 procedures for calculating diaphragm collector forces yield far smaller results than observed in this study, especially in taller structures. For example, results of the 12-story special SCBF and 12- and 20-story special RCMFs suggest that the current ASCE/SEI 7-10 provisions may underestimate collector forces by more than four times. It is not clear that these large discrepancies can be corrected by revising the static overstrength values, since the errors have more to do with how dynamic pulse (or higher mode) behavior is considered in the ASCE/SEI 7-10 force demand equations for diaphragm collectors. This study computed collector forces from the two-dimensional frame analyses as if the mass were rigidly connected to the frames at the floor levels (the conventional rigid diaphragm assumption). It is not clear that accounting for cracking and yielding of elements within the diaphragm and collector system will resolve all discrepancies observed. The rationale for applying the overstrength factor to collector force demands has less to do with the system overstrength and more to do with simply providing an extra margin of safety in the collectors. However, currently there is no reliability basis to establish appropriate margins (force demand and resistance factors).

- Design approaches that employ nonlinear dynamic analysis provide for explicit calculation of inelastic force demands in force-controlled components and, thereby, do not make use of Ω_O to calculate overstrength effects. Current standards and guidelines, such as Chapter 16 of ASCE/SEI 7-10, *Guidelines for Performance-Based Seismic Design of Tall Buildings* (PEER, 2010), and *An Alternative Procedure for Seismic Analysis and Design of Tall Buildings Located in the Los Angeles Region* (LATBSDC, 2011), generally include distinctions between deformation-controlled and force-controlled components, and they make allowances for the variability in force demands on force-controlled components. However, there are some striking differences between these documents: (1) ASCE/SEI 7-10 calculates demands at the Design Basis Earthquake (DBE) levels, whereas the PEER *Guidelines* calculate demands at MCE_R levels; (2) for force-controlled components, ASCE/SEI 7-10 uses the maximum of 7 ground motions to determine the required design force demand, whereas the PEER *Guidelines* impose a multiplier on the mean demands; and (3) component strengths are calculated differently in each document, i.e., expected or nominal material strengths are assumed and resistance factors, ϕ, are or are not included. Moreover, it is not clear that any of these provisions for design of force-controlled provisions have been statistically assessed for conformance with the expected collapse safety of the overall seismic force-resisting system.
- The nonlinear collapse analyses of the special RCMF and special SCBF archetypes, which were conducted for the overstrength study, provided an independent check of collapse analyses that were previously conducted in FEMA P-695 studies. In some cases, the nonlinear collapse analysis results in this study agreed fairly well with those of prior studies. However, in other cases the archetype analysis results were considerably different (up to a factor of about two in the calculated median collapse capacity) from those reported in prior studies. These results highlight the extent to which the FEMA P-695 evaluation of collapse safety is sensitive to model types and modeling assumptions used in the archetype analyses.

3.2.3 Discussion of Results Pertinent to Reformulation of Seismic Design Parameters

Given the limited and somewhat inconsistent use of Ω_O in current design standards, the inconsistency in calculated pushover strengths as compared to specified Ω_O for various systems, and the general difficulty and ambiguity in quantifying the overstrength factor, it is recommended to revise the general overstrength definition and provisions in current building codes and replace them with alternative requirements that are tailored to the specific design situation. For example, where material design provisions, such as the AISC *Seismic Provisions*, make reference to Ω_O, it is suggested that the references be replaced with specific strength requirements

based on capacity design that pertain to the specific situation. In other situations, such as for design of collectors, the analyses suggest that the issues related to the overstrength factor are less significant than the need for fundamental improvements in the way that collector force demands are calculated and the required margin of safety in collectors.

Specific aspects of overstrength reformulation should include the following:

- Force-sensitive limit states that are clearly controlled by a well-defined deformation-controlled response in a member, such as shear in special moment frame beams and connection forces in SCBF, should use local mechanism-based overstrength provisions similar to those in current material design standards. Studies using FEMA P-695 procedures, such as those in Appendix C, can be used to decide whether the particular limit state is clearly eligible for such provisions. The factors established to estimate appropriate upper bounds should be calibrated by reliability-based procedures.
- Force-sensitive limit states that require consideration of the ductile response of many members, or an entire system, such as the axial force in a column supporting a multi-story wall or braced frame (consider the three-dimensional effect of members supported by the wall above) should continue to be designed using specified values of Ω_O. The values of Ω_O for this purpose will require further study to assure that the design standards deliver the stated objectives, but the current values of Ω_O, 2, 2.5, and 3, have not been validated by this or prior studies based on FEMA P-695 Methodology. Validation of new values (or a single value) will require synthesis from studies of many different seismic force-resisting systems using archetype design and analysis concepts of the FEMA P-695 Methodology. Calibration of the appropriate overstrength values will require enhancements to the current FEMA P-695 Methodology to evaluate the reliability of force-sensitive components and their influence on collapse risk.

  Limit states that are considered force-sensitive, but for which limited ductility is feasible, such as collectors, could make use of intermediate values of Ω_O, or alternative procedures that allow for some amount of yielding. These values (or procedures) will also require validation by studies that make use of a modified FEMA P-695 Methodology that can assess risk to the force-sensitive components.

3.2.4 Conclusions

Some measure of system overstrength is integral to capacity-design provisions to provide inelastic response mechanisms and minimize the risk that overloading of force-controlled components will substantially impact the collapse safety of buildings. This study highlights limitations of the current ASCE/SEI 7-10 provisions that rely on a single overstrength factor, Ω_O, to characterize earthquake-induced force

demands for various force-controlled components throughout the structure. The single overstrength factor does not account for variations in member overstrength that can arise from specific design decisions (e.g., members that are oversized beyond what is required by the minimum seismic design requirements) or the effects of inelastic force redistributions that occur under dynamic earthquake loading. The study also highlights other shortcomings in capacity-design provisions that arise from: (1) inaccuracy in certain loading provisions to calculate force demands (e.g., forces on diaphragm collectors or column overturning forces in tall frames due to inelastic and higher mode effects); and (2) lack of consistent reliability basis to establish demand and capacity factors to account for the frequency of occurrence and variability in force demands.

Design specifications that rely on capacity-design requirements to control inelastic response tend to rely less on the amplified seismic loads (using Ω_O) towards provisions that are tailored to specific structural systems and components. Recognizing that such approaches are likely to lead to more accurate estimates of inelastic force demands, the overall recommendation of the overstrength study is to develop more case specific capacity-design requirements and to move away from the single overstrength system factors. Moreover, the capacity-design requirements should be developed and informed by a reliability basis that is consistent with the collapse safety targets implied in ASCE/SEI 7-10 and FEMA P-695.

3.2.5 Recommendations for Future Studies

The three most important needs to support the development of capacity design requirements to provide more risk-consistency in the design of force-controlled components are:

- Extension of the FEMA P-695 Methodology to evaluate the collapse risk associated with force-controlled components. Just as the FEMA P-695 Methodology provides a way to determine system response factors, extensions will provide the basis to evaluate force demand and capacity provisions applied in the design of force-controlled components.
- Studies to develop improved methods to determine median force demands in force-controlled components that are controlled by dynamic and inelastic response. Examples include methods to determine column axial forces due to overturning effects, shear demands in concrete and masonry walls, and diaphragm collector forces.
- Development of a reliability-based approach to establish risk-consistent demand and capacity factors for the design of force-controlled components.

3.3 Study of Long-Period Systems

Prior studies using the FEMA P-695 Methodology found that for long-period systems (structures with design period, $T = C_u T_a$, greater than 2 seconds) designed using the design spectrum and the same R factors as those used for systems with shorter periods, the collapse risk will be significantly higher. This is shown by the trend in the data plotted in Figure 2-1. The objectives of this study were to further investigate the collapse risk of long-period systems and to develop recommendations for modifying the design of long-period systems to achieve an approximately uniform collapse probability across all periods.

3.3.1 Overview of Study

In this study, presented in detail in Appendix D, the design base shear required to achieve a collapse risk of 10% under the MCE_R was computed for special reinforced concrete (special RCMF) and special steel moment frame (special SMF) archetypes designed and analyzed as part of the prior studies, and for special reinforced concrete core-wall (special RC core-wall) archetypes designed and analyzed as part of this study. Only archetypes designed for SDC D_{max} were considered and collapse risk was assessed using the FEMA P-695 Methodology. The required base shear data were then used to develop recommendations for design of long-period systems. The following sections discuss the design and collapse risk assessment of special RC core-wall archetypes, calculation of the base shear required to achieve a 10% collapse risk under the MCE_R, and evaluation of the required base shear data for the special RCMF, special SMF, and special RC core-wall archetypes.

Design of Long-Period Special Reinforced Concrete Core-Wall Archetypes

As part of the study, two sets of four special RC core-wall archetypes were designed in accordance with ACI 318-08, *Building Code Requirements for Structural Concrete and Commentary* (ACI, 2008) and ASCE/SEI 7-10. The recommendations of the PEER *Guidelines* were used to size walls for shear demand. Building archetypes were assumed to have a 100 feet by 100 feet footprint, a story height of 12 feet, and a core-wall configuration comprising two C-shaped walls. Building heights of 16, 20, 24, and 30 stories were used in the study.

Design was accomplished using elastic analysis and considering demands from gravity and earthquake loads (maximum demands for SDC D_{max}). Elastic analysis was conducted assuming flexural, shear, and axial stiffnesses equal to 50%, 100% and 100%, respectively, of the gross section stiffness, as recommended in ASCE/SEI 41-06, *Seismic Rehabilitation of Existing Buildings*, (ASCE, 2007). The designs were evaluated to verify capacity for wind loads (85 mph exposure C) and to assess wind-induced vibration. For one set of designs, demands from earthquake loads were determined using the ELF procedure. For the other set, demands were determined

using modal response spectrum analysis (RSA). In prior studies, it was found that archetypes analyzed with the RSA procedure anchored to 85% of the ELF base shear demands were producing collapse probabilities greater than archetypes designed by ELF. Based on this finding, in this study the RSA base shear demands were scaled up to 100% of the corresponding ELF demands. This modal scaling should become a reformulation consideration (also listed in Table 1-3 under Analysis Method).

Walls were designed for gravity and earthquake demands in accordance with ACI 318-08 and the PEER *Guidelines*. Basic assumptions employed in designing the walls were the following: (1) a minimum length, l_w, of 25 feet and a minimum thickness, t, of 18 inches; (2) concrete compressive strength, f_c, of 5000 psi and Grade 60 reinforcement; (3) an axial load at the base of the wall equal to $0.1f_cA_g$; (4) uniformly distributed longitudinal reinforcement with a target longitudinal reinforcement ratio of 1.00%; (5) fixed boundary conditions at the base of the wall with no consideration given to soil-foundation-structure interaction; and (6) no torsional demands. For walls designed using RSA demands wall length, l_w, and thickness, t, were determined by the shear demand and wall flange length, b_f, was determined by the flexural demand at the base of the wall. Shear stress demands were limited to $2-3\sqrt{f_c'}$ psi per the recommendations of PEER *Guidelines* and walls were designed to achieve the maximum shear strength based on ACI 318-08. For walls designed using ELF demands, wall design was determined primarily by flexural demands at the base of the wall. For all designs, the ratio of factored flexural strength to flexural demand, $\varphi M_n/M_u$, was 1.0 at the base of the wall. The ratio of factored shear capacity to shear demand, $\varphi V_n/V_u$, ranged from 1.7 to 1.9 for the RSA designs and from 2.8 to 3.2 for the ELF designs. In contrast to typical design practice, the design of the core-wall cross-section at the base of the wall was continued up the entire height of the wall. This was based on data from a Pugh (2012) in which the wall flexural and shear strengths were reduced up the height of the wall based on the demand profiles determined from RSA or the ELF procedure. Walls designed in this manner were found to exhibit large inelastic flexural deformation demands and develop shear demands in excess of shear capacity at heights above the base of the wall. Thus, to minimize inelastic flexural demands and to reduce the likelihood of shear demand-capacity ratios in excess of 1.0 above the base of the wall, the base cross-section was continued up the entire height of the wall.

Walls were analyzed for wind loading and found to have adequate capacity. Using expected material strength and stiffness, all but the 30-story RSA design was found to meet the 1-year acceleration limit for residential construction in ISO 6897:1984 (ISO, 1984). No modification was made to the 30-story RSA design to meet the ISO acceleration limit.

Figure 3-4 shows the plan view of the special RC core-wall archetype building. Table 3-1 lists configuration and design parameters for the walls. The computed

fundamental period of the buildings, T_1, is significantly longer than the design period, T, calculated according to ASCE/SEI 7-10. Because the design period is intended to represent the median of measured building periods, it is not surprising that the computed periods of the core-wall buildings differ from this value. However, anecdotal evidence suggests that although the computed fundamental period of a core-wall building designed for construction on the West Coast of the United States is typically longer than the design period, it is also typically less than the computed periods listed in Table 3-1. The greater flexibility of the archetype buildings designed for this project is attributed to the fact that these buildings were not designed to meet all performance requirements typical of practice, such as the ISO acceleration limit for wind loading for the 30-story archetype. Note that entries denoted with MRSA in the ID column were archetypes designed using demands determined from RSA and entries denoted with ELF were designed using demands determined from the ELF procedure.

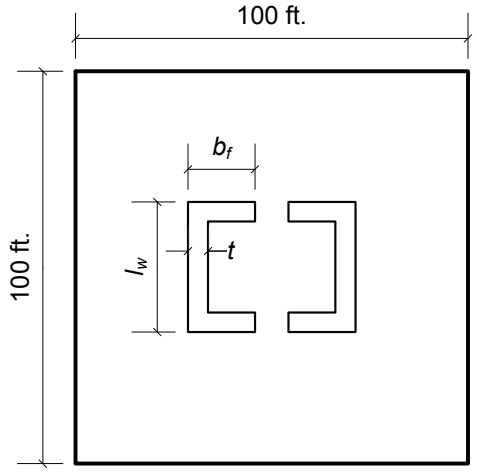

Figure 3-4 Plan view of special reinforced concrete core-wall archetype.

Table 3-1 Special Reinforced Concrete Core-Wall Archetype Configuration and Design Parameters

ID	No. of Stories	l_w (ft)	t (in)	b_f (ft)	T (sec)	T_1 (sec)	V/W (g)	ρ_{long} (%)	Base Shear Stress Demand / $\sqrt{f'_c}$ (psi)
MRSA1	16	25	18	4	1.44	3.52	0.069	1.00	2.5
MRSA2	20	25	18	7	1.71	4.57	0.059	1.00	2.6
MRSA3	24	25	18	10	1.96	5.74	0.051	1.00	2.7
MRSA4	30	25	18	15	2.31	7.58	0.044	1.00	2.9
ELF1	16	32	24	5	1.44	2.13	0.069	0.75	1.4
ELF2	20	32	24	7	1.71	2.98	0.059	1.00	1.5
ELF3	24	32	24	10	1.96	3.78	0.051	1.20	1.6
ELF4	30	32	24	15	2.31	5.03	0.044	1.40	1.7

Nonlinear Analysis of Special Reinforced Concrete Core-Wall Archetypes

Collapse risk was determined per the FEMA P-695 Methodology using the OpenSees platform and the Collapse Analysis Toolkit (Appendix E). Archetype buildings were modeled using nonlinear frame elements and linear shear springs to model concrete walls and an essentially zero-stiffness P-delta column to simulate base moment demand because of P-delta effects from gravity load. Displacement-based frame elements with nonlinear fiber-type cross-section models were used to simulate flexural and axial response. Four frame elements were used for each story at the base of the wall to provide accurate simulation of flexural response; one frame element per story was used elsewhere. Fiber-type cross-section models employed typical material response models; however, to limit mesh sensitivity, the typical stress-strain response models for concrete and steel were modified to account for the element length associated with each fiber section. One linear elastic shear spring was used per story to simulate shear deformation; gross-section shear stiffness was assumed. A uniformly distributed dead load was applied to the wall at each story; total axial load at the base of the wall was $0.1 f_c A_w$. The remainder of the applied gravity load (190 psf) was applied to the P-delta column. Hysteretic damping was supplemented by Raleigh damping of 2.5% in the first and third modes.

Previous research has shown that the above modeling procedure simulates the strength and stiffness well but overestimates drift capacity of wall specimens tested in the laboratory. Thus, to enable accurate assessment of collapse risk, the following empirical non-simulated collapse criteria were employed:

- Engineering judgment and other factors detailed in NIST GCR 10-917-8 suggest the use of 5% story drift as a limit. Drifts in excess of 5% were considered to result in excessive damage to the gravity system, causing direct loss of gravity load carrying capacity. Drifts in excess of 5% were also considered to result in a high likelihood of loss of lateral load carrying capacity for the wall, which in combination with P-delta effects would result in collapse.
- Maximum compressive strain of concrete is taken in excess of negative 0.01 in./in. Pugh (2012) found that walls exhibited initiation of strength loss when compressive strains in the extreme concrete fibers exceeded 0.01 inch magnitude. Again, initiation of loss lateral load carrying capacity in the wall was considered to represent the onset of collapse as P-delta effects could potentially cause collapse of the building if the wall does not have sufficient lateral strength and stiffness to resist overturning due to P-delta effects.

Additionally, as recent research indicates, the drift capacity of walls responding in flexure diminishes significantly with increasing shear demand (Birely, 2012; NIST, 2010), collapse risk was also determined using the above non-simulated collapse criteria as well as the linear model linking drift capacity with shear demand-capacity

ratio proposed by Birely (2012). Additional information about non-simulated collapse criteria is provided in Appendix D.

The FEMA P-695 Methodology was used to assess the collapse risk for the special reinforced concrete core-wall archetypes. Table 3-2 and Table 3-3 summarize the results of the analyses without and with consideration of the shear-based non-simulated collapse criterion. Data in these tables include the quantities used to determine collapse risk. The collapse criteria columns indicate the percentage of ground motion records for which collapse was determined by that particular criterion. The criteria are: (1) simulated collapse (Sim.); (2) concrete crushing as determined by a concrete compressive strain in excess of negative 0.01 in/in (Conc. Strain); (3) story drift in excess of 5% (Story Drift); and (4) the shear-based drift capacity model (Shear-Based). The latter two are non-simulated collapse criteria. The mean base shear demand-capacity ratio at the collapse intensity level is also indicated.

Results are presented without (Table 3-2) and with (Table 3-3) consideration of the shear-based collapse criterion because it is not known if the low Collapse Margin Ratio (*CMR*) values computed using this non-simulated collapse criterion are representative of long-period buildings in general or long-period walled buildings. When the shear-based criterion is considered, the low *CMR* values (and high collapse probabilities) are due to the following:

- The development of a flexural hinge at the base of the wall (which limits the moment at the base of the wall but not the shear demand at the base of the wall or the demands elsewhere up the height of the wall), the concentration of nonlinearity at the base of the wall, and higher-mode response all result in a drop in the effective height at which the seismic lateral loads act and an increase in the base shear demand.
- Flexural and shear demands interact at the base of the wall to increase principal compressive stress demand in the compression zone of the wall and reduce drift capacity.

While a few studies suggest that the amplification of base shear demands is not unique to core-wall systems (Haselton et al., 2011), it is not known if amplification of base shear occurs in all seismic force-resisting systems. Additionally, systems with core-walls are considered to be somewhat unique because a single element resists seismic shear and moment demand and these response modes interact to reduce deformation capacity even in code compliant elements. Moment frames could be considered to be somewhat similar to core walls in that seismic demands are transferred to the foundation through columns. However, in columns seismic demands are resisted through shear load, moment, and axial load and experimental data show that drift capacity of code-compliant columns is less sensitive to shear demand.

Table 3-2 Performance Evaluation Results without the Shear-Based Collapse Criterion

ID	No. of Stories	From Pushover		Collapse Probability Quantities			Criterion Determining Collapse			Mean Base Shear D/C Ratio at Collapse
		μ_T	*SSF*	*CMR*	*ACMR*	*Collapse Prob.*	Sim.	Conc. Strain	Story Drift	
MRSA1	16	12	1.6	1.81	2.87	2%	0%	35%	65%	1.40
MRSA2	20	10	1.6	1.58	2.55	4%	0%	0%	100%	1.56
MRSA3	24	8	1.6	1.61	2.59	4%	0%	0%	100%	1.69
MRSA4	30	7	1.6	1.59	2.48	4%	0%	0%	100%	1.98
ELF1	16	21	1.6	2.02	3.21	1%	0%	47%	53%	1.21
ELF2	20	16	1.6	1.98	3.19	1%	0%	7%	93%	1.47
ELF3	24	14	1.6	1.89	3.05	2%	0%	0%	100%	1.63
ELF4	30	11	1.6	2.21	3.55	1%	4%	0%	96%	2.17

Table 3-3 Performance Evaluation Results with the Shear-Based Collapse Criterion

ID	No. of Stories	From Pushover		Collapse Probability Quantities			Criterion Determining Collapse				Mean Base Shear D/C Ratio at Collapse
		μ_T	*SSF*	*CMR*	*ACMR*	*Collapse Prob.*	Sim.	Conc. Strain	Story Drift	Shear-Based	
MRSA1	16	12	1.6	1.00	1.59	19%	0%	0%	0%	100%	1.03
MRSA2	20	10	1.6	0.60	0.97	52%	0%	0%	0%	100%	1.00
MRSA3	24	8	1.6	0.61	0.98	52%	0%	0%	0%	100%	1.12
MRSA4	30	7	1.6	0.59	0.92	56%	0%	0%	0%	100%	1.23
ELF1	16	21	1.6	1.00	1.59	19%	0%	0%	0%	100%	0.98
ELF2	20	16	1.6	0.79	1.28	32%	0%	0%	0%	100%	0.98
ELF3	24	14	1.6	0.80	1.30	31%	0%	0%	0%	100%	1.10
ELF4	30	11	1.6	0.59	0.95	54%	0%	0%	0%	100%	1.31

The data in Table 3-2 show that if the shear-based non-simulated collapse criterion is not used, shear demand-capacity ratios at the collapse intensity are significantly larger than 1.0; while, if the shear-based criterion is employed (Table 3-3), shear demand-capacity ratios at the collapse intensity are approximately 1.0. These data suggest that high collapse probabilities, similar to those listed in Table 3-3, would be computed if the shear-based non-simulated collapse criterion was simplified from the linear model by Birely (2012) that links drift capacity with shear demand-capacity ratio to a pure strength-based model in which collapse is defined to occur when the shear demand-capacity ratio exceeds 1.0.

Calculation of the Base Shear Coefficient Required to Achieve Uniform Collapse Risk

Using the data in Table 3-1, Table 3-2, and Table 3-3, and data from previous studies, the base shear coefficient required to achieve a uniform collapse probability under the MCE_R of 10%, $C_{s10\%}$, was estimated using Equation 3-6:

$$Cs_{10\%} = V / W \left(\frac{ACMR_{10\%}}{ACMR} \right) \tag{3-6}$$

where:

V/W = normalized base shear (C_s coefficient) used for archetype design,

$ACMR$ = adjusted collapse margin ratio of archetype model of interest, and

$ACMR_{10\%}$ = acceptable value of $ACMR$ for the system of interest corresponding to a collapse probability of 10%.

Equation 3-6 is a derivative of Equation 2-1, and like Equation 2-1 provides a good estimate of the parameter of interest, $C_{s10\%}$, for values of the $ACMR$ approximately equal to 10% and may provide a poor estimate for significantly smaller or larger values of the $ACMR$, as is the case when the shear-based collapse criterion is considered. Figure 3-5 through Figure 3-8 show $C_{s10\%}$ for the complete data set (archetypes from previous studies and the core-wall archetypes); long-period wall data are identified as "Special RCSW Long Period" and shown in the figures using blue x's. Figure 3-5 and Figure 3-6 show $C_{s10\%}$ plotted versus the design period and versus the first-mode period determined from RSA for the case of collapse probability determined without the use of the shear-based collapse criterion. Figure 3-7 and Figure 3-8 show similar data for the case of collapse probability determined with the use of the shear-based collapse criterion.

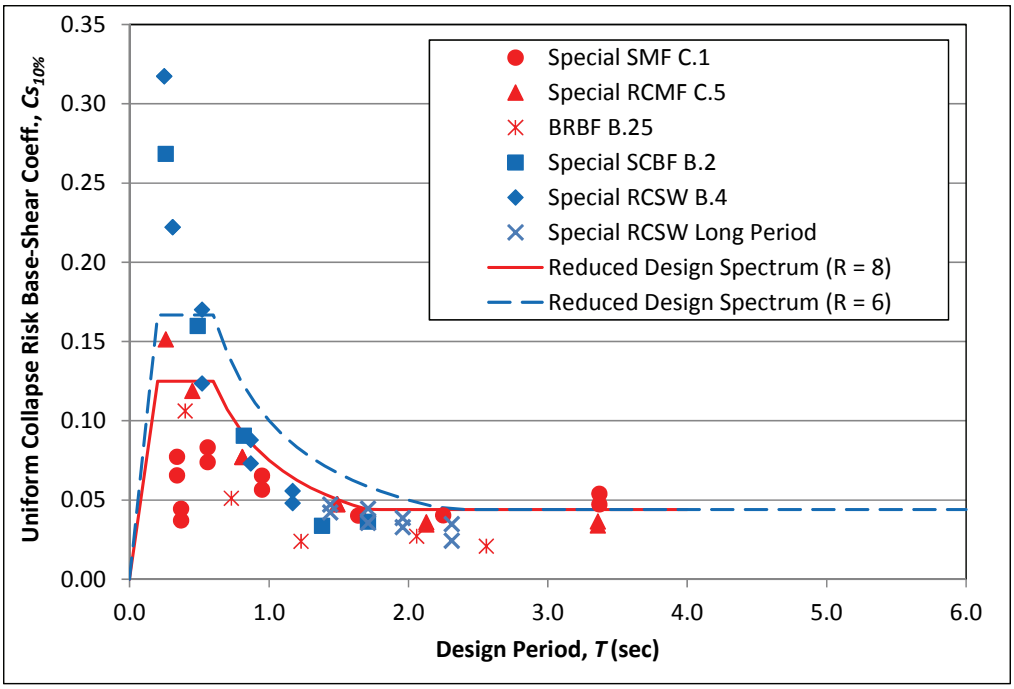

Figure 3-5 Base shear coefficient required to achieve uniform collapse risk of 10%, $C_{s10\%}$, versus design period, T, without shear-based collapse criterion used for determination of wall collapse.

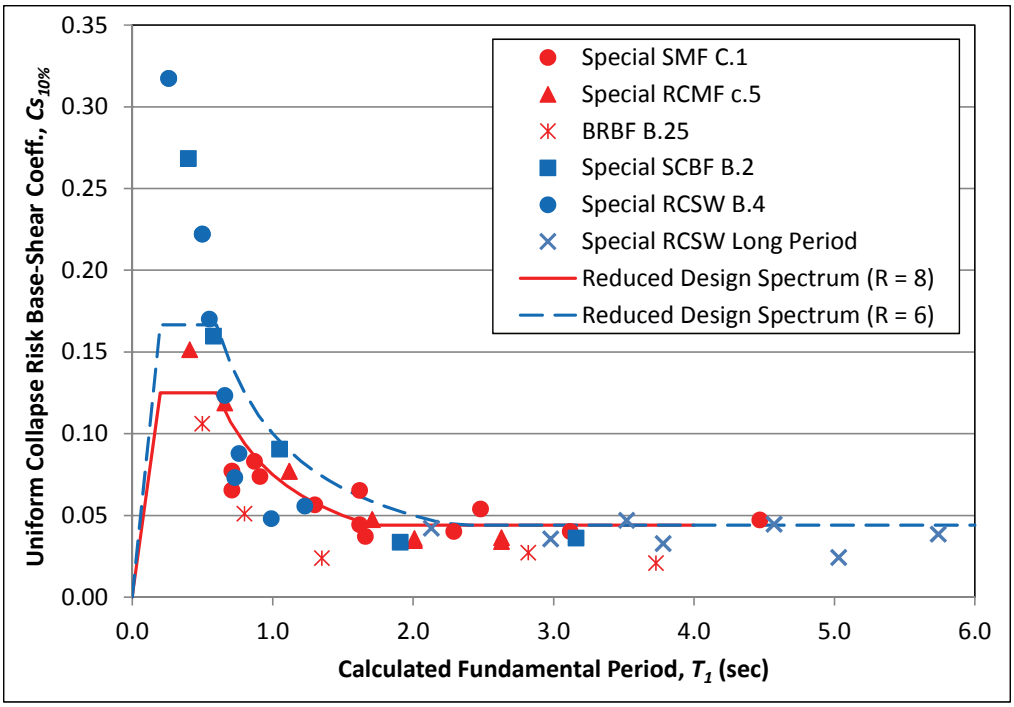

Figure 3-6 Base shear coefficient required to achieve uniform collapse risk of 10%, $C_{s10\%}$, versus calculated fundamental period from RSA, T_1, without shear-based collapse criterion used for determination of wall collapse.

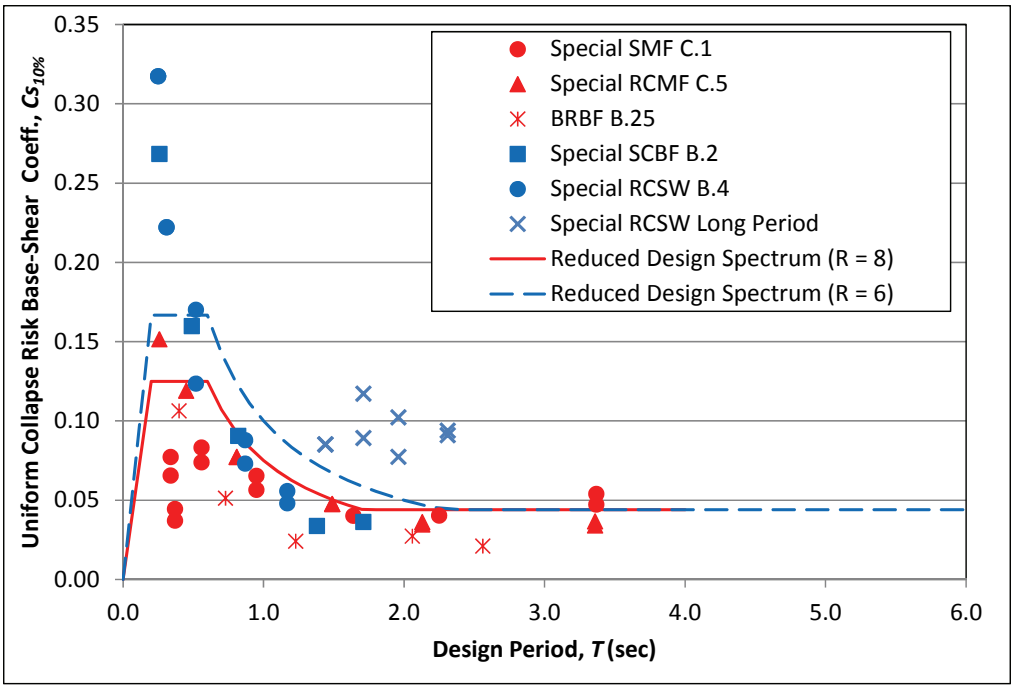

Figure 3-7 Base shear coefficient required to achieve uniform collapse risk of 10%, $C_{s10\%}$, versus design period, T, with shear-based collapse criterion used for determination of wall collapse.

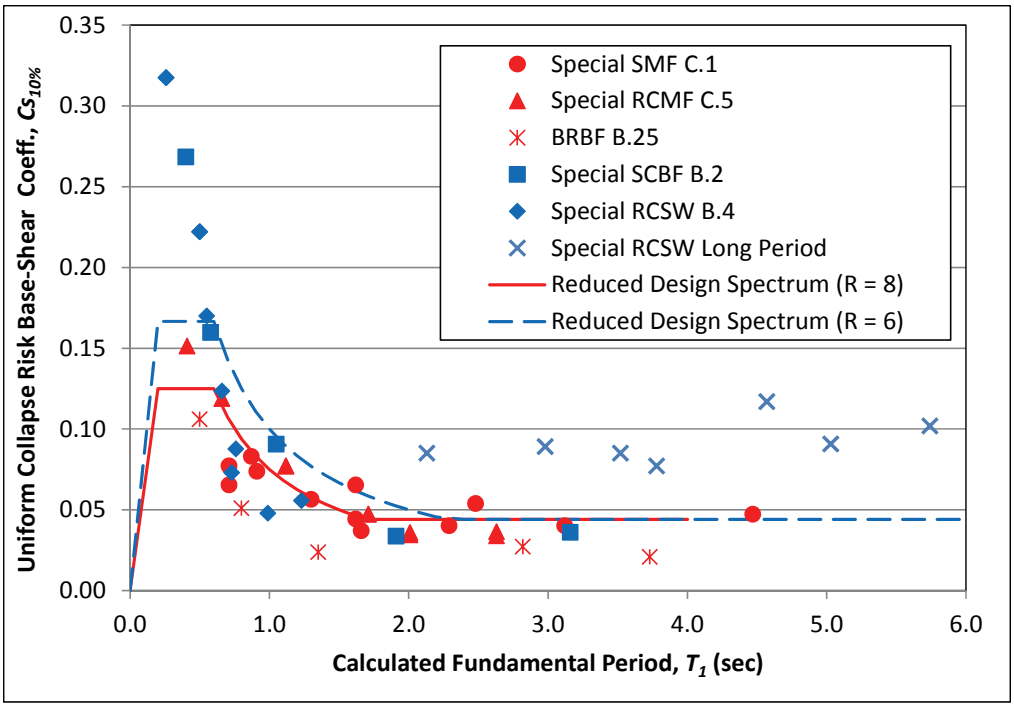

Figure 3-8 Base shear coefficient required to achieve uniform collapse risk of 10%, $C_{s10\%}$, versus calculated fundamental period from RSA, T_1, with shear-based collapse criterion used for determination of wall collapse.

3.3.2 Summary of Key Findings

The study of the collapse risk of long-period core-wall buildings indicates that revisions in design codes and the design process are required for these systems. Following are key findings and observations addressing seismic design and performance of long-period concrete walled buildings:

- The results of nonlinear analyses indicate that under design-level earthquake loading, base shear demands will greatly exceed those computed using either the ELF or RSA design methods. This amplification of the base shear demand is attributed to development of a flexural "hinge" at the base of the wall and higher-mode response; both of these mechanisms result in the base shear acting at a lower effective height. While the base moment is limited by flexural yielding of the wall, reduction of the effective height at which seismic lateral forces act results in an increased base shear demand.
- The results of nonlinear analyses indicate that walls in tall buildings typically develop a second flexural hinge above the base of the wall. If the vertical moment demand distribution determined using either the ELF or RSA design method is used to reduce the wall flexural capacity up the height of the wall, deformation demands at the location of this section hinge may be excessive and result in unacceptable performance.
- The data in Table 3-3 indicate that if the effect of shear demand-capacity on drift capacity is considered, long-period walls can have unacceptably high collapse probabilities under the MCE_R. These data apply to walls designed using linear analysis methods to achieve low shear stress demand at the base, to develop the maximum allowable (per ACI 318-08) cross-sectional shear strength at the base and to minimize flexural yielding and shear demand-capacity above the base.

On the basis of these general findings, the following are recommended: (1) additional research be done to assess amplification of shear demand in walls with shorter heights and in coupled walls; (2) additional research be done to determine strength and detailing requirements to ensure acceptable performance of flexural hinges located above the base of the wall; and (3) design recommendations for reduced shear stress demand in walls be developed and incorporated into design codes.

This investigation also resulted in observations and findings applicable to the FEMA P-695 Methodology. Primarily, scaling of earthquake ground motions based on the spectral acceleration at the design period of the structure resulted in essentially arbitrary scaling of the motions with respect to the design spectrum at shorter periods. Because higher modes of long-period systems can contribute significantly to the base shear demand (more than 60% for long-period walls), scaling ground motions to the design period may introduce significant uncertainty and bias in the computed collapse risk. Computation of the *CMR* using ground motions scaled to the

second mode period resulted in greatly reduced collapse risk. Further, pushover analyses using a load distribution determined by the first-mode shape may not be appropriate for long-period systems in which higher modes significantly affect response.

On the basis of these observations and findings, it is recommended that additional work be done to enhance the FEMA P-695 Methodology to provide better assessment of the collapse risk of long-period systems.

3.3.3 Discussion of Results Pertinent to Reformulation of Seismic Design Parameters

Results of this study of tall special RC core-wall buildings and prior studies of tall special reinforced concrete and steel moment frame buildings suggest that acceptable collapse risk can be achieved for long-period systems of any height designed using an appropriate value of minimum base shear. This conclusion presumes that collapse probabilities for long-period reinforced concrete wall buildings computed without consideration of reduced drift capacity because of shear demand are representative of long-period buildings in general.

As discussed previously, the shear-based collapse criterion for walls, in which the drift capacity of the wall is reduced as the shear demand-capacity ratio increases, is considered to be system specific. It is not known if issues similar to the amplification of shear demands and interaction of flexure-shear mechanisms for walls exist for other seismic force-resisting systems in the long-period range and could result in increased collapse probability for these systems. As such, in considering R factors and seismic demands for long-period systems in general, it is deemed appropriate to employ wall collapse probability data determined without consideration of the shear-based collapse criterion. These data combined with similar data for a few reinforced concrete and steel frames, as presented in Figure 3-5 and Figure 3-6, suggest that the current ASCE/SEI/SEI 7-10 requirements for determination of seismic demands, including the minimum base shear requirement but excluding limits on building height, result in acceptable collapse risks of less than 10% for long-period buildings.

Although the above data suggest that the desired collapse risk can be achieved using a minimum base shear demand in the long-period range and ignoring building height limits, the data are quite limited. The data in Figure 3-5 and Figure 3-6 are for structures designed for the maximum spectral acceleration intensity associated with SDC D; other design categories have not been considered. Additionally, the data in Figure 3-5 and Figure 3-6 include relatively few data points for reinforced concrete and steel frame buildings.

3.3.4 Conclusions

The data presented in Figure 3-5 and Figure 3-6, suggest that acceptable collapse risk can be achieved for long-period systems using a minimum base shear requirement. However, given the relatively small number of data points available for long-period systems, the specific form of a minimum base shear equation cannot be suggested at this time. It is expected that the form of a minimum base shear equation would depend on either the spectral acceleration intensity in the short period range, as defined by S_{MS}, or in the long period range, as defined by S_{M1} and, possibly, the strength reduction factor, R_M.

Thus, the equation defining the minimum base shear coefficient, $C_{sM} = V/W$, could take one of the following forms:

$$\begin{aligned} C_{sM} &\geq \alpha S_{MS} I_e \\ C_{sM} &\geq \alpha S_{M1} I_e \\ C_{sM} &\geq \alpha S_{M1} / (R_M / I_e) \\ C_{sM} &\geq \alpha S_{MS} / (R_M / I_e) \end{aligned} \tag{3-7}$$

3.3.5 Recommendations for Future Studies

The results of this and previous studies suggest that an acceptable collapse risk can be achieved for long-period systems if seismic demands are determined using a minimum base shear requirement. However, a more extensive data set is required to verify this. Thus, studies such as the one described above for special reinforced concrete core-walls must be conducted for several additional commonly employed systems, such as reinforced concrete and steel moment frames and steel braced frames, and for systems designed for construction in other Seismic Design Categories.

In designing structures as part of the additional study, efforts should be made to introduce a similar level of conservatism and clearly establish the design methodology employed. The results of this study suggest that to achieve acceptable collapse risk, long-period reinforced concrete core-wall buildings must be designed to achieve extremely low shear stress demands under design-level loading. It is expected that similar requirements may exist for other SFRS; for example, design of reinforced concrete and steel moment frames to achieve acceptable collapse risk may require column-to-beam strength ratios that exceed current code requirements.

Chapter 4
Conceptual Reformulation of Seismic Design Parameters

This chapter presents a conceptual reformulation of seismic design parameters and related criteria for possible future use in seismic codes and resource documents. Proposed reformulation of parameters and criteria is primarily conceptual, drawing from the results of prior collapse evaluation studies (summarized in Chapter 2) and the findings of problem-focused studies (summarized in Chapter 3) for specific recommendations of certain reformulated criteria.

4.1 Reformulation Objectives

The primary objective of reformulating seismic design parameters and related criteria is to improve the formulation and values of seismic design parameters to better and more uniformly achieve the collapse safety objective of current seismic codes, such as ASCE/SEI 7-10, *Minimum Design Loads for Buildings and Other Structures* (ASCE, 2010). That is, structures designed with improved values of design parameters should more uniformly achieve the safety objective of 10% probability of collapse given Maximum Considered Earthquake (MCE_R) ground motions occur.

The secondary objective of reformulation is to extend the risk-based framework of the FEMA P-695 Methodology used for designing buildings to meet life-safety (collapse) performance objectives to other seismic risk categories, namely protection of facility function and avoidance of economic loss. Extended risk categories apply to both structural and nonstructural systems in terms of overall performance objectives.

4.2 Reformulation Approach and Analytical Studies

This section summarizes the approach followed for reformulation of selected seismic design parameters and design criteria.

At the beginning of the project, an initial investigation of the results from prior studies based on the FEMA P-695 Methodology was performed to better understand issues, identify topics for detailed investigation, and develop draft reformulation material. A summary of prior collapse evaluation studies is presented in Chapter 2.

Next, a draft reformulation, composed of both conceptual reformulation topics which did not require analytical study and topics requiring specific areas of investigation by

problem-focused studies, was developed. Problem-focused studies (summarized in Chapter 3) were performed to investigate each study topic in regards to the formulation of seismic design parameters.

The draft reformulation and results of problem-focused studies were presented and discussed at a project workshop with invited experts, including participants from seismic code committees and industry. The draft reformulation was updated to incorporate findings of problem-focused studies (e.g., revised methods for design of long-period systems) and input received from workshop participants. Although complex terms and concepts are used in this report as required to develop, explain, and clarify underlying concepts, the final reformulation is kept as simple as possible for potential use in seismic codes and resource documents.

4.3 Reformulation Scope

The scope of the reformulation includes both the conceptual topics and the topics related to short-period performance, overstrength, and long-period performance listed in Table 1-1. In addition, two "big picture" topics were also investigated. This section provides a brief introduction of the conceptual and big picture topics. The reformulation utilizing all topics is given in the next section.

4.3.1 Conceptual Topics from Table 1-1

Basis for *R* Factors. Changing the basis for the *R* factors from design ground motions to MCE_R ground motions, would eliminate the 2/3 factor. The new factor, labeled R_M, can be directly applied to spectral response acceleration of MCE_R ground motions.

This reformulation topic is strictly conceptual, but would require revising a number of provisions throughout ASCE/SEI 7-10 to be compatible with the new definition of R_M, including the seismic design criteria of Chapter 11 and the site-specific seismic criteria of Chapter 21.

Components of the R_M Factor. The R_M factor can be separated conceptually into a ductility component, R_{Md}, and an overstrength component, R_O, where $R_M = R_{Md}R_O$.

Investigation of results from prior FEMA P-695 collapse evaluations shows that the *R* factor can be conceptually separated into ductility and overstrength components. Figure 2-5 illustrates a method of selecting reasonable "lower-bound" values of the overstrength component, R_O, when collapse has been evaluated for a sufficiently large number of archetypes of the system of interest.

Although challenging, the primary issue is not the mechanics of separating the R_M factor into components, but rather how these components should be used in the design process. Prior FEMA P-695 studies have shown that large variability in the

overstrength of different archetypes of the same system make it difficult to assign a single value of overstrength to a given system. Studies of alternative approaches to system overstrength (Section 3.2) suggest that the R_O factor (Ω_O factor) may not be the best approach to capacity design. If so, then the components, R_O and R_{Md}, would still be necessary to develop appropriate values of the R_M factor, but would not be used directly by practitioners for design (i.e., only the R_M factor would appear in Table 12.2-1 of ASCE/SEI 7-10).

Lower Limit for *R* Factor Values. There is no lower limit on the values of the *R* factor and the values can be as small as required to meet FEMA P-695 collapse performance criteria. Prior studies have not indicated a need for very small values of the *R* factor to meet FEMA P-695 criteria. Nonetheless, values of *R* less than 1.0 are possible and values of $R = 0.67$ ($R_M = 1.0$) are considered.

Simplification of the R_M Factor Table. When developing a set of "standardized" discrete values of the R_M factor similar to Table 12.2-1 of ASCE/SEI 7-10, it is necessary to balance minimizing the number of different values of the R_M factor with maintaining a broad range of possible values (e.g., $1.0 \le R_M \le 15$). The key issue is determining an appropriate spacing of a limited number of discrete values from the smallest value of R_M to the largest value of R_M.

A number of other changes are possible to simplify Table 12.2-1. For example, based on FEMA P-695 collapse performance criteria, which define the deflection amplification factor, C_d, in terms of *R* (and system damping), there is no need for a separate set of values of the MCE_R-based deflection amplification factor, C_{dM}. Values of the C_{dM} parameter can be specified by a formula in terms of the value of R_M factor (and damping, if other than 5% of critical, as described in the next section).

Other possible changes to Table 12.2-1 include deleting the system overstrength factor, Ω_O, in lieu of new design requirements that focus on capacity design of specific elements of the seismic force-resisting system (i.e., as suggested by the findings of the overstrength studies presented in Section 3.2), and eliminating or greatly modifying current limits on height and system usage. In concept, the FEMA P-695 Methodology could be used to provide a rational basis to either eliminate or improve current, judgmental limits on, for example, building height.

Damping Level of Design Response Spectrum. The definition of the design response spectrum and related spectral response acceleration parameters can be generalized to include system-dependent values of damping other than the 5% value used in ASCE/SEI 7-10.

The FEMA P-695 Methodology defines C_d as equal to R/B_I, where the value of B_I depends on system damping, β_I. Since ASCE/SEI 7-10 already defines B_I and β_I, and specifies values of B_I given the value of β_I, the only outstanding issue for the use of

these terms is the need to determine an appropriate value of β_I for each system. For most systems, the current implicit assumption of β_I = 5% damping would likely still be appropriate (for which B_I = 1.0), so only a limited number of systems would need to be addressed (i.e., need not be a new column of system damping terms in Table 12.2-1 of ASCE/SEI 7-10).

4.3.2 Big Picture Topics

Multi-Period Design Response Spectrum. A design response spectrum with a multi-period shape can be developed and related definitions of spectral response acceleration parameters can be revised.

Advances in earth science and web-based sources of ground motion design parameters have made it possible to specify site-specific ground motions at multiple response periods that define the design response spectrum more accurately than the traditional two-domain shape of the design response spectrum of Figure 11.4-1 of ASCE/SEI 7-10. It should be investigated whether a future change to a multi-period design response spectrum would affect reformulation of the *R* factor and others, and if so, how reformulation would be affected.

Performance Objectives (other than those addressed by FEMA P-695). Rationally based design requirements that address performance objectives related to functional and economic risk and the enhanced performance objectives of Risk Category III and Risk Category IV structures can be developed. Although life-safety risk is the primary concern of the seismic codes, economic and functional risks are also very important, particularly for critical facilities.

The FEMA P-695 Methodology determines appropriate values of the *R* factor, and other criteria for design of the seismic force-resisting system of interest, on the basis of collapse performance and an acceptable probability of collapse of 10% given MCE_R ground motions. The 10% collapse objective is deemed appropriate for Risk Category II structures, but might be too liberal for Risk Category III and Risk Category IV structures (and too conservative for Risk Category I structures). The issue here is the value of seismic importance factor, I_e (Table 1.5-2, ASCE/SEI 7-10).

Adequate collapse performance of the seismic force-resisting system alone does not ensure adequate functional or economic performance of the structural system or adequate performance of nonstructural systems. In fact, nonstructural systems sensitive to acceleration demand are, in general, more susceptible to damage (and loss of function) in structures that are made stiffer and stronger to resist collapse. So, there may be competing interests in terms of meeting both structural and nonstructural performance objectives. It is important to broadly consider how all structural and nonstructural performance objectives (life-safety, functional, and

economic) could and should be addressed in a consistent manner with the concepts and methods of FEMA P-695 for collapse evaluation.

4.4 Reformulation of Seismic Performance Factors and Related Criteria

This section provides specific recommendations for reformulation of seismic performance factors, other parameters, and related design criteria.

4.4.1 Maximum Considered Earthquake Basis for the R_M Factor

When the *R* factor is reformulated in terms of MCE_R ground motions (and labeled as R_M to distinguish this term from its predecessor), MCE_R ground motions and seismic coefficients, S_{MS} and S_{M1}, should be substituted for design earthquake ground motions and seismic coefficients, S_{DS} and S_{D1}, in all cases, throughout ASCE/SEI 7-10. The intent of this proposed change is to eliminate the 2/3 factor of Equation 11.4-3 and Equation 11.4-4 of ASCE/SEI 7-10 and base designs directly on MCE_R ground motions. Use of the 2/3 factor obscures the performance objective for life-safety design which is an acceptably small (10 %) probability of collapse for MCE_R ground motions.

Values of the new R_M factor for existing seismic force-resisting systems of Table 12.2-1 of ASCE/SEI 7-10 should be determined by FEMA P-695 collapse evaluations. In general, values of the R_M factor are expected to be about 50% greater than current values of the *R* factor:

$$R_M \approx 1.5R \tag{4-1}$$

where:

R_M = MCE_R-based response modification coefficient (example values given in Table 4-1), and

R = response modification coefficient as given in Table 12.2-1 of ASCE/SEI 7-10.

The net effect of this reformulation on building design should be small, except for those systems found by FEMA P-695 evaluation to have collapse performance significantly different from the safety objective (i.e., 10% given MCE_R ground motions).

4.4.2 Components of the R_M Factor

The R_M factor should be characterized as the product of two components, a ductility (and damping) factor, R_{Md}, and an overstrength factor, R_O, as follows:

$$R_M = R_{Md} R_O \tag{4-2}$$

where:

R_M = MCE_R-based response modification factor,

R_{Md} = component of R_M related to total system ductility and damping, and

R_O = component of R_M related to system overstrength, representing a lower-bound on the overstrength of the system of interest.

The ductility component, R_{Md}, is not proposed for direct use in design, but is a useful parameter when interpreting the results of FEMA P-695 collapse evaluations. Similarly, the overstrength component, R_O, is also not proposed for use in design, but provides a measure of the lower-bound amount of overstrength assumed to be contained in the specified value of the R_M factor of the system of interest. Certain design requirements directly related to the value R_M might be relaxed for structures shown to have a substantially larger amount of overstrength than that of the overstrength component, R_O.

Table 4-1 provides hypothetical values of the R_M, R_{Md}, and R_O factors for five seismic force-resisting systems. Hypothetical values are selected from the proposed sets of standardized values of R_M, R_{Md}, and R_O factors, described later in this section, and are based very approximately on the "uniform risk" processing of prior study results, as described in Section 2.3.

Table 4-1 Hypothetical Values of R_M, Corresponding Example Values of Ductility Component, R_{Md}, and Corresponding Example Values of Overstrength Component, R_O

	Response Modification Coefficient and Components		
Seismic Force-Resisting System	R_M	R_{Md}	R_O
A. BEARING WALL SYSTEMS			
A.15 Light-frame (wood) walls sheathed with wood structural panels rated for shear resistance	9.5	4.7	2.0
B. BUILDING FRAME SYSTEMS			
B.2 Special steel concentrically braced frames	12	9.5	1.25
B.4 Special reinforced concrete shear walls	12	7.5	1.6
C. MOMENT-RESISTING FRAME SYSTEMS			
C.1 Special steel moment frames	12	4.7	2.5
C.5 Special reinforced concrete moment frames	12	7.5	1.6

The hypothetical values of R_M given in Table 4-1 are the product of example values of R_O and R_{Md}. Example values of R_O were developed from plots of $R_{UR10\%}$ versus $R_{d10\%}$ data shown in Figure 2-5, represent lower-bound values of overstrength of the

system of interest, recognizing that substantially higher values of overstrength could be expected for certain system configurations or design criteria. For example, FEMA P-695 studies found that light-frame wood shear walls (A.15) with high aspect ratios have substantially larger amounts of overstrength than walls with low aspect ratios as a result of design requirements intended to achieve parity in lateral displacement of systems with high- and low-aspect ratio walls. In this case, it would be inappropriate to use the additional overstrength of high-aspect walls to define a larger value of the R_M factor, because larger values of the R_M factor would defeat the purpose of achieving parity in the displacement of systems with low- and high-aspect-ratio walls.

Example values of R_{Md} were estimated as 1.5 times the typical value of $R_{d10\%}$ (data plotted in Figure 2-4) for archetypes with representative periods in the range of about 0.5 seconds to 2.0 seconds. Using data in this period range presumes that potentially inferior collapse performance of structures with very long or very short periods is either ignored or precluded by other design criteria, such as minimum base shear criteria. Even for a limited range of periods, considerable judgment was required to determine an appropriate value of R_{Md} from the scatter in the example data. This is to be expected and simply reinforces the importance of the FEMA P-695 requirement for peer review by a team of knowledgeable experts.

The hypothetical values of R_M, R_{Md}, and R_O shown in Table 4-1 are based on limited number of collapse evaluations (i.e., incomplete sets of archetype models). Actual values of R_M, R_{Md}, and R_O and other reformulated factors should be based on FEMA P-695 results from a sufficiently large number of collapse performance evaluations of each system. A larger number of collapse evaluations would be expected to improve the reliability of the trends in the values of $R_{UR10\%}$ and $R_{d10\%}$ but not eliminate the need for judgment in the selection of R_{Md} and R_O for the system of interest.

4.4.3 Simplified R_M Factor Table

Reformulating the R_M factor as the product of the R_{Md} and R_O components follows the traditional concept of defining R_M by a limited set of discrete values, but in a more logical manner than the current values in ASCE/SEI 7-10. Two premises for redefining discrete values of the R_M (and R_{Md} and R_O) factors are as follows:

- A sufficient number of discrete values of the R_M factor should be included to enable differences in system collapse performance to be distinguished, but not more than about a dozen or so values, since finer resolution is unnecessary and would imply a precision unwarranted by either the design methods or FEMA P-695 evaluations.

- The discrete values of the R_M factor should increase as a uniform multiple of the previous value, because the R_M factor is used in the denominator of the base shear equation to reduce response spectral acceleration.

On the basis of the above premises, ten discrete values of the R_M factor per decade are proposed to be spaced logarithmically as follows:

$$R_{M,\ i+1} = \left(10^{0.1}\right) R_{M,\ i} \tag{4-3a}$$

Since the R_M factor is the product of the ductility and overstrength components, discrete values of the R_{Md} and R_O factors are proposed to be spaced logarithmically as follows:

$$R_{Md,\ i+1} = \left(10^{0.1}\right) R_{Md,\ i} \tag{4-3b}$$

$$R_{O,\ i+1} = \left(10^{0.1}\right) R_{O,\ i} \tag{4-3c}$$

Implementing the above equations requires assuming a range of values for the R_M factor and the components thereof. R_M (and R_{Md}) is assumed to range from $R_{M,1} = 0.95$ (rounded to 1.0) to $R_{M,11} = 15$, and R_O is assumed to range from $R_{O,1} = 1.0$ to $R_{O,7} = 4.0$. Table 4-2 implements these formulas with some rounding, showing that 13 discrete values of the R_M factor are required for all possible combinations of the ductility factor, R_{Md}, and overstrength factor, R_O.

Table 4-2 Discrete Values of R_M Factor as the Product of Discrete Values of R_{Md} and R_O Factors Based on Ten Increments per Decade Spaced Logarithmically

R_{Md} Factor	R_O Factor						
	1.0	*1.25*	*1.6*	*2.0*	*2.5*	*3.1*	*4.0*
1.0	1.0	1.2	1.5	2.0	2.5	3.0	3.8
1.2	1.2	1.5	2.0	2.5	3.0	3.8	4.7
1.5	1.5	2.0	2.5	3.0	3.8	4.7	6.0
2.0	2.0	2.5	3.0	3.8	4.7	6.0	7.5
2.5	2.5	3.0	3.8	4.7	6.0	7.5	9.5
3.0	3.0	3.8	4.7	6.0	7.5	9.5	12
3.8	3.8	4.7	6.0	7.5	9.5	12	15
4.7	4.7	6.0	7.5	9.5	12	15	
6.0	6.0	7.5	9.5	12	15		
7.5	7.5	9.5	12	15			
9.5	9.5	12	15				
12	12	15					
15	15						

Recognizing that a smaller number of less closely-spaced values of the R_M factor may be desirable, five discrete values of the R_M factor per decade are alternatively proposed to be spaced logarithmically as follows:

$$R_{M,\,i+1} = \left(10^{0.2}\right) R_{M,i} \tag{4-4}$$

Following logic similar to that underlying Table 4-2, Table 4-3 implements Equation 4-4 with some rounding, showing that as few as 7 discrete values of the R_M factor are required for all possible combinations of the ductility factor, R_{Md}, and overstrength factor, R_O.

The discrete values of the R_M factor given in Table 4-2 represent the finest spacing (and largest number of different values of R_M) that can be reliably supported by the FEMA P-695 Methodology. That is, there would be no practical difference in the collapse performance of systems designed using a value the R_M factor selected from a larger set of discrete values. Conversely, the set of discrete values of the R_M factor given in Table 4-3 represent the crudest spacing (minimum number of different values) that could be used without undue loss of accuracy.

Table 4-3 Discrete Values of R_M Factor as the Product of Discrete Values of R_{Md} and R_O Factors Based on Five Increments per Decade Spaced Logarithmically

R_{Md} Factor	R_O Factor			
	1.0	*1.5*	*2.5*	*4*
1.0	1.0	1.5	2.5	4
1.5	1.5	2.5	4	6
2.5	2.5	4	6	10
4	4	6	10	15
6	6	10	15	
10	10	15		
15	15			

4.4.4 Minimum Value of the Base Shear Coefficient, C_{sM}

Reformulation of the R_M factor, as described above, will rely on new lower-bound limits of the base shear coefficient, C_{sM}, to achieve the collapse performance objective for long-period systems (i.e., systems with periods of about 2 seconds or greater).

The study of long-period systems found that limiting base shear coefficient values to greater than 0.04W to 0.05W would be sufficient to affect adequate collapse performance of certain long-period systems designed with high seismic (SDC D) loads. Accordingly, a new minimum base shear formula (or formulas), based on

either short-period or 1-second MCE_R response and possibly incorporating the response modification factor, is proposed. Study of additional long-period systems is required to define the specific form and values of the new minimum base shear formula (or formulas). Subject to additional study, the new minimum base shear criteria are proposed for design of all long-period systems in lieu of current drift criteria (to achieve acceptable collapse performance).

4.4.5 Deflection Amplification Factor, C_{dM}

The deflection amplification factor, C_d, is proposed to be reformulated as follows:

$$C_{dM} = \frac{C_{dS} R_M}{B_I} \tag{4-4}$$

where:

C_{dM} = deflection amplification factor corresponding to MCE_R ground motions,

C_{dS} = short-period inelastic deflection amplification factor (see also Section 3.1 recommendations regarding the formulation of the C_{dS} factor),

R_M = MCE_R-based response modification coefficient,

B_I = damping reduction factor, as set forth in Table 18.6-1 of ASCE/SEI 7-10 for effective damping, β_I, and period, T, and

β_I = component of effective damping (including hysteretic energy dissipation) of the structure due to the inherent dissipation of energy by elements of the structure, at or just below the effective yield displacement of the seismic force-resisting system, Section 18.6.2.1 of ASCE/SEI 7-10.

Most seismic force-resisting systems are assumed to have a value of effective damping, $\beta_I = 5\%$ (of critical damping) for which the corresponding value of the damping factor is, $B_I = 1.0$. Rather than adding a column of damping factors to Table 12.2-1 of ASCE/SEI 7-10 (most of which would have the same value, $B_I = 1.0$), acceptable values of the damping factor should be specified by material or system type in a separate (smaller) table (see the subsequent section on system damping).

There are two important considerations in the proposed reformulation of the C_{dM} factor that affect a number of design criteria, including the determination of story drift (e.g., Section 12.8.6 of ASCE/SEI 7-10), the evaluation of P-delta effects (e.g., Section 12.8.7 of ASCE/SEI 7-10) and current limits on story drift and lateral deformation (e.g., Section 12.12 of ASCE/SEI 7-10). First, story drift and stability criteria, formerly evaluated for design earthquake ground motions, would now be evaluated for MCE_R ground motions (i.e., 1.5 times design ground motions). Second, current values of the C_d factor in ASCE/SEI 7-10 are typically only a fraction of the

corresponding R factor (e.g., $C_d = 5.5$ versus $R = 8$ for special steel moment frames). Thus, for most systems with nominal, 5% effective damping, reformulating the deflection amplification factor as C_{dM} with $B_I = 1.0$ and R_M will substantially increase story drift demand (e.g., by 1.5(8/5.5) = 2.2 for special steel moment frames). Hence, current story drift limits, stability criteria, and other deformation-related requirements (e.g., structural separations) would require significant revision for evaluating deflections corresponding to MCE_R ground motions.

The above discussion of deflection amplification applies to both long-period and short-period structures. Additional inelastic deflection of short-period structures (i.e., additional inelastic deflection beyond elastic deflection) is well known and is the likely contributor to relatively poor collapse performance of short-period archetypes observed in prior analytical studies (e.g., see Figure 2-1). Inelastic deflection amplification has been traditionally ignored in seismic codes, in part, because drift and stability criteria do not influence the design of short-period structures. The proposed reformulation of C_{dM} includes an additional, short-period, inelastic deflection amplification factor, C_{dS}, although it is not clear if this term is of practical significance.

4.4.6 Reformulation of the Overstrength Factor, Ω_O

The overstrength factor, Ω_O, is intended to represent a reasonable, upper-bound value of overstrength for capacity design of force-controlled components of the system of interest. This upper-bound value should not be confused with the lower-bound value of the overstrength, R_O, which is a component of the R_M factor of the system of interest.

FEMA P-695 requires system overstrength, Ω_O, to be based on the envelop of overstrength, Ω, values calculated for individual archetypes of the system of interest (not to exceed $\Omega_O = 3.0$). Prior studies have typically found system overstrength to vary greatly between different archetypes of the same system, with at least some archetypes found to have large values of overstrength, making the determination of the overstrength factor problematic.

Rather than perpetuate the use of a poorly defined and possibly overly conservative value of the system overstrength, it is proposed to eliminate this factor in lieu of a more focused, element-based approach anchored in reliability concepts (see Section 3.2 for details). Alternatively (or as an interim measure), values of overstrength, ranging from 1.5 to 3.0, could be specified in terms of their specific application, rather than as functions of the type of seismic force-resisting system (e.g., 1.5 for design of collectors and 3.0 for design of elements supporting discontinuous walls).

4.4.7 Drift Limits

The proposed reformulation of the R_M factor, including the new minimum base shear coefficient, C_{sM}, criteria, is assumed to preclude the need to design the seismic force-resisting system for drift to meet collapse objectives.

Drift limits are still necessary to achieve other risk objectives, including life-safety protection of nonstructural components (e.g., stairwells), to evaluate stability of elements supporting gravity loads, and to detail certain structural elements. In these cases, drift limits should correspond to deflections corresponding to MCE_R ground motions, and current drift and deformation requirements (e.g., Section 12.12 of ASCE/SEI 7-10) would require significant revision for evaluating deflections corresponding to MCE_R ground motions.

Additionally, new drift limits would be required for design of the structural system (and nonstructural components) to meet economic or functional risk objectives should reformulation explicitly embrace such objectives (see also Section 4.7 for discussion of economic and functional performance objectives).

4.4.8 Damping Level of Design Response Spectrum

The elastic design response spectrum of MCE_R ground motions is defined in terms of an assumed value of 5% damping (i.e., equivalent viscous damping is defined as 5% of critical damping). Although 5% is a reasonable value for fundamental mode of many systems considering also the effects of nonstructural components, actual damping, at or just below yield, is not the same for all structures (or modes of vibration). Systems that incorporate viscous dampers can have substantially larger amounts of damping at or just below the yield of the structure, as recognized by the design provisions of Chapter 18 of ASCE/SEI 7-10.

Conceptually, the design response spectrum (of elastic response) of MCE_R ground motions should be based on the effective damping level at or just below yield of the system of interest. That is, the appropriately damped design spectrum would accurately reflect peak response (e.g., peak displacement) of the fundamental mode of the system of interest (after adjustment for modal participation). If the system of interest could be accurately modeled as a single-degree-of-freedom (SDOF) system, then peak response could be read directly from the appropriately damped response spectrum.

While it is possible to reformulate design response spectra to have different levels of damping (and the U.S. Geological Survey could be asked to provide maps of MCE_R ground motions for different levels of damping), this would be an unnecessary complication of the design process, particularly for equivalent lateral force (ELF) design. Rather, it is easier to use an arbitrary, but uniform, level of damping (i.e.,

traditional 5% damping) to define a single set of MCE_R ground motions and adjust design factors to account for actual damping other than 5%.

In the case of the ductility component of the R_M factor, response modification implicitly includes both adjustments for inelastic response (ductility) as well as adjustments, if any, for damping other than the 5% value used to define MCE_R spectral response. That is, the archetype models developed as part of FEMA P-695 collapse evaluations include structural damping as part of the hysteretic behavior of the structural system and some additional viscous damping to simulate energy dissipation arising from structural and nonstructural components. Thus, the value of the R_{Md} component based on FEMA P-695 collapse evaluation implicitly includes both a "ductility" component and a "damping" component that can be characterized as follows:

$$R_{Md} = R_{\mu} B_I \tag{4-5}$$

where:

R_{Md} = component of R_M related to total system "ductility" (including damping),

R_{μ} = component of R_{Md} related to inelastic response beyond the effective yield displacement of the seismic force-resisting system, and

B_I = damping reduction factor, as set forth in Table 18.6-1 of ASCE/SEI 7-10 for effective damping, β_I, and period, T, as defined previously.

While the damping reduction factor, B_I, is not explicitly used to define design forces (because it is implicitly part of the R_M factor), it is used in the calculation of peak displacement (drift) of the system. That is, Equation 4-4 defines the deflection amplification in proportion to the ratio R_M/B_I, effectively amplifying the design displacement by $R_O R_{\mu}$, rather than $R_O R_{Md}$, such that peak inelastic displacement is equal to MCE_R response spectral displacement (i.e., for SDOF response) at the effective damping, β_I of the system of interest. Again, explicit incorporation of damping in Equation 4-4 is only of importance for those systems that have effective damping, β_I, other than 5% of critical.

Table 4-4 provides values of effective damping, β_I, at or just below yield for various materials representing selected seismic force-resisting systems. In general, these values are based on the recommendations of Newmark and Hall (1982). An exception is a new system with a metal frame proposed for addition to future editions of seismic codes and has less than 5% damping, at or just below yield (Uang and Smith, 2011). Table 4-4 also shows the corresponding values of the damping reduction factor, B_I, based on Table 18.6-1 of ASCE/SEI 7-10. The damping reduction factors of Table 4-4 are valid for all periods $T > T_0$.

The example values of damping given in Table 4-4 are generally representative of the damping, at or just below yield, of the system of interest, but they are not unique. Other values are possible depending on system configuration and influence of nonstructural components. Additional guidance would be required for selection of a value of damping appropriate for the system of interest.

While the focus has been on the use of effective damping, other than 5% of critical, for a more accurate ELF calculation of peak inelastic response, the values of effective damping given in Table 4-4 could also be used in modal response spectrum analysis (RSA) to better define elastic spectral response of the fundamental mode of the structure.

Table 4-4 Example Values of Damping Reduction Factor, B_I, and Effective Damping, β_I, for Selected Seismic Force-Resisting Systems

Type of Structure/Material	Representative Seismic Force-Resisting System	Effective Damping β_I	Damping Reduction Factor, B_I
Prefabricated Metal Frames	New (Uang and Smith, 2011)	2	0.8
Welded Steel	SCBF(B.1), SMF(C.1)	5	1.0
Prestressed Concrete		5	1.0
Reinforced Concrete Shear Walls	RCSW (B.4, B.5)	7	1.1
Reinforced Masonry Shear Walls	RMSW (A.7, A.9)	7	1.1
Reinforced Concrete Frames and Flexural Walls	RCMF (C.5), RCSW (B.4)	10	1.2
Reinforced Masonry Flexural Walls	RMSW (A.7)	10	1.2
Bolted Steel		10	1.2
Bolted Wood		10	1.2
Nailed Wood Shear Walls	NWSW (A.15)	15	1.35

4.5 Illustration of Reformulation Concepts

Figure 4-1 illustrates the underlying concepts of the FEMA P-695 Methodology as adapted for the proposed reformulation of the R_M factor and related terms. For reference, Figure 4-1 may be compared with Figure 1-2 of FEMA P-695 report. Although the R_M factor is now based on MCE_R ground motions (rather than design earthquake ground motions) and parsed into overstrength, R_O and ductility, R_{Md}, components, the process used to evaluate collapse performance of the system of interest remains true to the methods of FEMA P-695. It should also be noted that while Figure 4-1 illustrates proposed reformulation concepts with a number of complex, interrelated terms, appropriate for commentary, only the R_M factor would be

used by practitioners to determine design base shear (i.e., for design of Risk Category II structures to meet collapse safety objectives).

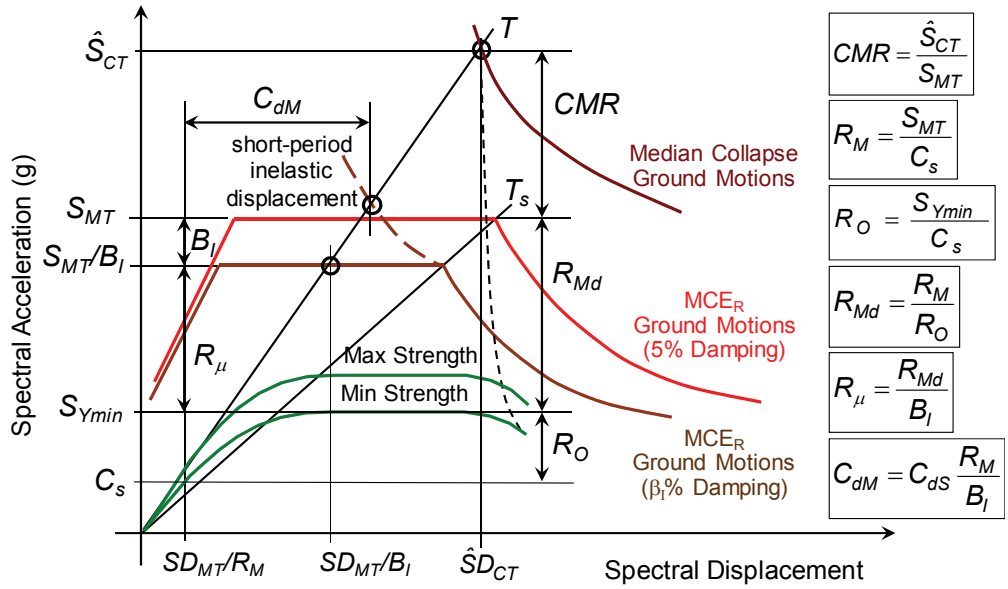

Figure 4-1 Illustration of the underlying concepts of the R_M factor and other reformulated terms.

As defined in FEMA P-695, the collapse margin ratio, *CMR,* is the ratio of the median 5%-damped spectral acceleration of the collapse level ground motions, $\hat{S}_{CT}$, to the 5%-damped spectral acceleration of the MCE$_R$ ground motions, S_{MT}, at the fundamental period of the seismic force-resisting system. Proposed reformulation of the R_M factor (and related terms) has the objective of achieving a more uniform (10%) probability of collapse given MCE$_R$ ground motions for different configurations of the system of interest. Thus, the value of *CMR* after adjustment by the spectral shape factor, *SSF*, should result in an adjusted collapse margin ratio, *ACMR*, that is approximately equal to the acceptable value of the adjusted collapse margin ratio, $ACMR_{10\%}$.

Provided the value of the *CMR* adjusted by *SSF* is sufficient to meet the collapse safety objective (i.e., no more than a 10% probability of collapse given MCE$_R$ ground motions), then an acceptable value of the R_M factor is defined by the ratio of the 5%-damped spectral acceleration of the MCE$_R$ ground motions, S_{MT}, and the value of seismic coefficient, C_s, used for design of the system of interest. Additional reformulation criteria for short-period systems (i.e., systems with design period, T, less than about 0.5 seconds) and long-period systems (i.e., systems with T greater than about 2.0 seconds), such as minimum base shear requirements (not illustrated in Figure 4-1), may also be necessary to achieve the 10% collapse objective, effectively reducing the value of the R_M factor at very short and very long periods.

Acceptable values of the R_M factor and related criteria proposed for reformulation (e.g., minimum base shear requirements) would be determined using the same incremental nonlinear dynamic analysis methods and collapse evaluation criteria as those required by FEMA P-695 to establish an acceptable value of the R factor. However, reformulation would require the value of the R_M factor used for design to be selected from a predefined set of discrete values of the R_M factor, as described in Section 4.4.3.

Equation 4-2 conceptually defines the R_M factor as the product of an overstrength component, R_O, and a ductility component, R_{Md}. Acceptable values of the overstrength factor, R_O, would be determined using the same nonlinear static (pushover) methods as those required by FEMA P-695 to establish an acceptable value of the system overstrength factor, Ω_O. However, the value of R_O would be based on the ratio of lower-bound system strength, S_{Ymin}, and the value of the seismic coefficient, C_s, rather than on the upper-bound of system strength required by FEMA P-695 to determine an acceptable value of Ω_O. The value of R_O would be selected from a predefined set of discrete values of the R_O factor, as described in Section 4.4.3. Reformulation recommends that the system overstrength factor, Ω_O, be eliminated in lieu of a more element-based approach anchored in reliability concepts.

The value of the ductility component, R_{Md}, of the R_M factor is the ratio of the acceptable value of the R_M and the corresponding value of the R_O factor for the system of interest. Equation 4-5 conceptually defines the R_{Md} factor as the product of a (pure) ductility component, R_μ, and a damping component, B_I, representing the inherent damping of the system of interest. While reformulation does not require direct use of the (pure) ductility component for design, the R_μ factor provides a useful measure of the inelastic response capacity of the system of interest.

The B_I factor modifies 5%-damped MCE_R response spectral acceleration of systems with effective damping other than 5% of critical, at or just below the yield displacement. Table 18.6-1 of ASCE/SEI 7-10 provides the value of the damping factor, B_I, given the value of inherent damping, β_I. Determining an appropriate value of inherent damping, β_I, for the system of interest is not within the scope of FEMA P-695 methods, and would require separate determination of this parameter for different systems and materials of interest, as described in Section 4.4.7.

Equation 4-4 conceptually defines the deflection amplification factor, C_{dM}, as the product of the short-period deflection amplification factor, C_{dS}, and the response modification factor, R_M, divided by the damping factor, B_I. Consistent with the methods of FEMA P-695, peak inelastic displacement is assumed to be equal to β_I-damped spectral displacement of the MCE_R ground motions at the fundamental period of the system of interest. The short-period deflection amplification factor, C_{dS}, is included in the reformulation of the deflection amplification factor to account for

additional inelastic displacement of systems with periods less than the transition period, T_s (e.g., less than about 0.5 seconds), although the C_{dS} factor would not likely be of practical significance to the design of most short-period systems. Additional short-period displacement is illustrated in Figure 4-1 by the dashed curve extending upward from the response spectrum of β_I%-damped MCE_R ground motions spectrum at periods less than T_s.

4.6 Use of Multi-Period Design Response Spectra

This section discusses the possibility of replacing the current two-domain design spectrum (i.e., Figure 11.4-1 of ASCE/SEI 7-10) with a multi-period design spectrum that has a more realistic shape that better characterizes the frequency content of earthquake ground motions.

The characterization of earthquake ground motions has improved greatly since the time that seismic codes first began to distinguish seismic design forces on the basis of building period. Science can now provide multi-period design response spectrum for sites in the United States. However, the use of a multi-period spectrum would complicate the design process.

There is a very real need to balance improved accuracy of earthquake loads with the associated changes and complications to the design process that would occur, if adopted. Although incorporation of a multi-period design response spectrum would seem an inevitable improvement to earthquake design, such changes may take some time to be embraced by seismic codes and practice.

Figure 4-2 shows an example comparison of a multi-period spectrum (red curve) for a stiff soil site (Site Class D) in a region of high seismicity in the Western United States and the corresponding 2-domain spectrum (blue curve) that have approximately the same values of short (0.25 second) and 1 second response spectral acceleration.

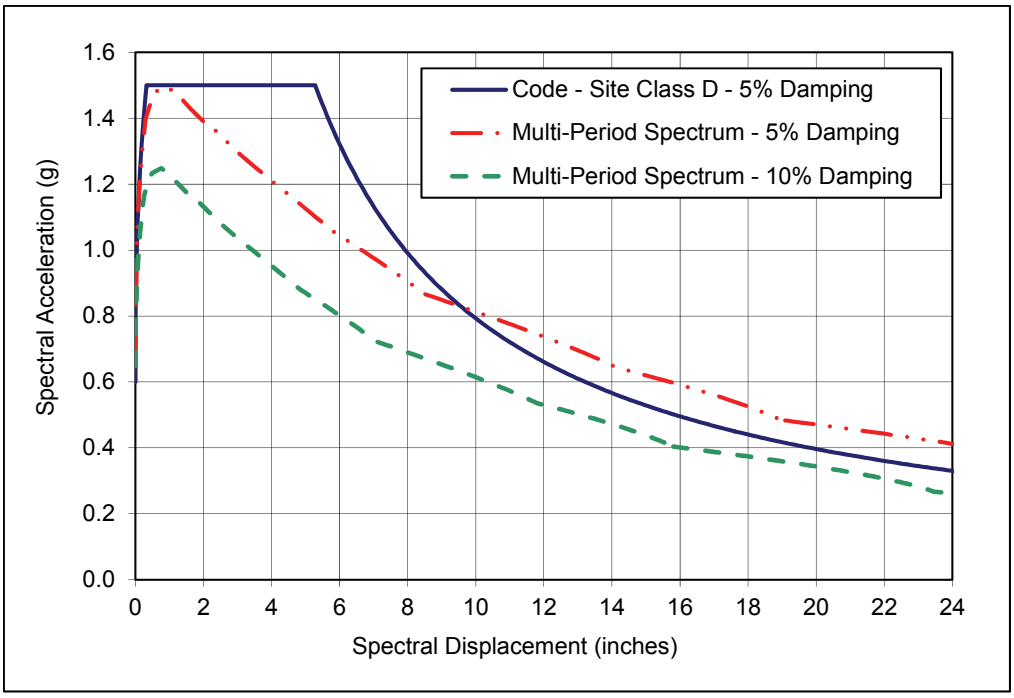

Figure 4-2 Comparison of multi-period and 2-domain spectra with comparable short-period and 1-second response spectral accelerations.

As seen in Figure 4-2, the multi-period spectrum defines ground motions that are substantially different than the two-domain spectrum near the transition period (i.e., 0.6 seconds) and at long periods. Use of the multi-period spectrum would better address earthquake risk by improving the accuracy of design loads as a function of building period. In particular, multi-period spectra would improve the description of design loads on long-period structures, avoiding possible underestimation (or overestimation) of earthquake demand. Multi-period spectra would also affect greater consistency between ELF design forces and those of RSA and response-history analysis.

Multi-period spectra are currently available from the U.S. Geological Survey for sites in the Western United States (WUS) but not yet available for sites in the Central and Eastern United States (CEUS). In general, however, multi-period response spectra are not available for other countries which could affect future use of ASCE/SEI 7 for earthquake design outside of the United States.

Of particular importance to this report is that the reformulation concepts proposed in previous sections of this chapter would work equally well with either the current two-domain design spectrum or the multi-period design spectrum of the future, although certain methods of FEMA P-695 would require some adjustment, if ASCE/SEI 7 adopted a new, multi-period design spectrum.

4.7 Risk-Based Design Criteria Considering Life-Safety, Economic, and Functional Objectives

This section discusses possible adoption of the risk-based concepts of FEMA P-695, which explicitly address life-safety (collapse) risk, to also address economic and functional risk objectives, and the development of appropriate design criteria based on expanded risk objectives. This section describes a conceptual framework for incorporating economic and functional risk objectives in ASCE/SEI 7 design criteria; however, developing specific risk objectives would be the responsibility of seismic code committees.

Risk-based design criteria necessarily combine performance objectives with seismic hazard (ground motion intensity). For life-safety objectives ASCE/SEI 7-10 requires only a single ground motion intensity (MCE_R), defined probabilistically as ground motions having a 1% probability of causing structural collapse in 50 years. Those ground motions are very rare, typically having a return period of about 2,000 years, and are, in general, not appropriate for design to meet economic or functional risk objectives. Hence, one or two other ground motion intensity levels would likely be required to explicitly address economic and functional risk objectives. For this purpose, the conceptual framework defines two new levels of earthquake intensity: risk-based functional level (FLE_R) ground motions, and risk-based service level (SLE_R) ground motions. Like MCE_R ground motions, FLE_R and SLE_R ground motions are defined by 50-year risk and conditional probabilities, and would be calculated from the same set seismic hazard functions.

This section also describes a simple approach for developing rational values of the importance factor, I_e, based on differences in defined risk objectives for each of the four risk categories (i.e., risk categories of Table 1.5-1 of ASCE/SEI 7-10). Conceptually, the importance factor would bias ground motion intensity as required to meet the performance objectives of different risk categories, avoiding the need to define additional hazard levels and corresponding sets of design value maps.

Although this section focuses on structural performance and risk criteria, nonstructural systems and contents are also important to life safety, typically dominate economic loss, and can govern loss of function. Thus, it is envisioned that the conceptual framework described in this section also applies to nonstructural systems and components, although different design parameters and methods would be required to meet risk objectives.

4.7.1 Structural Risk Criteria of ASCE/SEI 7-10

Table 4-5 summarizes structural risk criteria of ASCE/SEI 7-10 as described in Table C.1.3.1b, where life-safety risk is defined as either total or partial structural collapse.

Blank cells indicate that ASCE/SEI 7-10 does not define structural risk criteria for either economic loss or functional failure.

Table 4-5 Performance Objectives, Risk Probabilities, Ground Motion Intensities, and Primary Structural Design Parameters of ASCE/SEI 7-10

	Seismic Risk Objective					
		Risk Probability				
Generic Risk Subject	Acceptable Facility Performance	Absolute (50 years)	Conditional (on Ground Motion)	Ground Motion Intensity	Primary Structural Design Parameter	Basis for Risk Parameters and Values
Risk Category I (structures posing low risk to life safety)						
Life Safety	No Collapse	1%	10%	MCE_R	*R*	FEMA P-695
Function						
Economic						
Risk Category II (structures not in Risk Categories I, III, or IV)						
Life Safety	No Collapse	1%	10%	MCE_R	*R*	FEMA P-695
Function						
Economic						
Risk Category III (structures posing high risk to life safety, economic impact or disruption)						
Life Safety	No Collapse	< 1%	6%	MCE_R	*R*/1.25	FEMA P-695
Function						
Economic						
Risk Category IV (essential facilities required to maintain functionality)						
Life Safety	No Collapse	< 1%	3%	MCE_R	*R*/1.5	FEMA P-695
Function						
Economic						

For Risk Category I and Risk Category II structures, i.e., $I_e = 1.0$, acceptable life-safety risk is defined by an "absolute" collapse probability of 1% in 50 years and a "conditional" probability of 10% given MCE_R ground motions. As noted previously, the conditional probability of 10% is based on FEMA P-695 Methodology. The absolute, 1% in 50-year, and the conditional, 10% given MCE_R ground motions, probabilities were used by the U.S. Geological Survey to develop the probabilistic MCE_R ground motions of ASCE/SEI 7-10.

The conditional probabilities of 6% (Risk Category III structures) and 3% (Risk Category IV structures) shown in Table 4-5 represent improved reliability anticipated for structures designed with an importance factor, I_e, greater than 1.0. Although not specifically stated by ASCE/SEI 7-10 commentary, it may be presumed that Risk Category III and Risk Category IV structures have absolute collapse probability

objectives that are less than a 1% in 50 year (i.e., due to design using an importance factor of $I_e > 1.0$).

4.7.2 Hypothetical Risk Criteria of Future Editions of ASCE/SEI 7

Table 4-6 provides a tentative conceptual framework and hypothetical criteria illustrating how the current risk criteria of Table 4-5 could be expanded to address economic and functional risk, as well as life-safety risk, and to address nonstructural, as well as structural performance.

In Table 4-6, "No Collapse" is used to describe acceptable life-safety performance, "Green Tag" and "10% LR" are simply short-hand terms for much more detailed sets of system-specific performance criteria that would need to be developed to define acceptable functional and economic performance. "Green Tag," implies acceptable functional performance of a facility; the building could have some damage, but would not be closed. Acceptable economic performance of a facility is shown as "10% LR," (where LR stands for loss ratio) implies that a building would not sustain damage requiring more than 10% of the replacement value to repair.

The hypothetical criteria shown in Table 4-6 are intended solely as a starting point for code committee discussions of acceptable risk and would be expected to change, perhaps significantly, during such discussions (e.g., design for economic risk may be deemed inappropriate; and, hence, performance objectives and criteria would not be defined for this risk category).

Table 4-6 Hypothetical Performance Objectives, Risk Probabilities, Ground Motion Intensities and Primary Design Parameters Used to Illustrate a Risk-Based Framework

	Seismic Performance Objectives				Primary Design Parameter[1]		
		Risk Probability					
Generic Risk Subject	Acceptable Facility Performance	50Years	Conditional (on Ground Motion)	Ground Motion Intensity	Structural	Nonstructural	Basis for Values of Design Parameters
Risk Category I (structures posing low risk to life safety)							
Life Safety	No Collapse	≈ 2%	20%	MCE_R	R_M/I_e		(FEMA P-695)
Function	None						
Economic	None						
Risk Category II (structures not in Risk Categories I, III, or IV)[2]							
Life Safety	No Collapse	1%	10%	MCE_R	R_M/I_e	R_M/I_p	FEMA P-695
Function[3]	Green Tag	10%	10%	FLE_R			
Economic[4]	10% LR	50%	10%	SLE_R			
Risk Category III (posing high risk to life safety, economic impact, or disruption)							
Life Safety	No Collapse	≈ 0.5%	5%	MCE_R	R_M/I_e	R_M/I_p	(FEMA P-695)
Function[3]	Green Tag	≈ 7%	5%	FLE_R			
Economic	10% LR	≈ 40%	5%	SLE_R	Drift[5]	TBD[6]	Hazus/FEMA P-58[7]
Risk Category IV (essential facilities required to maintain functionality)							
Life Safety	No Collapse	≈ 0.3%	2.5%	MCE_R	R_M/I_e	R_M/I_p	(FEMA P-695)
Function	Green Tag	≈ 5%	2.5%	FLE_R	Drift[5]	TBD[6]	Hazus/FEMA P-58[7]
Economic[4]	10% LR	≈ 30%	2.5%	SLE_R			

1. Other parameters and criteria include minimum value of the base shear coefficient, C_{sM}, etc.
2. ASCE/SEI 7-10 defines probabilistic MCE_R ground motions in terms of the following: (1) a 1% probability of collapse in 50 years; and (2) a 10% probability of collapse given these ground motions occur. The 10% conditional collapse probability is based on design of the seismic force-resisting system using R (I_e = 1.0) and other design parameters that are consistent with FEMA P-695 acceptance criteria appropriate for Risk Category II structures.
3. In this example, protection against loss of function for Risk Category II and Risk Category III structures is assumed to be provided implicitly by response limits associated with life-safety criteria for MCE_R ground motions (for Risk Category II structures) and by economic loss criteria for SLE_R ground motions (for Risk Category III structures).
4. In this example, protection against unacceptable economic loss for Risk Category II and Risk Category IV structures is assumed to be provided implicitly by response limits associated with life-safety criteria for MCE_R ground motions (for Risk Category II structures) and by loss of function criteria for FLE_R ground motions (for Risk Category IV structures).
5. In general, current story drift limits of Table 12.12-1 of ASCE/SEI 7-10 do not provide adequate damage control to meet functional and/or economic loss objectives and would require substantial revision.
6. To Be Determined (TBD). Design of nonstructural systems to meet functional and economic performance objectives is complex, requiring consideration of structure response (e.g., calculation of in-structure response spectra) and special qualification testing of certain components.
7. Structural fragility data developed for FEMA P-58 (FEMA, 2012b) or the *HAZUS-MH MR1 Advanced Engineering Building Module Technical and User's Manual* (FEMA, 2003) may be used to define appropriate system-specific story drift limits for limiting damage to the structural system

It is important to note the interdependency of 50-year risk and conditional probabilities, and ground motion intensity (including the importance factor). Specifying both the 50-year risk probability (e.g., 1% probability of collapse in 50 years) and the conditional probability (e.g., 10% probability of collapse given MCE_R ground motions) defines a specific ground motion intensity (e.g., MCE_R ground motions, $I_e = 1.0$), in this case for Risk Category II structures. Specifying a lower absolute collapse probability or a lower conditional collapse probability (e.g., for Risk Category III or Risk Category IV structures) increases design forces (e.g., by the value of the I_e factor applied to MCE_R ground motions) as required to achieve the more stringent life-safety risk objectives. For example, design of Risk Category III structures using an importance factor value of $I_e = 1.25$ reduces the conditional probability of collapse given MCE_R ground motions from 10 percent to 5 percent and the 50-year risk probability from 1 percent to about 0.5 percent. The conceptual basis for the reduction in the conditional probability is explained in Section 4.7.3. The 50-year risk probability reduces approximately in proportion to the reduction in the conditional probability. Precise values of the 50-year risk probability require integration of the derivative of collapse fragility (representing the reduced conditional probability of failure) and site-specific hazard, and therefore would be somewhat different for different sites.

In Table 4-6, FLE_R and SLE_R ground motions are based on the same conditional probability of 10% as that of MCE_R ground motions for Risk Category II structures (i.e., the most common structure type). Unlike the 1% in 50 year probability of collapse risk, FLE_R ground motions are based on 10% in 50 years probability of loss of function, and SLE_R ground motions are based on 50% in 50 years probability of economic loss. That is, the hypothetical values of 50-year risk shown in Table 4-6 establish a risk-based hierarchy: collapse should be very unlikely (1% probability), loss of function should be unlikely (10% probability), but modest economic loss could be likely and still be acceptable (50% probability of 10% loss ratio).

Although risk-based seismic performance objectives are defined for each of the three risk subjects, Table 4-6 requires explicit design for life-safety objectives only, assuming that economic and functional objectives would be met implicitly (i.e., single-level design approach, like that of ASCE/SEI 7-10). Table 4-6 requires consideration of dual risk objectives for design of Risk Category III and Risk Category IV structures. In this example, Risk Category III structures would be designed for the more critical of life-safety and economic loss objectives (to avoid adverse economic impacts as well as structure collapse); and Risk Category IV structures would be designed for the more critical of life-safety and functional loss objectives (to maintain functionality of critical facilities as well as to avoid structure collapse). The hypothetical criteria of Table 4-6 are intended solely to illustrate risk-based concepts, and actual criteria could be quite different.

Table 4-6 includes two columns listing the "primary design parameter" that relate the risk-based performance objectives to applicable design requirements of seismic codes. In this example, the primary design parameter for life-safety design is shown as the R_M factor, developed by FEMA P-695 collapse evaluations, divided by the importance factor, where the R_M factor would be.

For functional and economic objectives, Table 4-6 shows "Drift" as the primary structural design parameter to indicate that controlling damage requires drift-related, as well as force-related, design criteria, and "TBD" as the primary nonstructural design parameter to acknowledge the additional complexity of designing nonstructural components to meet risk objectives. At this time, there is no methodology that addresses economic and functional risk equivalent to FEMA P-695 for life-safety.

As shown in Table 4-6, the same three hypothetical sets of ground motions (MCE_R, FLE_R, and SLE_R) are listed for possible use with each risk category. While ground motions are the same, design values vary by risk category in accordance with the value of the importance factor, as required to meet 50-year risk and conditional probabilities.

Example values of short-period ground motions are shown in Table 4-7, and example values of 1-second ground motions are shown in Table 4-8 for three 50-year risk probabilities (i.e., 1%, 10%, and 50% probability in 50 years). Ground motions are provided for 34 cities located in high seismic areas or densely populated regions of the continental United States (see Table 4-9 for city and population data). In all cases, ground motion values are based on a conditional probability of 10% (i.e., Risk Category II structures) and are adjusted to represent Site Class D conditions. Ground motions corresponding to a 1% in 50-year risk are the same as the probabilistic MCE_R ground motions of ASCE/SEI 7-10. The other two risk levels illustrate the reduction in ground motion spectral acceleration and return period with increase in 50-year risk probability.

Of particular note is the significant reduction in SLE_R ground motions (based on 50% risk of 10% economic loss) and, to a lesser degree, FLE_R ground motions (based on 10% risk of loss of function) for sites of low and moderate seismicity in the CEUS region. Because of the underlying shape of seismic hazard functions, SLE_R ground motions and, to a lesser degree, FLE_R ground motions are relatively low in the CEUS, effectively eliminating the need for designs to meet economic and possibly functional objectives (i.e., even if otherwise required by the dual risk objectives of Risk Category III and Risk Category IV structures, seismic forces would be too small to govern design).

Table 4-7 ASCE/SEI 7-10 Values of Short-Period Probabilistic MCE_R Ground Motions and Example Values of Short-Period SLE_R and FLE_R Ground Motions for 34 Cities Assuming Site Class D Conditions Based on a Conditional Risk Probability of 10 Percent

		MCE_R (1% in 50yr)		FLE_R (10% in 50yr)		SLE_R (50% in 50yr)	
Region	City (Site Location)	Spectral Acceleration (g)	Return Period (yrs)	Spectral Acceleration (g)	Return Period (yrs)	Spectral Acceleration (g)	Return Period (yrs)
Southern California	Los Angeles	2.30	1,861	0.93	195	0.29	33
	Century City	2.05	1,916	0.88	189	0.28	33
	Northridge	1.85	2,069	0.89	176	0.30	33
	Long Beach	1.57	1,879	0.74	200	0.26	31
	Irvine	1.48	2,109	0.70	197	0.26	31
	Riverside	1.65	2,310	0.88	170	0.34	30
	San Bernardino	2.99	1,999	1.19	178	0.37	35
	San Luis Obispo	1.14	1,959	0.55	198	0.20	30
	San Diego	1.29	1,894	0.50	237	0.17	31
	Santa Barbara	2.78	1,789	0.97	211	0.22	36
	Ventura	2.30	1,908	0.91	194	0.26	35
	Weighted Mean	**1.88**	**1,990**	**0.84**	**195**	**0.28**	**32**
Northern California	Oakland	2.67	2,015	1.13	172	0.35	34
	Concord	2.59	1,896	1.08	185	0.33	34
	Monterey	1.44	1,901	0.71	198	0.25	31
	Sacramento	0.79	2,393	0.40	185	0.16	29
	San Francisco	1.90	2,112	0.91	175	0.31	33
	San Mateo	2.18	1,865	0.93	192	0.30	33
	San Jose	1.99	2,479	1.00	170	0.38	31
	Santa Cruz	1.56	1,973	0.80	185	0.28	32
	Vallejo	1.76	2,296	0.90	168	0.33	32
	Santa Rosa	2.99	1,797	1.06	205	0.26	36
	Weighted Mean	**1.99**	**2,143**	**0.93**	**180**	**0.31**	**32**
Pacific Northwest	Seattle	1.29	1,979	0.64	189	0.20	33
	Tacoma	1.23	2,002	0.65	186	0.21	33
	Everett	1.24	1,977	0.59	196	0.19	33
	Portland	1.08	1,897	0.44	207	0.10	39
	Weighted Mean	**1.21**	**1,956**	**0.58**	**195**	**0.17**	**35**
Other WUS	Salt Lake City	1.62	1,826	0.50	250	0.09	38
	Boise	0.47	2,051	0.15	199	0.04	33
	Reno	1.46	1,876	0.71	191	0.22	34
	Las Vegas	0.69	2,145	0.22	204	0.07	32
	Weighted Mean	**1.00**	**2,018**	**0.35**	**214**	**0.09**	**34**
CEUS	St. Louis	0.65	1,937	0.16	239	0.026	40
	Memphis	1.15	1,842	0.28	284	0.032	41
	Charleston	1.26	1,989	0.25	294	0.014	48
	Chicago	0.23	2,308	0.05	225	0.008	40
	New York	0.47	2,274	0.08	250	0.011	42
	Weighted Mean	**0.49**	**2,233**	**0.09**	**244**	**0.012**	**41**

Table 4-8 ASCE/SEI 7-10 Values of 1-Second Probabilistic MCE_R Ground Motions and Example Values of 1-Second SLE_R and FLE_R Ground Motions for 34 Cities Assuming Site Class D Conditions Based on a Conditional Risk Probability of 10 Percent

		MCE_R (1% in 50yr)		FLE_R (10% in 50yr)		SLE_R (50% in 50yr))	
Region	City (Site Location)	Spectral Acceleration (g)	Return Period (yrs)	Spectral Acceleration (g)	Return Period (yrs)	Spectral Acceleration (g)	Return Period (yrs)
Southern California	Los Angeles	1.20	1,929	0.51	191	0.17	32
	Century City	1.14	1,964	0.49	193	0.16	32
	Northridge	0.98	2,069	0.49	177	0.17	32
	Long Beach	0.88	1,999	0.40	197	0.15	30
	Irvine	0.81	2,226	0.39	192	0.15	30
	Riverside	0.97	2,129	0.50	173	0.18	32
	San Bernardino	1.94	1,889	0.70	185	0.20	36
	San Luis Obispo	0.64	2,000	0.32	193	0.11	31
	San Diego	0.74	1,996	0.30	222	0.11	30
	Santa Barbara	1.46	1,777	0.53	210	0.13	36
	Ventura	1.30	1,937	0.52	196	0.15	34
	Weighted Mean	**1.06**	**2,022**	**0.47**	**193**	**0.16**	**32**
Northern California	Oakland	1.49	1,948	0.62	178	0.19	35
	Concord	1.36	1,883	0.58	187	0.18	34
	Monterey	0.80	1,934	0.38	199	0.13	32
	Sacramento	0.49	2,417	0.26	178	0.11	29
	San Francisco	1.18	1,955	0.53	184	0.16	34
	San Mateo	1.42	1,784	0.54	204	0.15	34
	San Jose	1.05	2,216	0.53	170	0.19	32
	Santa Cruz	0.88	1,912	0.42	188	0.14	33
	Vallejo	0.94	2,157	0.50	169	0.18	32
	Santa Rosa	1.87	1,790	0.62	208	0.14	37
	Weighted Mean	**1.13**	**2,050**	**0.52**	**183**	**0.17**	**33**
Pacific Northwest	Seattle	0.77	1,943	0.36	196	0.10	35
	Tacoma	0.73	1,942	0.35	191	0.10	35
	Everett	0.72	1,939	0.33	200	0.09	35
	Portland	0.67	1,851	0.26	221	0.05	40
	Weighted Mean	**0.72**	**1,913**	**0.32**	**204**	**0.08**	**36**
Other WUS	Salt Lake City	0.89	1,945	0.26	252	0.05	38
	Boise	0.24	2,062	0.08	193	0.02	34
	Reno	0.75	1,935	0.35	195	0.10	34
	Las Vegas	0.35	2,176	0.13	192	0.04	33
	Weighted Mean	**0.55**	**2,072**	**0.18**	**209**	**0.05**	**35**
CEUS	St. Louis	0.37	1,833	0.08	258	0.012	41
	Memphis	0.62	1,917	0.13	300	0.013	42
	Charleston	0.65	2,110	0.09	303	0.008	45
	Chicago	0.15	1,947	0.04	232	0.006	39
	New York	0.18	2,293	0.04	225	0.007	39
	Weighted Mean	**0.24**	**2,136**	**0.04**	**234**	**0.007**	**39**

Table 4-9 Site Locations, Associated Counties, and Populations at Risk

Region	City and Location of Site			County or Metro Statistical Area	
	Name	Latitude	Longitude	Name	Population
Southern California	Los Angeles	34.05	-118.25	Los Angeles	9,948,081
	Century City	34.05	-118.40		
	Northridge	34.20	-118.55		
	Long Beach	33.80	-118.20		
	Irvine	33.65	-117.80	Orange	3,002,048
	Riverside	33.95	-117.40	Riverside	2,026,803
	San Bernardino	34.10	-117.30	San Bernardino	1,999,332
	San Luis Obispo	35.30	-120.65	San Luis Obispo	257,005
	San Diego	32.70	-117.15	San Diego	2,941,454
	Santa Barbara	34.45	-119.70	Santa Barbara	400,335
	Ventura	34.30	-119.30	Ventura	799,720
	Total Population - S. California		**22,349,098**	**Population - 8 Counties**	**21,374,778**
Northern California	Oakland	37.80	-122.25	Alameda	1,502,759
	Concord	37.95	-122.00	Contra Costa	955,810
	Monterey	36.60	-121.90	Monterey	421,333
	Sacramento	38.60	-121.50	Sacramento	1,233,449
	San Francisco	37.75	-122.40	San Francisco	776,733
	San Mateo	37.55	-122.30	San Mateo	741,444
	San Jose	37.35	-121.90	Santa Clara	1,802,328
	Santa Cruz	36.95	-122.05	Santa Cruz	275,359
	Vallejo	38.10	-122.25	Solano	423,473
	Santa Rosa	38.45	-122.70	Sonoma	489,290
	Total Population - N. California		**14,108,451**	**Population - 10 Counties**	**8,621,978**
Pacific Northwest	Seattle	47.60	-122.30	King WA	1,826,732
	Tacoma	47.25	-122.45	Pierce WA	766,878
	Everett	48.00	-122.20	Snohomish WA	669,887
	Portland	45.50	-122.65	Portland Metro OR (3)	1,523,690
	Total Population - OR and WA		**10,096,556**	**Population - 6 Counties**	**4,787,187**
Other WUS	Salt Lake City	40.75	-111.90	Salt Lake UT	978,701
	Boise	43.60	-116.20	Ada/Canyon ID (2)	532,337
	Reno	39.55	-119.80	Washoe NV	396,428
	Las Vegas	36.20	-115.15	Clarke NV	1,777,539
	Total Population - ID/UT/NV		**6,512,057**	**Population - 5 Counties**	**3,685,005**
CEUS	St. Louis	38.60	-90.20	St. Louis MSA (16)	2,786,728
	Memphis	35.15	-90.05	Memphis MSA (8)	1,269,108
	Charleston	32.80	-79.95	Charleston MSA (3)	603,178
	Chicago	41.85	-87.65	Chicago MSA (7)	9,505,748
	New York	40.75	-74.00	New York MSA (23)	18,747,320
	Total Population - MO/TN/SC/IL/NY		**48,340,918**	**Population - 57 Counties**	**32,912,082**

4.7.3 Rational Basis for the Importance Factor, I_e

Consistent with the risk-based framework described in the previous section, the importance factor may be thought of as the ratio of the ground motion intensity required to achieve a given conditional risk probability and the ground motion intensity corresponding to the conditional risk probability of 10% used to develop MCE_R ground motions for Risk Category II structures (i.e., $I_e = 1.0$).

Using FEMA P-695 methods, the importance factor may be calculated as the ratio of acceptable *ACMR* values of Section 7.4 of FEMA P-695 corresponding to the conditional collapse probabilities of interest (and an appropriate value of total system collapse uncertainty, β_{TOT}).

$$I_e = \frac{ACMR_{XX\%}}{ACMR_{10\%}} \tag{4-6}$$

where:

$AMCR_{XX\%}$ = acceptable value of *ACMR* for the system of interest corresponding to a collapse probability of XX% and an appropriate value of β_{TOT} (same as that of $ACMR_{10\%}$), and

$AMCR_{10\%}$ = acceptable value of *ACMR* for the system of interest corresponding to a collapse probability of 10% and an appropriate value of β_{TOT}.

Table 4-10 provides example values of the importance factor, I_e, based on Equation 4-6 for conditional collapse risk probabilities ranging from 2% to 25% for two values of the total system collapse uncertainty factor ($\beta_{TOT} = 0.6$ and $\beta_{TOT} = 0.8$).

Although values of the importance factor in Table 4-10 are calculated using acceptable values of the *ACMR*, the underlying concepts apply equally well to other risk parameters whose conditional probability (i.e., fragility) can be characterized by a lognormal distribution.

Table 4-10 Example Values of the Importance Factor, I_e, for Hypothetical Values of the Conditional Risk Probability

Conditional Risk Probability	β_{TOT} = 0.6		β_{TOT} = 0.8	
	$ACMR_{XX\%}$	I_e	$ACMR_{XX\%}$	I_e
2%	3.43	1.59	5.17	1.85
2.5%	3.24	1.50	4.80	1.72
3%	3.09	1.43	4.50	1.62
4%	2.86	1.33	4.06	1.46
5%	2.68	1.24	3.73	1.34
6%	2.54	1.18	3.47	1.24
8%	2.32	1.08	3.08	1.10
10%	2.16	1.00	2.79	1.00
12%	2.02	0.94	2.56	0.92
15%	1.86	0.86	2.29	0.82
20%	1.66	0.77	1.96	0.70
25%	1.50	0.69	1.72	0.62

Chapter 5

Summary, Findings, and Recommendations

This chapter summarizes the investigations of the current formulation of building seismic performance factors and provides recommendations for reformulation of these factors and related design requirements.

5.1 Summary of Investigations

Seismic performance factors, such as R, C_d, Ω_O, and related criteria are used to estimate force and deformation demands on seismic force-resisting systems that are designed using linear methods of analysis but are responding in the nonlinear range. The seismic design requirements of ASCE/SEI 7-10, *Minimum Design Loads for Buildings and Other Structures*, (ASCE, 2010) define these criteria and specify system-specific values of the seismic performance factors in Table 12.2-1, based largely on judgment. The intent of ASCE/SEI 7-10 is that Risk Category II structures (designed using these criteria with requisite detailing and properly constructed) would have no more than a 10% probability of total or partial collapse given the occurrence of Maximum Considered Earthquake (MCE_R) ground motions.

The 10% collapse probability objective of ASCE/SEI 7-10 is based on the acceptance criteria of the FEMA P-695 Methodology required for evaluation of seismic performance factors proposed for a new seismic force-resisting system. At the heart of the investigations of this study is the notion that the existing systems of ASCE/SEI 7-10 Table 12.2-1 should also comply with the 10% collapse probability objective. However, prior studies have shown that existing systems do not meet this collapse probability objective, thus a study of the R factor (and other related performance factors) is necessary. Prior to undertaking such a major effort, the basic formulation of the seismic performance factors and related criteria were investigated and proposed reformulations of seismic performance factors and related criteria were developed, such that improved values of these factors and criteria would be appropriate for use in future editions of the *NEHRP Recommended Seismic Provisions*, ASCE/SEI 7, and other seismic codes.

Initial investigations of reformulation began with the identification of topics of interest that greatly exceeded the number that could be investigated in this project. Certain topics were conceptual in nature (e.g., reformulation of R factor as R_M based directly on MCE_R ground motions) that require serious consideration before

adoption, but would not benefit from analytical study. Other topics of interest that would benefit from analytical study (using the FEMA P-695 Methodology) were ranked and the three most promising areas of study with respect to reformulation were identified as topics related to the following: (1) short-period systems; (2) overstrength; and (3) long-period systems.

The topical studies of this report build upon the results of prior FEMA P-695 studies, summarized in Chapter 2. These studies found that existing systems generally had collapse probabilities less than 10% but that collapse probabilities also varied significantly by system, by design period, and by other factors for the same system. Although the prior studies evaluated 10 commonly used seismic force-resisting systems, these systems represent only a fraction of the 84 systems in Table 12.2-1 of ASCE/SEI 7-10. Further, existing studies of these systems generally did not have the completeness required for full FEMA P-695 evaluation, so results could not be considered as definitive for any specific system. Nonetheless, certain trends in the collapse results of these studies were found to be strong and consistent among the different systems investigated. Of particular note, short-period archetypes of a given system were found to have significantly higher collapse probabilities (often greater than 10%) than archetypes with longer periods.

In the review of the results of prior studies, Chapter 2 introduced the notion of "uniform risk" adjustment of collapse results, whereby the trial value of the R factor used for design of archetypes in a FEMA P-695 collapse evaluation could be adjusted to correspond approximately to the desired collapse probability (i.e., 10% probability of collapse). This technique permits estimation of an appropriate value of the R factor (or R_M factor) for the system of interest from FEMA P-695 analyses whose results typically have collapse probabilities above or below the desired objective, and thus avoids the need for iterative redesign and reanalysis of archetypes for different trial values of the R factor. FEMA P-695 analyses can be time consuming and this technique would greatly expedite the number of analyses required for investigation and reevaluation of the R factors of existing systems of ASCE/SEI 7-10 Table 12.2-1.

Topical studies of short-period systems, overstrength, and long-period systems, summarized in Chapter 3, developed and analyzed archetype models using the FEMA P-695 Methodology. Results were typically found to be similar to those of prior FEMA P-695 studies of comparable archetypes. When possible, results of these and prior studies were used to develop general recommendations for reformulation (Chapter 4), although in most cases specific recommendations could not be made without additional study. Similar to the prior FEMA P-695 studies, the topical studies of this report increased the understanding of system behavior and collapse performance, discovered potential safety issues (e.g., with tall shear-wall buildings), and confirmed shortcomings in current design methods (e.g., scaling criteria for response spectrum analysis).

Conceptual reformulation of seismic performance factors and related criteria, described in Chapter 4, include the following: (1) basing the *R* factor (and reformulating as R_M factor) directly on MCE_R ground motions; (2) theoretically representing the R_M factor as the product of a ductility component and an overstrength component; (3) using a standardized set of R_M factors; (4) revising minimum base shear criteria; (5) revising the deflection amplification factor; and (6) explicitly incorporating effective damping in the design spectrum (for systems which do not have 5% effective damping). Most of these reformulation concepts are not new, rather notions that have been well developed by prior research and often found in existing resource documents. For example, *SEAOC Blue Book: Seismic Design Recommendations of the SEAOC Seismology Committee* (SEAOC, 1999) defined the *R* factor as the product of ductility and overstrength components. What is new in this case is not the concept, rather the FEMA P-695 Methodology, which now provides a rational basis to quantify values of the ductility and overstrength components of the R_M factor.

Chapter 4 also investigated two "big picture" topics: (1) the possibility of using a multi-period design spectrum, in lieu of the traditional, two-domain design spectrum; and (2) the extension of the collapse risk-based concepts of FEMA P-695 to future design requirements that would explicitly address functional and economic risks (e.g., for Risk Category III and Risk Category IV structures) and include design of nonstructural, as well as structural, systems. These big picture topics, although of tremendous potential significance to future code development, do not affect conceptual reformulation of the R_M factor to better address collapse risk.

5.2 General Findings Related to Reformulation of Seismic Design Parameters

This section summarizes general findings related to reformulation, addressing topics that require additional investigation either before, or as part of future reformulation studies using the FEMA P-695 Methodology.

5.2.1 Consistent Archetype Models

There is a need to achieve greater uniformity of the archetype models (i.e., consistency of modeling methods and failure criteria) used in FEMA P-695 collapse evaluations.

Analytical modeling of the nonlinear inelastic behavior and failure mechanisms of structural elements is both challenging and evolving as the associated research progresses. In some cases, different researchers working independently have developed archetype models of the same or similar system configuration using reasonable but somewhat different assumptions and properties that produced significantly different results. Future applications of the FEMA P-695 Methodology

reevaluating seismic performance factors and related criteria of current systems will require consistency of the methods used to model archetypes and the criteria used to evaluate collapse.

5.2.2 Consistent Archetype Designs

There is a need to achieve greater uniformity of archetype designs (i.e., consistency of the system configurations, design methods, and properties) used in FEMA P-695 collapse evaluations.

Archetype design involves developing appropriate properties of structural elements of typical configurations that when properly modeled and evaluated using FEMA P-695 Methodology would produce representative collapse results for the system of interest. Archetype design is challenging because it necessarily must use a limited number of relatively simple (typically 2-D) configurations to represent a wide range of actual building geometries. Further, while archetype designs are not intended to capture all "outliers" of the system of interest, they should still in some reasonable manner represent the minimum design requirements of ASCE/SEI 7-10. In some cases, different researchers (or practitioners) working independently have developed significantly different archetype designs of the same system. Future application of the FEMA P-695 Methodology reevaluating seismic performance factors and related criteria of current systems will require consistency of the methods used to develop archetype designs and confidence that these designs are representative of the systems of interest.

5.2.3 Reliability of FEMA P-695 Evaluations

There is a need to investigate and improve the reliability of the procedures and results of FEMA P-695 evaluations.

Because a FEMA P-695 evaluation can be quite sensitive to archetype design, nonlinear analysis models, and modeling assumptions, it would be useful to examine appropriate and effective ways to ensure reliability in the procedures. This may, for example, lead to more specific reporting requirements that summarize key assumptions and modeling criteria or requirements for performing complementary archetype studies by two independent entities, including a requirement that they identify and resolve significant differences in archetype designs and archetype model attributes, and agree on a common set of analysis model assumptions and criteria. Associated with this, the study could examine the extent to which observed variations in the analysis results are consistent with establishing the judgment-based variability in collapse assessment and acceptance criteria.

5.2.4 Consistent Archetype Periods

There is a need to better understand and reconcile significant differences in the calculated fundamental period, T_1, of some archetype models and the design period, $T = C_u T_a$, typical of actual building periods.

The fundamental vibration period formulas of ASCE/SEI 7-10 for steel moment frames, reinforced concrete moment frames and masonry and reinforced concrete shear walls are based on the recommendations of Chopra et al. (1998) and related studies (Goel and Chopra, 1997a, 1997b, and 1998). The formulas of ASCE/SEI 7-10 for the approximate period, T_a, represent lower-bound estimates (best fit minus 1σ) of the fundamental vibration periods of 42 steel moment frames, 37 reinforced concrete moment frames, and 16 reinforced concrete shear wall buildings measured during 8 major California earthquakes occurring between and including the 1971 San Fernando Earthquake and the 1994 Northridge Earthquake. The C_u factor modifies values of T_a to approximately represent upper-bound values of measured periods. These formulas are an update of those published in ATC 3-06, *Tentative Provisions for the Development of Seismic Regulations for Buildings*, (ATC, 1978) which introduced the notion of basing the period on measurements of actual buildings of comparable construction and height.

Comparison of archetype periods shows that the values of the analytical model period of short-period buildings tend to be shorter than the corresponding values of the actual building period which is based on measurements of the fundamental periods of actual buildings. Shorter analytical model periods are most likely due to omission of diaphragm, base/foundation, and other sources of flexibility that are typically not included in the analytical models of short-period buildings. Conversely, values of the analytical model period of tall buildings tend to be somewhat longer than the corresponding values of actual building period. In this case, longer analytical model periods could be due to omissions of stiffness effects of the gravity system, partition walls, or cladding, which are typically not included in the analytical models of tall buildings. Relatively poor computed performance of very short-period building archetypes is likely influenced by underestimation of building period (and the corresponding overestimation of ductility demand). Relatively poor computed performance of certain tall (very long-period or flexible) building archetypes may be influenced by overestimation of building period (and the corresponding overestimation of building drift).

5.2.5 Evaluation of Failures Governed by Higher-Mode Response

There is a need to improve current FEMA P-695 methods for evaluation of archetypes, or critical components of archetypes, whose response and associated failure is dominated by higher modes of vibration.

FEMA P-695 Methodology presumes collapse to be governed by large displacements of archetypes. Earthquake records are scaled to the design period, *T*, similar to incremental dynamic analysis methods, and the spectrum shape factor (*SSF*) is used to increase the collapse margin ratio (*CMR*) to account for changes in ground motion intensity anticipated for buildings responding beyond yield (i.e., due to period elongation). Potential overestimation of ground motion intensity at periods less than the design period is ignored assuming that such overestimation would not significantly affect archetype displacements and collapse performance. Findings of prior studies (summarized in Chapter 2) support this assumption and the associated methods of FEMA P-695. However, the topical study of overstrength that investigated response of force-controlled elements and the topical study of long-period buildings both found that failure can be significantly overestimated when failure is governed by higher modes of vibration at periods much less than that of the fundamental mode. In such cases, scaling of earthquake records to match ground motion intensity at the design period, *T*, is not appropriate.

5.2.6 Evaluation of Failures Governed by Force-Controlled Limit States

There is a need to improve current FEMA P-695 methods for evaluation of archetypes or critical components of archetypes whose response and associated failure is governed by force-controlled limit states.

A study should be undertaken to identify important design criteria that cannot be accurately evaluated by the current FEMA P-695 procedures and to develop appropriate adaptations to the FEMA P-695 procedures to consider these criteria. For example, the evaluation of diaphragm and collector forces revealed that force demands associated with higher mode response can be significantly overestimated by earthquake records scaled to first-mode response (first-mode period). More fundamentally, the current FEMA P-695 framework, which employs nonlinear analyses of models based on median properties, does not provide a rigorous basis to evaluate seismic design criteria for force-controlled components (except insofar as through the judgment-based procedures for determining the inherent variability in system response).

5.3 Specific Findings of Problem-Focused Studies

This section summarizes specific findings of the three problem-focused studies.

5.3.1 Short-Period Systems

Collapse Risk of Short-Period Buildings

Short-period buildings appear to have a greater risk of collapse than buildings with longer-periods, although the amount of additional collapse risk could not be reliably quantified.

Short-period systems appear to be at higher risk of collapse than systems with longer periods, particularly for archetypes with very short periods prone to relatively large residual displacements and ductility demands. However, the archetype models used in the study were too simplistic to accurately quantify the degree of additional risk and the associated amount of adjustment in seismic performance factors and related criteria (e.g., design base shear) that would be required to achieve approximate parity in collapse performance with that of archetypes with longer periods.

Realistic Archetype Models

More realistic archetype models of short-period systems are required to better represent experimental behavior and observed collapse performance of short-period buildings.

The topical study of short-period systems found results and trends in collapse performance similar to those of prior FEMA P-695 studies and previous research but not necessarily consistent with actual collapse damage observed for short-period buildings in earthquakes. In general, short-period building archetypes studied have very simple configurations (i.e., designs might not be realistic), have not incorporated all sources of flexibility (i.e., model periods could be unrealistically short), and evaluated collapse using conservative failure criteria. Significantly different collapse results would likely be found if more realistic models and associated failure criteria of short-period systems were used.

Improved Archetype Model Periods

Fundamental periods of short-period archetype models are often significantly shorter than those estimated using the actual building period, particularly for single-story systems with very stiff walls in plane.

The short-period studies using single-degree-of-freedom (SDOF) models generally show acceptable collapse performance for archetypes that have a model period of about 0.5 seconds, or greater, and very poor collapse performance for the same archetypes (i.e., same nonlinear behavior) that have a model period of 0.1 seconds, indicating the importance of the model period to collapse performance. Calculated periods of short-period models that do not fully incorporate all sources of flexibility can be significantly shorter than those of actual buildings, estimated using the period formula, $T = C_u T_a$. Results suggest that incorporation of diaphragm flexibility, base flexibility including foundation effects, and other sources of flexibility typical of real buildings would lengthen the calculated period of models with very short periods, decrease inelastic demand on initially stiff elements, and better represent collapse performance of the system of interest.

Improved Collapse Criteria

Failure of stiff wall elements in shear is likely too conservative as the collapse metric for evaluation of short and stiff shear wall systems (e.g., single-story structures).

Short and stiff shear wall systems are assumed to collapse when the wall fails (i.e., as characterized by significant loss of lateral strength). For a single-story archetype, shear failure can occur at relatively small displacements even for "ductile" systems (e.g., less than a drift ratio of about 0.01, or about 1 inch). Although stiff walls may have lost a significant fraction of their lateral strength at a displacement of about 1 inch, it is unlikely that a real building would have collapsed at this relatively small displacement. Results suggest that a more realistic displacement-based metric be developed for collapse evaluation of short and stiff shear wall systems.

5.3.2 Overstrength

Overstrength Criteria for Capacity Design of Force-Controlled Limit States

The traditional concept of system overstrength does not provide a reliable measure of the maximum force demands on force-controlled limit states and should be replaced with new "element overstrength criteria" for capacity design that distinguish between component force demands controlled by yielding of nearby components versus overall system response, and the sensitivity of collapse risk to failure of the force-controlled limit states.

Some force-controlled limit states are effectively controlled by ductile yielding behavior of nearby components, and relatively simple element-specific design provisions can yield reliable performance of the system, at least with regard to capacity design for these particular limit states. Examples of this include shear-force demands in beams and columns that are limited by flexural hinging in these components or connection-force demands in connections for braces that are designed to undergo inelastic yielding. Other force-controlled limit states are not currently amenable to simple element-specific design provisions and require more study. Examples include axial force in columns and diaphragm collector forces, especially in taller buildings.

Implementation of element overstrength criteria would require ASCE/SEI 7 to distinguish between "local" and "system" force-controlled limit state behavior, and the overall requirements for the application of both types would need to be improved.

For components whose force demands are governed by local behavior, requirements should be established based on the strength of the yielding components, the frequency with which the earthquake-induced force demands develop, and the consequence of component failure on system collapse.

For components whose force demands are governed by overall system behavior, procedures and criteria should be developed to determine force demands that may or may not be limited by the inelastic pushover strength of the structure. This procedure would take the place of the current amplified earthquake load equation that is based on overstrength system factors, Ω_O. To be effective, the procedure will likely need to differentiate and be tailored to specific systems, components, and limit states. As a minimum, such procedures should accurately evaluate forces in axial column forces because of overturning in moment frames and braced frames and because of supports under walls and discontinuous walls. The procedures should employ appropriate design factors to control the reliability index for failure of the force-controlled components. Default values of the overstrength factor, Ω_O, equal to 1.5 to 3 (depending on the component type) could be defined as an interim measure (for all structural systems) until more detailed provisions are developed.

Limitations of Static Pushover Analysis

The system overstrength, calculated based upon static pushover analysis, is not an accurate measure of maximum component forces that can develop in the structure.

Since pushover analysis is performed using an applied force distribution that is patterned after the first-mode response, the inelastic mechanisms and internal forces observed in the pushover analyses do not capture higher mode effects that can arise during dynamic inelastic response. As such, the calculation of overstrength by pushover analysis should be replaced with a more reliable method of determining maximum force demands. This has implications on both the FEMA P-695 Methodology, which specifies the use of static pushover analysis to calculate system overstrength factors, and on design standards that employ such factors to evaluate seismic demands on force-controlled components.

Consideration of Inelastic Response in Modeling Force-Controlled Limit States

Improved models and failure criteria are required to evaluate force-controlled limit states that account for limited inelastic response of the force-controlled actions.

Whereas the component actions associated with force-controlled limit states are often modeled as being infinitely rigid, this modeling assumption may overestimate the force demands on these limit states and components. This is particularly true where the force demands are due to high frequency input motions or higher mode response, which may occur in the lower stories of buildings where high frequency transients of the ground accelerations may be transmitted into the structure. For example, where inelastic shear deformations are not modeled in structural walls, the peak shear forces that are calculated may overestimate the failure probability. Alternatively, where floor diaphragms and collectors are modeled as rigid, the likelihood of failure is likely to be overestimated because the transient forces may have very short durations

(with little strain or deformation demands). Force demands and capacity checks in these situations are likely not realistic representations of actual force-controlled element failure and may overstate the risk of collapse resulting from their failure.

Frequency of Maximum Force Demands for Capacity-Design Limit States

Maximum force demands in capacity-designed elements can develop for ground motions that occur much more frequently than MCE_R ground motions.

Ground motions less intense (and more frequent) than MCE_R ground motions can cause full yielding of highly ductile (high R or R_M) systems, essentially increasing the likelihood of maximum forces occurring over the life of the building and associated risk of failure of force-controlled elements (e.g., due to uncertainty in element capacity). Therefore, force-controlled components whose failure may precipitate collapse may require higher margins than other components to achieve comparable collapse risk to that implied by the FEMA P-695 Methodology.

Improved Design Requirements for Diaphragm Collectors

There is a need for improvement of the calculation of force demands and capacity requirements in diaphragm collectors, considering the possibility of limited inelastic response of collectors and diaphragms.

The overstrength study indicates that current building code requirements appear to significantly underestimate collector force demands, even where the system overstrength factor is considered in the design. Therefore, a study should be undertaken to establish more accurate provisions for determining force demands in diaphragms and collectors. Such a study should consider how collector forces are affected by both inertia effects and inelastic force redistributions in the structure and by the dynamic response of floor diaphragms and collectors, considering the beneficial effects of inelasticity in the diaphragms and collectors. This will likely require the definition of new archetype configurations and analysis models that accurately reflect diaphragm behavior, in contrast to the simplified archetype models used in the overstrength study of Appendix C, where the diaphragm and collectors were modeled as rigid. The proposed study should also consider whether it is appropriate and necessary to design collectors for a larger safety margin, which is implied by current design requirements that apply overstrength factors to the design of collector elements but not to the floor diaphragms to which they are attached.

Reliability-Based Criteria for Capacity Design

There is a need for development of a reliability-based procedure to establish force demand and capacity criteria for capacity design of force-controlled components that are consistent with the collapse risk implied in ASCE/SEI 7-10.

For force-controlled components where the imposed force demands are due to yielding of adjacent members, efforts should be continued to develop and refine a reliability-based methodology that can be employed by specification committees to develop risk-consistent capacity design factors and requirements for design by elastic analysis. This could, for example, employ a methodology that is similar to the first-order second moment methods employed in the original development of Load Resistance Factor Design provisions, except that the force demands are determined based on the yielding deformation-controlled elements. The method should incorporate consideration of factors that increase the overstrength, including the following: (1) differences between the design strength and expected strengths of structural components; (2) oversizing of members, due to drift limits, architectural constraints, or other reasons; and (3) influence of system redundancy and strain hardening behavior on the maximum forces developed in a system. The underlying reliability factors (reliability index) should be consistent with the collapse risk implied by the FEMA P-695 and ASCE/SEI 7-10 procedures.

5.3.3 Long-Period Systems

Tall Building Design for Minimum Base Shear

In lieu of current drift limits, it appears that long-period systems could be designed for minimum base shear to achieve acceptable collapse risk, although the specific form and appropriate values of minimum base shear could not be determined.

Studies of a limited number of long-period systems indicate that tall buildings designed for appropriate minimum base shear criteria (in lieu of current drift limits) would achieve acceptable collapse probabilities consistent with other (shorter period) buildings. However, additional studies of other long-period systems are required to establish the specific form and appropriate values of minimum base shear criteria and to verify that elimination of current drift limits would not adversely affect other performance characteristics of tall buildings, such as adequate stiffness to preclude occupant motion sickness.

Improved Archetype Model Periods

Fundamental periods of long-period archetype models can be significantly longer than those of actual buildings, particularly for tall slender core-wall buildings.

Fundamental periods calculated for tall (core-wall) archetype models used in this study are substantially longer than the periods of actual tall buildings of comparable height, estimated using the period formula, $T = C_u T_a$. The degree to which these longer periods might influence collapse performance is not known, although shorter, more representative, values of the fundamental period would not be expected to eliminate issues with higher-mode domination of response of very tall structures.

Shear-Related Collapse Failure Mode Models

Performance of tall, core-wall buildings was found to be highly dependent on the assumptions used to model shear-related collapse failure modes.

Tall core-wall buildings that develop a single flexural hinge at the base of the wall under earthquake loading also develop base shear demands that greatly exceed those determined using linear analysis methods. As a result, collapse performance was found to be very different for long-period archetypes modeled with and without non-simulated shear-related failure modes. Tall core-wall archetypes modeled without non-simulated shear-related failure modes have acceptably low probabilities of collapse. The same archetypes modeled with non-simulated shear-related failure modes have very poor collapse performance.

Although assumptions used to model shear-related failure are likely conservative, the high base shear demand-capacity ratios observed when the shear-related failure criterion is not employed suggest that the issue cannot be ignored. There is a need for additional research for the following reasons: (1) to verify that this amplification of base shear is unique to concrete core walls; (2) to verify that shear demand and collapse risk computed using the shear-related failure criterion are not exacerbated by scaling ground motions at the fundamental period, which determines demands for long-period structures; and (3) to develop capacity-based shear design procedures for core-wall systems.

Design Using Response Spectrum Analysis Methods

Tall building collapse performance was found to be inferior for long-period archetypes designed using modal response spectrum analysis (RSA) methods than for the same archetype configurations designed using equivalent lateral force (ELF) methods.

Tall core-wall building archetypes designed using RSA methods (except when base shear was scaled to 100% of the ELF value, rather than 85% of the ELF value as currently permitted by ASCE/SEI 7-10), had collapse performance only slightly worse than the same archetype configurations designed using ELF methods. It may be assumed that collapse performance of these tall core-wall building archetypes designed using RSA methods would be substantially worse than the corresponding archetypes designed using ELF methods if the RSA designs had been based on 85% of ELF base shear. Prior FEMA P-695 studies also found inferior collapse performance for building archetypes designed using the RSA design method.

Collapse Risk of Tall Core-Wall Buildings

Results of FEMA P-695 evaluations suggest that tall core-wall buildings designed to the minimum requirements of ASCE/SEI 7-10 could pose a potentially significant and unacceptable collapse risk.

A number of assumptions and factors affect the data supporting this finding. Factors that could be expected to reduce collapse risk include the following:

- The non-simulated collapse criterion used to determine the impact on collapse risk of shear demand-capacity ratio is likely conservative for core walls,
- MCE_R demands are defined by spectral acceleration at the fundamental mode; this may not be appropriate for long-period structures for which higher modes determine response,
- The core walls designed for this project were not designed to exhibit significant inelastic action above the base,
- Development of a second flexural hinge above the base of the structure could reduce shear demand, and
- Core-wall buildings designed in practice are designed to achieve strength and performance objectives beyond those associated with earthquake demands, typically resulting in thicker walls with higher shear strength and shorter fundamental period.

It should also be noted that core walls designed as part of this study were designed per the recommendations of *Guidelines for Performance-Based Seismic Design of Tall Buildings* (PEER, 2010), to achieve a shear stress demand under design loads of $2\sqrt{f_c'}$ psi and to have the maximum shear strength allowed by ACI 318-08, *Building Code Requirements for Structural Concrete* (ACI, 2008); this is a more conservative approach to design for shear than is required by ASCE/SEI 7-10 and typically employed in practice.

5.4 Recommendations for Reformulation of Seismic Design Parameters

This section provides recommendations for reformulation and improvement of current ASCE/SEI 7-10 design requirements including new values of seismic performance factors and recommendations for future studies to support reformulation.

5.4.1 Proposed Reformulation of Current Criteria

The reformulation concepts described in Section 4.4 are recommended for consideration by seismic code committees, including the Provisions Update Committee (PUC) of the Building Seismic Safety Council and the Seismic

Subcommittee (SSC) of the ASCE 7 Standards Committee of the American Society of Civil Engineers. The PUC is currently developing new material for the 2014 Edition of the *NEHRP Recommended Seismic Provisions for New Buildings and Other Structures* (2014 *NEHRP Provisions*) that, if adopted, would also be considered by the SSC for possible incorporation in ASCE/SEI 7-16.

Although the list of proposed reformulation topics is relatively short and primarily conceptual (i.e., commentary material), proper incorporation into the 2014 *NEHRP Provisions* (and subsequently ASCE/SEI 7-16) requires significant work by the responsible seismic code committees. In particular, proposed changes, such as basing design directly on MCE_R ground motions, have implications for a number of current design earthquake-based criteria sprinkled throughout various sections of the 2009 *NEHRP Provisions* and ASCE/SEI 7-10 that would require careful review and modification. For example, current drift limits and stability criteria based on the design earthquake would require changes to apply to MCE_R shaking intensity.

There would also be opportunities for greatly simplifying current design requirements. For example, current ASCE/SEI 7-10 design requirements for seismically isolated structures (Chapter 17) and structures with damping systems (Chapter 18) that are now based on both the design earthquake and MCE_R ground motions could be significantly shortened to be based solely on MCE_R ground motions in the future.

5.4.2 Risk-Based Concepts

Proposed reformulation of current criteria, recommended above, addresses improvements to the 2014 *NEHRP Provisions* and ASCE/SEI 7-16 specific to structural design to meet life-safety (collapse) risk objectives. It is recommended that the seismic code committees consider conceptual framework described in Section 4.7 for expanding risk-based criteria to address functional and economic, as well as life-safety objectives, and to address nonstructural, as well as structural systems.

These concepts are already being considered for inclusion in the 2014 *NEHRP Provisions*. However, the scope of the PUC effort is necessarily limited to defining risk and performance objectives (i.e., replacing the hypothetical criteria shown in Table 4-6 with PUC-approved criteria), and does not include development of new, or revision of existing, design requirements necessary to reliably implement these objectives. A major study similar to that of the ATC-63 Project, which developed the collapse risk-based methodology of FEMA P-695, would likely be required to develop risk-based design criteria to meet functional and economic performance objectives.

5.4.3 New Seismic Ground Motion Data

New seismic ground motion data are recommended for development by the U.S. Geological Survey, as part of their ongoing National Seismic Hazard Mapping Project. These new data include set(s) of risk-based ground motions (in addition to the current set of MCE_R ground motions) and ground motion data at response periods ranging from 0.1 to 10 seconds (in addition to current response periods of 0.2 seconds and 1.0 second).

New sets of seismic ground motion data will be required for risk-based design to meet functional or economic performance objectives. These ground motion sets can be developed from the same set of hazard functions used to calculate MCE_R ground motions, although the process or calculation may be somewhat different to address different risk objectives.

New data at response periods ranging from 0.1 to 10 seconds will be required for description of multi-period design spectra (as described in Section 4.6). The new response periods should be sufficient in number and their values spaced as required to permit accurate linear interpolation of ground motions at other response periods within the range of interest.

5.4.4 Investigation and Validation of Risk Objectives

ASCE/SEI 7-10 Table C.1.3.1b lists anticipated life-safety risk objectives for Risk Category I and Risk Category II structures as 10% probability of collapse conditioned on the occurrence of MCE_R ground motions, which is based on the acceptance criteria of FEMA P-695. FEMA P-695 studies found that a conditional probability of 10% was not inconsistent with the anticipated collapse performance of existing systems. ASCE/SEI 7-10 Table C.1.3.b also lists conditional collapse probabilities of 6% for Risk Category III structures and 3% for Risk Category IV structures, based loosely on the 10% conditional collapse probability objective for Risk Category II structures. However, in a broader context, whether the stakeholders who are actually at risk of death or serious injury consider these collapse objectives as providing adequate life-safety protection should be considered.

Further, do the life-safety (collapse) objectives provide acceptable performance for other related risks? For example, the Canterbury Earthquake of February 2011, which caused extended closure of the city center of Christchurch, New Zealand, and had a severe impact on the economy and function of the city (and the nation), destroyed, but did not collapse, more than 10% of the buildings and killed less than 200 people. Arguably, life-safety (collapse) objectives were met for ground motions essentially of MCE_R intensity, but the impact of extensive building damage on the city and society were not acceptable to the stakeholders.

Thus, risk objectives, including economic and functional as well as life-safety objectives that are used by seismic code committees to establish design requirements, should be selected in terms of anticipated damage and loss and overall impact to the affected city or region, not just in terms of damage or failure of the elements of an individual building. Although well beyond the scope of FEMA P-695 study, it is recommended that the risk objectives used to develop seismic code requirements be investigated and validated, perhaps using earthquake loss technologies such as that of HAZUS-MH (FEMA, 2012a) or FEMA P-58 (FEMA, 2012b) to relate regional earthquake consequences to specific building risk objectives.

Appendix A
Data from Prior Studies

A.1 Compilation of Design Properties, Nonlinear Analysis Results, and Collapse Evaluation Parameters

Design properties, nonlinear analysis results, and collapse performance parameters for each archetype of each performance group of each of the ten seismic-force-resisting systems of interest studied in the FEMA P-695 and NIST GCR 10-917-8 reports were compiled. Table A-1 summarizes the seismic design criteria for 35 performance groups, including two special steel moment frame archetypes designed using RSA methods, which were excluded from the considerations in Chapter 2, in each of the ten seismic force-resisting systems (using ASCE/SEI 7-10 system labels).

Table A-2 and Table A-3 contain values of design properties, nonlinear analysis results and collapse evaluation parameters that are representative of the archetypes of the performance group of interest (e.g., average of individual archetype values). Table A-2 summarizes representative values of design properties for each of the 35 selected performance groups. Values of Seismic Design Categories (SDC) are also shown to represent the seismic design level that controls collapse performance. Table A-3 summarizes representative values of nonlinear analysis results for each of the 35 selected performance groups (corresponding to the seismic design criteria of Table 2-3).

Table A-1 ASCE/SEI 7-10 Seismic Design Criteria of Previously Evaluated Seismic Force-Resisting Systems

Performance Group (PG) Reference Number	PG No. of Prior Study	System ID No.	Seismic Force-Resisting System Design Criteria - ASCE 7-10 Table 12.2-1							
			Design Coefficients and Factors			Structural System and Height Limits (ft.) Seismic Design Category (SDC)				
			R	Ω_O	C_d	B	C	D	E	F
Bearing Wall Systems										
A.7.H.S A.7.H.L A.7.L.S A.7.L.L	PG-1S PG-2S PG-5S PG-6S	A.7	5	2.5	3.5	NL	NL	160	160	100
A.9.H.S A.9.H.L A.9.L.S A.9.L.L	PG-1O PG-2O PG-5O PG-6O	A.9	2	2.5	1.75	NL	160	NP	NP	NP
A.15.L.S A.15.L.L A.15.H.S A.15.H.L	PG-1 PG-4 PG-9 PG-12	A.15	6.5	3	4	NL	NL	65	65	65
Building Frame Systems										
B.2.2X.S B.2.2X.L	PG-1SCB PG-2SCB	B.2	6	2	5	NL	NL	160	160	100
B.4.H.S B.4.H.L B.4.L.S B.4.L.L	PG-1S PG-2S PG-5S PG-6S	B.4	6	2.5	5	NL	NL	160	160	100
B.5.H.S B.5.H.L B.5.L.S B.5.L.L	PG-1O PG-2O PG-5O PG-6O	B.5	5	2.5	4.5	NL	NL	NP	NP	NP
B.25.S B.25.L	PG-3BRB PG-4BRB	B.25	8	2.5	5	NL	NL	160	160	100
Moment Frame Systems										
C.1.ESA.S C.1.ESA.L C.1.RSA.S C.1.RSA.L	PG-1ELF PG-2ELF PG-1RSA PG-2RSA	C.1	8	3	5.5	NL	NL	NL	NL	NL
C.5.P.S C.5.P.05.L C.5.P.L	PG-5 PG-6 PG-6(R)	C.5	8	3	5.5	NL	NL	NL	NL	NL
C.7.S.L C.7.P.L C.7.S.L (C) C.7.P.L (C)	PG-10 PG-14 PG-18 PG-17	C.7	3	3	2.5	NL	NP	NP	NP	NP

Table A-2 Representative Design Properties of Selected Performance Groups of Previously Evaluated Systems

Performance Group (PG) Reference Number	Archetype Design Properties - Average/Typical Value of Governing PG								
	PG No. of Prior Study	No. of Stories	Gravity Loads	Seismic Design Criteria					
				SDC	*R*	*T* (sec)	T_1 (sec)	*V/W*	$S_{MT}(T)$ (g)
Bearing Wall Systems									
A.7.H.S	PG-1S	1,2,4	High	D_{max}	5	0.32	0.15	0.20	1.50
A.7.H.L	PG-2S	8,12	High	D_{max}	5	0.89	0.74	0.14	1.05
A.7.L.S	PG-5S	1,2,4	Low	D_{max}	5	0.32	0.16	0.20	1.50
A.7.L.L	PG-6S	8,12	Low	D_{max}	5	0.89	0.77	0.14	1.05
A.9.H.S	PG-1O	1,2	High	C_{max}	2	0.27	0.15	0.25	0.75
A.9.H.L	PG-2O	4,8,12	High	C_{max}	2	0.79	0.62	0.14	0.43
A.9.L.S	PG-5O	1,2	Low	D_{max}	2	0.27	0.14	0.25	0.75
A.9.L.L	PG-6O	4,8,12	Low	D_{max}	2	0.79	0.64	0.14	0.43
A.15.L.S	PG-1	1,2,3	Nominal	D_{max}	6.5	0.29	0.48	0.17	1.50
A.15.L.L	PG-4	3	Nominal	D_{min}	6.5	0.41	0.93	0.06	0.75
A.15.H.S	PG-9	1,2,3,4,5	Nominal	D_{max}	6.5	0.37	0.45	0.17	1.50
A.15.H.L	PG-12	3,4,5	Nominal	D_{min}	6.5	0.51	0.80	0.06	0.75
Building Frame Systems									
B.2.2X.S	PG-1SCB	2,3	Typical	D_{max}	6	0.38	0.49	0.17	1.50
B.2.2X.L	PG-2SCB	6,12,16	Typical	D_{max}	6	1.30	2.04	0.08	0.76
B.4.H.S	PG-1S	1,2,4	High	D_{max}	6	0.36	0.44	0.17	1.50
B.4.H.L	PG-2S	8,12	High	D_{max}	6	1.02	0.88	0.11	0.90
B.4.L.S	PG-5S	1,2,4	Low	D_{max}	6	0.36	0.47	0.17	1.50
B.4.L.L	PG-6S	8,12	Low	D_{max}	6	1.02	0.98	0.11	0.90
B.5.H.S	PG-1O	1,2	High	C_{max}	5	0.28	0.31	0.10	0.75
B.5.H.L	PG-2O	4,8,12	High	C_{max}	5	0.85	0.66	0.05	0.39
B.5.L.S	PG-5O	1,2	Low	D_{max}	5	0.28	0.31	0.10	0.75
B.5.L.L	PG-6O	4,8,12	Low	D_{max}	5	0.85	0.69	0.05	0.39
B.25.S	PG-3BRB	2,3	Typical	D_{min}	8	0.61	0.97	0.05	0.54
B.25.L	PG-4BRB	6,12,16	Typical	D_{min}	8	2.09	3.55	0.02	0.16
Moment Frame Systems									
C.1.ESA.S	PG-1ELF	1,2	Typical	D_{max}	8	0.45	0.79	0.13	1.50
C.1.ESA.L	PG-2ELF	4,8,12,20	Typical	D_{max}	8	2.16	1.89	0.06	0.64
C.1.RSA.S	PG-1RSA	1,2	Typical	D_{max}	8	0.45	0.81	0.11	1.50
C.1.RSA.L	PG-2RSA	4,8,12,20	Typical	D_{max}	8	2.88	2.88	0.05	0.54
C.5.P.S	PG-5	1,2	Low	D_{max}	8	0.36	0.54	0.13	1.50
C.5.P.05.L	PG-6	4,8,12,20	Low	D_{max}	8	1.95	1.87	0.05	0.60
C.5.P.L	PG-6(R)	4,8,12,20	Low	D_{max}	8	1.95	1.87	0.06	0.60
C.7.S.L	PG-10	2,4,8,12	High	B_{max}	3	1.40	1.84	0.04	0.20
C.7.P.L	PG-14	2,4,8,12	Low	B_{max}	3	1.40	2.75	0.04	0.20
C.7.S.L (C)	PG-18	4,12	Low	C_{max}	3	1.58	1.94	0.05	0.24
C.7.P.L (C)	PG-17	4,12	Low	C_{max}	3	1.58	2.62	0.05	0.24

Table A-3 Representative Nonlinear Analysis Results of Selected Performance Groups of Previously Evaluated Systems

Performance Group (PG) Reference Number	Nonlinear Analysis Results (average/typical value of governing performance groups)							
	PG No. of Prior Study	NSA	*NDA*			*CMR Adjustment*		
		Ω	$S_{MT}(T)$ (g)	$S_{CT}(T)$ (g)	*CMR*	μ_T	*SSF*	*ACMR*
Bearing Wall Systems								
A.7.H.S	PG-1S	2.00	1.50	1.61	1.07	8.4	1.31	1.41
A.7.H.L	PG-2S	1.75	1.05	1.65	1.63	10.5	1.41	2.30
A.7.L.S	PG-5S	1.80	1.50	1.94	1.29	8.3	1.31	1.71
A.7.L.L	PG-6S	1.53	1.05	1.65	1.63	28.2	1.44	2.33
A.9.H.S	PG-1O	1.89	0.75	1.07	1.42	2.1	1.06	1.51
A.9.H.L	PG-2O	2.08	0.43	0.56	1.35	5.2	1.14	1.54
A.9.L.S	PG-5O	1.91	0.75	1.41	1.87	2.1	1.06	1.98
A.9.L.L	PG-6O	1.67	0.43	0.89	2.26	7.4	1.17	2.69
A.15.L.S	PG-1	2.17	1.50	2.14	1.43	9.8	1.32	1.89
A.15.L.L	PG-4	2.10	0.75	1.98	2.64	7.0	1.13	2.98
A.15.H.S	PG-9	3.42	1.50	2.85	1.90	7.7	1.31	2.48
A.15.H.L	PG-12	3.57	0.75	2.12	2.82	6.3	1.13	3.18
Building Frame Systems								
B.2.2X.S	PG-1SCB	1.43	1.50	1.95	1.30	5.2	1.25	1.64
B.2.2X.L	PG-2SCB	1.66	0.76	1.97	2.68	2.5	1.25	3.37
B.4.H.S	PG-1S	1.98	1.50	1.69	1.13	14.7	1.33	1.50
B.4.H.L	PG-2S	1.54	0.90	1.91	2.16	20.5	1.47	3.18
B.4.L.S	PG-5S	2.08	1.50	1.97	1.32	11.3	1.33	1.75
B.4.L.L	PG-6S	1.70	0.90	1.97	2.18	29.5	1.47	3.20
B.5.H.S	PG-1O	2.85	0.75	1.16	1.55	33.5	1.14	1.77
B.5.H.L	PG-2O	3.43	0.39	1.66	4.76	37.0	1.21	5.87
B.5.L.S	PG-5O	2.85	0.75	1.16	1.16	33.5	1.14	1.77
B.5.L.L	PG-6O	2.36	0.39	1.87	5.23	61.7	1.21	6.42
B.25.S	PG-3BRB	1.78	0.54	1.20	2.44	8.6	1.17	2.87
B.25.L	PG-4BRB	1.29	0.16	0.53	3.48	3.8	1.21	4.20
Moment Frame Systems								
C.1.ESA.S	PG-1ELF	4.16	1.50	3.62	2.41	4.2	1.24	2.97
C.1.ESA.L	PG-2ELF	3.67	0.61	1.04	1.57	3.2	1.22	1.94
C.1.RSA.S	PG-1RSA	4.70	1.50	3.57	2.37	3.9	1.22	2.91
C.1.RSA.L	PG-2RSA	2.61	0.54	0.76	1.37	3.0	1.28	1.76
C.5.P.S	PG-5	1.70	1.50	2.01	1.34	16.8	1.33	1.79
C.5.P.05.L	PG-6	1.88	0.60	0.82	1.23	8.1	1.50	1.84
C.5.P.L	PG-6(R)	1.63	0.60	0.90	1.49	9.4	1.53	2.27
C.7.S.L	PG-10	3.20	0.20	0.42	2.08	3.6	1.17	2.44
C.7.P.L	PG-14	1.60	0.20	0.39	1.91	3.3	1.15	2.20
C.7.S.L (C)	PG-18	2.40	0.24	0.44	1.78	4.0	1.20	2.12
C.7.P.L (C)	PG-17	1.45	0.24	0.33	1.29	2.9	1.15	1.48

Appendix B
Study of Short-Period Systems

B.1 Introduction

Prior studies summarized in Chapter 2 found that there was a general trend that structures with shorter fundamental periods of vibration ($T_1 \leq 0.6$s) were more likely to fail the acceptance criteria than structures with longer periods ($T_1 > 0.6$s) of the same basic structural material and configuration. In the FEMA P-695 report, *Quantification of Building Seismic Performance Factors* (FEMA, 2009), none of the systems with shorter periods actually failed the acceptance criteria, but these systems tended to have the lowest ratio of computed Adjusted Collapse Margin Ratio (*ACMR*) to the acceptable *ACMR* for individual archetypes ($ACMR_{20\%}$) of a given performance group. Problems with short-period archetypes were particularly evident in the special reinforced masonry and special reinforced concrete shear wall systems evaluated in the NIST GCR 10-917-8 report, *Evaluation of the FEMA P-695 Methodology for Quantification of Building Seismic Performance Factors* (NIST, 2010), where several of the short-period systems failed or came close to failing the acceptance criterion. The "short-period problem" has been recognized for decades and is attributed to the use of *R* factors in the region of the design acceleration spectrum where it is recognized that the "equal-displacement" basis of seismic response is not applicable. A variety of approaches have been developed for dealing with the problem.

The most common approach is to reduce the value of *R* as periods decrease below 0.6 seconds (while maintaining the detailing requirements that would be associated with a higher *R* factor). A related problem in the low-period region is the use of C_d to adjust computed elastic design level displacements up to the expected inelastic displacements. This adjustment, which is also based on the equal-displacement concept, is theoretically applicable only to longer-period systems and may be unconservative for systems with very short periods. Thus, adjustments (reductions) to *R* for short-period systems may need to be accompanied by increased values of C_d (or multipliers on C_d). Chapter 4 suggests the term C_{ds} for the short-period displacement multiplier.

A second approach that has been recommended for short-period systems is to increase the ductility supply of the systems as the period reduces. More detail will be provided on this approach in Section B.3.

In both of the above approaches, the solution attempts to force short-period systems to be designed on the basis of a paradigm that applies only to systems with longer periods. Thus, a third way to resolve the short-period problem is to recognize that the traditional approach of dissipating energy through inelastic material behavior is not viable for systems with extremely short periods. Instead, the system could be designed to respond through controlled sliding or rocking but with limited displacements so that the nonstructural system is protected.

A final possible approach is to make no modifications to design rules or system behavior and accept the increased probability of collapse (from the perspective of FEMA P-695 Methodology) on the basis that there is little experimental or post-earthquake evidence that the short-period problem exists outside of the theoretical arena. Additionally, it should be noted that the non-simulated collapse metrics used in prior studies were not particularly realistic for these buildings because a total system collapse (complete loss of the structure) would not occur as a result of the non-simulated collapse parameter being exceeded. As described later, however, the opposite argument might be made in those cases where serious loss of strength in a system, such as complete loss of bracing at a story, was not used as a non-simulated collapse parameter.

These and other issues related to the short-period problem are discussed in the remainder of this appendix. Section B.2 summarizes the short-period issues observed in the test applications of the FEMA P-695 Methodology in the NIST GCR 10-917-8 Report. In Section B.3, the short-period problem is addressed from both a historical and theoretical basis. This review helps to set the stage for detailed analysis of short-period archetypes of special reinforced masonry shear walls and buckling-restrained braced frame systems, presented in Section B.4. Section B.5 presents observations and findings, Section B.6 provides recommendations and Section B.7 lists possible future studies on short-period systems.

B.2 Short-Period Issues Identified in the NIST GCR 10-917-8 Report

Table B-1 summarizes the results of the special reinforced masonry shear wall systems studied in the NIST GCR 10-917-8 Report, with archetypes of 1, 2, 4, and 8 stories. Twelve-story systems were also analyzed but these are not included in Table B-1. As may be observed, where all of the one-story systems failed and one of the two-story systems failed, all of the 4- and 8-story systems passed the acceptance criterion, which is ratio of computed $ACMR$ to $ACMR_{20\%} \geq 1$. Table B-2 provides a similar summary for the special reinforced concrete shear wall systems, where it is observed that all of the one- and two-story systems failed or came very close to failing (note ratio less than 1.05 for S16). Gray shading in these tables indicates systems that failed the acceptance criterion.

In Table B-1 and Table B-2 the period of vibration, T, shown in the tables is the calculated empirical period $C_u T_a$, with a lower limit of 0.25 seconds as specified in the FEMA P-695 report, whereas the T_1 column is computed by using an eigenvalue analysis. In Table B-1, T_1 values for 1-, 2-, and 4-story masonry wall models are consistently less than the T values. For example, the computed eigenvalue period for the two-story S2 masonry archetype is 0.13 seconds, while the empirical period is 0.26 seconds. The opposite is true for the two-story S2 reinforced concrete wall archetype in Table B-2, where the computed eigenvalue period, 0.50 seconds, is greater than the empirical period of 0.31 seconds.

In the eigenvalue analysis for the computation of periods, all of the analytical models were based on a rigid support condition, not including the flexibility inherent in the underlying soils. This issue is revisited later in this report, where it is shown that computed periods would be significantly increased if foundation flexibility were included in the analysis.

Table B-1 Summary of Results for Special Reinforced Masonry Shear Wall Systems

Archetype	NS	SDC	Grav.	T (sec)	T_1(sec)	Ω	$ACMR$	$ACMR_{20\%}$	$ACMR/ACMR_{20\%}$
S1	**1**	**D_{max}**	**High**	**0.25**	**0.10**	**1.84**	**0.66**	**1.56**	**0.42**
S2	**2**	**D_{max}**	**High**	**0.26**	**0.13**	**2.28**	**1.52**	**1.56**	**0.97**
S3	4	D_{max}	High	0.45	0.21	1.87	2.06	1.56	1.32
S4	8	D_{max}	High	0.75	0.55	1.89	1.76	1.56	1.13
S6	**1**	**D_{min}**	**High**	**0.25**	**0.14**	**1.62**	**1.19**	**1.56**	**0.76**
S7	2	D_{min}	High	0.28	0.19	2.61	2.18	1.56	1.40
S8	4	D_{min}	High	0.48	0.35	1.65	1.88	1.56	1.21
S9	8	D_{min}	High	0.80	1.12	1.63	2.03	1.56	1.30
S11	**1**	**D_{max}**	**Low**	**0.25**	**0.10**	**1.84**	**0.66**	**1.56**	**0.42**
S12	2	D_{max}	Low	0.26	0.13	1.82	2.27	1.56	1.46
S13	4	D_{max}	Low	0.45	0.26	1.73	2.19	1.56	1.40
S14	8	D_{max}	Low	0.75	0.61	1.59	1.82	1.56	1.17
S16	**1**	**D_{min}**	**Low**	**0.25**	**0.14**	**1.62**	**1.19**	**1.56**	**0.76**
S17	2	D_{min}	Low	0.28	0.21	1.80	2.71	1.56	1.74
S18	4	D_{min}	Low	0.48	0.43	1.41	1.88	1.56	1.21
S19	8	D_{min}	Low	0.80	1.16	1.64	2.05	1.56	1.37

NS: Number of stories

Gray shading highlights systems that failed the acceptance criterion.

Table B-2 Summary of Results for Special Reinforced Concrete Shear Wall Systems

Archetype	NS	SDC	Grav.	T(sec)	T_1(sec)	Ω	$ACMR$	$ACMR_{20\%}$	$ACMR/ACMR_{20\%}$
S1	**1**	**D_{max}**	**High**	**0.25**	**0.26**	**2.39**	**1.05**	**1.56**	**0.67**
S2	**2**	**D_{max}**	**High**	**0.31**	**0.50**	**1.82**	**1.50**	**1.56**	**0.96**
S3	4	D_{max}	High	0.52	0.55	1.72	1.96	1.56	1.25
S4	8	D_{max}	High	0.87	0.76	1.45	2.68	1.56	1.72
S6	**1**	**D_{min}**	**High**	**0.25**	**0.25**	**2.98**	**1.60**	**1.56**	**1.03**
S7	**2**	**D_{min}**	**High**	**0.31**	**0.38**	**1.83**	**1.40**	**1.56**	**0.90**
S8	4	D_{min}	High	0.52	0.53	2.91	3.42	1.56	2.19
S9	8	D_{min}	High	0.87	0.71	4.44	5.71	1.56	3.66
S11	**1**	**D_{max}**	**Low**	**0.25**	**0.26**	**2.39**	**1.05**	**1.56**	**0.60**
S12	**2**	**D_{max}**	**Low**	**0.31**	**0.50**	**1.82**	**1.50**	**1.56**	**0.96**
S13	4	D_{max}	Low	0.52	0.66	2.03	2.70	1.56	1.73
S14	8	D_{max}	Low	0.87	0.73	1.89	3.22	1.56	2.06
S16	1	D_{min}	Low	0.25	0.25	2.98	1.60	1.56	1.03
S17	**2**	**D_{min}**	**Low**	**0.31**	**0.38**	**1.83**	**1.40**	**1.56**	**0.90**
S18	4	D_{min}	Low	0.52	0.53	1.85	3.42	1.56	2.19
S19	8	D_{min}	Low	0.87	0.74	5.64	2.21	1.56	1.42

NS: Number of stories

Gray shading highlights systems that failed the acceptance criterion.

Next, it is important to look at the empirical and computed periods in the context of the design spectrum and in relation to the median ground motion spectrum used in the FEMA P-695 analysis of the systems.

Figure B-1 shows the response spectrum for Seismic Design Category (SDC) D_{max} and D_{min} for Maximum Considered Earthquake (MCE) level ground motions. The figure also shows spectral acceleration values computed at periods determined by eigenvalue analysis for the 1-, 2-, and 4-story masonry systems with heavy gravity load. As may be seen, all of the points lie on the constant acceleration part of the spectrum with the exception of the 1-story SDC D_{max} archetype, which falls just to the left of the $0.2T_s$ transition period. This plot can be used to dispel the notion that systems with very short periods have reserve capacity because they are designed for the peak amplified acceleration, whereas the true spectrum tends towards the peak ground acceleration as T approaches zero. It is highly unlikely that any real building structure will have a computed period less than $0.2T_s$, and only one archetype (the one shown in Figure B-1) in the entire set of archetypes run for the NIST GCR 10-917-8 studies had such a low period.

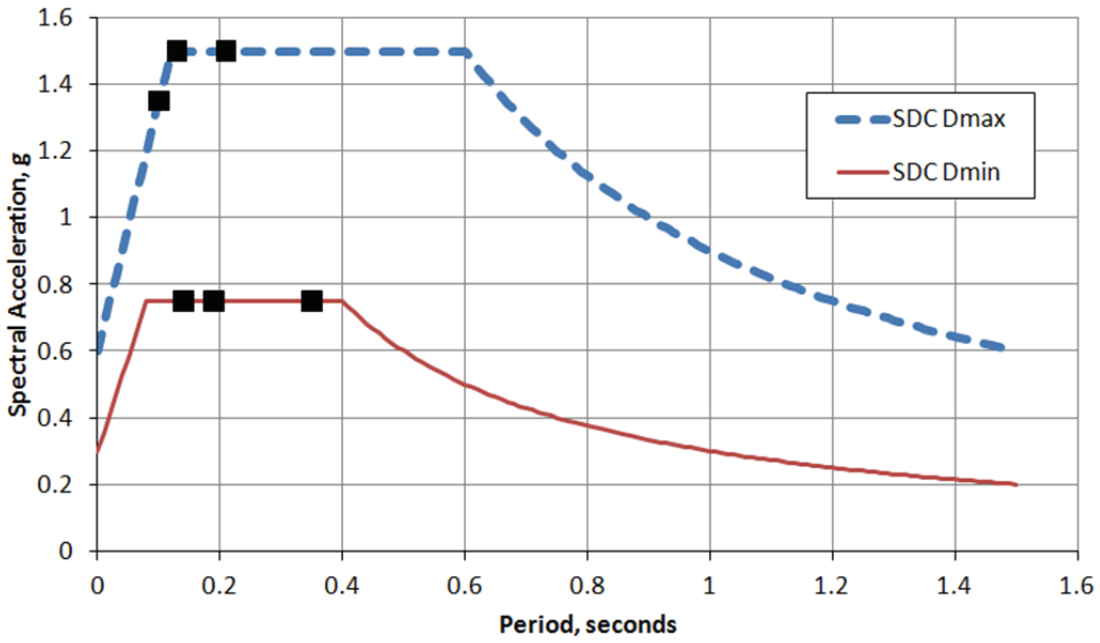

Figure B-1 MCE spectrum and spectral ordinates for the 1-, 2-, and 4-story (heavy gravity load) reinforced masonry shear wall archetypes.

Figure B-2 shows the median MCE ground motion spectrum for all (44) of the far-field records from FEMA P-695 as compared to the design spectrum, where the median spectrum has been scaled to match the design spectrum at periods of 0.2, 0.4, and 0.6 seconds. This figure indicates that median spectral accelerations from the ground motions are similar to the spectral accelerations computed from the design spectrum when matched to periods of 0.2 and 0.4 seconds. For the 0.6 second match, there is a 30% increase in ground motion accelerations relative to the code spectrum, but these would be applicable at the higher modes, which do not contribute significantly to the response of the short-period systems. Differences in ground motion spectra and design spectra are likely not a significant contributor to the relatively poor performance of the short-period systems.

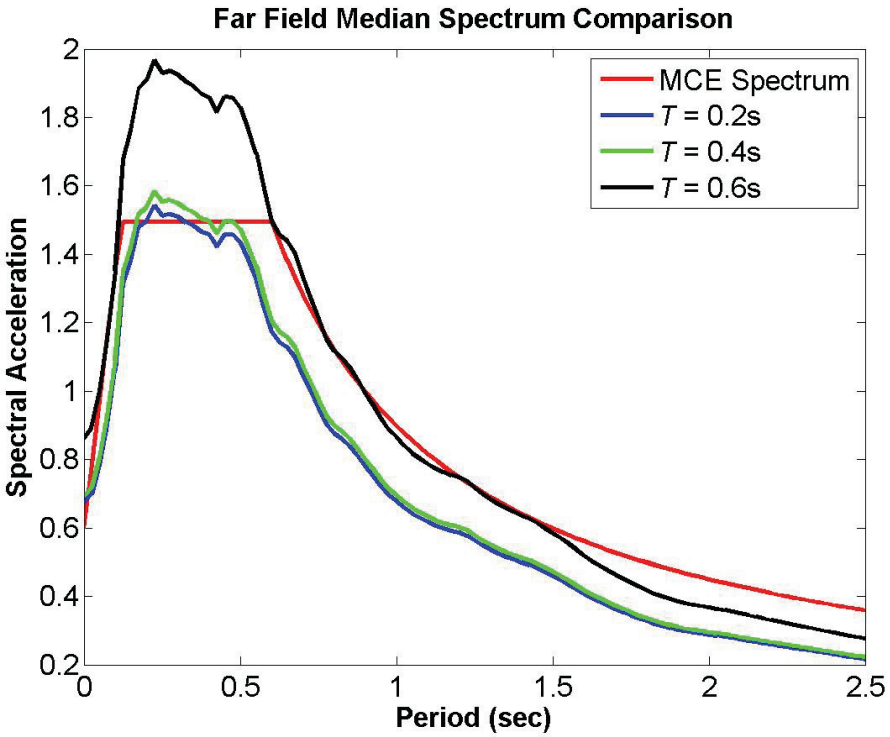

Figure B-2 Comparison of MCE design spectrum for SDC D_{max} with median ground motion spectra scaled to match the design spectrum at periods of 0.2, 0.4, and 0.6 seconds.

According to NIST GCR 10-917-8, the poor performance of the short-period reinforced masonry shear wall archetypes is due to the high ductility demand that earthquake ground motions placed on these archetypes and on the lower ductility capacity of shorter walls (as observed in Figure 3-10 through Figure 3-14 of NIST GCR 10-917-8). The collapse drift ratio of the 2-story high axial load SDC D_{max} archetype was approximately 0.015, and the collapse drift ratio for the 4-story high axial load SDC D_{max} archetype was 0.005. (The collapse drift ratio of the one-story model was not reported.) These collapse values were based on strain limits in the steel and concrete fibers of the mathematical model and were used as non-simulated collapse parameters in the FEMA P-695 analysis of the archetypes.

In regards to the definition of collapse of the reinforced masonry shear wall systems, Chapter 3 of NIST GCR 10-917-8 states:

> "Observed results were sensitive to assumptions made about the collapse behavior of reinforced masonry walls and decisions made in nonlinear modeling. Because of difficulties in quantifying collapse for low-rise walls, it was decided that collapse would be defined as excessive crushing of the masonry cross section or rupture of a significant percentage of the cross section. Neither of these conditions would necessarily lead to collapse in the low-rise shear wall system. Rather, collapse would more likely be expected

to occur when drifts are so large that other gravity-load carrying systems lose their ability to carry vertical loads."

The low collapse displacement parameters mentioned earlier indicate that the systems did not experience large drifts, and thus a gravity load related collapse was not likely.

This appendix reports on studies conducted on a broadened reinforced masonry design space. In association with these studies, the behavior of the 1-, 2-, and 4-story reinforced masonry shear wall archetypes from the NIST GCR 10-917-8 report were investigated through the use of cyclic pushover analysis, which was not done in the original work. Such curves are shown in Figure B-3 for the original 2-story archetype designed for SDC D_{max} and heavy gravity load. As may be observed, the hysteretic response is flag shaped. This behavior is attributed to almost free-rocking of the wall after the reinforcement ruptures. Such behavior has been seen in laboratory testing of unreinforced masonry walls (Franklin et al., 2001) but was unexpected in reinforced masonry shear walls. For the wall height-to-width ratios used in the analysis of these systems (12/24, 20/32, and 40/32 for the 1-, 2-, and 4-story systems, respectively), it is unlikely that such rocking, particularly when limited to the non-simulated collapse displacements used in the analysis, would initiate a true "collapse" of the systems.

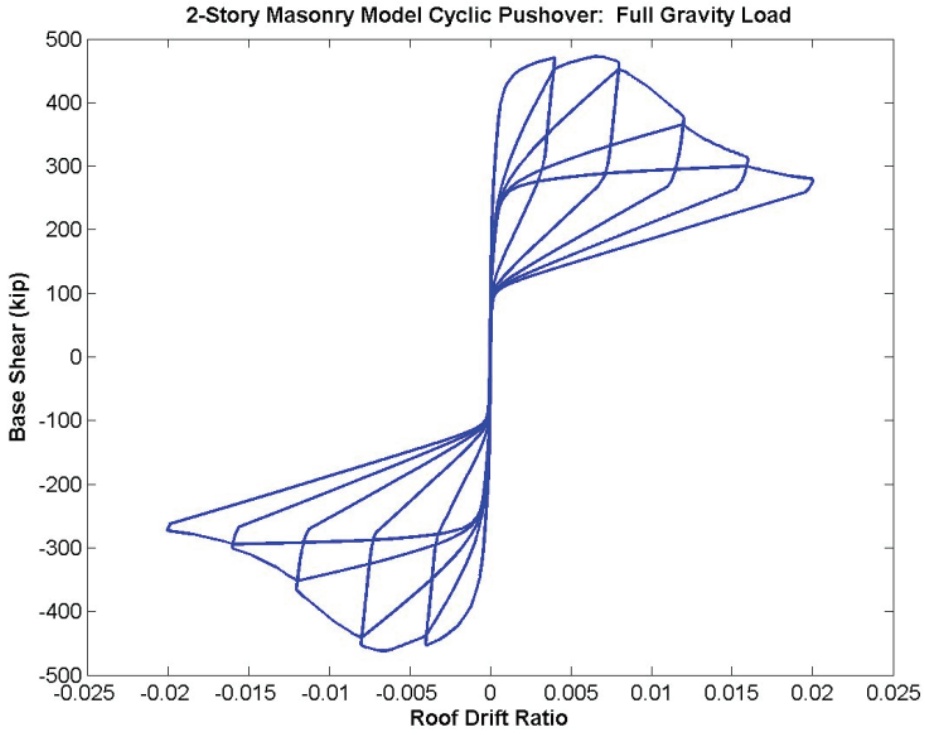

Figure B-3 Cyclic pushover results showing rocking of the 2-story special reinforced masonry shear wall archetype with heavy gravity load.

However, the rocking behavior identified in systems designed for heavy gravity loads is not evident for the more lightly loaded systems. Figure B-4 shows cyclic pushover curves for the 2-story system designed for SDC D_{max} and light (1/4 of system in Figure B-3) gravity load. It is observed that the rocking behavior has effectively disappeared. With regards to the failures of the short-period systems analyzed in the NIST GCR 10-917-8 report, however, there did not appear to be a specific trend related to the level of gravity load.

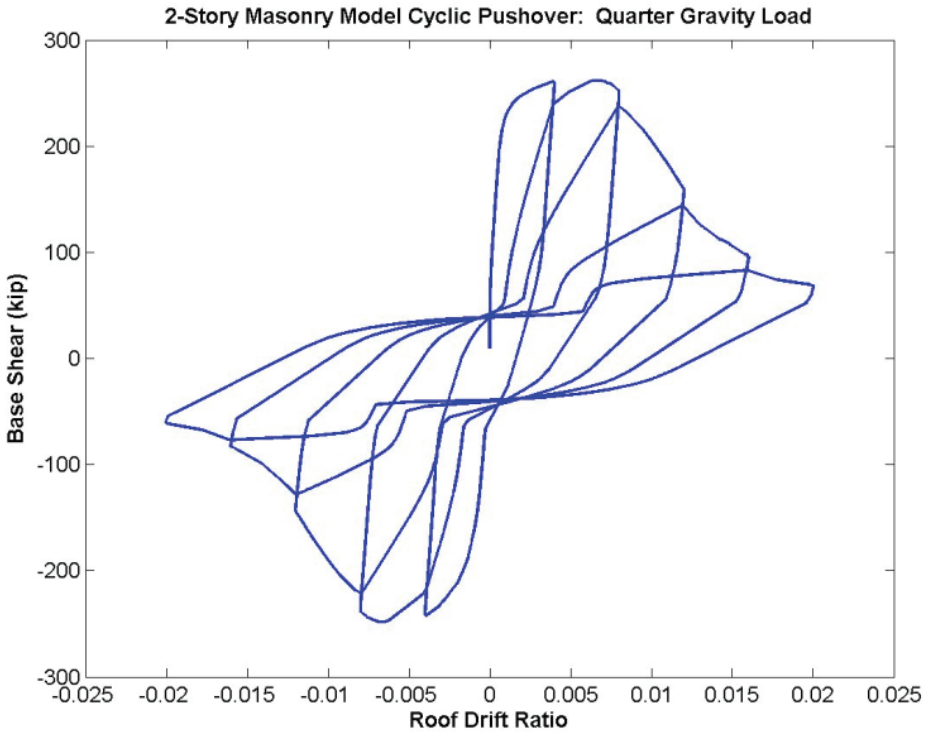

Figure B-4 Cyclic pushover results showing rocking of the 2-story special reinforced masonry shear wall archetype with light gravity load.

Chapter 3 of the NIST GCR 10-917-8 report concludes with the following comment regarding the adequacy of current code provisions that use the same value of *R* for all special reinforced masonry systems:

> "Current code provisions do not adequately distinguish between the wide range of performance characteristics of different masonry wall systems for which the use of the same *R* factor might not be appropriate. In particular, current codes do not account for the fact that the ductility demands induced by an earthquake ground motion on low-rise walls and high-rise walls can be very different. Their ductility capacities can be very different as well, so that different *R* factors may be needed for low-rise and high-rise walls."

Chapter 4 of NIST GCR 10-917-8 had similar observations regarding the special reinforced concrete wall systems:

> "One and 2-story archetypes failed to achieve acceptable collapse margin ratios primarily because shear failures used as a proxy for collapse occurred at relatively low drift levels (below 1.5 %). In general, collapse of low-rise shear wall buildings has not been observed in earthquakes, except in cases where the floor system failed (e.g., precast parking structures). This suggests that findings related to low-rise walls were biased by the modeling assumptions and potentially conservative criteria used to assess collapse. At this time, however, insufficient information exists to establish more liberal failure criteria."

All of the special steel concentrically braced frame (SCBF) and BRBF systems studied in NIST GCR 10-917-8 passed the acceptance criterion, with the exception of the 2-story SCBF archetype $2SCBFD_{max}$. This system with $C_u T_a$=0.25 seconds and T_1 of 0.4 seconds had an *ACMR* of 1.27 with an $ACMR_{20\%}$ of 1.56 (a ratio of 0.81). Thus, it is suggested that design *R* values should be period dependent and use of the equal energy formula to show that a design *R* value of 3.3 would be needed if the target ductility was 6.0. However, this revised *R* value does not address the overstrength that is inherent in *R* (ATC, 1995).

In some analyses, archetypes did not collapse (in a simulated sense), even though there was a complete loss of load-carrying capacity in the braces due to low-cycle fatigue. The lack of collapse was attributed to the backup capacity of the remaining moment frame as provided by fully welded beam-column connections in the braced frame systems. These welded connections were not modeled to capture all deterioration modes associated with plastic hinging in the beams. It is possible, therefore, that if collapse had been defined as loss of load carrying capacity in the braces or if the plastic hinges had been more accurately modeled, more systems would have failed the acceptance criteria. (The modeling of the plastic hinges in the beams, including cyclic deterioration of flexural capacity, is discussed further in Section B.4.2 of this appendix. Findings presented in that section indicate that collapse margin ratios of BRBF systems are reduced somewhat if cyclic deterioration is included in the analysis.)

Based on the above discussion, the following summary points are offered:

- There is a general trend for short-period systems to fail the FEMA P-695 acceptance criteria, whereas systems with longer periods using the same basic design and detailing requirements generally pass.
- The failure of the short-period systems is attributable, in part, to the increased ductility demands that are inherent. This is the driving motivation for developing an *R* value that is period-dependent.

- Mathematical modeling limitations (inherent in the software) and modeling decisions made by the analysts, given those limitations, directly affect the collapse margin ratios computed for a given system. It is not clear whether these decisions are biased for or against low-period systems or whether there is no bias at all. However, more conservative modeling (e.g., modeling that is more likely to produce simulated or non-simulated collapse) will probably push a larger percentage of low-period systems into the unacceptable category, relative to systems with longer periods.
- The definition of collapse and the associated selection of collapse metrics (both simulated and non-simulated) influence the results. For masonry models, for example, a non-simulated collapse associated with concrete and steel strain was used, although it was recognized that a physical system collapse was unlikely for systems with shorter periods. Similar observations were made for reinforced concrete systems. On the other hand, steel braced frames systems were not deemed to collapse, even when there was a total loss of the load-carrying capacity of the braces.

B.3 The Short-Period Problem

The short-period problem is reflective of the fact that the equal displacement concept, wherein lateral displacements for an inelastic system, δ_I, are approximately equal to the elastic displacements, δ_E, of an elastic system of the same initial stiffness, does not hold for systems with natural periods less than about 1.0 second. A consequence of the violation of the equal displacement rule is that inelastic design forces, F_I, cannot be taken as $1/\mu$ times the elastic force demand, F_E, where μ is the ductility supplied by the system.

B.3.1 Historical Background

Veletsos et al. (1965) developed period-dependent expressions for estimating the inelastic force demand in terms of the elastic force demand and the expected inelastic displacement in terms of the elastic displacement, as follows:

For periods less than 0.03 seconds:

$$\frac{F_I}{F_E} = 1.0 \text{ and } \frac{\delta_I}{\delta_E} = \text{undetermined} \qquad \text{(B-1a, B-1b)}$$

For periods between 0.125 seconds and 0.5 seconds (equal energy realm):

$$\frac{F_I}{F_E} = \frac{1}{\sqrt{2\mu - 1}} \text{ and } \frac{\delta_I}{\delta_E} = \frac{\mu}{\sqrt{2\mu - 1}} \qquad \text{(B-2a, B-2b)}$$

For periods greater than 1.0 seconds (equal displacement realm):

$$\frac{F_I}{F_E} = \frac{1}{\mu} \text{ and } \frac{\delta_I}{\delta_E} = 1.0 \qquad \text{(B-3a, B-3b)}$$

R_d is the inverse of ratio of the inelastic force demand to the elastic force demand. Thus, from Equations B-1 through B-3,

$R_d = 1$ when $T < 0.03$ seconds
$R_d = \sqrt{2\mu - 1}$ when 0.125 seconds < T < 0.5 seconds
$R_d = \mu$ when $T > 1.0$ seconds

A host of other researchers, e.g., Qi and Moehle, (1991), Krawinkler and Nasser (1992), Miranda and Bertero (1994), Miranda (2000), Ruiz-Garcia and Miranda (2003, 2004), Chopra and Chintanapakdee (2004), have found similar relationships that were based on systematic response-history analysis of simple elastic-plastic and bilinear systems under various ground motions and various site conditions.

In all of the cases mentioned above, values of R_d tend towards 1.0 when the period of vibration approaches zero, but no guidance is provided for adjusting the computed elastic displacement as the period approaches zero. This is the reason that the inelastic to elastic displacement ratio is given as "undetermined" in Equation B-1b. If an R_d value of 1.0 implies a linear elastic behavior, the displacement ratio is presumably 1.0. If, however, the $R_d = 1$ system yields under the design event, the true ratio of inelastic to displacement can be quite large, as explained subsequently in this appendix.

For systems in the period range of 0.125 to 0.5 seconds, Equations B-2a and B-2b provide the required R_d and elastic displacement multipliers. As noted earlier, the R_d value is only the ductility part of R, and this must be multiplied by the overstrength part, R_o, to determine the design R value. To provide insight into the use of Equations B-2a and B-2 b and for use in future discussion, Table B-3 provides computed values for R_d, R, and δ_I/δ_E for a range of ductilities. R_o was taken as 2.5 for the purpose of computing R.

Table B-3 Values of R_d, R, and Ratio of Inelastic Displacement to Elastic Displacement using Equation B-2a and Equation B-2b

μ	R_d	R	δ_I/δ_E
1	1.00	2.5	1.00
2	1.73	4.32	1.15
3	2.27	5.62	1.32
4	2.65	6.62	1.51
5	3.00	7.50	1.67
6	3.31	8.27	1.82

Instead of modifying the design R value, it might be possible to achieve acceptable performance for short-period systems by requiring enhanced ductility. For example, Section 5.2.3.4 of Eurocode 8 (CEN, 2004) requires that the curvature ductility supplied in critical regions of concrete structures be tied to the system period, as follows:

$$\mu_\phi = 2q_0 - 1 \text{ if } T_1 \geq T_c \tag{B-4}$$

$$\mu_\phi = 1 + 2(q_o - 1)\frac{T_c}{T_1} \text{ if } T_1 < T_c \tag{B-5}$$

where μ_ϕ is the required curvature ductility, q_o is the reduction factor (similar to R_d), T_1 is the computed period of vibration, and T_c is the transition period (similar to T_S in ASCE/SEI 7-10). Values of q_o are as low as 3.0 for uncoupled walls with moderate detailing and as high as 4.5 for systems with ductile detailing. In some cases the value of q_o can be increased to account for expected overstrength and redundancy.

For $q_o = 3$ and $T_c = 0.6$ seconds, the following curvature ductility requirements are obtained using Equation B-5:

$T_1 = 0.2$	$\mu_\phi = 13$
$T_1 = 0.3$	$\mu_\phi = 9$
$T_1 = 0.4$	$\mu_\phi = 7$
$T_1 = 0.5$	$\mu_\phi = 5.8$
$T_1 = 0.6$	$\mu_\phi = 5$

The above requirement is based on work done by Vidic et al. (1994) in which a period dependent R is given as follows:

$$R = 1 + c_1(\mu - 1)^{c_R} \text{ if } T > T_0 \tag{B-6}$$

$$R = 1 + c_1(\mu - 1)^{c_R}\frac{T}{T_0} \text{ if } T \leq T_0 \tag{B-7}$$

$$\text{where } T_0 = c_2\mu^{c_T}T_1 \tag{B-8}$$

The coefficients c_1, c_2, c_R, and c_T depend on assumptions regarding hysteretic and damping behavior. T_1 is the transition period, similar to T_s in ASCE/SEI 7.

Sample values computed using c_1, c_2, c_R, and c_T values from Vidic et al. give the following R values when the ductility $\mu = 6.0$:

$T = 0.0$	$R = 1.00$
$T = 0.2$	$R = 2.58$
$T = 0.3$	$R = 3.36$
$T = 0.4$	$R = 4.15$
$T = 0.5$	$R = 4.94$

$T = 0.6$ $R = 5.72$
$T = 0.64$ $R = 6.00$

While it is unlikely that building systems will have periods less than 0.03 seconds, the behavior at these periods is of some interest as a limiting case. Physically, an elastic-plastic system with a very high initial stiffness may be idealized as a rigid block on a frictional interface, as shown in Figure B-5. The total displacement of the block is equal to the elastic shear deformation plus the "inelastic" sliding deformation. As the stiffness of the block increases, the elastic deformation in the block decreases while the sliding deformation stays relatively constant. Thus, it is impossible for the inelastic and elastic displacements to be similar. Additionally, the ductility demand of the system will approach infinity as the block becomes stiffer because the yield displacement approaches zero while the total displacement demand stays relatively constant.

B.3.2 Parametric Response-History Analysis of a Simple Single-Degree-of-Freedom System

For the sliding block of Figure B-5, there is no restoring force from the elastic deformation in the block; thus, it is likely that there will be significant residual deformation at the end of the event. Such deformations may also be dominant in the transitional period range from 0.03 seconds to 0.125 seconds and even into the "equal energy" realm between 0.125 seconds and 0.5 seconds. Such behavior was reported by Jennings (1963) but is rarely mentioned in other studies dealing with computation of R.

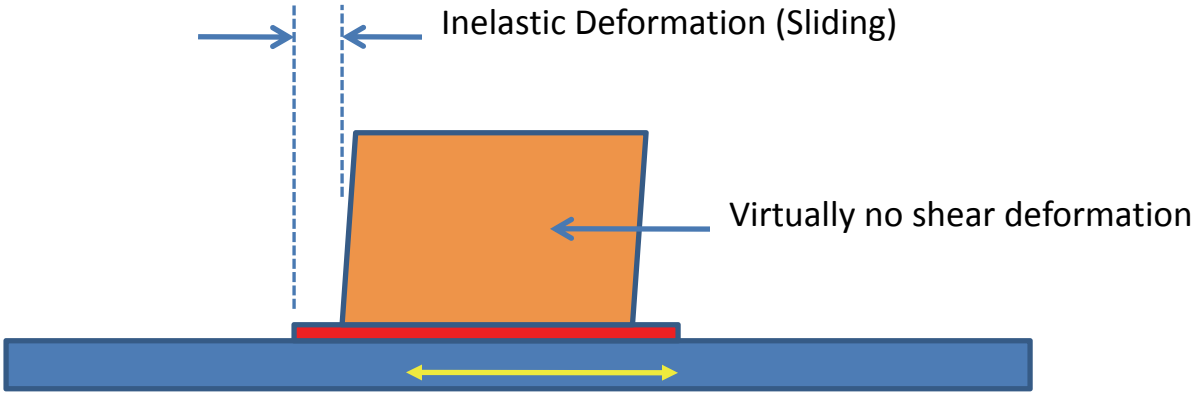

Figure B-5 Model of short-period system as block sliding on friction plane.

Additional insight into the short-period problem can be found from the analysis of a simple structure. Consider, for example, a single-degree-of-freedom (SDOF) elastic-plastic system subjected to the Oakland Outer Wharf record from the Loma Prieta Earthquake. The properties of the system are as follows:

- Mass = 1.0 k-sec^2/in.
- Damping = 2.5% critical

- F_y = 40 kips
- Secondary (strain hardening) stiffness = 0.0
- P-Delta effects not included

The system was repeatedly analyzed for cases where the initial stiffness varied such that T ranged from 0.1 to 1.0 seconds/cycle. All of the nonlinear dynamic analyses were performed using NONLIN-EQT software (Charney et al., 2010).

The results of the analysis of systems with a constant strength of 40 kips are summarized in Table B-4. The table indicates that the ratio of the inelastic to elastic displacement is in the neighborhood of 1.0 for the systems with periods greater than 0.5 seconds. However, when the period falls below 0.5 seconds the ratio of inelastic to elastic displacement increases dramatically and is much larger than predicted by Equation B-2b. Associated with large inelastic displacement are large ductility demands. Ductility demands above 6 are not sustainable for most systems.

Table B-4 Response of Elasto-Plastic System to the Loma Prieta Ground Motion with Constant f_y

T (sec)	K (k/in)	Elastic Displacement (in)	Inelastic Displacement (in)	Residual Displacement (in)	Ductility Demand	Yield Excursions	Inelastic to Elastic Disp. Ratio
1.0	39.5	4.42	5.92	3.84	5.84	8	1.34
0.9	48.7	3.61	4.27	1.68	5.20	9	1.18
0.8	61.7	5.18	3.10	0.79	4.79	7	0.60
0.7	80.6	5.54	2.97	0.56	5.99	11	0.54
0.6	108.7	4.20	2.66	0.52	7.28	24	0.63
0.5	159.7	1.56	2.43	1.57	9.58	21	1.55
0.4	246.7	1.12	3.07	2.27	18.9	23	2.73
0.3	438.6	0.60	2.18	1.26	23.9	39	3.63
0.2	987.0	0.23	1.83	1.31	45.2	39	7.97
0.1	3984.8	0.03	1.51	0.96	148.6	13	45.6

Figure B-6 shows the displacement histories computed for two systems with the same yield strength (40 kips) but with different periods of vibration, 0.8 seconds and 0.2 seconds. Also shown in the figure are the responses for each system had it remained elastic during the ground shaking. The system with a period of 0.8 seconds has similarities in the elastic and inelastic behavior because both responses are dominated by a transient response. For the system with a period of 0.2 seconds, however, the characters of the elastic and inelastic responses are completely different with the behavior being dominated by a single displacement pulse, followed by a relatively large residual deformation.

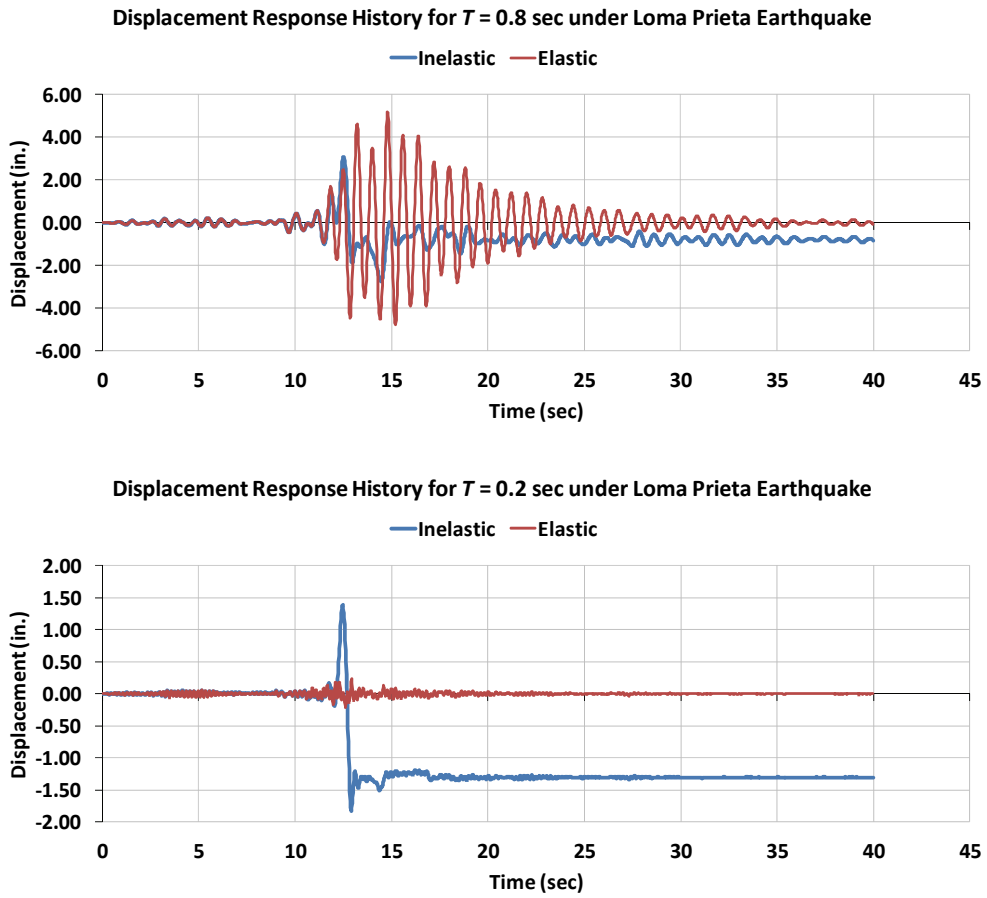

Figure B-6 Response history comparisons for systems with constant strength with: (a) T = 0.8 seconds; (b) T = 0.2 seconds.

Similar results are provided in Table B-5 and Figure B-7 for a series of systems designed for a constant ductility. Table B-5 shows that the strength demand for the system increases significantly as the period decreases. In the constant acceleration range of the ASCE 7 spectrum (T is less than approximately 0.5 seconds), the strength demands have increased by approximately 50%, and the inelastic displacements are significantly larger than the elastic displacement. For the system with a period of 0.1 seconds, the displacement ratio is 4.24. This suggests that a strategy of decreasing the R value to control the short-period problem may need to be accompanied by adjustments to C_d. This is contrary to the conclusion from the FEMA P-695 study that the C_d factors should be set equal to R.

It is important to note that the behavior shown in Figure B-6 and Figure B-7 was common among several similar analyses performed using a variety of different ground motion methods.

Table B-5 Response of Elasto-Plastic System to the Loma Prieta Ground Motion with Constant Ductility Demand

T (sec)	K (k/in)	Elastic Displacement (in)	Inelastic Displacement (in)	Residual Displacement (in)	f_y (kips)	Yield Excursions	Inelastic to Elastic Disp. Ratio
1.0	39.5	4.42	5.86	3.97	38.6	9	1.32
0.9	48.7	3.61	4.12	2.07	33.9	11	1.15
0.8	61.7	5.18	3.12	1.51	32.2	11	0.60
0.7	80.6	5.54	2.97	0.56	39.9	11	0.54
0.6	108.7	4.20	2.58	0.28	47.2	22	0.61
0.5	159.7	1.56	2.56	1.30	67.4	14	1.64
0.4	246.7	1.12	1.89	0.82	77.5	13	1.68
0.3	438.6	0.60	1.06	0.17	77.5	19	1.77
0.2	987.0	0.23	0.432	0.25	71.1	13	1.87
0.1	3984.8	0.03	0.140	0.12	92.2	3	4.24

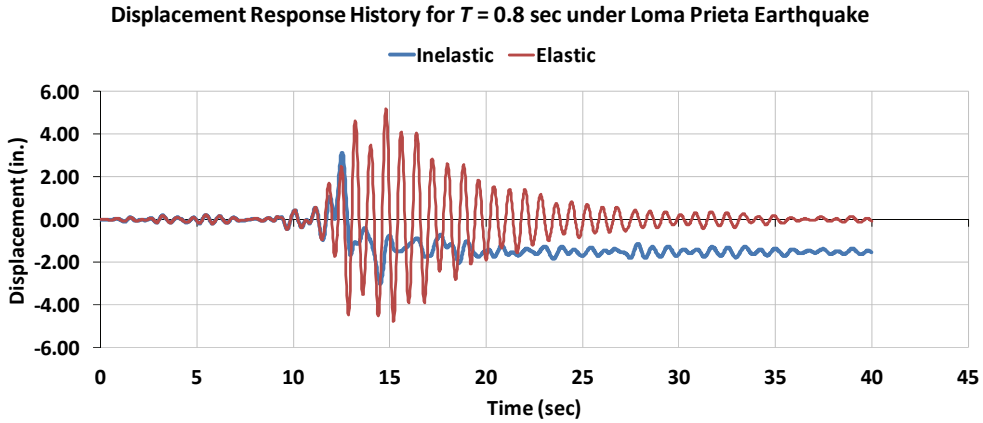

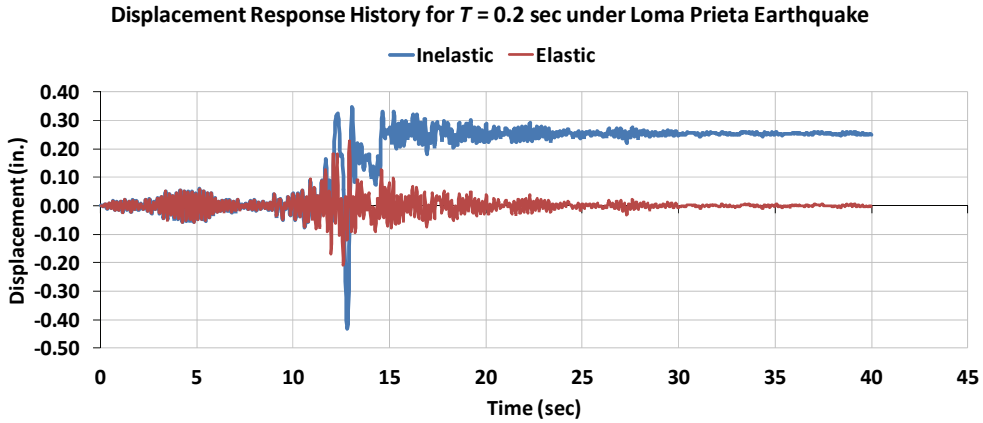

Figure B-7 Response history comparisons for systems with constant ductility with: (a) T = 0.8 seconds; (b) T = 0.2 seconds.

B.3.3 FEMA P-695 Analysis of Simple Single-Degree-of-Freedom Systems

In this section, the systematic FEMA P-695 analysis of a design space consisting of SDOF systems is presented. This analysis provides additional insight to the performance of short-period systems and sets the stage for the analysis of the RMSW and BRBF systems in Section B.4.

The SDOF systems studied consisted of simple bilinear models with positive, zero, or negative strain hardening slope. Models were also run using a gradual transition into yielding, and the results were not significantly different than those obtained for the bilinear models. Although a large variety of post-yield slopes were used in the full study, only the results for the models with strain hardening ratios of 0.10, 0.0, and -0.10 are presented herein (3 slopes).

In the analyses, collapse was defined as occurring when the ductility demand exceeds a given threshold. For most of the analysis reported herein, the ductility threshold was taken as 10. Design, Test Data, and Analysis uncertainties were taken as B (Good).

Models were designed for SDC D_{max} in accordance with FEMA P-695 Methodology. For each of these systems, the design space consisted of models with periods ranging from 0.1 second to 1.0 second in 0.1 second increments (10 periods), designed for *R* values of 1, 2, 4, 6, 8, and 10 (six *R* values). This resulted in the evaluation of $3 \times 10 \times 6 = 180$ models. The FEMA P-695 Methodology was applied to each model, and adjusted collapse margin ratios were computed and compared to the acceptable values for both a 10% and 20% probability of collapse. Using these results, the target *R* value (which results in an *ACMR* of 1.0 for the given probability of collapse) can be interpolated and plotted versus period.

Also computed and plotted versus period is the probability of collapse associated with each *ACMR*, and the ratio of median inelastic displacement to elastic displacement at the MCE levels of ground motion. All analyses were performed using the FEMA P-695 Analysis Toolkit that is described in Appendix E of this report.

The results for systems with 0% strain hardening (alpha = 0) and with no consideration for P-delta effects (alphaPD = 0) are shown in Figure B-8. Figure B-8a shows the ratio of the computed *ACMR* to the $ACMR_{10\%}$ value. Ratios less than 1.0 indicate failure to meet the performance criterion for a performance group.

The curves in Figures B-8a may be used to interpolate the *R* value at which the *ACMR* to $ACMR_{10\%}$ ratio would be exactly 1.0. The interpolated *R* values are shown in Figure B-8b. If the *R* value is based on a 10% probability of collapse, it would

increase from 1 for a system with a very low period to approximately 4 for a system with a period of 1.0 second.

Probabilities of collapse are shown in Figure B-8c. Only the system with $R = 1$ has a probability of collapse less than 0.1 for all period values. Again, the behavior of systems with longer periods improves relative to the behavior of systems with lower periods.

Ratios of inelastic to elastic drift are shown in Figure B-8d. As expected, the ratios are considerably in excess of 1.0 for the lower period systems, with R greater than 1.0, indicating a lack of adherence to the equal displacement concept (which appears to hold reasonably well for systems with longer periods).

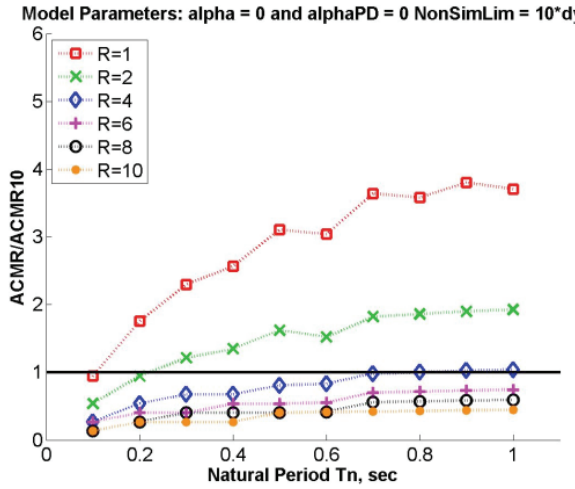

(a) *ACMR* ratios for 10% probability of collapse

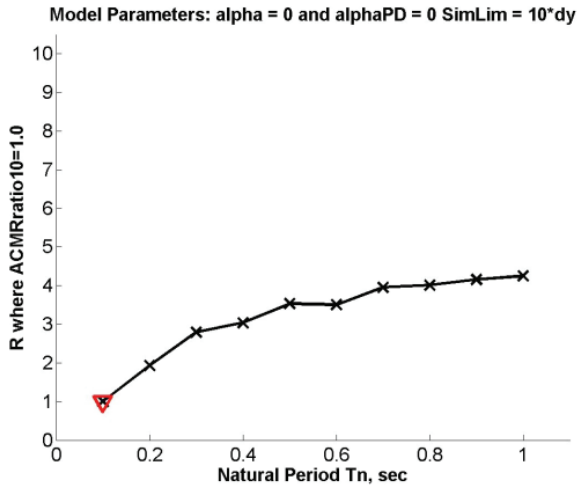

(b) *R* values for 10% probability of collapse

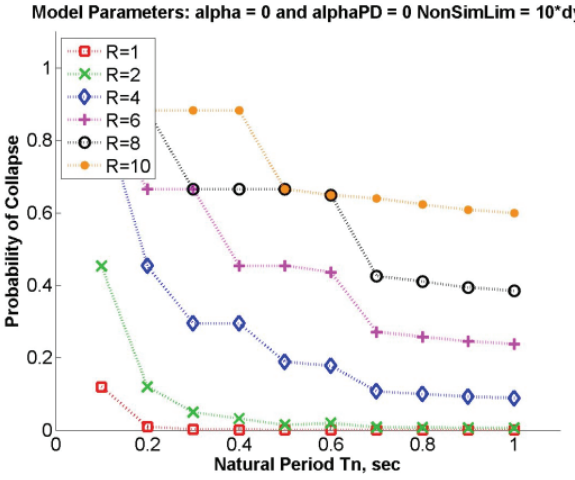

(c) Probability of collapse

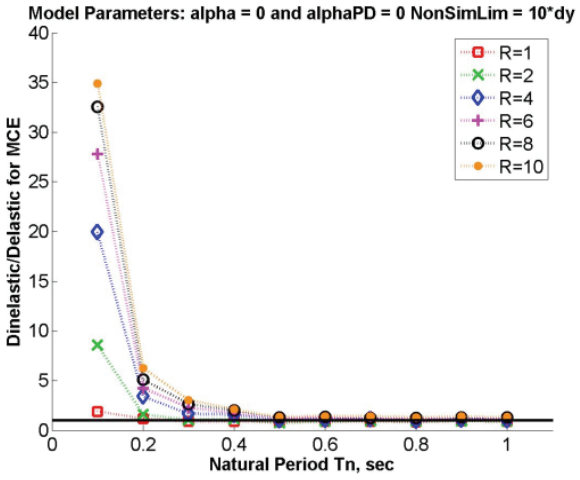

(d) Inelastic to elastic drift ratios

Figure B-8 Results for SDOF systems with 0% strain hardening and a ductility limit of 10.

The results for the system with a positive 10% strain hardening are shown in Figure B-9. The same basic trends as discussed for the 0% strain hardening models are observed, and as expected, the interpolated R values for systems with longer periods are increased

and reach 5 to 6 at periods in the range from 0.6 to 1.0 seconds. *R* values for systems with lower periods still tend towards 1.0 as the period approaches 0.1 seconds. Ratios of inelastic drift to elastic drift are somewhat lower for systems with 10% strain hardening than with 0% strain hardening. For the shorter periods, however, these ratios are still in excess of those predicted using the "equal energy" rule.

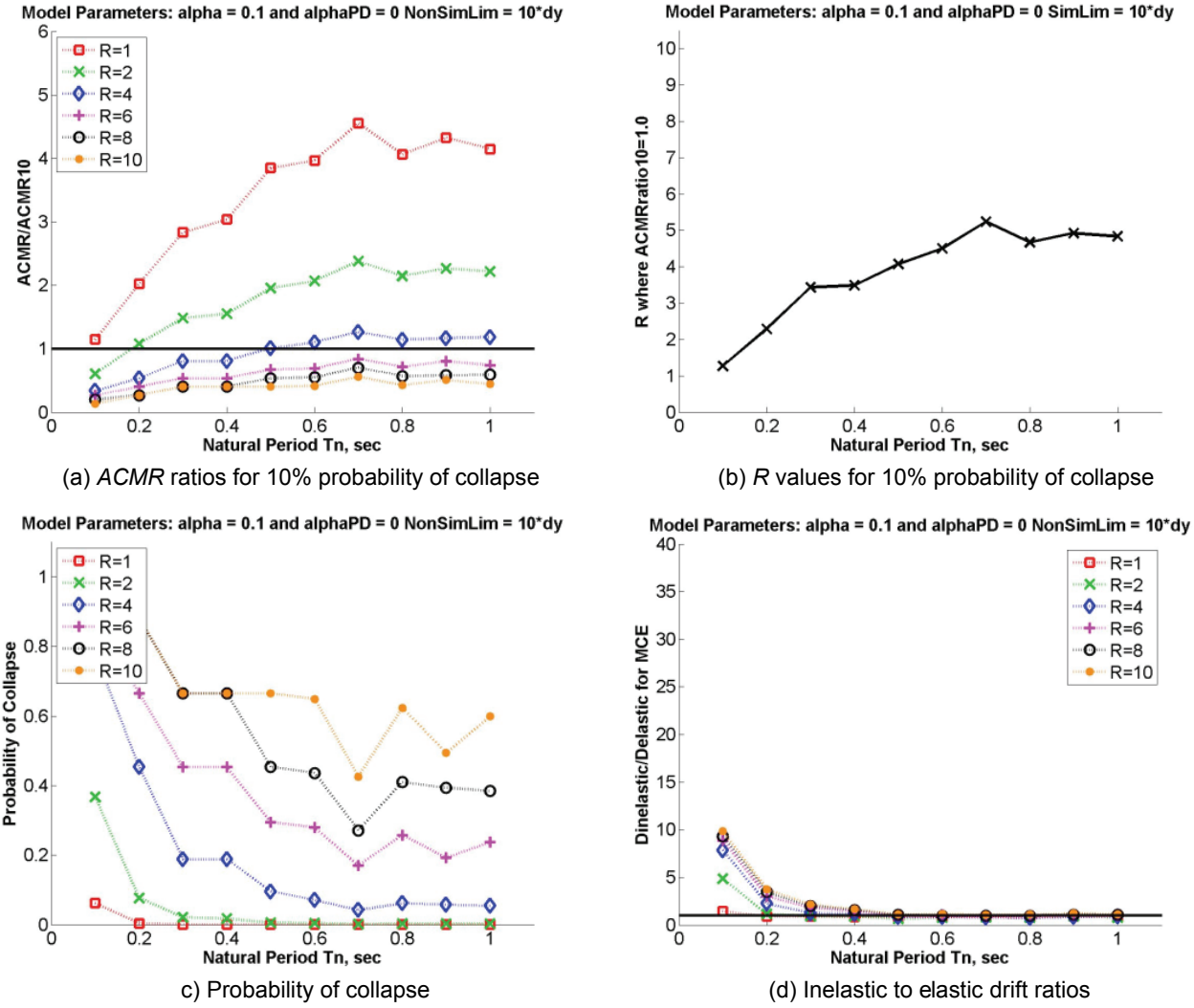

(a) *ACMR* ratios for 10% probability of collapse

(b) *R* values for 10% probability of collapse

c) Probability of collapse

(d) Inelastic to elastic drift ratios

Figure B-9 Results for SDOF systems with 10% strain hardening and a ductility limit of 10.

Results for the system with negative 10% strain hardening are presented in Figure B-10. Here, only systems with *R* of 1 to 2 are acceptable, with the interpolated value just reaching 2.0 for systems with higher periods when the *ACMR* is based on 10% probability of collapse (Figure B-10b). Figure B-10d shows that the ratios of inelastic to elastic drift follow no discernable pattern. The reason is that the results are dominated by dynamic instability, which occurs at all period values. The tendency towards dynamic instability can be seen in Figure B-11, where part (a) is the response history at one IDA level, and part (b) is the response at a slightly larger level of ground motion.

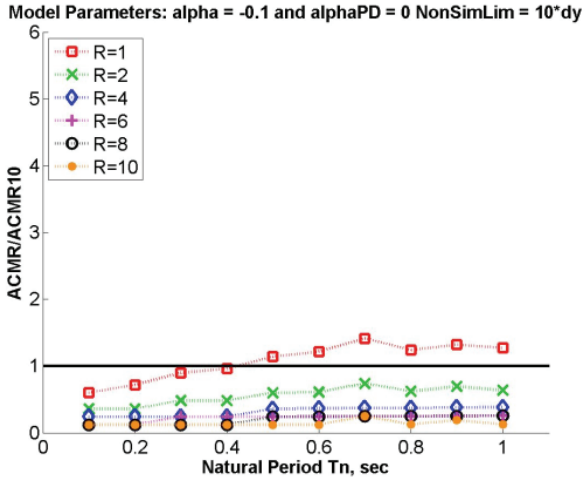

(a) *ACMR* ratios for 10% probability of collapse

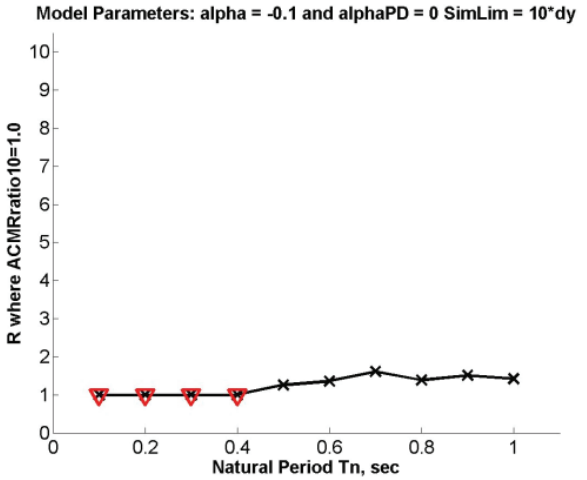

(b) *R* values for 10% probability of collapse

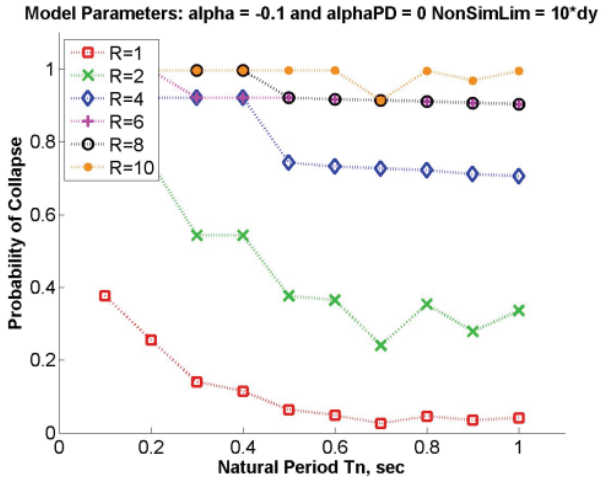

(c) Probability of collapse

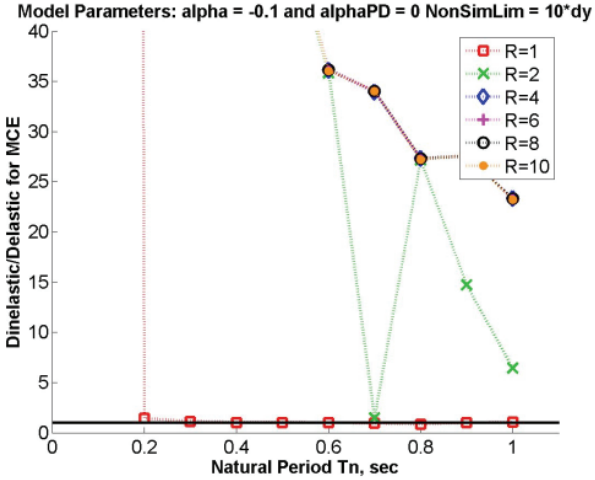

(d) Inelastic to elastic drift ratios

Figure B-10 Results for SDOF systems with negative 10% strain hardening and a ductility limit of 10.

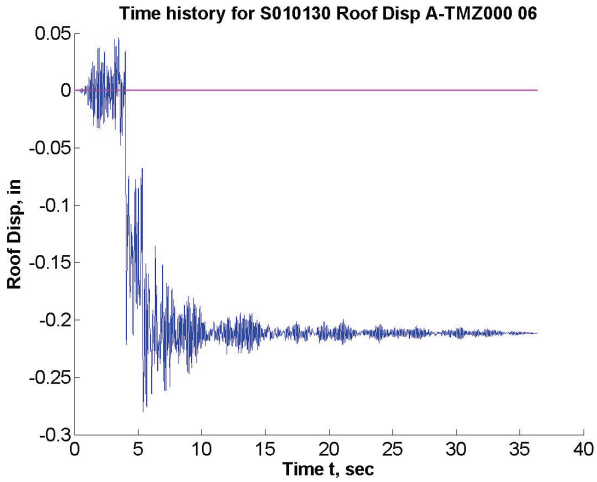

(a) Response at IDA Increment 06

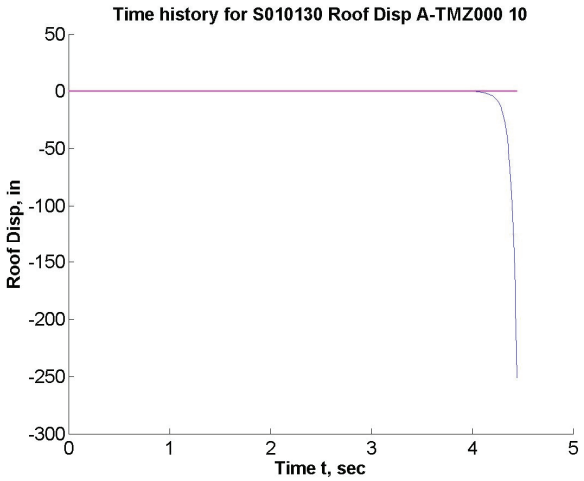

(b) Response at IDA Increment 10

Figure B-11 Response histories for negative 10% strain hardening for two IDA increments.

Figure B-12 illustrates how the system behavior changes if the non-simulated collapse ductility for the 0% strain hardening is increased to 20. When compared to the results with 0% strain hardening with a ductility limit of 10, the *ACMR* ratios and the interpolated *R* value have increased. This indicates to some extent the validity of the Eurocode approach that requires that systems with shorter periods be detailed for enhanced ductility.

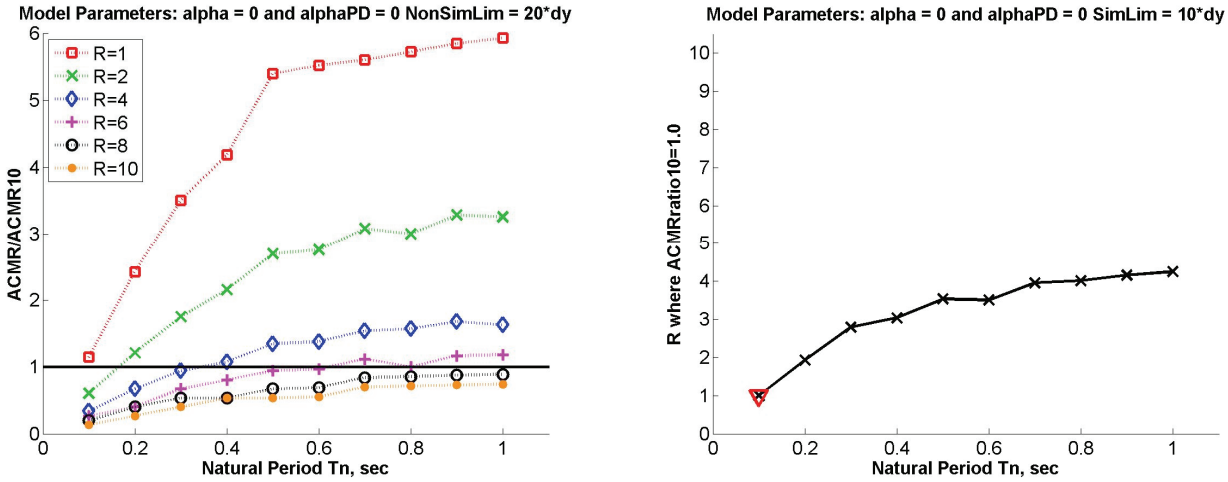

(a) ACMR ratios for 10% probability of collapse

(b) R values for 10% probability of collapse

Figure B-12 Results for SDOF systems with 0% strain hardening and a collapse ductility limit of 20.

B.4 FEMA P-695 Analysis of Special Reinforced Masonry Shear Wall and Buckling-Restrained Braced Frame Systems

B.4.1 Special Reinforced Masonry Shear Wall Systems

As shown in Table B-1, all of the 1-story and one of the 2-story special reinforced masonry shear wall archetypes analyzed as part of the NIST GCR 10-917-8 study failed to achieve an individual archetype probability of collapse of less than 20% for the MCE ground shaking. Each of these systems was designed using an *R* of 5.0, and C_d was taken as equal to *R* as recommended by the FEMA P-695 Methodology. These values are somewhat different from the design values of *R* and C_d from ASCE/SEI 7-05, which are 5.5 and 4, respectively.

In this study, 1-, 2-, and 4-story archetypes, subjected to heavy gravity load and SCD D_{min} and D_{max} shaking, were redesigned using *R* values of 1, 2, 4, 6, and 8 and analyzed using the FEMA P-695 Methodology to determine how the collapse margin ratios vary with design *R* values. Also computed were the ratios of the peak computed inelastic displacement to the peak elastic displacement.

The archetype designs followed the latest standards for the design of masonry structures (TMS, 2011). The designs used the gravity loads developed for the NIST

GCR 10-917-8 models. Table B-6 provides the basic details for the walls, and Table B-7 through Table B-12 provide the reinforcement details.

Table B-6 Basic Design Parameters for All Special Reinforced Masonry Shear Wall Archetypes

Number of Stories	f'_m	Wall length	Total Wall height	Nominal Thickness
1 at 12 ft	1.5	24 ft	12 ft	8.0 in
2 at 10 ft	2.5	32 ft	20 ft	8.0 in
4 at 10 ft	3.0	32 ft	40 ft	8.0 in

Table B-7 Reinforcement for 4-Story Wall Designed for SDC D_{max}

Design *R* Value	System Designation	Story Level	Reinforcement
1	M4DmaxR1	4	#4 at 16”
		3	#5 at 8”
		2	#7 at 8”
		1	#9 at 8”
2	M4DmaxR2	4	#4 at 32”
		3	#4 at 16”
		2	#6 at 16”
		1	#8 at 16”
4	M4DmaxR4	4	#4 at 32”
		3	#4 at 32”
		2	#4 at 32”
		1	#4 at 16”
6	M4DmaxR6	4	#4 at 32”
		3	#4 at 32”
		2	#4 at 32”
		1	#4 at 32”
8	M4DmaxR8	4	#4 at 32”
		3	#4 at 32”
		2	#4 at 32”
		1	#4 at 32”

Table B-8 Reinforcement for 2-Story Wall Designed for SDC D_{max}

Design *R* Value	System Designation	Story Level	Reinforcement
1	M2DmaxR1	2	#4 at 8”
		1	#7 at 8”
2	M2DmaxR2	2	#4 at 16”
		1	#4 at 8”
4	M2DmaxR4	2	#4 at 32”
		1	#4 at 32”
6	M2DmaxR6	2	#4 at 32”
		1	#4 at 32”
8	M2DmaxR8	2	#4 at 32”
		1	#4 at 32”

Table B-9 Reinforcement for 1-Story Wall Designed for SDC D_{max}

Design *R* Value	System Designation	Story Level	Reinforcement
1	M1DmaxR1	1	#6 at 8”
2	M1DmaxR2	1	# 5 at 16”
4	M1DmaxR4	1	#4 at 16”
6	M1DmaxR6	1	#4 at 32”
8	M1DmaxR8	1	# 4 at 32”

Table B-10 Reinforcement for 4-Story Wall Designed for SDC D_{min}

Design *R* Value	System Designation	Story Level	Reinforcement
1	M4DminR1	4	#4 at 32”
		3	#4 at 32”
		2	#4 at 16”
		1	#8 at 16”
2	M4DminR2	4	#4 at 32”
		3	#4 at 32”
		2	#4 at 32”
		1	#6 at 16”
4	M4DminR4	4	#4 at 32”
		3	#4 at 32”
		2	#4 at 32”
		1	#4 at 16”
6	M4DminR6	4	#4 at 32”
		3	#4 at 32”
		2	#4 at 32”
		1	#4 at 32”
8	M4DminR8	4	#4 at 32”
		3	#4 at 32”
		2	#4 at 32”
		1	# 4 at 32”

Table B-11 Reinforcement for 2-Story Wall Designed for SDC D_{min}

Design *R* Value	System Designation	Story Level	Reinforcement
1	M2DminR1	2	#4 at 16”
		1	#4 at 8”
2	M2DminR2	2	#4 at 32”
		1	#4 at 32”
4	M2DminR4	2	#4 at 32”
		1	#4 at 32”
6	M2DminR6	2	#4 at 32”
		1	#4 at 32”
8	M2DminR8	2	#4 at 32”
		1	#4 at 32”

Table B-12 Reinforcement for 1-Story Wall Designed for SDC D_{min}

Design *R* Value	System Designation	Story Level	Reinforcement
1	M1DminR1	1	#5 at 16”
2	M1DminR2	1	#4 at 16”
4	M1DminR4	1	#4 at 32”
6	M1DminR6	1	#4 at 32”
8	M21minR8	1	#4 at 32”

The OpenSees (http://opensees.berkeley.edu/) models used in this analysis were developed for the studies summarized in NIST GCR 10-917-8 report. The analysis of these models, without modification of any kind, did not produce exactly the same results for computed period of vibration and pushover behavior as presented in NIST GCR 10-917-8. In some cases, the correlation in behavior was very good (e.g. for the 2-story SDC D_{max} model), but in others (e.g. the 4-story SDC D_{max} model), the correlation was not good, particularly for pushover analysis.

These models were used as-is, with the following exceptions:

- Leaning column loads were included in all analyses.
- Live load was not included in seismic mass.
- The reinforcement pattern was modified as required for each member of the design space.
- Masonry was modeled as uncracked. Use of cracked *EI* for the walls increases the period of vibration from 10% to 25% for the 1- and 4-story models, respectively. It is not expected that use of cracked *EI* for the walls would have significantly altered the fundamental conclusions provided by the analysis reported in this appendix.

Two displacement-based fiber elements were used at the first story of each model, and a single displacement-based fiber element was used in the upper stories. The length of the lowermost element in the first story was set to the expected plastic hinge length for the wall. Concrete was modeled using the Park-Kent stress-strain relationship, and reinforcing steel was allowed to rupture in tension and buckle in compression. Inelastic shear deformation was not considered, but elastic shear deformations were included in the manner described in NIST GCR 10-917-8. Both concrete and steel constitutive relationships were regularized to account for localization issues. All walls were assumed to be completely fixed at the base (no foundation flexibility was included).

As with the original models, non-simulated collapse was assumed when the strains in the steel or concrete reached a limiting strain of 30% into the section as measured from the extreme fiber. The displacements at which the strains were exceeded were computed using nonlinear static pushover analysis. Pushover curves for the full design set are provided in Figure B-13 through Figure B-15. A black asterisk is provided on each curve to show the drift ratio at which a non-simulated collapse would occur. The design drift ratio limit for cantilever masonry walls is 0.01 in ASCE 7.

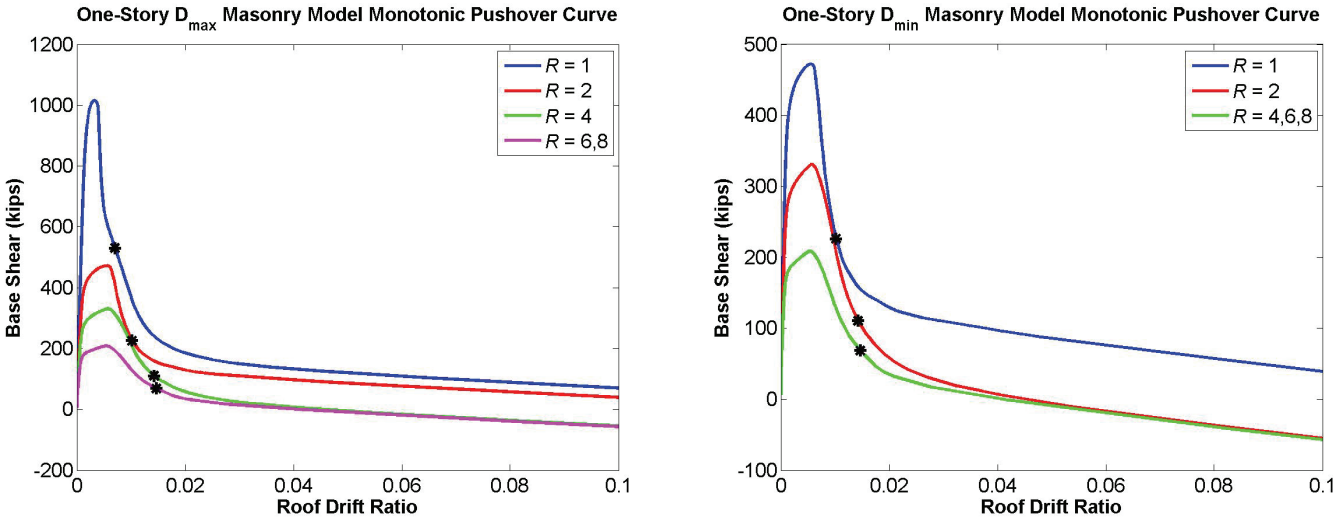

Figure B-13 Monotonic pushover curves for 1-story systems.

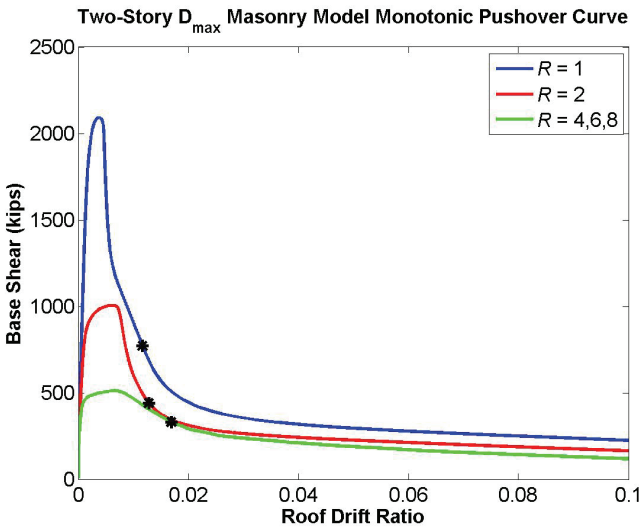

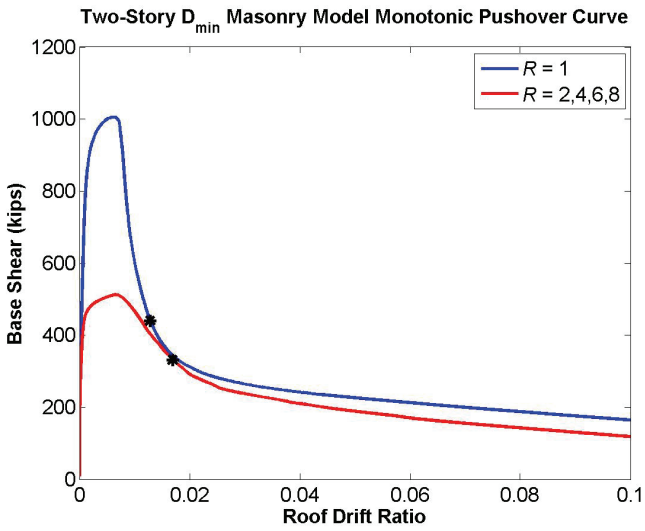

Figure B-14 Monotonic pushover curves for 2-story systems.

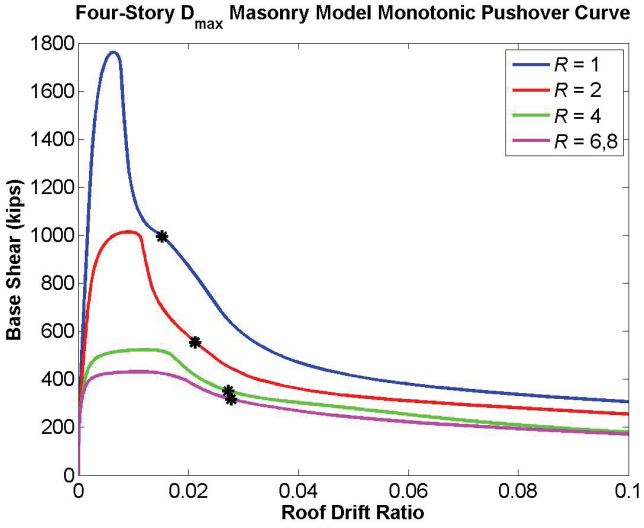

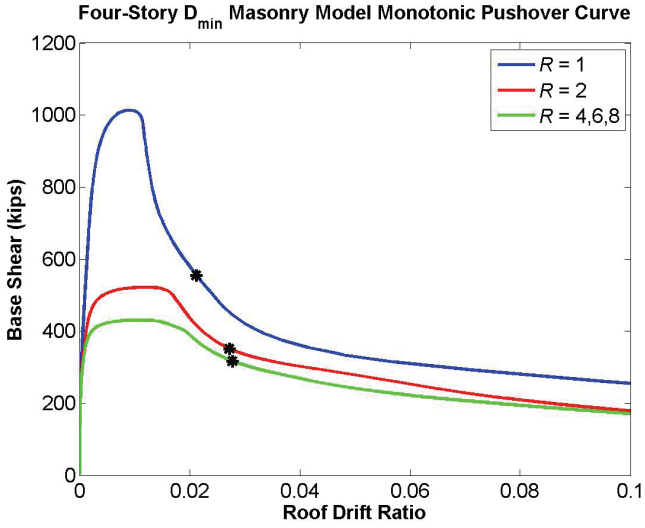

Figure B-15 Monotonic pushover curves for 4-story systems.

Prior to running the dynamic analysis, a cyclic pushover analysis was performed for selected members of the design space. Curves obtained for the $R = 2$ and $R = 6$ designs of the 2- and 4-story archetypes with SDC D_{max} are shown in Figure B-16 through Figure B-19. Figure B-17 and Figure B-19 show that the cyclic curves indicate rocking behavior for the $R = 6$ systems but little or no rocking for the $R = 2$ systems that have significantly more reinforcement.

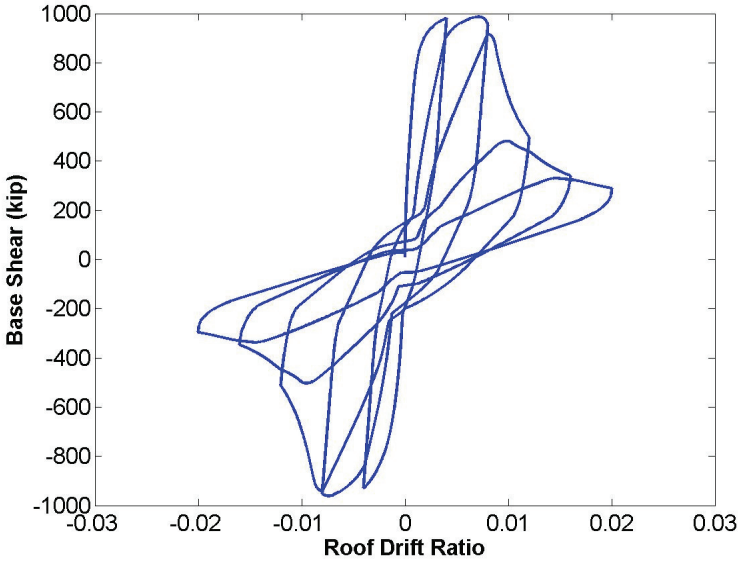

Figure B-16 Cyclic pushover curve for the 2-story, R = 2, SDC D_{max} system.

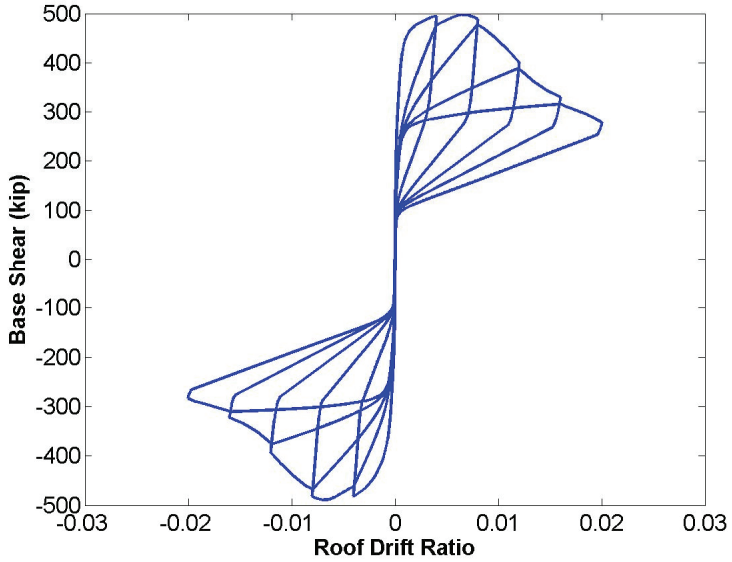

Figure B-17 Cyclic pushover curve for the 2-story, R = 6, SDC D_{max} system.

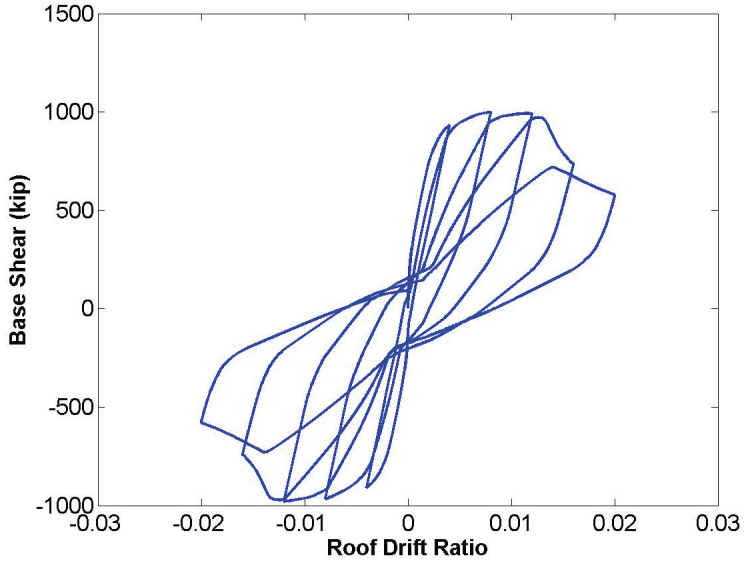

Figure B-18 Cyclic pushover curve for the 4-story, R = 2, SDC D_{max} system.

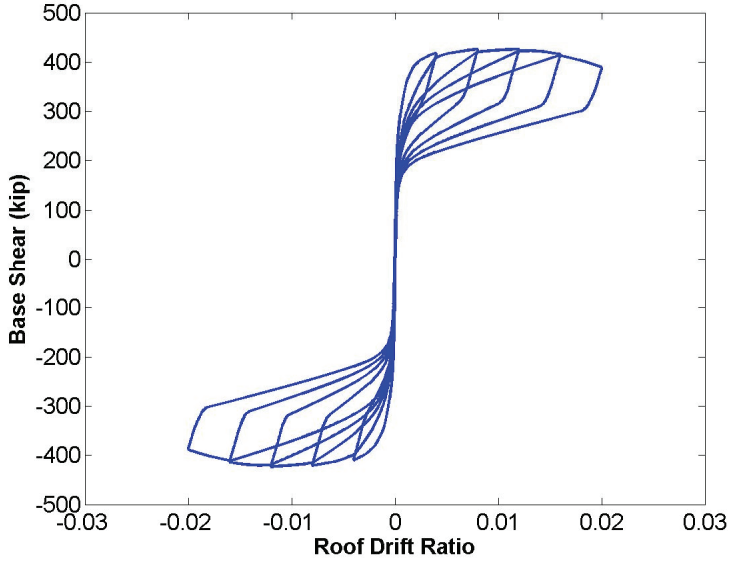

Figure B-19 Cyclic pushover curve for the 4-story, R = 6, SDC D_{max} system.

An overview of the results of the FEMA P-695 analysis is presented for all archetypes in Table B-13. As may be seen in the last column of the table, the R = 2, 4, 6, and 8 archetypes for the 1-story SDC D_{max} systems failed the FEMA P-695 requirements for individual archetypes (20% probability of collapse given the MCE shaking), while all of the other systems passed.

In Table B-14, the 1- and 2-story SDC D_{max} models are arranged as performance groups. Again, the R = 2, 4, 6, and 8 groups fail, but the R = 1 group passes. Failure is dominated by the poor performance of the 1-story systems. The same result (only R = 1 systems passing) would be obtained for the full group even if the 4-story

systems were included in the performance group. Results arranged into performance groups for the 1- and 2-story models for SDC D_{min} systems are provided in Table B-15. All of these systems passed the FEMA P-695 performance requirements.

Table B-13 Analysis Results for all Special Reinforced Masonry Archetypes

NS	SDC	*R*	*T* (sec)	T_1 (sec)	Static Ω	*CMR*	μ_T	SSF	*ACMR*	$ACMR_{20\%}$	*ACMR* / (*Accept.* $ACMR_{20\%}$)
		8	0.25	0.108	2.58	0.8	6.4	1.29	1.03	1.56	0.66
		6	0.25	0.108	1.93	0.8	6.4	1.29	1.03	1.56	0.66
1	D_{max}	4	0.25	0.108	2.04	1.0	4.2	1.23	1.23	1.56	0.78
		2	0.25	0.108	1.46	1.2	2.5	1.15	1.39	1.56	0.92
		1	0.25	0.106	1.57	1.6	0.7	1.00	1.60	1.56	1.14
		8	0.25	0.108	5.09	1.6	6.4	1.12	1.80	1.56	1.15
		6	0.25	0.108	3.87	1.6	6.4	1.12	1.80	1.56	1.15
1	D_{min}	4	0.25	0.108	2.58	1.6	6.4	1.12	1.80	1.56	1.15
		2	0.25	0.108	2.04	1.9	4.2	1.09	2.08	1.56	1.33
		1	0.25	0.108	1.46	2.2	2.5	1.07	2.35	1.56	1.56
		8	0.26	0.099	3.44	1.4	8.0	1.33	1.86	1.56	1.19
		6	0.26	0.099	2.59	1.4	8.0	1.33	1.86	1.56	1.19
2	D_{max}	4	0.26	0.099	1.72	1.4	8.0	1.33	1.86	1.56	1.19
		2	0.26	0.099	1.69	1.8	2.9	1.18	2.12	1.56	1.36
		1	0.26	0.097	1.76	2.5	0.8	1.00	2.50	1.56	1.79
		8	0.28	0.099	6.93	2.8	7.3	1.13	3.17	1.56	2.03
		6	0.28	0.099	5.18	2.8	7.3	1.13	3.17	1.56	2.03
2	D_{min}	4	0.28	0.099	3.44	2.8	7.3	1.13	3.17	1.56	2.03
		2	0.28	0.099	1.72	2.8	7.3	1.13	3.17	1.56	2.03
		1	0.28	0.099	1.69	3.4	2.5	1.07	3.64	1.56	2.40
		8	0.45	0.161	3.01	2.4	8.0	1.33	3.19	1.56	2.04
		6	0.45	0.161	2.27	2.4	8.0	1.33	3.19	1.56	2.04
4	D_{max}	4	0.45	0.160	1.82	2.4	8.0	1.33	3.19	1.56	2.04
		2	0.45	0.158	1.77	2.6	2.6	1.16	3.01	1.56	1.98
		1	0.45	0.153	1.54	3.0	1.0	1.00	3.00	1.56	2.14
		8	0.48	0.161	6.07	5.5	8.0	1.14	6.27	1.56	4.02
		6	0.48	0.161	4.53	5.5	8.0	1.14	6.27	1.56	4.02
4	D_{min}	4	0.48	0.161	3.01	5.5	8.0	1.14	6.27	1.56	4.02
		2	0.48	0.160	1.82	5.7	7.1	1.13	6.45	1.56	4.13
		1	0.48	0.158	1.77	6	2.3	1.07	6.39	1.56	4.28

NS: Number of stories

Table B-14 Analysis Results for 1- and 2-Story SDC D_{max} Masonry Archetypes Arranged into Performance Groups

R	SDC	No. of stories	T (sec)	T_1 (sec)	Static Ω	*CMR*	μ_T	SSF	*ACMR*	*Accept. ACMR*	*ACMR/ (Accept. ACMR)*
		1	0.25	0.108	2.58	0.8	6.4	1.29	1.03	1.56	0.66
8	D_{max}	2	0.26	0.099	3.44	1.4	8.0	1.33	1.86	1.56	1.19
		Avg			3.01				1.45	1.96	0.74
		1	0.25	0.108	1.93	0.8	6.4	1.29	1.03	1.56	0.66
6	D_{max}	2	0.26	0.099	2.59	1.4	8.0	1.33	1.86	1.56	1.19
		Avg			2.26				1.45	1.96	0.74
		1	0.25	0.108	2.04	1.0	4.2	1.23	1.23	1.56	0.78
4	D_{max}	2	0.26	0.099	1.72	1.4	8.0	1.33	1.86	1.56	1.19
		Avg			1.88				1.54	1.96	0.79
		1	0.25	0.108	1.46	1.2	2.5	1.15	1.39	1.56	0.92
2	D_{max}	2	0.26	0.099	1.69	1.8	2.9	1.18	2.12	1.56	1.36
		Avg			1.57				1.75	1.96	0.89
		1	0.25	0.106	1.57	1.6	0.7	1.00	1.60	1.56	1.14
1	D_{max}	2	0.26	0.097	1.76	2.5	0.8	1.00	2.50	1.56	1.79
		Avg			1.66				2.05	1.96	1.05

Table B-15 Analysis Results for 1- and 2-Story SDC D_{min} Masonry Archetypes Arranged into Performance Groups

R	SDC	No. of stories	T (sec)	T_1 (sec)	Static Ω	*CMR*	μ_T	SSF	*ACMR*	*Accept. ACMR*	*ACMR / (Accept. ACMR)*
		1	0.25	0.108	5.09	1.6	6.4	1.12	1.80	1.56	1.15
8	D_{max}	2	0.28	0.099	6.93	2.8	7.3	1.13	3.17	1.56	2.03
		Avg			6.01				2.49	1.96	1.27
		1	0.25	0.108	3.87	1.6	6.4	1.12	1.80	1.56	1.15
6	D_{max}	2	0.28	0.099	5.18	2.8	7.3	1.13	3.17	1.56	2.03
		Avg			4.53				2.49	1.96	1.27
		1	0.25	0.108	2.58	1.6	6.4	1.12	1.80	1.56	1.15
4	D_{max}	2	0.28	0.099	3.44	2.8	7.3	1.13	3.17	1.56	2.03
		Avg			3.01				2.49	1.96	1.27
		1	0.25	0.108	2.04	1.9	4.2	1.09	2.08	1.56	1.33
2	D_{max}	2	0.28	0.099	1.72	2.8	7.3	1.13	3.17	1.56	2.03
		Avg			1.88				2.62	1.96	1.34
		1	0.25	0.108	1.46	2.2	2.5	1.07	2.35	1.56	1.56
1	D_{max}	2	0.28	0.099	1.69	3.4	2.5	1.07	3.64	1.56	2.40
		Avg			1.58				3.00	1.96	1.53

Figure B-20 provides a plot of probability of collapse versus period of vibration ($T = C_u T_a$) for all of the SDC D_{max} archetypes. There is a dramatic increase in probability of collapse as periods progress from about 0.45 seconds for the 4-story systems to 0.25 seconds for the 1-story system. Figure B-21 is a plot of the ratio of median peak inelastic displacement to median peak elastic displacement for the systems subjected to MCE level motions. These ratios increase exponentially at the lowest periods and are much larger than would be predicted from the "equal energy" rule (see Equation B-2b). Similar results are shown for the SDC D_{min} designs in Figure B-22 and Figure B-23.

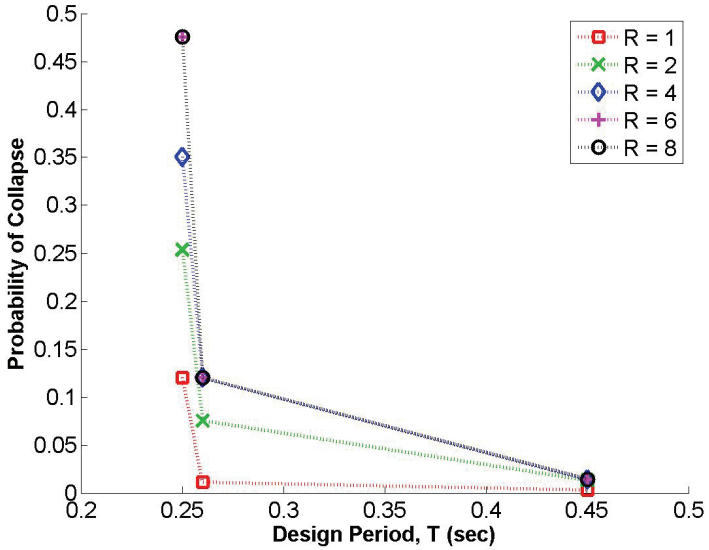

Figure B-20 Probability of collapse for SDC D_{max} archetypes.

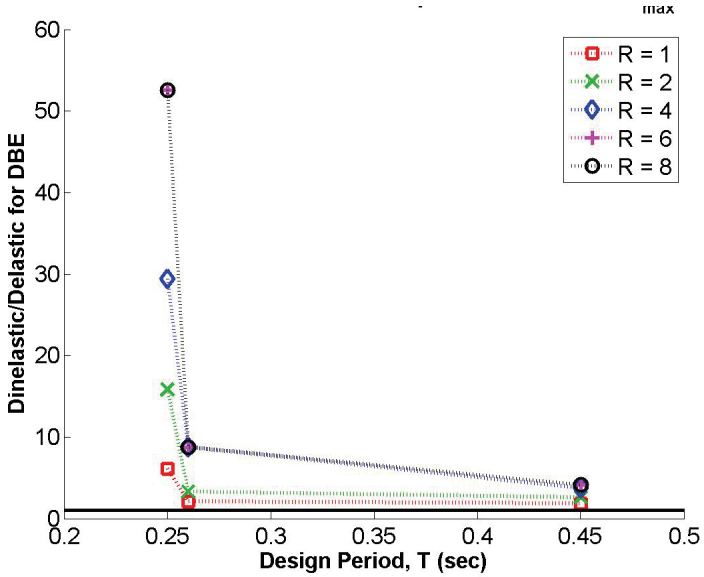

Figure B-21 Roof displacement ratios for SDC D_{max} archetypes.

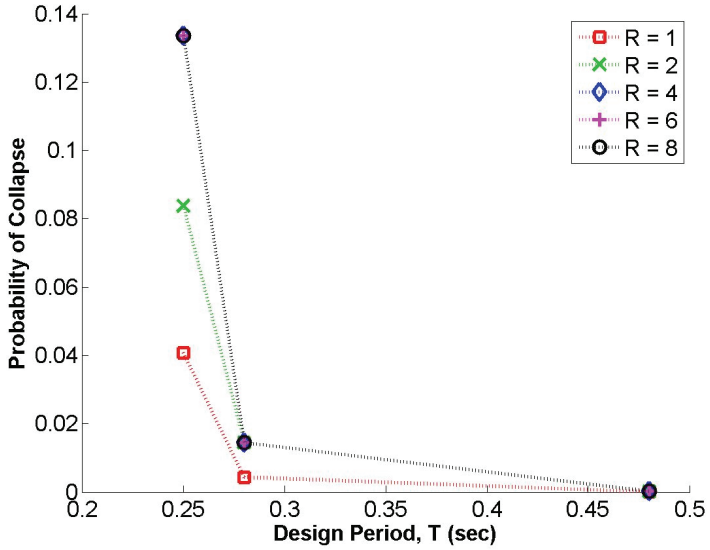

Figure B-22 Probability of collapse for SDC D_{min} archetypes.

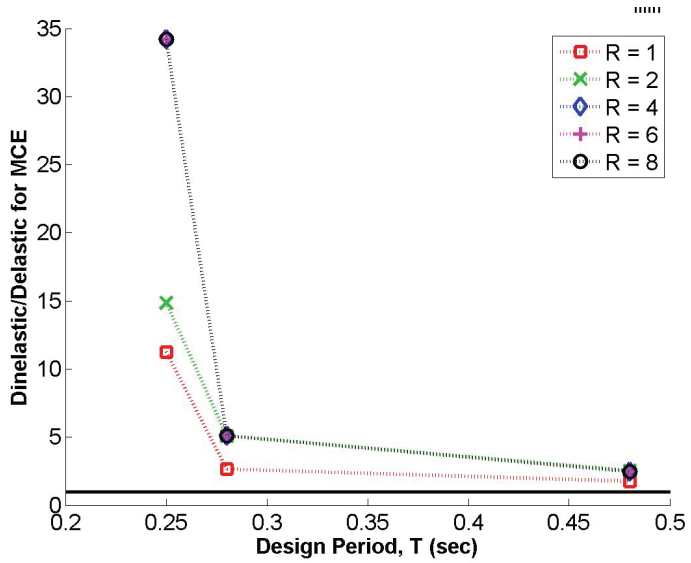

Figure B-23 Displacement ratios for SDC D_{min} archetypes.

Influence of Foundation Flexibility on Period of Vibration

All analyses discussed assumed that the walls were fixed at the base, which resulted in very short periods of vibration for all of the systems, particularly for the 1- and 2-story systems. Prior studies have indicated that foundation flexibility, when included in the development of acceleration spectra, has the tendency to reduce spectral accelerations at all periods, particularly at short periods. Figure B-24 shows such a spectrum that was developed as part of the FEMA 440 report (FEMA, 2005). As may be observed from the figure, spectral accelerations are reduced approximately 15% to 25% in the short-period constant acceleration region.

On the basis of the reduced accelerations shown in Figure B-24, there is some potential for foundation flexibility to affect the results of the analysis of the masonry

wall systems. Direct inclusion of the foundation flexibility was outside the scope of the studies presented herein but is recommended for future work. Short of performing such studies, the influence of foundation flexibility on computed period of vibration was investigated for the work reported herein. In this analysis, it was assumed that the walls were supported on a spread footing extending the length of the wall with a width of 24 inches and a depth of 18 inches. In this analysis, stiff clay, very stiff clay, hard clay, and rock (fixed base) foundations (soils) were considered.

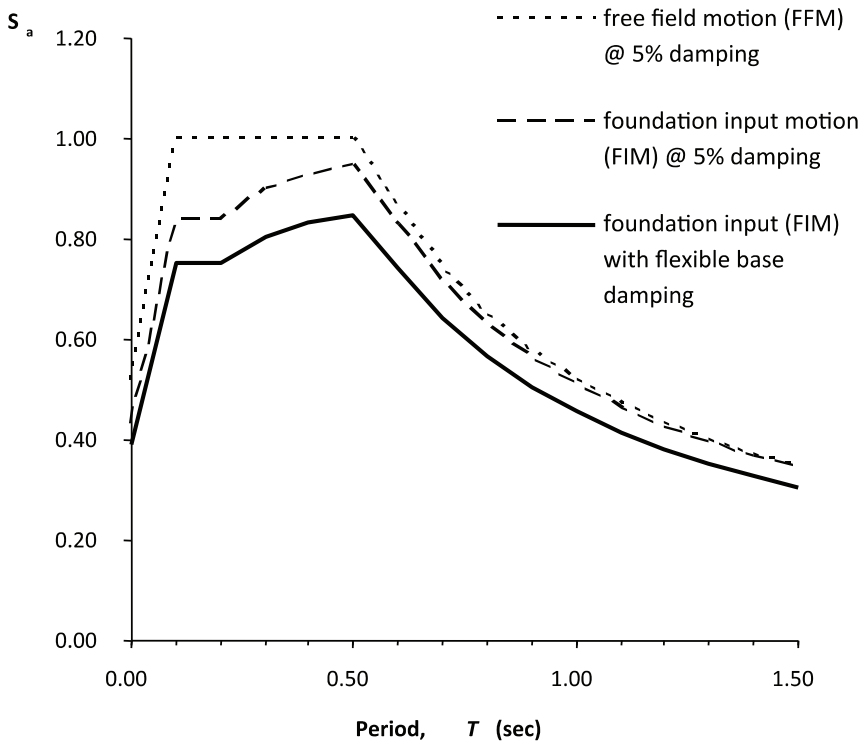

Figure B-24 Acceleration spectrum modified to include foundation flexibility.

In each analysis, the footing was treated as a rigid beam on elastic foundation, and it was assumed that vibration would occur without uplift. The results of the analyses in Table B-16 show that there is a significant increase in period as the soils become softer. For example, the period of vibration of the 1-story system increased from 0.11 seconds for the fixed base to 0.34 seconds when supported on hard clay and from 0.11 seconds to 0.65 seconds when founded on stiff clay.

Table B-16 Influence of Foundation Flexibility on Computed Period of Vibration

Model	Stiff Clay		Very Stiff Clay		Hard Clay		Fixed
	k_θ (kip-in/rad)	T_1 (sec)	k_θ (kip-in/rad)	T_1 (sec)	k_θ (kip-in/rad)	T_1 (sec)	T_1 (sec)
1-story	4.15E+06	0.65	8.29E+06	0.47	1.66E+07	0.34	0.11
2-story	9.83E+06	0.68	1.97E+07	0.48	3.93E+07	0.35	0.10
3-story	9.83E+06	1.19	1.97E+07	0.84	3.93E+07	0.60	0.15

Summary of Analysis of Masonry Archetypes

The basic findings from the analysis of the short-period special RMSW systems are as follows:

- Special RMSW systems with very short periods ($T < 0.125$ seconds) modeled with fixed base conditions would need to be designed using $R = 1$ if it is desired that these systems have less than a 20% probability of collapse under MCE shaking.
- Performance groups containing 1- and 2-story walls would need to be designed using $R = 1$ if it is desired to limit performance group probabilities of collapse to 10%. These findings are similar to those reported by other researchers when investigating the design and behavior of systems with very short periods.
- It is difficult, if not impossible, to predict the inelastic displacements of special RMSW systems with very short periods ($T < 0.125$ seconds) in terms of the displacement of the same system modeled as linear elastic. This is seen by the very large ratios of inelastic to elastic displacement shown in Figure B-18 and Figure B-20.

B.4.2 Buckling-Restrained Braced Frame (BRBF) Systems

The design space for the 1- and 2-story buckling-restrained braced frame systems is presented in Table B-17 through Table B-21. The design space consists of 1- and 2-story systems designed for SDC D_{max} and D_{min} ground motions and for $R = 2$, 4, 6, and 8. Thus a total of sixteen systems were design and evaluated.

Each of these systems consisted of frames with story heights of 13 feet, bay widths of 25 feet, and a "lightning bolt" bracing configuration. Table B-18 through Table B-20 provide section sizes for the braced cores, beams, and columns in each system, and Table B-21 provides a summary of the complete design space, including period of vibration and seismic coefficient. Wall layout and loading were the same as those used for the special concentrically braced frames analyzed in NIST GCR 10-917-8. Gravity loads were based on Steel TIPS report (Lopez and Sabelli, 2004) and Chapter 5 of NIST GCR 10-917-8. The equivalent lateral force (ELF) procedure was used for the design of all models.

Table B-17 Section Sizes for 1-Story BRBF Systems Designed for SDC D_{max}

Design *R* Value	Story Level	Brace Area	Column Size	Beam Size
2	1	8.0 in.^{2}	W14x53	W18x55
4	1	4.0 in.^{2}	W14x38	W18x46
6	1	2.5 in.^{2}	W14x38	W18x46
8	1	2.0 in.^{2}	W14x38	W18x46

Table B-18 Section Sizes for 2-Story BRBF Systems Designed for SDC D_{max}

Design *R* Value	Story Level	Brace Area	Column Size	Beam Size
2	2	11	W14x132	W21x73
	1	18	W14x132	W27x146
4	2	6	W21x74	W18x46
	1	9	W14x74	W21x83
6	2	4	W14x68	W18x46
	1	6	W14x68	W21x68
8	2	3.5	W14x68	W18x48
	1	4.5	W14x68	W21x68

Table B-19 Section Sizes for 1-Story BRBF Systems Designed for SDC D_{min}

Design *R* Value	Story Level	Brace Area	Column Size	Beam Size
2	1	4.0 in.^{2}	W14x48	W18x46
4	1	2.0 in.^{2}	W14x38	W18x46
6	1	1.5 in.^{2}	W14x38	W18x40
8	1	1.0 in.^{2}	W14x38	W18x40

Table B-20 Section Sizes for 2-Story BRBF Systems Designed for SDC D_{min}

Design *R* Value	Story Level	Brace Area	Column Size	Beam Size
2	2	4.0	W14x68	W18x46
	1	7.0	W14x68	W18x71
4	2	2.0	W14x48	W18x46
	1	3.5	W14x48	W18x50
6	2	1.5	W14x48	W18x40
	1	2.5	W14x48	W18x46
8	2	1.0	W14x48	W18x40
	1	2.0	W14x48	W18x46

Beam-column connections at the braces were assumed to be fully restrained due to gusset plate connections. Beam-column elements were modeled to capture the deterioration modes associated with plastic hinging (Lignos and Krawinkler, 2011). Columns were fixed at the base and were oriented to resist lateral forces through strong-axis bending. Beam column members were designed using ASTM A992 steel with f_y = 50 ksi.

Table B-21 Summary of BRBF System Properties

Archetype ID	NS	SDC	R	T(sec)	T_1(sec)	V/W	$S_{MT}(T)$ (g)
1S-LB-25B-Dmax-R8	1	D_{max}	8	0.29	0.51	0.125	1.5
1S-LB-25B-Dmax-R6			6		0.46	0.167	1.5
1S-LB-25B-Dmax-R4			4		0.38	0.250	1.5
1S-LB-25B-Dmax-R2			2		0.29	0.500	1.5
1S-LB-25B-Dmin-R8	1	D_{min}	8	0.31	0.65	0.062	0.75
1S-LB-25B-Dmin-R6			6		0.57	0.083	0.75
1S-LB-25B-Dmin-R4			4		0.51	0.125	0.75
1S-LB-25B-Dmin-R2			2		0.38	0.249	0.75
2S-LB-25B-Dmax-R8	2	D_{max}	8	0.48	0.64	0.125	1.5
2S-LB-25B-Dmax-R6			6		0.59	0.167	1.5
2S-LB-25B-Dmax-R4			4		0.50	0.250	1.5
2S-LB-25B-Dmax-R2			2		0.37	0.500	1.5
2S-LB-25B-Dmin-R8	2	D_{min}	8	0.52	0.97	0.048	0.58
2S-LB-25B-Dmin-R6			6		0.87	0.064	0.58
2S-LB-25B-Dmin-R4			4		0.77	0.097	0.58
2S-LB-25B-Dmin-R2			2		0.57	0.193	0.58

NS: Number of stories

Braces were assumed to have pinned end connections to the framing. Each brace was modeled with a corotational truss element. Equivalent elastic modulus was used to model the effect of various regions of the brace (yielding core, non-yielding core, and connection) between the brace ends. The fatigue material of OpenSees was used to model low cycle fatigue failure of BRBFs. Recommended values by Uriz and Mahin (2008) were used for low cycle fatigue parameters. A 42 ksi steel was used for the BRBF core plate yield strength. A leaning column was used to model second order effects. Two percent inherent damping was used for nonlinear dynamic analyses.

Low cycle fatigue of the braces was explicitly modeled. In addition, a non-simulated collapse criterion of 10% of maximum interstory drift was used as a measure of column fracture. Although an excessive strain that would cause failure of the brace was not assigned in the OpenSees fatigue material, 10% interstory drift corresponds to 4% brace strain according to the model geometry used. Thus, it is considered a collapse whenever a brace failed because of low cycle fatigue or a story drift reached 10%. Even though it is possible that the structure may still stand after losing the brace because of the moment resisting beam-column connections, this was never observed in the analyses.

In terms of quality rating, B (Good) was used for Test Data, Design Requirements, and Nonlinear Models. Nonlinear static pushover curves are shown for all of the models in Figure B-25 and Figure B-26.

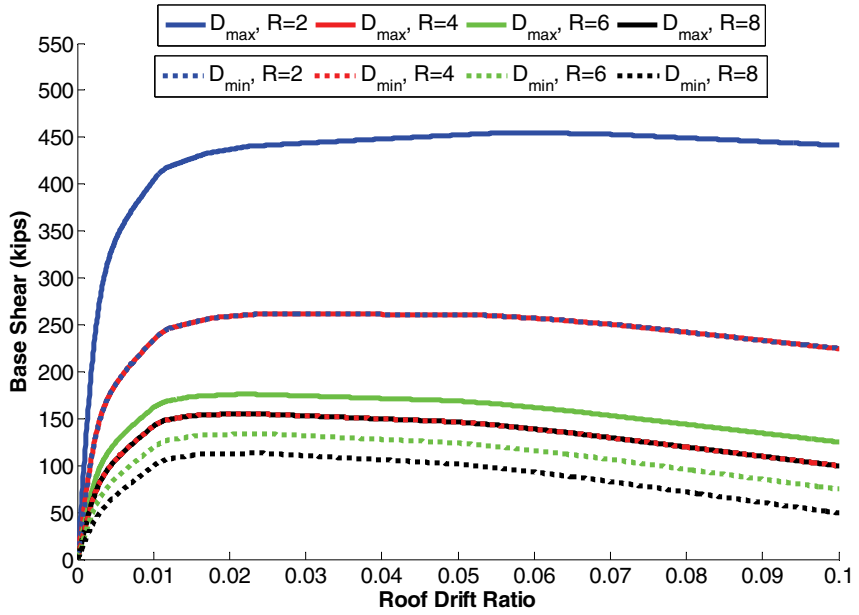

Figure B-25 Pushover curves for 1-story BRBF systems.

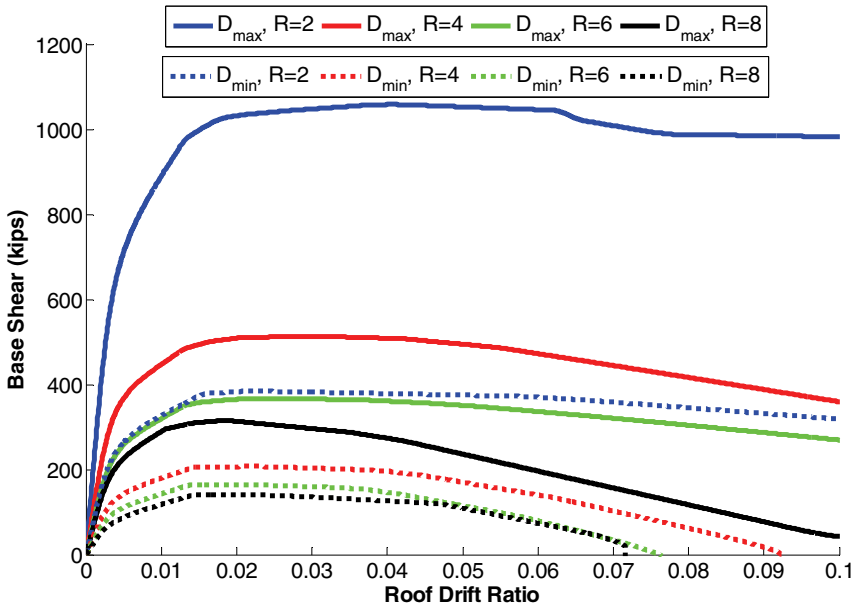

Figure B-26 Pushover curves for 2-story BRBF systems.

The results for the FEMA P-695 analysis of BRBF systems are provided in Table B-22, where all archetypes had less than a 10% probability of collapse under the MCE ground motions. The 1-story system with $R = 8$ under SDC D_{max} ground motions had the lowest ratio (1.22) of computed *ACMR* to $ACMR_{10\%}$. Ratios of inelastic drift to elastic drift at MCE and Design Basis Earthquake (DBE) levels are summarized in the last two columns of Table B-22, and these values are in the vicinity of 1.0 as predicted using the equal displacement concept.

Table B-22 Summary of FEMA P-695 Analyses of BRBF Systems

Archetype ID	T (sec)	T_1 (sec)	R	SDC	$ACMR$ / $ACMR_{10\%}$	$ACMR$ / $ACMR_{20\%}$	$ACMR_{10\%}$/ $ACMR$	$ACMR_{20\%}$/ $ACMR$	Probability of Collapse (%)	Inelastic/ Elastic at MCE	Inelastic/ Elastic at DBE
1S-LB-25B-Dmax-R8	0.29	0.51	8	D_{max}	1.22	1.53	0.82	0.65	4.82	1.079	0.880
1S-LB-25B-Dmax-R6	0.29	0.46	6		1.36	1.71	0.74	0.59	3.12	1.252	1.096
1S-LB-25B-Dmax-R4	0.29	0.38	4		1.90	2.39	0.53	0.42	0.61	1.108	0.985
1S-LB-25B-Dmax-R2	0.29	0.29	2		2.85	3.58	0.35	0.28	0.05	1.096	1.036
1S-LB-25B-Dmin-R8	0.31	0.65	8	D_{min}	1.74	2.19	0.57	0.46	0.96	0.850	0.826
1S-LB-25B-Dmin-R6	0.31	0.57	6		1.86	2.34	0.54	0.43	0.68	0.786	0.767
1S-LB-25B-Dmin-R4	0.31	0.51	4		2.21	2.78	0.45	0.36	0.26	0.864	0.791
1S-LB-25B-Dmin-R2	0.31	0.38	2		3.14	3.95	0.32	0.25	0.03	0.921	0.894
2S-LB-25B-Dmax-R8	0.48	0.64	8	D_{max}	1.49	1.88	0.67	0.53	2.04	1.062	0.893
2S-LB-25B-Dmax-R6	0.48	0.59	6		1.63	2.05	0.61	0.49	1.35	0.883	0.785
2S-LB-25B-Dmax-R4	0.48	0.50	4		1.90	2.39	0.53	0.42	0.61	0.847	0.738
2S-LB-25B-Dmax-R2	0.48	0.37	2		2.85	3.58	0.35	0.28	0.05	0.810	0.830
2S-LB-25B-Dmin-R8	0.52	0.97	8	D_{min}	1.86	2.34	0.54	0.43	0.68	0.859	0.852
2S-LB-25B-Dmin-R6	0.52	0.87	6		2.09	2.63	0.48	0.38	0.36	0.933	0.886
2S-LB-25B-Dmin-R4	0.52	0.77	4		2.44	3.07	0.41	0.33	0.14	0.792	0.781
2S-LB-25B-Dmin-R2	0.52	0.57	2		4.07	5.12	0.25	0.20	0.00	0.772	0.836

A series of plotted results are provided in Figure B-27 through Figure B-29. The upper part of each figure plots the results with the $T = C_u T_a$ period on the horizontal axis, and the lower part of the figure plots the same information versus the period determined from eigenvalue analysis.

It is clear from these analyses that the short-period problem is not present for the BRBF systems, likely because the true periods, T_1, from eigenvalue analysis are greater than 0.5 seconds for all of the $R = 8$ systems. The periods for the $R = 2$ systems are somewhat lower (as low as 0.29 seconds), but these systems have sufficient reserve capacity to eliminate collapse.

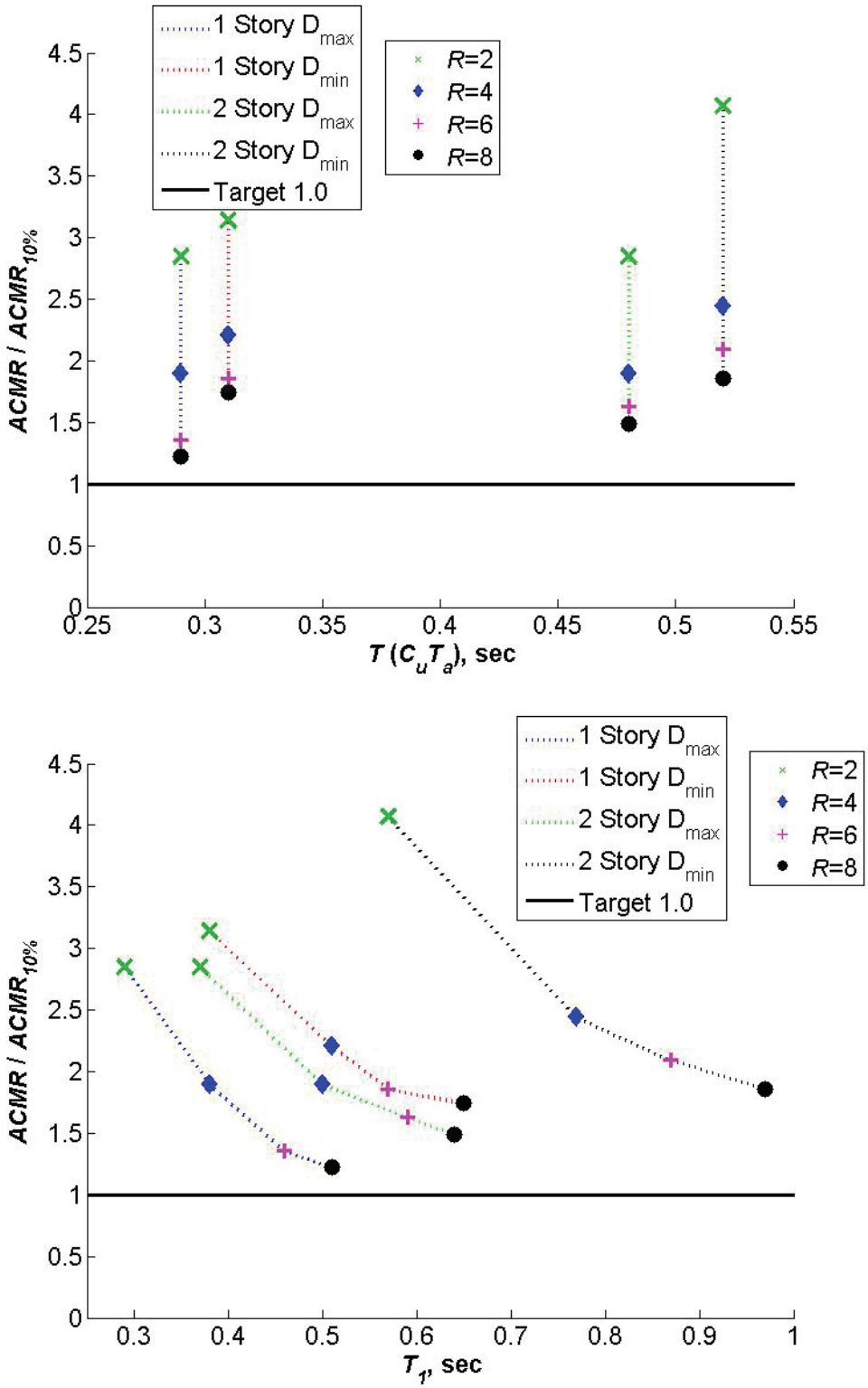

Figure B-27 Computed *ACMR* / $ACMR_{10\%}$ ratios for BRBF systems.

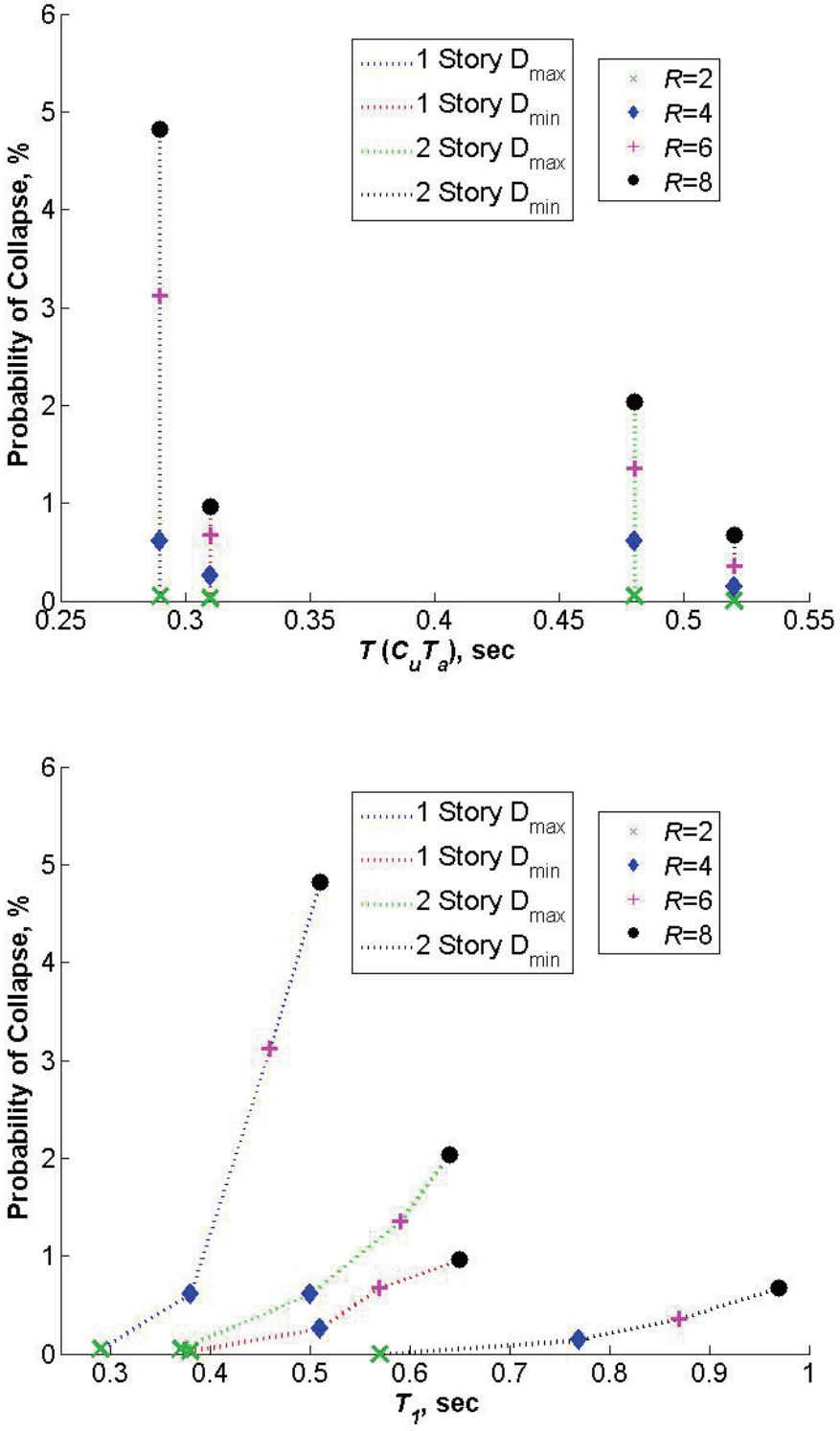

Figure B-28 Computed probabilities of collapse for BRBF systems.

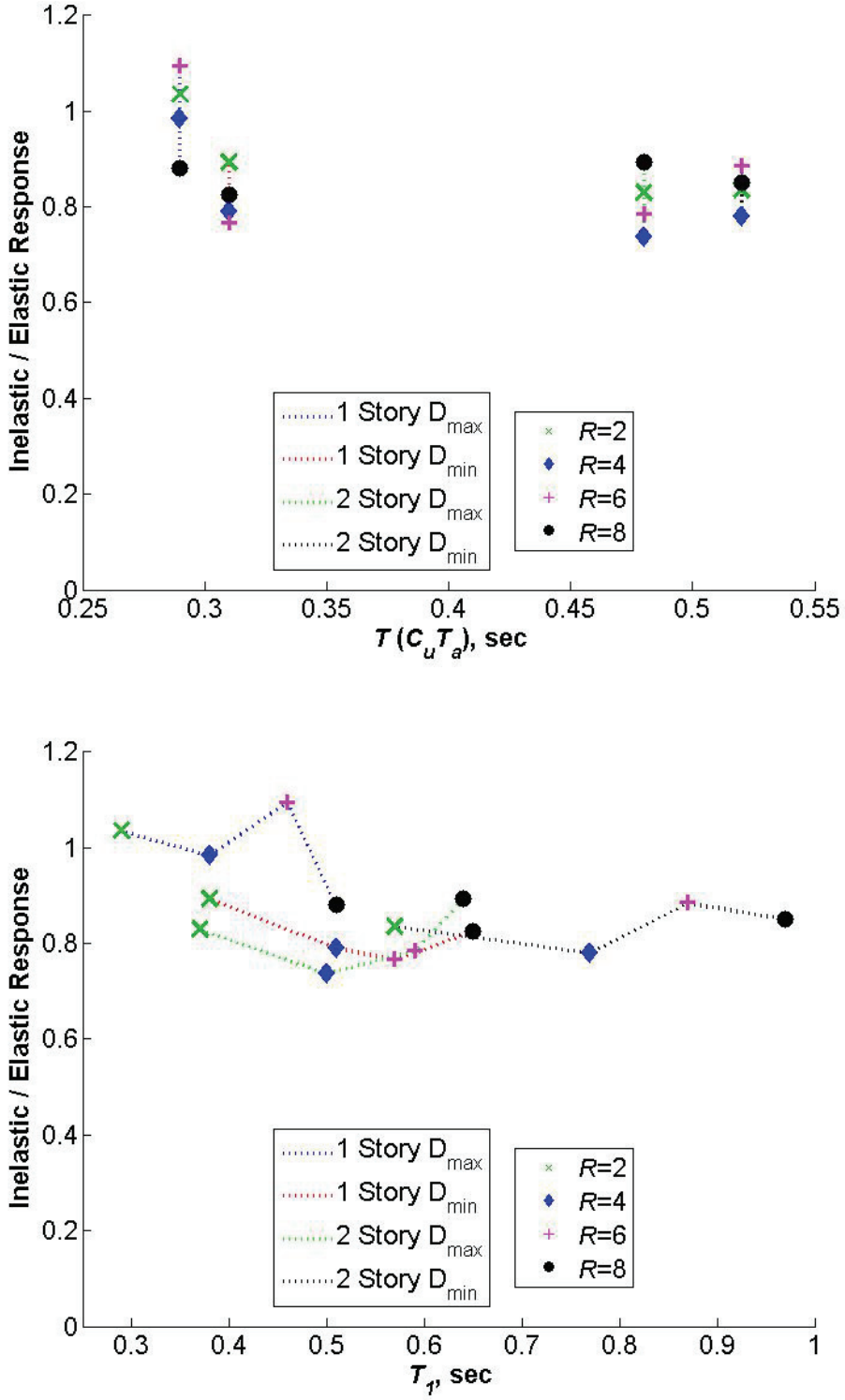

Figure B-29 Inelastic to elastic drift ratios for BRBF systems at the DBE level.

B.5 Observations and Findings

FEMA P-695 analyses of a variety of structural systems indicates a general tendency for shorter period archetypes (T less than about 0.5 seconds) of a given system to have a greater probability collapse than archetypes of the same structural system with longer periods. In particular, several of the 1- and 2-story reinforced masonry shear wall and reinforced concrete shear wall archetypes analyzed in the NIST GCR 10-917-8 report failed the FEMA P-695 acceptance criterion.

In order to investigate the above trends, design spaces of SDOF systems, reinforced masonry shear wall systems, and buckling-restrained braced frame systems were systematically analyzed using the FEMA P-695 Methodology. Each design space consisted of a basic system (e.g., a 1-story reinforced masonry shear wall), which was designed for a variety of R values, ranging from a low of 1 for all systems to a high of 10 for the SDOF systems. For each basic system analyzed, the probability of collapse and the ratio of maximum computed median inelastic displacement to the maximum computed median elastic displacement were recorded together with the R values used for the design of that archetype.

B.5.1 General Findings

The general results of these analyses are summarized as follows:

- For systems designed using some value of R, there is a clear trend of increased probability of collapse as the system period of vibration decreases from approximately 0.6 seconds to about 0.1 seconds.
- For systems designed using some value of R, there is a clear trend of the ratio of computed inelastic displacements to computed elastic displacements exceeding 1.0 as the system period decreases from about 0.5 seconds to about 0.1 seconds. At periods less than about 0.3 seconds, the ratio of inelastic to elastic displacement can be orders of magnitude greater than the ratios predicted using the equal energy concept.

B.5.2 Specific Findings

In the SDOF study, simple bilinear systems were designed with periods ranging from 0.1 seconds to 1.0 second in intervals of 0.1 seconds. The systems were designed using R values ranging from 1 to 10. Other variables included strain hardening stiffness (in terms of initial stiffness) and the ductility demand at which "collapse" was defined. The results of the analysis are summarized as follows:

- If it is desired to maintain a probability of collapse of 10% in 50 years under MCE ground motions, the design R values should be between 1 for systems with periods less than about 0.2 seconds and 5 for systems with periods of about 0.6

seconds. The probability of collapse is not strongly sensitive to the *R* value for periods from 0.6 seconds to 1.0 seconds. Figure B-8c and Figure B-9c clearly demonstrate this behavior.

- The ratio of computed inelastic displacement to computed elastic displacement is about 1.0 for systems with periods ranging from 0.6 seconds to 1.0 seconds but increases exponentially as the period decreases from about 0.6 seconds to 0.1 seconds. Figure B-8d and Figure B-9d demonstrate this behavior. In the period range of 0.1 to 0.6 seconds, the computed ratios of inelastic to elastic displacement far exceed those predicted using the equal energy concept, given by Equation B-1b.

The RMSW systems studied demonstrate a behavior that is entirely consistent with items above for the SDOF systems. Such behavior is observed in Figure B-20 through Figure B-23. Thus, 1-story archetypes consistently failed the FEMA P-695 acceptance criterion of no more than 20% probability of collapse for individual archetypes. While the 2-story archetypes all passed the FEMA P-695 criteria for individual archetypes, the short-period performance groups containing 1- and 2-story archetypes consistently failed to meet the 10% probability of collapse criteria because of the very poor performance of the 1-story systems.

The BRBF systems studied show a clear trend of increased probability of collapse as the system period decreases, and there was some tendency for the ratios of inelastic to elastic displacement to increase as the design period decreased. Such behavior is shown in Figure B-28 and Figure B-29. However, none of the BRBF systems failed the FEMA P-695 acceptance criteria, and the ratios of inelastic to elastic displacement never exceeded 1.1, even for the system with the shortest period.

As has been observed by many previous researchers, systems with very short periods do not behave in a manner consistent with the equal displacement principle. At periods less than about 0.6 seconds, the behavior of the systems shifts from a transient response to a behavior that is dominated by impulsive displacement and residual deformations. When the period is less than about 0.2 seconds, the response is completely dominated by the impulsive behavior. At these same low periods, the ratio of the computed displacement to the computed elastic displacement far exceeds 1.0, and far exceeds the ratio predicted by the equal energy concept.

If it is desired to maintain a 10% probability of collapse across all periods less than 0.6 seconds (given a constant collapse metric, such as a limited strain in shear wall reinforcement), it is necessary to reduce the design *R* value as the period decreases, with a limited value of $R = 1$ being required when the period is less than about 0.2 seconds. However, the reduction in *R* towards the limiting value of 1.0 is needed because the ratio of inelastic displacement to elastic displacement increases

exponentially as the period decreases. For very short systems it is impossible to provide sufficient ductility to accommodate this behavior, so a design *R* value of 1 is needed.

As noted in NIST GCR 10-917-8, it is doubtful that exceeding the collapse metric for the reinforced masonry and reinforced concrete shear wall systems would lead to a true collapse of the system, where collapse in this sense would include the loss of the gravity-load-resisting system. If, for example, the wall reaches its strain-based collapse at an interstory drift of 1.0%of the story height and the system loses its gravity load resisting capacity at an interstory drift of 2.5% of the story height, there is a range of 1.5% drift in which the wall must be able to continuously rotate or slide after the strain limit is reached. If the wall is detailed to accommodate that additional deformation, the system will not collapse so long as the 2.5% drift limit is not exceeded. If the FEMA P-695 collapse metric is adjusted to represent the full system failure and not the wall failure, the probability of true collapse could be determined. It is recognized that this is not the intent of the FEMA P-695 Methodology, and thus the use of the FEMA P-695 collapse metric in this context is debatable.

B.5.3 Mitigation of the Short-Period Problem

As mentioned previously, the results of any FEMA P-695 analysis are highly dependent on the measure of collapse used in the analysis. However, the observed trends for higher probability of collapse and increase in the inelastic to elastic displacement ratios for shorter period systems relative to longer period systems is largely independent of the collapse metric.

There are several options for dealing with the observed trends in the context of code requirements for building structures. Among these options are the following:

1. Make no modifications to current specifications (and therefore accept a higher probability of collapse), on the basis that there is a not a substantial body of field evidence that short-period buildings utilizing a given lateral-load-resisting system have a greater tendency to collapse than do buildings with longer periods of the same system type. In this context, collapse could be due to the failure of the lateral system or the gravity system or both. (While most of the FEMA P-695 analyses performed to date have included gravity systems in the leaning column sense, the strength and stiffness of gravity systems were not included.)
2. Make modifications to detailing requirements so that the modes of failure of the lateral-load-resisting system, such as rocking or sliding in the reinforced masonry shear wall systems, are accommodated or controlled in such a way that the integrity of building structure is not jeopardized. Such modifications would not alter the computed probabilities of collapse in the sense of a FEMA P-695 analysis.

3. Make modifications to the design specifications such that the probability of collapse of the short-period systems is the same as that of buildings with longer periods using the same system. Such modifications would require a substantial reduction in the value of R (or R_M) used to establish the required strength of the system. For the purpose of predicting inelastic displacements, it would also be necessary to introduce short-period deflection amplification factor, C_{ds}. This factor is needed because the computed ratio of inelastic displacement to elastic displacement increases well beyond that predicted by the equal displacement or equal energy concepts when the period of vibration falls below about 0.4 seconds.

The above options are not mutually exclusive. The best approach to solving the short-period problem will likely include some combination of the approaches.

Additional research is necessary before specific recommendations can be made regarding Option 1 and Option 2. Additional research is also needed for Option 3, but there is sufficient information to formulate at least a basis of the types of modifications that are needed.

Chapter 4 of this report presents possible recommended changes to ASCE/SEI 7-10, wherein an MCE_R based value of R, designated as R_M, is used. R_M consists of the product of ductility and overstrength components, as follows:

$$R_M = R_{Md} R_o \tag{B-9}$$

The short-period adjustment would be placed on the full value of R_{Md}, because the studies for masonry systems indicate that a design value of $R = 1$ is required for systems with periods less than about 0.2 seconds. (This warrants some discussion of what the meaning of overstrength is for $R = 1$ systems.) If it is desired to have a uniform probability of collapse across all periods, the relationship between R_{Md} and period would look like Line E on Figure B-30. Line A on the same figure represents the current approach wherein the same reduction value is used for all periods and where the probability of collapse increases significantly at very short periods. Each line on Figure B-30 is defined mathematically as follows:

For $T \le T_{min}$ $\qquad R = R_{Md,\,min}$

For $T_{min} < T < T_{max}$ $\qquad R_{Md} = R_{Md,\,min} + \left[R_{Md,\,max} - R_{Md,\,min} \right] \dfrac{T - T_{min}}{T_{max} - T_{min}}$ (B-10)

$T \ge T_{max}$ $\qquad R_{Md} = R_{Md,\,max}$

If, for example, T_{min} was set to 0.2 seconds, T_{max} was set to 0.6 seconds, $R_{Md,\,min}$ was taken as 1.0, and $R_{Md,\,max}$ was taken as 6.0, the expression for the sloping part of Line E would be:

$$R_{Md} = 1 + 10(T - 0.2) \tag{B-11}$$

For a system designed using Line E in Figure B-30, the value of the short-period displacement magnification factor, C_{ds}, would be 1.0 for all periods. This is because for low periods ($T < 0.2$s) the system is responding elastically ($C_{ds} = 1$), and for periods greater than 0.6 seconds, the value of C_{ds} is also 1.0. There is no basis for varying the value of C_{ds} above 1.0 in the intermediate period range.

However, if the value for R_{Md} does not depend on period (the probability of collapse of greater than 10% for a performance group is accepted), it is theoretically necessary to provide a short-period displacement amplifier in the very short period range ($T < T_{min}$) and to transition this multiplier to 1.0 for periods greater than T_{max}. Such a transition is provided graphically by Line A in Figure B-31. Here the maximum short-period deflection multiplier is 5.0 for very low periods. This value is in the general range of inelastic to elastic deflection ratios determined from the analysis of SDOF systems. Line E in Figure B-31 corresponds to the case where R_{Md} is modified to produce a constant probability of collapse across all periods. A general expression for the short-period multiplier is provided in the equations below.

$$\text{For } T \le T_{min} \qquad C_{ds} = C_{ds,\,max}$$

$$\text{For } T_{min} < T < T_{max} \qquad C_{ds} = C_{ds,\,max} - \left[C_{ds,\,max} - C_{ds,\,min} \right] \frac{T - T_{min}}{T_{max} - T_{min}} \tag{B-12}$$

$$T \ge T_{max} \qquad C_{ds} = C_{ds,\,min}$$

The sloping part of Line A in Figure B-31 would have the following expression:

$$C_{ds} = 5 - 10(T - 0.2) \tag{B-13}$$

Lines B, C, or D on Figures B-30 and B-31 could be used if an intermediate design was desired. However, the same alphabetically designated line would be used from each figure (for example, one would use Line D from each figure and not Line D from Figure B-30 and Line B from Figure B-31).

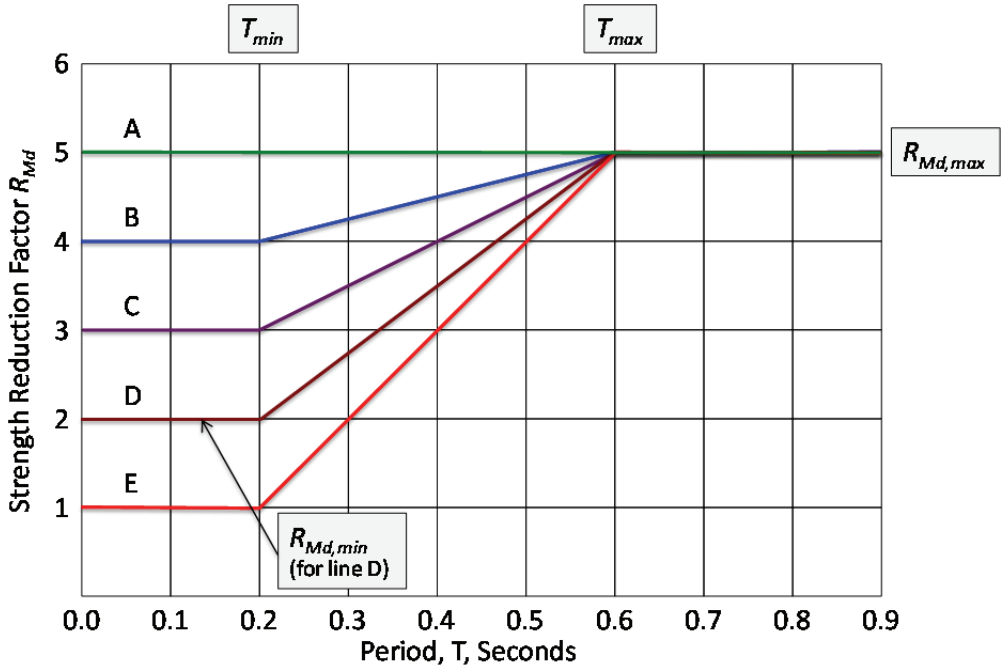

Figure B-30 Variation in R_{Md} with period of vibration.

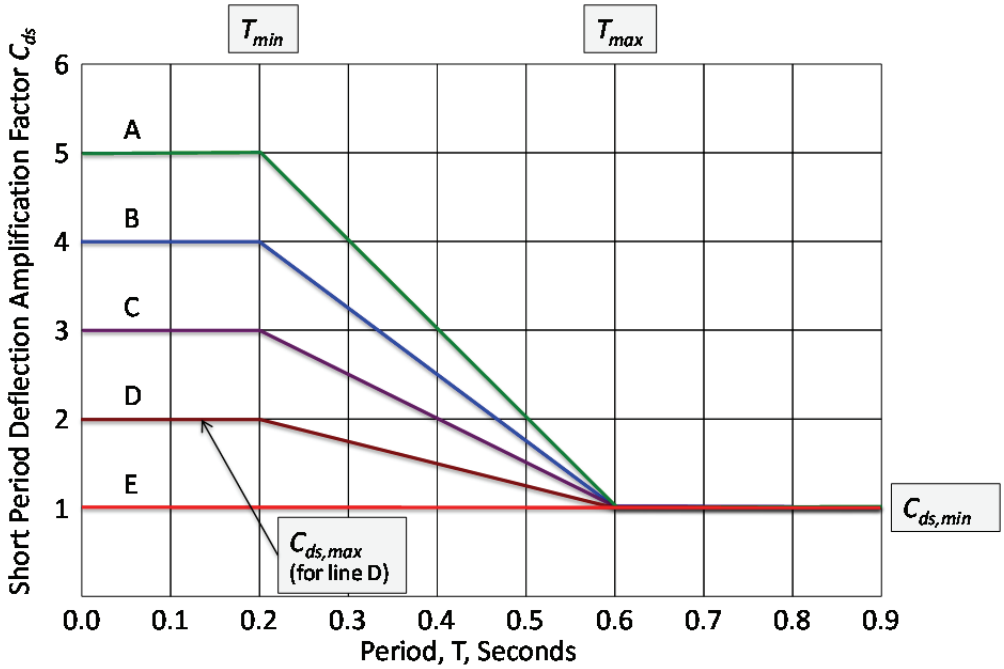

Figure B-31 Variation in C_{ds} with period of vibration.

Clearly, the use of Line E would have a great impact on the required strength of structures and may not be economically justifiable given the scarcity of evidence that short-period systems are indeed problematic. The use of Line A, which increases displacements at short periods, may not be as severe a penalty because short-period systems are rarely drift controlled. In all cases, significant research would be required to determine the appropriate period bounds and upper and lower limits on

R_{Md} and C_{ds} in Figure B-30 and Figure B-31. Another factor in the research is whether the period limits should be based on empirical or computed periods of vibration. The use of expressions as illustrated in Figure B-30 and Figure B-31 would, of course, be system dependent, and in some cases (e.g., steel moment frames), the figures would probably not be needed because even 1-story systems often have periods exceeding 0.4 seconds.

B.6 Recommendations

Given the lack of clear evidence that short-period systems are problematic outside of the computational and theoretical arena, it seems unwise to proceed with a recommendation to make significant adjustments to R_{Md} for short-period systems. However, adjustments to the computed deflection of short-period systems might be warranted. Thus, the principal recommendation from the work completed to date is to make no modification to R_{Md} but to further develop a perio-dependent relationship for C_{ds}.

The above recommendation is based on the ability of the system to deform beyond the point that the main lateral-load-resisting system reaches its ductile deformation limit and is then able to deform in a controlled manner up to the point that the gravity system loses its capacity. The main point of the development of the C_{ds} factor is to provide an improved way of predicting that maximum displacement.

The disadvantage of the above recommendation is that the probability of collapse, using previously established collapse metrics in association with FEMA P-695 analysis of two-dimensional models of systems that include only the lateral-load-resisting elements and fixed base conditions, will not be uniform across all periods (even when designs are modified to accommodate increased drifts). However, more refined analysis and alternate collapse metrics may show that probabilities of collapse are less than currently computed.

B.7 Future Studies

The basic recommendation and the related disadvantages motivate the need for the following future work related to the study of short-period systems:

- Revision of mathematical models of the structure to include axial-flexural-shear interaction. Such models were not available at the time of the original analysis.
- Revision of mathematical models of the structure to include reasonable stiffness and flexibility estimates of the foundation.
- Revision of mathematical models of the structures to include the gravity load-resisting systems, including the structural diaphragms and collectors. Such models would be three dimensional.

- Reconsideration of collapse metrics used for the analysis of reinforced masonry and reinforced concrete shear wall systems. Such metrics should be established not only for the lateral load-resisting system but for the gravity system as well.
- Review of the detailing of problematic short-period systems to determine if required sliding and rocking can be accommodated.
- Performance of FEMA P-695 analysis of a subset of short-period archetypes of reinforced masonry and reinforced concrete systems, modeled as described above and using revised collapse metrics. The results would be used to determine if the short-period problem persists. If the problem does persist, either from a strength, R_{Md}, perspective or from a deformation, C_{ds}, perspective, the required reformulation relationships described in Section B.5 should be further developed. All analyses will be based on the variable R_M design space utilized in previous research.

Appendix C

Study of Overstrength

C.1 Introduction

Structural overstrength has two related but distinct influences on seismic design. The first influence is the contribution of overstrength to the seismic response modification coefficient, *R* factor, which can be considered as the product of static overstrength, R_o, and a dynamic ductility response factor, R_d. In this regard, the overstrength provides a beneficial effect to the system, where for a given ductility the overstrength increases the available *R* factor (i.e., $R = R_O R_d$), or, alternatively, for a given *R* factor the overstrength reduces the required ductility (i.e., $R_d = R/ R_O$). The second influence is the increase of force demands on so-called force-controlled components, which are typically designed using some type of capacity design requirements. The overstrength used for capacity design is referred to as the Ω_O factor, which is specified in ASCE/SEI 7-10, *Minimum Design Loads for Buildings and Other Structures*, (ASCE, 2010) for use in the amplified seismic force demand calculation.

The study presented in this chapter is concerned with the second of these effects, i.e., the role of overstrength in establishing capacity design requirements for force-controlled components. This study is motivated by the following considerations:

- Prior studies of system archetypes, as summarized in Chapter 2, indicate that overstrength values, calculated using static pushover analyses, can vary considerably from the specified values of Ω_O in ASCE/SEI 7-10. For example, special steel and reinforced concrete moment frame archetypes had reported overstrength values ranging from 1.6 to 5.5, as compared to specified value of Ω_O equal to 3 for moment frames in ASCE/SEI 7-10. Thus, the studies presented in FEMA P-695, *Quantification of Building Seismic Performance Factors*, (FEMA, 2009) and NIST GCR 10-917-8, *Evaluation of the FEMA P-695 Methodology for Quantification of Building Seismic Performance Factors*, (NIST, 2010) reports raise questions as to whether the specified system overstrength factors provide consistent reliability of force-controlled components that are designed using Ω_O. As a practical measure, the FEMA P-695 Methodology for defining Ω_O limits the maximum value to 3, regardless of the calculated system overstrength factors from pushover analyses of the archetype configurations.
- In addition to the large variability in calculated overstrength values, there are basic questions as to whether the overstrength, as determined by a static pushover analysis, is an accurate measure of force demands that develop in force-controlled components during earthquake shaking. As shown in Figure C-1, in a

study of collapse resistance of special reinforced concrete moment frames, the collapse mechanisms varied for different ground motions, and the mechanism from the static pushover analysis was only observed in 17% of the dynamic analysis collapse cases. Thus, this raises the question as to whether the inelastic force demands from a pushover analysis are generally representative of component forces developed during strong ground shaking.

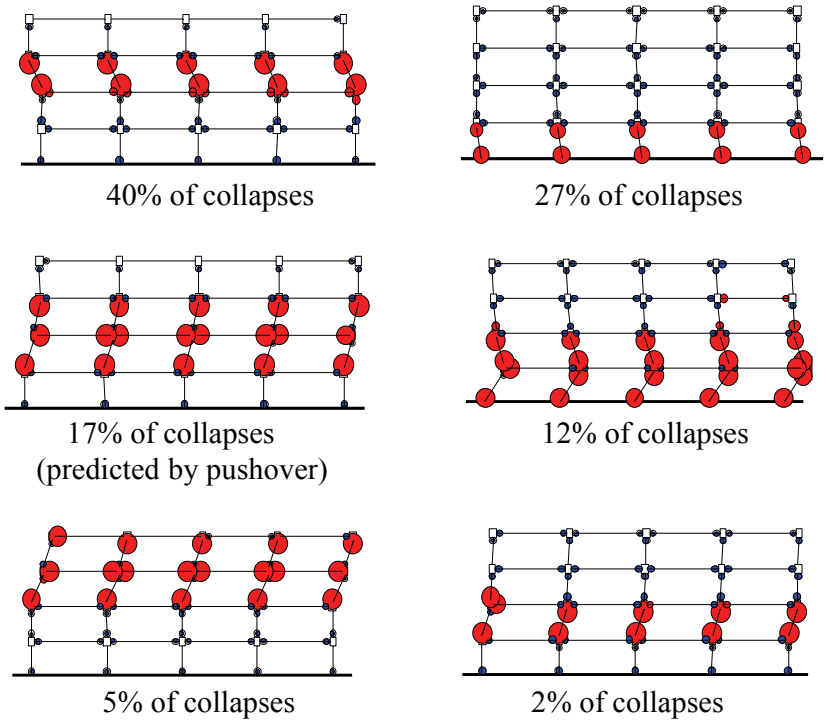

Figure C-1 Collapse modes of 4-story special reinforced concrete moment frames calculated by nonlinear dynamic analysis (Haselton and Deierlein, 2007).

- Material specifications, notably ANSI/AISC 341-10, *Seismic Provisions for Structural Steel Buildings*, (AISC, 2010) include requirements for capacity-based design of force-controlled components, yet they typically do not rely on the system overstrength factor and instead employ more specific checks based on the expected strength of deformation-controlled (yielding) elements. This raises the question as to whether the existing system overstrength factors and amplified force equation are still as relevant and necessary for design as implied by their prominence in the ASCE/SEI 7-10 seismic design provisions.
- Emerging use of performance-based design methods, including those that employ nonlinear response-history analysis, have drawn attention to the significance of uncertainties in establishing appropriate criteria for force-controlled components. Thus, the role of "overstrength" cannot considered with characteristic (central value) force demands alone. Rather, the design of force-controlled components

involves consideration of the following: (1) at what ground motion intensities the force demands should be calculated; (2) reliability considerations of the uncertainties in force demands and component strengths; and (3) how the failure of force-controlled components affect the system collapse safety. This raises the question of how the FEMA P-695 Methodology could be extended to more accurately evaluate the reliability of design procedures and criteria for force-controlled components. Insights gained by investigating this question in relation to the FEMA P-695 Methodology would serve to inform and improve other design procedures that rely on nonlinear response-history analyses to determine seismic force and deformation demands on structural systems and components.

Considering these factors, the initial motivation of this study to assess the Ω_O values specified in ASCE/SEI 7-10 was expanded to more broadly consider capacity design requirements for force-controlled components of seismic systems.

Section C.2 provides a review of the way current design provisions, including ASCE/SEI 7-10 and the underlying material specifications, use the amplified seismic load and other provisions for design of force-controlled components. The review of design criteria also includes criteria from recently published guidelines for design of tall buildings by nonlinear analysis. Section C.3 briefly looks at some emerging research and standards development related to force demands and capacity design of force-controlled components. Sections C.4 and C.5 present results from nonlinear analysis of special steel concentrically braced frame (SCBF) and special reinforced concrete moment frame (RCMF) archetypes to examine force demands and how accurately they are reflected in design criteria for force-controlled components. The appendix concludes with Sections C.6, C.7, and C.8, which present a summary of the results and recommendations for strategies and future work to improve the specification of design requirements for force-controlled components.

C.2 Building Code Provisions for Capacity Design

C.2.1 Conventional Design by Elastic Analysis

Requirements for capacity design of force-controlled components and other checks related to system overstrength are specified at several locations in ASCE/SEI 7-10 and the referenced material specifications. The basic overstrength provision is specified in ASCE/SEI 7-10 Section 12.4.3, where the amplified horizontal seismic force is defined as the product of Ω_O and Q_E, and where Ω_O is specified in ASCE/SEI 7-10 Table 12.2-1 and Q_E is the lateral seismic force as calculated by the equivalent lateral force (ELF) procedure, the response spectrum analysis (RSA) procedure, or other methods. With the exception of a few nonductile systems, the tabulated values of Ω_O range between 2 and 3, typically equal to about one-quarter to one-half of the R values for ductile systems permitted in Seismic Design Category (SDC) D and above.

This amplified force is then invoked by other provisions of ASCE/SEI 7-10 or the underlying material design standards.

In contrast to common perception, there are relatively few components whose design is specified using the overstrength factor. Summarized in Table C-1 are instances where the amplified seismic force provision or other capacity design requirements for force-controlled components are specified in ASCE/SEI 7-10 and in referenced material standards, ANSI/AISC 341-10, ACI 318-11, *Building Code Requirements for Structural Concrete and Commentary*, (ACI, 2011), and TMS 402-05/ACI 508-05/ASCE 5-08, *Building Code Requirements for Masonry Structures*, (TMS, 2005). There are also capacity design features in the American Iron and Steel Institute (AISI) standards for shear walls constructed with cold-formed steel framing and the American Wood Council (AWC) standard for wood structures, although some of them are not particularly apparent. As indicated, ASCE/SEI 7-10 specifies the use of Ω_O for the following: (1) supports of discontinuous walls; (2) collectors; (3) certain transfer diaphragms; and (4) as an upper limit check for systems with a weak story. In other material specifications for steel, concrete, masonry, and wood structures the only specific references to the amplified seismic load are a few instances as an upper limit on force demands in steel-framed structures and a lower limit for shear in columns of intermediate reinforced concrete moment frames. Otherwise, capacity-design requirements (several for steel structures, a few for concrete and masonry structures, and almost none for wood structures) are defined by the expected strengths of yielding members. This summary deals only with overstrength and amplified force provisions for conventional structural building systems and does not include provisions for seismically isolated structures, structures with added damping, and non-building structures.

C.2.2 Design by Nonlinear Response-History Analysis

As design using nonlinear response-history analysis is finding its way into practice, it is useful to consider how current practice treats the design of force-controlled components. Related design requirements include those of Chapter 16 of ASCE/SEI 7-10 and recommended guidelines provided by the *Guidelines for Performance-Based Seismic Design of Tall Buildings* (PEER, 2010) and *An Alternative Procedure for Seismic Analysis and Design of Tall Buildings Located in the Los Angeles Region* (LATBSDC, 2011).

Table C-1 Capacity Design Provisions in Design Standards

Component or System	Design Standard	Ω_O	Description of Capacity Demand Requirements
Weak story	ASCE/SEI 7-10 12.3.3.2	X	Extreme weak stories (65% less strength) shall not be over 2 stories or 30ft in height, unless the weak story can resist Ω_O times the design force.
Components supporting discontinuous walls	ASCE/SEI 7-10 12.3.3.3	X	Columns, beams trusses, or slabs and their connections supporting discontinuous walls or frames or structures with horizontal irregularity, Type 4 of Table 12.3-1 (out-of-plane offsets) or vertical irregularity Type 4 of Table 12.3-2 (in-plane offsets) shall be designed to resist the minimum axial force that can develop in accordance with load combinations with overstrength factor, Ω_O, per Section 12.4.3.2.
Diaphragm forces	ASCE/SEI 7-10 12.10.1.1	X	Transfer diaphragms in structures assigned to seismic design categories D, E, or F shall be designed for a 25% increase in seismic forces or in accordance with load combinations with overstrength factor, Ω_O, per Section 12.4.3.2.
Collector forces	ASCE/SEI 7-10 12.10.2.1	X	Collector elements in structures assigned to seismic design categories C, D, E, or F shall be designed for seismic forces accordance with load combinations with overstrength factor, Ω_O, per Section 12.4.3.2.
RC wall shear strength	ACI 318-11 9.3.4		In Seismic Design Categories D, E, and F structural walls, columns and beams resisting shear from seismic effects shall have $\varphi = 0.60$ (instead of $\varphi = 0.75$) unless the nominal shear strength is greater than the shear force associated with the development of the nominal flexural strength of the member under any load combination including seismic effects. Also, diaphragms shall be designed such that the capacity reduction factor, φ, for shear shall not exceed the smallest such factor for shear used for any member in a vertical element of the seismic force-resisting system.
Shear in beams of intermediate RCMF	ACI 318-11 21.3.3.1		Required shear force in beams shall be based on lesser of (a) shear due to nominal flexural strength applied at the joints faces and factored tributary gravity load along span, and (b) force based on design load combinations with *E* assumed to be twice that prescribed by code.
Shear in columns of intermediate RCMF	ACI 318-11 21.3.3.2	X	Required shear force in columns shall be based on lesser of: (1) shear due to nominal flexural strength applied at column ends under reverse curvature bending, and (2) force based on design load combinations with *E* amplified by Ω_O.
Shear in Beams and Columns of special RCMF	ACI 318-11 21.5.4.1 21.6.5.1		Required shear force shall be based on probable maximum flexural strength M_{pr} applied at the joints faces and factored tributary gravity load along span. M_{pr} based on a steel yield strength of $1.25f_y$. For columns, the provisions also allow for limiting the shear demands based on the probable strengths of beams framing into the columns.
Column strength in special RCMF	ACI 318-11 21.6.2.2		The sum of the nominal flexural strength of columns framing into a joint, ΣM_{nc}, (calculated for the factored axial force) shall be greater than 1.2 times the sum of the nominal flexural strength of the beams ΣM_{nc}.
Joint strength in special RCMF	ACI 318-11 21.7.2.1		Forces at joint face shall be determined by assuming the flexural stress in longitudinal reinforcement is $1.25f_y$.
Shear in flexural masonry members (including shear walls)	TMS 402 3.1.3		The design shear strength ϕV_n shall exceed the shear corresponding to the development of 1.25 times the nominal flexural strength, M_n, except the nominal strength, V_n, need not exceed 2.5 times the required shear strength V_u.

Table C-1 Capacity Design Provisions in Design Standards (continued)

Component or System	Design Standard	Ω_O	Description of Capacity Demand Requirements*
Columns in steel seismic systems	ANSI/AISC 341-10 D1.4	X	Required axial strength provisions shall be based on the following: (1) amplified seismic load; (2) load from yielding members including the effects of material overstrength and strain hardening; (3) limiting resistance of foundation.
Column splices in steel seismic systems	ANSI/AISC 341-10 D2.5		Required strength of welded splices in seismic resisting system shall be based on 200% of calculated loading effect or at least 50% of the strength of the expected yield strength of column flanges ($R_yF_yb_ft_f$).
Column bases in steel seismic systems	ANSI/AISC 341-10 D2.6	X	Required strength of bases shall be lesser of M_{pc}/H (shear) and $1.1R_yF_yZ_x$ (moment) or the shear/moment calculated using the amplified seismic load.
Special SMF connections	ANSI/AISC 341-10 E3.6		Required shear strength of beam column connections shall be based on load combinations with amplified seismic load, $E = 2[1.1R_yM_p/L_h]$. Other design aspects covered by pre-qualified connection provisions or demonstrated by tests.
Special SMF columns	ANSI/AISC 341-10 E3.4		Minimum required column flexural strengths shall be determined without ϕ factors and compare with beam flexural strengths calculated based on $1.1R_y F_yZ_x$.
Special SCBF columns	ANSI/AISC 341-10 F2.3	X	Required strength shall be based on larger of load from all braces at their expected strength or tension braces at their expected strength and compression braces at their expected post-buckling strength but never to exceed load from amplified seismic load in which all compression braces have been removed.
EBF link-column connection	ANSI/AISC 341-10 F3.6		Required strength of link-to-column connection is the nominal shear strength of the link V_n at the maximum rotation angle. Testing is required to demonstrate deformation capacity of connection for some cases.
EBF braces	ANSI/AISC 341-10 F3.4		Minimum required strength equal to axial force associated with 1.25 or 1.4 (I-shaped/box shaped) times expected shear strength of link, R_yV_n.
EBF beams	ANSI/AISC 341-10 F3.4		Minimum required strength equal to moment and axial force associated with 1.25 or 1.4 (I-shaped/box shaped) times expected shear strength of link, $R_y V_n$. The available beam strength may also be increased by R_y.
EBF beam-column connections	ANSI/AISC 341-10 F3.6		For EBF's with moment connections, the required strength of beam-column connections is the same as for ordinary moment frames, $1.1R_yM_p$.
BRBF beams and adjoining members	ANSI/AISC 341-10 F4.2		Required strength of adjacent members (e.g., chevron beams) and their connections shall be based on adjusted brace strengths, $\beta\omega R_yP_{ysc}$, in compression and ωR_yP_{ysc} in tension.
BRBF brace connections	ANSI/AISC 341-10 F4.6		Required strength of brace connections shall be 1.1 times the adjusted brace strengths in tension and compression.

ASCE/SEI 7-10 Chapter 16 specifies that the force demands be established using analysis results based on seven pairs of ground motions that are scaled to the Design Basis Earthquake (DBE) intensity. For force-controlled components, ASCE/SEI 7-10 specifies that force demands should be determined from the maximum value

obtained from the seven record-pair analyses by setting the component's design strength, ϕR_n, to be equal to or larger than the force demand. The component design strength is presumably determined using the usual materials standards.

The PEER *Guidelines* require that force demands for force-controlled components be calculated based on mean forces calculated under the Maximum Considered Earthquake (MCE) intensity using at least seven pairs of ground motions. To account for uncertainties in force demands, the mean values are increased by a factor ranging from 1.2 to 1.5, depending on whether the variability in force demands is constrained by yielding of nearby elements. The force-controlled component is then checked by comparing the calculated demands to the expected design strength, $\phi R_{n,exp}$, calculated by the usual materials standards, except that expected material strengths are used in lieu of nominal (minimum specified) strengths. The use of expected strengths is justified since this check is made at MCE, as opposed to DBE, ground motion intensities.

The LATBSDC *Procedure* is similar to those of the PEER *Guidelines*, except for one notable difference. Whereas the PEER *Guidelines* use the expected design strength, $\phi R_{n,exp}$, the LATBSDC *Procedure* specifies the design check using the expected strength, $R_{n,exp}$, without a resistance factor. As a result, there is a significant difference in the inherent reliability between the two procedures.

Thus, in considering how nonlinear analysis design methods should achieve parity with conventional elastic design, it is important to consider the following: (1) at what ground motion intensities the design check is made; (2) how uncertainties in the force demands are considered; and (3) what strength (nominal versus expected strength, with or without resistance factors) is used in the design check.

C.3 Previous Studies of Capacity-Design Requirements

There are relatively few studies that have systematically evaluated force demands on force-controlled components. Some studies have addressed force demands in specific components of specific systems, whereas others have discussed capacity design requirements in more general terms.

C.3.1 Disaggregation of the R Factor

Mitchell et al. (2003) describe the background to changes made in *National Building Code of Canada 2005* (NRC, 2005), where the *R* factor was disaggregated into the product of R_o and R_d, where R_o is the static overstrength. The authors discuss how the static overstrength, R_o, is further disaggregated into five contributions: (1) R_{size} resulting from oversizing of members that occurs because of various design considerations including those related to drift (minimum stiffness) requirements, discrete member sizing, architectural requirements, and construction practicality; (2)

R_ϕ, the effect of the resistance factor to increase the effective member strength; (3) R_{yield} reflecting the difference between expected and minimum nominal specified material strengths; (4) R_{sh} due to strain hardening; and (5) R_{mech} due to inelastic force redistribution that reflects the difference between the first yield and the peak strength. As the goal of their study is to establish minimum values of R, their proposed overstrength factors reflect minimum values, which would not be appropriate for determination of Ω_O. However, the disaggregation approach to describing R_o could be adapted to help establish minimum values for Ω_O.

C.3.2 Column Axial Force Demands in Braced Frames

Richards (2009) examines axial force demands in seismically designed steel braced frames through the use of nonlinear static and dynamic analyses. Pushover strengths in the range of 1.5 to 2.0 are reported for SCBF and buckling-restrained braced frame (BRBF) systems. The study draws attention to the dramatic change in behavior when brace buckling occurs and the influence of building height on the axial column force demands. Design standards that assume all braces are at their expected tensile or compression strengths tend to underestimate the column force demands in the upper stories and overestimate demands in the lower stories. For special SCBFs, an approach to determine column design forces using an analysis that reflects the post-buckling brace strengths, either by reducing the compression brace forces or removing entirely the buckled braces from the analysis model, is recommended. Richards's research is reflected in the latest revisions to ANSI/AISC 341-10 for special SCBFs, which cap the required column forces as those calculated using $\Omega_O Q_E$ force demands where compression braces are removed from the analysis model.

C.3.3 Shear Force Demands in Walls

Calvi et al. (2008) and others have conducted nonlinear dynamic analyses to examine shear demands in concrete shear walls, pointing out that the actual shear demands are usually quite higher than those determined by conventional design approaches. The amplification of shear force issue is not necessarily capped by the flexural overstrength in the wall, as might be determined by a pushover analysis. Instead, the way large shear forces occur due to higher modes, which tend to respond elastically even when the wall base is hinging, is described. Calvi et al. (2008) recommend a procedure whereby the shear demands are determined by the elastic higher mode response at the ground motion intensity of interest.

C.3.4 Diaphragm Forces

Several studies have examined the calculation of diaphragm forces in buildings. Gardener et al. (2008) conducted nonlinear analyses to assess diaphragm forces in dual frame-wall system buildings ranging in height from 3- to 12-stories. The importance of differentiating diaphragm forces arising from inertial effects and

inelastic load transfer, the latter of which occurs between frames and walls in dual systems or in any system where there are significant force transfers from one lateral force resisting subsystem to another is discussed, and a method to calculate inertial diaphragm forces that employs an overstrength factor on the elastic seismic design forces and a lower bound value based on the peak ground acceleration (PGA) is proposed. Although the proposed method for inertial effects is shown to work well, the way diaphragm transfer forces, calculated by inelastic analyses, can be significantly (up to ten times) larger than those calculated by elastic analysis is also described. Rodriguez et al. (2002) report dynamic analysis results for 3-, 6-, and 12-story shear wall buildings, which show how the inertial diaphragm forces are influenced by PGA, higher mode effects and inelastic action. A procedure to calculate diaphragm forces that uses superposition of modal responses, where the first-mode (sway) response is reduced for inelastic effects and elastic response is assumed in calculating higher mode effects, is proposed.

C.3.5 Reliability Considerations in Force-Controlled Components

As noted previously with regard to the requirements for design by nonlinear dynamic analysis, reliability considerations are important in the design of force-controlled components so as to properly consider the uncertainty in the force-demands and component strengths, and target reliability of the force-controlled component, considering the ground motion intensities and influence of component failure on collapse. Victorsson et al. (2011) have developed a reliability approach to address these concerns, which is based on an adaptation of the reliability formulation used for load resistance factor design. For seismic design of force-controlled components, the target reliability index is based on the permissible collapse rate, the slope of the ground motion hazard curve, and the influence of component failure on overall collapse.

C.4 Special Steel Concentrically Braced Frame (SCBF) Studies

In order to investigate the capacity design requirements for force-controlled components and how well the force demands are calculated by the system overstrength factor or other methods, force demands are calculated by nonlinear analyses of structural archetypes for special steel concentrically braced frame systems.

Shown in Figure C-2 are three special SCBF archetypes that were studied. These designs are the same as those investigated in the NIST GCR 10-917-8 report. OpenSees models (http://opensees.berkeley.edu/) of each of the three archetypes were developed that are similar to the models developed previously, except for one very significant difference. In this study, the beam and column hinges were modeled using strength degrading (softening) hinge models, whereas in the previous study the beams and columns were modeled with non-degrading fiber hinges that do not

degrade. As the frame action provides significant lateral resistance, the difference between non-degrading and degrading beam and column models is expected to have a significant influence on collapse capacity. The degrading hinges in the beams and columns were modeled using the Krawinkler-Ibarra model that followed the backbone curve shown in Figure C-3 and using parametric equations from PEER/ATC-72-1, *Modeling and Acceptance Criteria for Seismic Design and Analysis of Tall Buildings*, (PEER/ATC, 2010), to determine the hinge rotation capacities. The braces were modeled in a similar way to the previous study, using fiber type beam-column elements that included steel material yielding, geometric out-of-straightness, and a low-cycle fatigue model that together simulate brace yielding, buckling, and fracture.

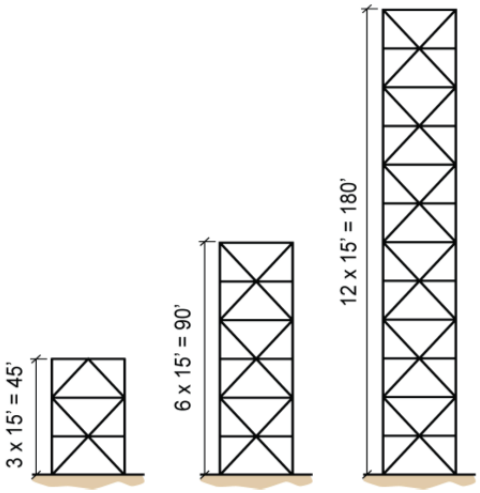

Figure C-2 Special SCBF archetypes.

C.4.1 Results from Static Pushover Analyses

Shown in Figure C-4 is a pushover curve for the 3-story archetype, which is generally representative of the pushover results for each of the special SCBF archetypes. Generally, the deformations concentrated in one story, leading to large drift ratios and, ultimately, loss of lateral strength. The static overstrength, Ω, calculated for each of the archetypes are summarized in Table C-2, along with values calculated in the previous study.

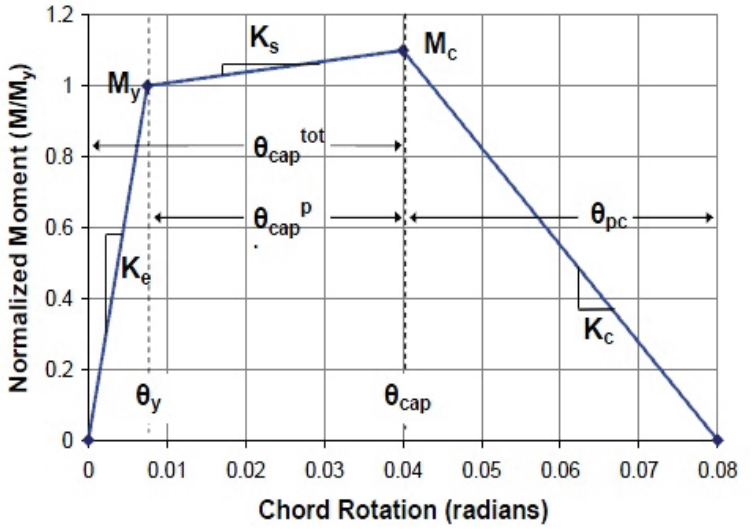

Figure C-3 Illustration of monotonic hinge backbone curve for flexural members in special SCBF and RCMF archetype models.

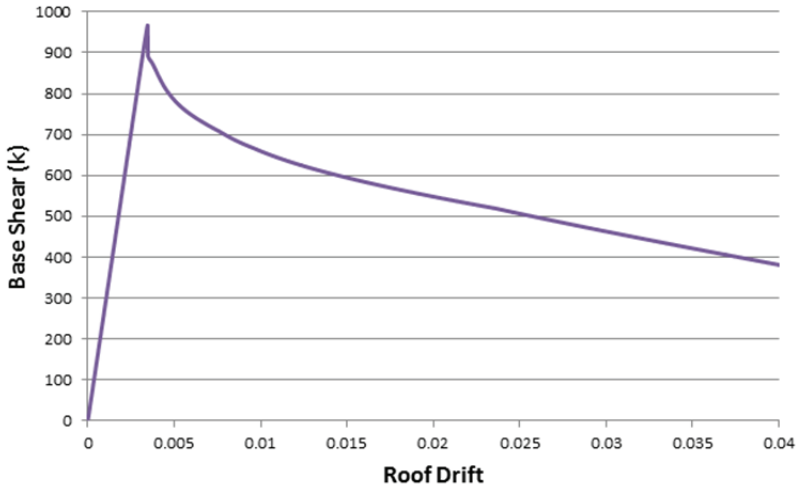

Figure C-4 Illustration of monotonic pushover curve for 3-story special SCBF archetype.

Considering the contribution of the resistance factor ($\phi = 0.9$) and expected material strength factor ($R_y = 1.4$ for hollow structural section braces), the calculated overstrength values of Ω of 1.8 to 2.1 indicate remaining overstrength factors of about 1.2 to 1.4, which reflect the effects of member sizing, strain hardening, and the relative strength of tension versus compressive brace strengths. While the special SCBF designs used in this study were the same as those in the previous study, as summarized in Table C-2, the static overstrength values calculated in this study were up to 50% larger. These differences are thought to be due to variations in the brace models because as shown in Figure C-4, the peak response associated with brace buckling is likely to be sensitive to the assumed initial imperfections, rigid end offsets, and brace end fixity.

Table C-2 Summary of Special SCBF Archetype Nonlinear Analysis Results

	Design and Model Data			Static Ω		Dynamic Collapse S_{CT} (g)	
Special SCBF	T (sec)	T_1 (sec)	S_{MT} (g)	*Prior Study*	*This Study*	*Prior Study*	*This Study*
3-story	0.5	0.6	1.50	1.4	2.1	2.4	2.1
6-story	0.8	1.1	1.10	1.3	1.8	2.4	1.5
12-story	1.4	1.4	0.65	1.6	1.8	2.1	0.7

C.4.2 Results from Dynamic Analyses

Incremental nonlinear dynamic analyses were run up to collapse, and force demands were recorded for the following force-controlled components: brace and brace connection force, column axial force, and diaphragm collector force. The FEMA P-695 far field ground motions were used for all cases, and the ground motions were scaled as a set at the first-mode period, T, as specified in FEMA P-695.

While the primary focus of this study is on the force demands, the analyses conducted as part of this study provide an opportunity to examine the significance of modeling assumptions on the calculated collapse capacity. As summarized in Table C-2, the median collapse capacity, S_{CT}, for the 3-story special SCBF calculated in this study is close to that calculated previously in the previous study, i.e., S_{CT} of 2.1g calculated in this study versus 2.4g calculated previously. The lower value calculated in this study is explained by the fact that the beam and column models in this study simulated strength degrading hinges (Figure C-4), whereas the previous models used fiber-type beam and column elements that do not degrade. The differences in collapse capacities for the 6- and 12-story frames are much more dramatic, where there is a difference of three times in the calculated S_{CT} for the 12-story frame. It is not clear whether or not these large differences in the computed collapse capacities for the 6- and 12-story frames can be explained by the differences in the hinge properties alone. Numerical convergence and tolerances may also play a role. For example, with the addition of the degrading beam and column hinge models, convergence of the OpenSees model was quite sensitive to the numerical tolerances and solution algorithms. Nevertheless, as both studies were carefully conducted using defensible models, the large differences highlight the potential sensitivity of the collapse results to modeling assumptions.

The calculated force demands from the dynamic analyses are compared to various types of checks to estimate the maximum demands. Some of the force demand checks are based on ones currently specified in ASCE/SEI 7-10 and ANSI/AISC 341-10, whereas other checks are not required by building code standards but are intended to assess the accuracy of calculating demands through the elastic design force demand multiplied by the system overstrength, Ω.

C.4.3 Evaluation of Brace Force Demands

The brace force demands are important for capacity design of the connection braces and for evaluation of force demands in columns and beams of the braced frame. Maximum brace force demands, developed in each story of each of the special SCBF archetypes under increasing ground motion intensity, are plotted in Figure C-5. The maximum force demands correspond to median values from dynamic analyses of the FEMA P-695 far-field ground motion set. In Figure C-5 the median force demands are normalized by the expected brace yield strengths, $P_{y,exp}$, equal to $R_y F_y A_g$, where $R_y F_y$ is the expected steel yield strength and A_g is the gross area of the braces. The spectral acceleration corresponding to the MCE design basis for each frame is indicated by the vertical line in each plot. The following observations are made about brace force demands:

- In general, brace force demands in all three frames tend to saturate close to or slightly below the expected yield strength. The variability in normalized brace forces between each floor is very small in the 6-story frame, whereas the variability is somewhat higher (with a slightly lower median value) in the 12-story frame. This saturation close to the expected yield strength confirms the accuracy of the AISC design requirements for brace connections, where the connection design strength, ϕR_n, is required to exceed $P_{y,exp}$.
- Table C-3 shows that the record-to-record variability in the maximum brace forces at the MCE level has values of Coefficient of Variation (COV) that are generally less than about 10%. This is in contrast to the record-to-record variability of 40% to 50%, which is generally observed in story drifts and collapse statistics.
- Table C-4 shows that the maximum brace forces tend to saturate at ground motion intensities that range from 0.2 to 0.4 (discounting a few higher values in upper stories) of the MCE intensity. The rapid increase in forces at low intensities is significant because such an increase implies that the maximum brace forces will occur much more frequently (lower return periods) than implied by MCE level design checks. This has implications on establishing an appropriate reliability index for establishing the brace connection design requirements, i.e., load and resistance factors applied to connection design.
- The results shown in Figure C-5 and Table C-3 and Table C-4 are for special SCBF designs where the braces have been optimally sized. In a study of similar frames, Victorsson et al. (2011) considered brace force demands in a 6-story design where the brace sizes in the first story were maintained up the height of the building. As shown in Figure C-6, the braces in the upper stories did not yield, such that the expected brace yield strength overestimates the forces developed in the braces at the upper (fifth and sixth) stories.

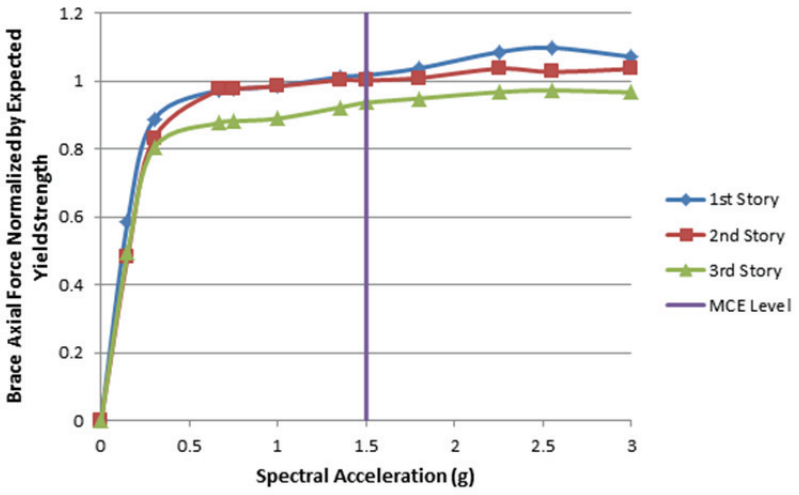

(a)

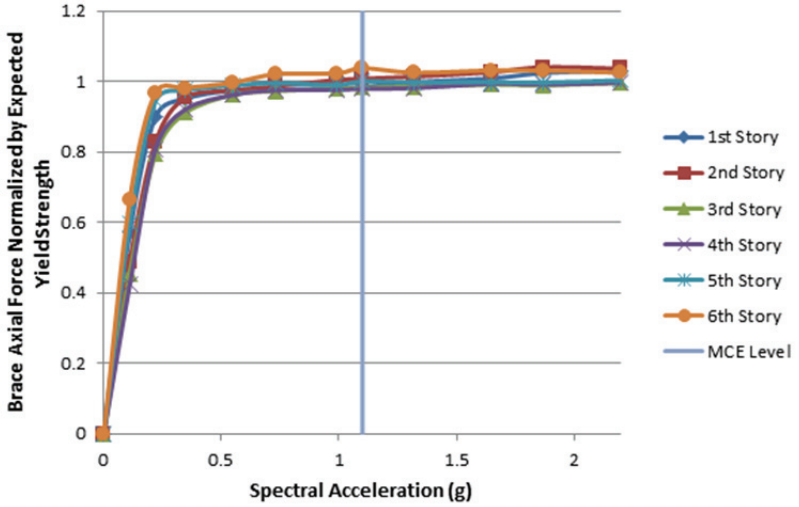

(b)

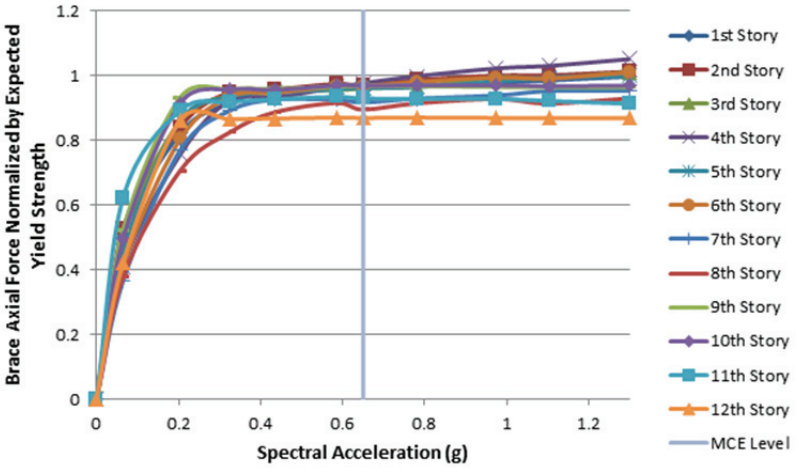

(c)

Figure C-5 Normalized brace force demands for special SCBF archetypes: (a) 3-story; (b) 6-story; and (c) 12-story.

Table C-3 Record-to-Record Variability in Special SCBF Force Demands

	Coefficient of Variation		
	Braces	Columns	Collectors
3-story	8 to 9%	6%	4 to 15%
6-story	3 to 7%	7 to 10%	4 to 18%
12-story	6 to 12%	10 to 16%	14 to 30%

Table C-4 Normalized Ground Motion Saturation Intensity for Special SCBF Components

	$S_{a,saturation}/S_{a,MCE}$		
	Braces	Columns	Collectors
3-story	0.4	0.4	0.4
6-story	0.2 to 0.3	0.2 to 0.7	0.2 to > 1
12-story	0.3 to 0.7	0.3 to 0.7	0.3 to > 1

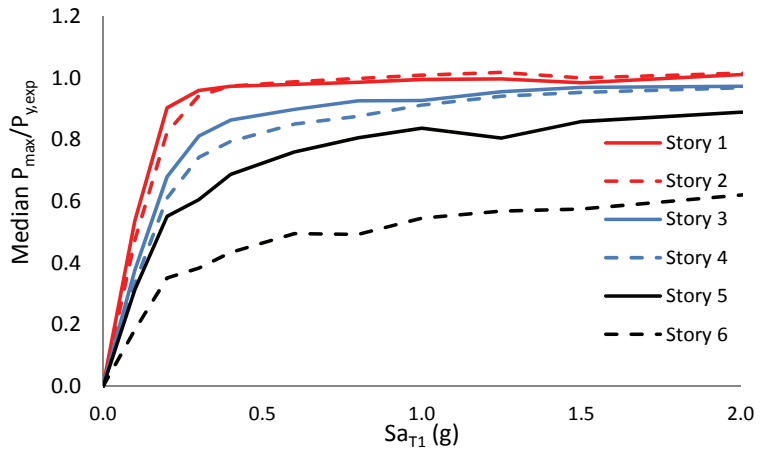

Figure C-6 Normalized brace force demands for 6-story special SCBF archetypes with constant brace sizes (Victorsson et al., 2011).

C.4.4 Evaluation of Column Force Demands

Column axial force demands are important because the ANSI/AISC 341-10 requires that the axial strength of the columns should exceed the maximum axial load that can develop in the columns. Summarized in Figure C-7 are median axial force demands in the columns for the three special SCBF archetypes. In these plots, the median demands are normalized by the minimum required strength as specified in ANSI/AISC 341-10, which is specified as the greater of the following criteria:

1. Column force developed by all of the braces simultaneously reaching their expected strengths in tension or compression,

2. Column force developed by all of the braces simultaneously reaching their expected strengths in tension or expected post-buckling strengths in compression, and

3. Column force calculated as $1.0D + 0.5L + \Omega_O E$, where $\Omega_O = 2$ and E is the elastic design force, as calculated by either the ELF or RSA analysis procedure.

4. *Exception.* The maximum force as calculated by these three methods need not exceed the force calculated by $1.0D + 0.5L + \Omega_O Ec$, where $\Omega_O = 2$ and Ec is the elastic design force determined by an ELF analysis where the compression braces are removed from the model.

In the 3- and 6-story special SCBFs, the column design forces were generally governed by criterion 1 (braces simultaneously reaching their expected strength in tension or compression), and in the 12-story special SCBF the design forces were governed by the upper limit exception ($1.0D + 0.5L + \Omega_O Ec$).

Similar to the brace forces, the maximum axial forces in the columns tended to increase quickly at low intensities and saturate well before the MCE ground motion intensity. Table C-4 shows that the forces saturated at about 0.2 to 0.7 of the MCE intensity. Table C-3 shows that the record-to-record variability in the maximum column axial column forces was also fairly low, on the order of COV equal to 6% to 16%.

Also, Figure C-7 shows that in the 3- and 6-story special SCBFs where the required axial column strength is based on the expected brace capacities, the required strengths match the median demands pretty well (i.e., with values saturating between 0.9 and 1.15). On the other hand, in the 12-story special SCBF, the median demands tend to cluster at either 1.2 or 0.8 of the required column strengths, which in this case are controlled by the exception above, i.e., where a design force of $\Omega_O Ec$ with $\Omega_O = 2$ is applied to a model that excludes the braces in compression.

To further investigate the accuracy of various methods to determine the required axial column forces, the median force demands at MCE intensities are plotted against four possible demand calculations in Figure C-8. One demand is based on the expected brace strength (Br Capacity) and the other three are based on amplified design forces, using an ELF (W-ELF), RSA (W-RSA), or compression braces removed (W-ELFC) analysis. To better ascertain the accuracy of the overstrength amplifier, in these comparisons, the forces are amplified by the measured overstrength, Ω, for each archetype.

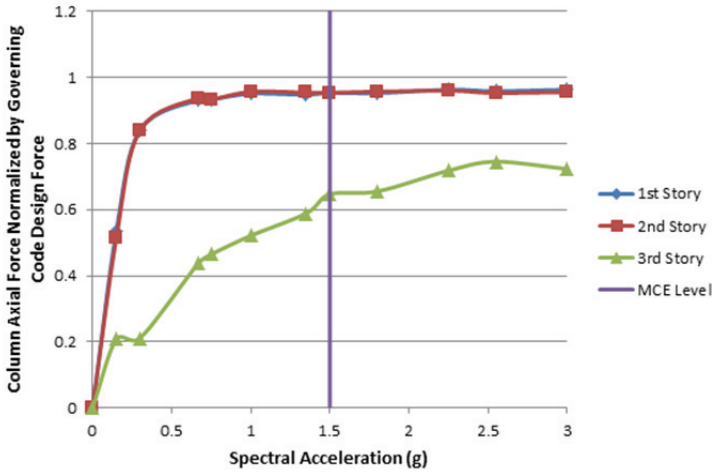

(a)

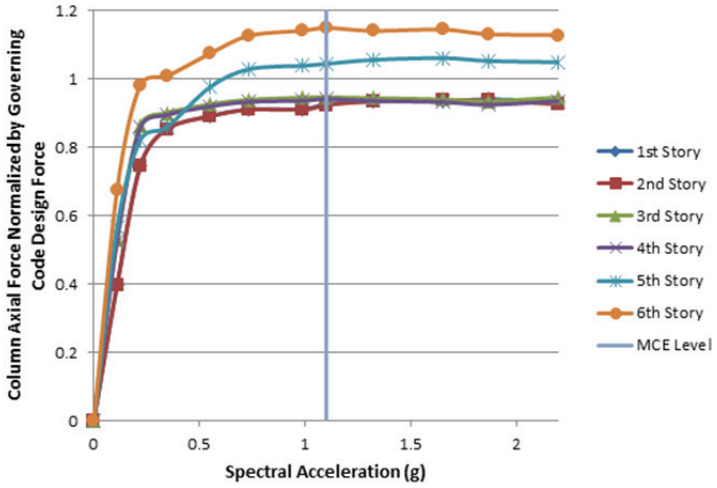

(b)

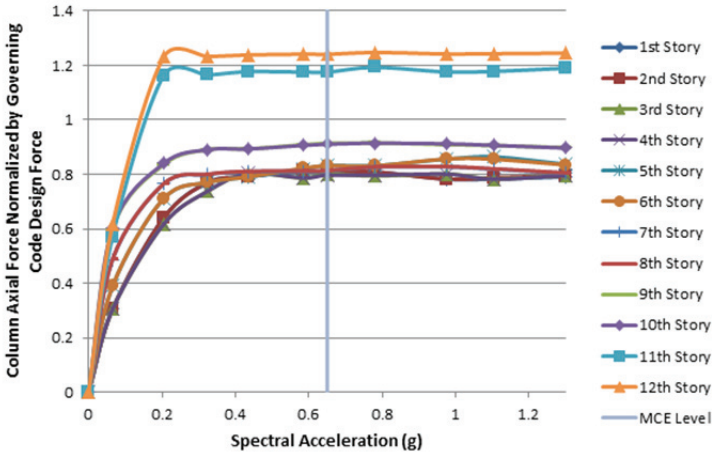

(c)

Figure C-7 Normalized column axial force demands for special SCBF archetypes: (a) 3-story; (b) 6-story; and (c) 12-story.

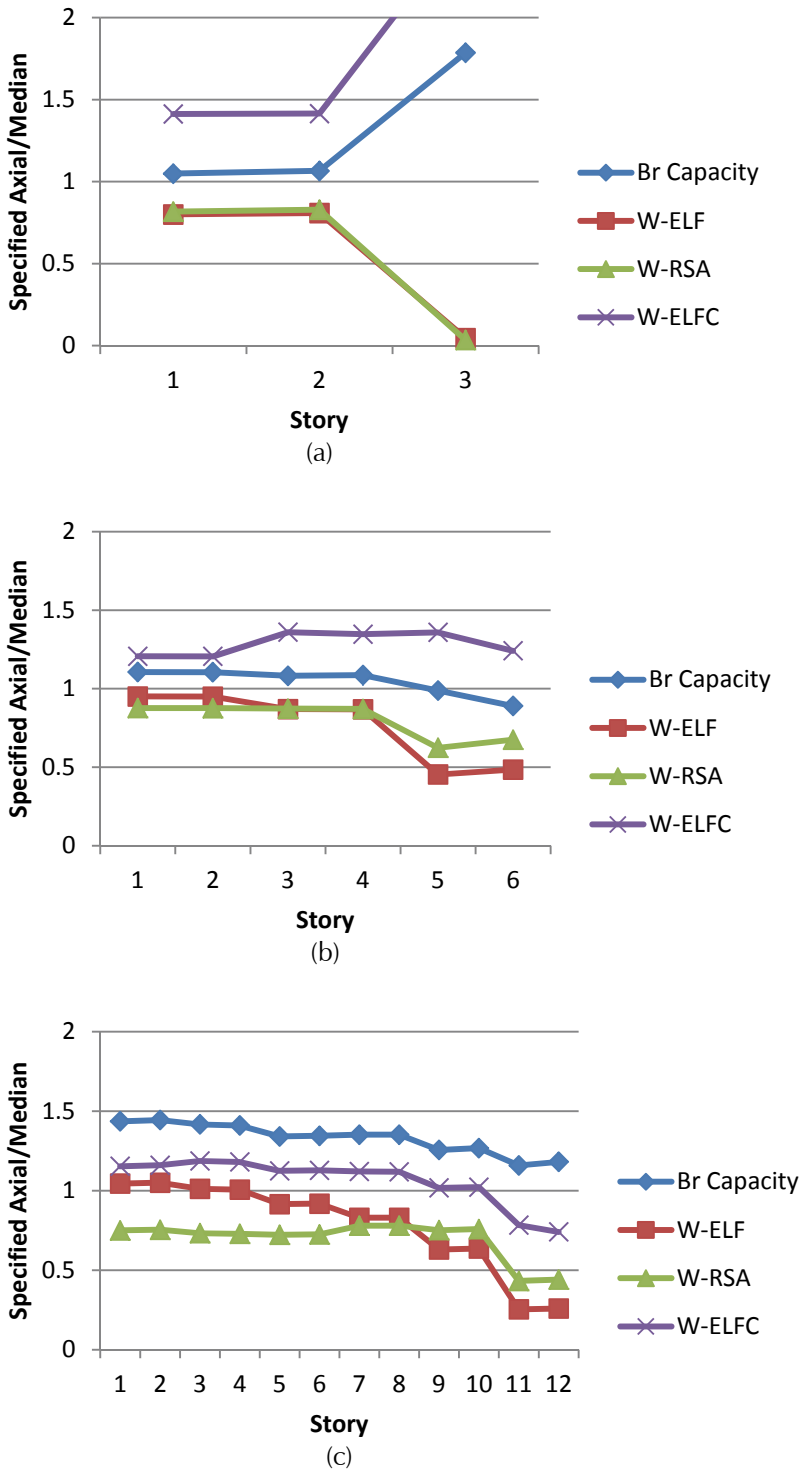

Figure C-8 Specified axial column force normalized by median demands at MCE intensity for special SCBF archetypes: (a) 3-story; (b) 6-story; and (c) 12-story.

In Figure C-8, of the four methods, the one based on brace strengths (Br Capacity) tends to provide the most consistent measure. The Br Capacity values are close to the medians (ratio close to 1) in the 3- and 6-story archetypes. In the 12-story archetype, the Br Capacity value is fairly stable, although slightly conservative, ranging between 1.2 to 1.4 times the maximum of the median values across all stories. The amplified force with the ELF model with compression braces removed also provides fairly good agreement (ratio close to 1) in the 12-story archetype, whereas the more conventional amplified ELF and RSA values tend to underestimate the median demands.

There are further potential complications for column force demands. Even two-dimensional analyses can include the effect of vertical ground motion, and this may have significance. Further study may show that the significant effect is limited to near-fault locations, or optimistically, not even be there. Real structures behave in three dimensions, and column axial forces are particularly susceptible to inadvertent three dimensional effects. For example, the inherent continuity of beams and floor slabs not part of a seismic force-resisting system can result in the shifting of gravity load to uplifting columns at the end of braced frames or shear walls, with a resultant increase in the compression at the far end of the wall or braced frame. Studies to date have not treated these effects comprehensively.

C.4.5 Evaluation of Diaphragm Collector Force Demands

ASCE/SEI 7-10 requires that collector forces be designed as force-controlled components, using force demand equations specified in ASCE/SEI 7-10 Sections 12.10.1.1 and 12.10.2.1. These sections require calculation of the collector forces using the criteria below. The forces should be the minimum of criteria 1, 2, 3, and less than the upper bound criterion 4:

1. $\Omega_O F_x$, where F_x is calculated by analysis (here assumed as the ELF procedure).
2. $\Omega_O F_{px}$, where F_{px} is calculated by the ASCE/SEI 7-10 diaphragm force Equation 12.10-1.
3. $F_{px,\,min} = 0.2 S_{DS} I_e w_{px}$ (assuming $I_e = 1$, $S_{DS} = 1$g for SDC D_{max})
4. $F_{px,\,max} = 0.4\, S_{DS} I_e w_{px}$ (assuming $I_e = 1$, $S_{DS} = 1$g for SDC D_{max})

The overstrength factor is only applied to the calculated forces in criterion 1 and criterion 2. The minimum and maximum limits calculated by criterion 3 and criterion 4, respectively, are related to peak ground acceleration, and these are not amplified by the overstrength factor. These collector force requirements are illustrated for the 12-story special SCBF archetype in Figure C-9, using the measured Ω value of 1.8 in lieu of the value of Ω_O of 2.0 as specified in ASCE/SEI 7-10. As shown, the minimum criterion 3 controls collector design for the first six floors, above which criterion 2 controls.

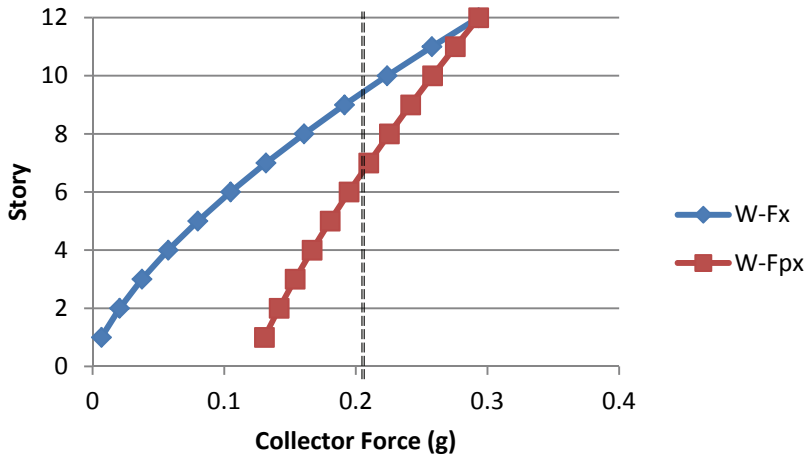

Figure C-9 Collector force demands for 12-story special SCBF archetype as specified by ASCE/SEI 7-10.

The diaphragm collector forces were calculated as the difference in story shears, immediately above and below each floor. Thus, the calculated collector forces assume perfectly rigid floor diaphragms and collectors. The median collector forces are plotted for each of the special SCBFs in Figure C-10, where they are normalized by the floor weight (mass). In contrast to the previous cases, there is considerably more variability in the normalized collector forces up the height of the building, and the forces tend to saturate less than the brace or column forces. According to Table C-4 and Figure C-10, the values tend to saturate at ground motion intensities of 0.2 to 0.4 times the MCE intensity at the upper floors, and they saturate less and at higher intensities in the lower floors. As shown in Table C-3, the record-to-record variability is also larger for collector forces, with maximum COV values of 15% to 30%, generally increasing with the number of stories. Shown in Figure C-11 are plots showing how the median collector forces at the MCE intensity (normalized by tributary floor weights) vary up the building height. In contrast to what one would infer from ELF design procedures (or from ASCE/SEI 7-10 Equation 12.10.1), the collector forces tend to be larger near the base of the building.

The accuracy of the four collector force criteria described previously are evaluated further in Figure C-12, based on median force demands at the MCE ground motion intensity. In these plots, the maximum of the blue diamonsd (criterion 1, $\Omega F_{x,ELF}$) or red squares (criterion 2, ΩF_{px}) will control, subject to the upper and lower limits of $F_{px,max}$ and $F_{px,min}$, indicated by the dashed and solid black lines. As in the column force example, in these comparisons, the measured overstrength values, Ω, for each special SCBF archetype are used (i.e., Ω from Table C-2, rather than the specified value of $\Omega_O = 2$). Comparing the plots in Figure C-12, in the 3-story frame, criterion 2, ΩF_{px}, provides a force demand that is about 50% less than the calculated demand. In the 6-story and 12-story special SCBFs, the predicted demands are controlled about equally

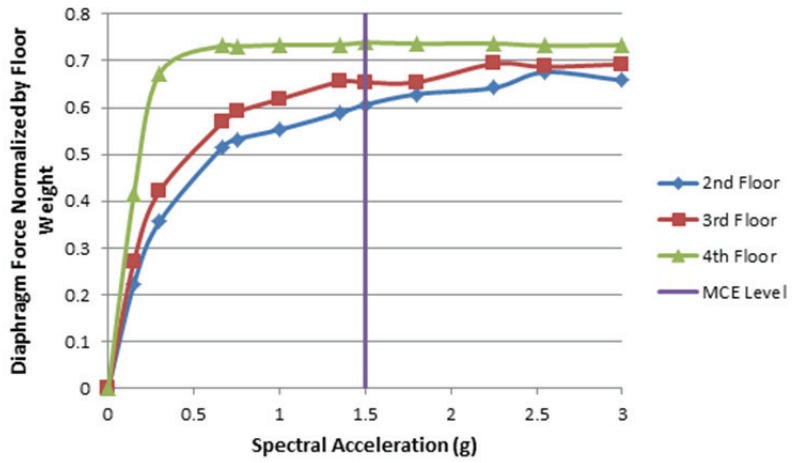

(a)

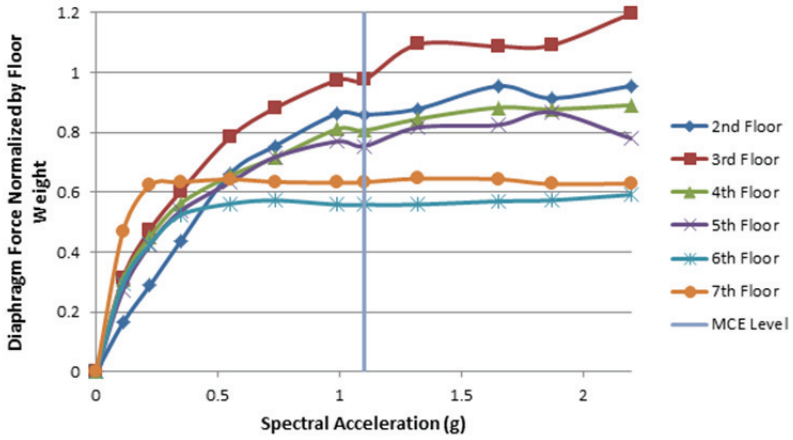

(b)

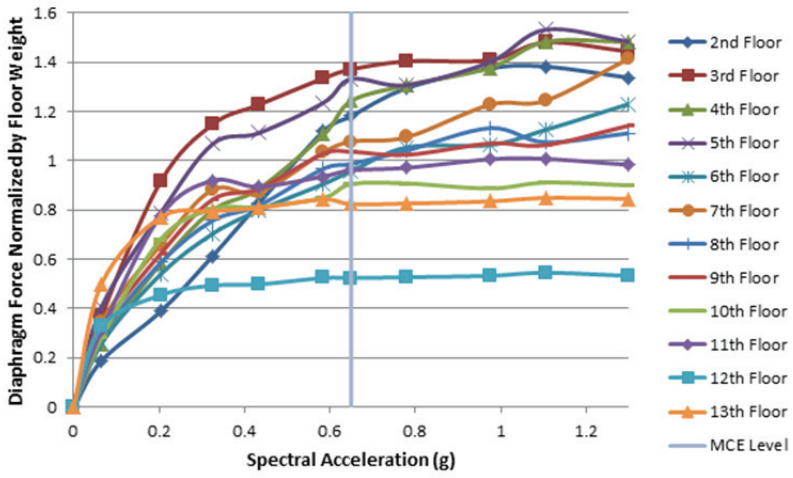

(c)

Figure C-10 Normalized collector force demands for special SCBF archetypes: (a) 3-story; (b) 6-story; and (c) 12-story.

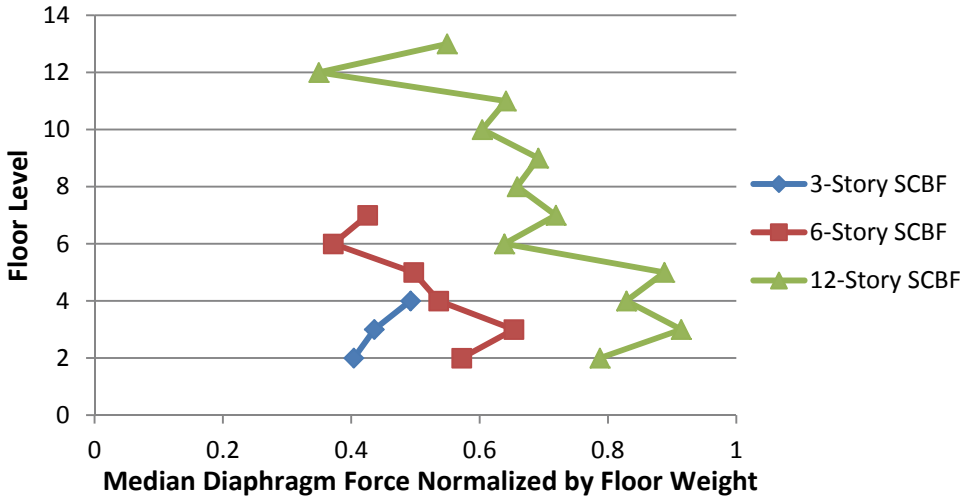

Figure C-11 Collector force demands normalized by floor weight at MCE intensity for special SCBF archetypes.

by criterion 2 or criterion 3 (which is not modified by overstrength). More significantly, the required strengths in the taller frames are up to 80% less than the median demands in the lower floors and 50% less in the upper floors.

Taken at face value, these results for diaphragm and collector forces indicate that the current provisions in ASCE/SEI 7-10 significantly underestimate the actual forces. However, there are three mitigating effects that should be considered when interpreting these results:

- The appropriateness of comparing the median values at the MCE intensity to the ASCE/SEI 7-10 design criteria, which are defined at DBE levels (2/3 of MCE intensity) should be considered. In cases where the force demands saturate, this will not make much difference; however, because the collector forces in the lower floors do not saturate, the difference between DBE and MCE demands could result in a difference of up to 2/3.
- The FEMA P-695 approach to scaling ground motions can, in certain cases, lead to an overestimation of earthquake induced effects that are associated with vibration periods that are significantly shorter than the first-mode period. This situation arises because the shape of the median spectrum for the FEMA P-695 far-field record set differs from the shape of the code spectrum (e.g., see Figure A-2 of FEMA P-695 report), such that scaling of the median to match at one period may lead to large discrepancies at other periods. Because the diaphragm and collector forces in lower floors tend to be closely associated with PGA, discrepancies can arise when the ground motions are scaled to first mode periods above about 1.5 seconds. The discrepancies can be estimated by the plot in Figure C-13, which shows the median PGA that results when the far-field record

set is scaled to the MCE D_{max} spectra at the periods noted. For example, whereas correct PGA for the MCE D_{max} spectra is about 0.84g, effective PGA's of over twice this amount can occur when the ground motions are scaled to match the SDC D_{max} spectrum at periods longer than about 3 seconds. For special SCBF archetypes with first-mode periods of 0.5, 0.8, and 1.4 seconds, the effective PGA values are about 30% higher than the SDC D_{max} values (about 1.07g versus 0.84g).

- The degree to which the resulting high frequency force are significant for diaphragm and collector design should be considered. For example, if the diaphragms and collectors were modeled as flexible, the higher frequency responses would likely be reduced. To explore this effect, the diaphragm force time history from one ground motion was filtered using a moving average filter, which changes the characteristic time interval from 0.01 seconds in the original record to 0.1 seconds and 0.2 seconds (roughly equivalent to filtering frequencies about 10Hz or 5Hz, respectively). As shown in Figure C-14, the filtering reduces the peak force demand by 30% and 50%, respectively. The results shown in this figure are for the second floor of the 6-story frame, and the high frequency filter reductions are generally less in the upper floors.

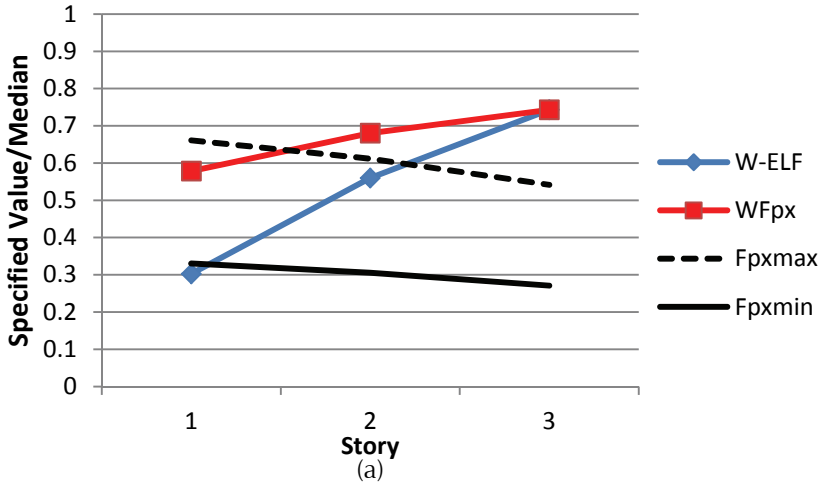

(a)

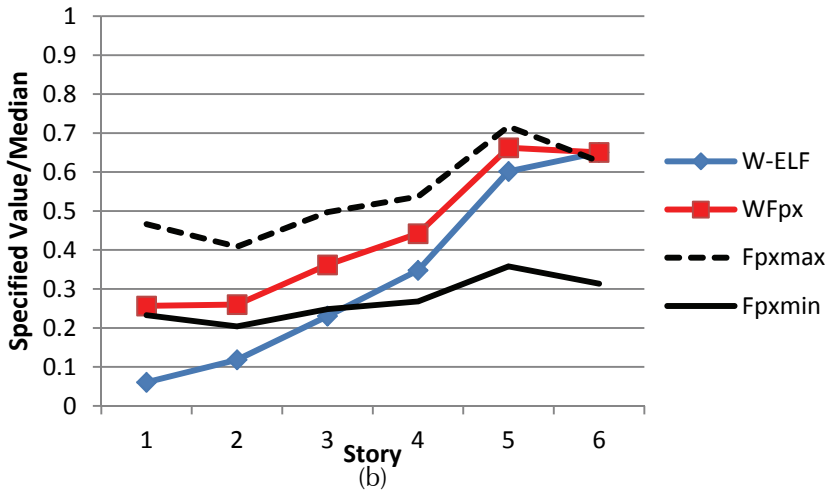

(b)

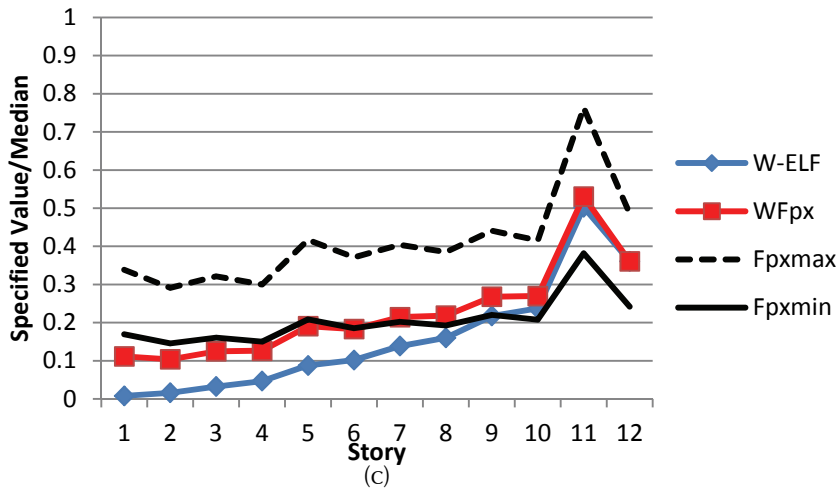

(c)

Figure C-12 Specified collector force normalized by median demands at MCE intensity for special SCBF archetypes: (a) 3-story; (b) 6-story; and (c) 12-story.

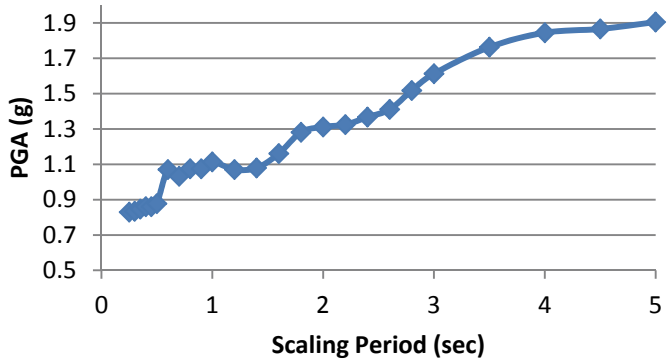

Figure C-13 Median PGA of far-field ground motion set when scaled to SDC D_{max} at the designated period.

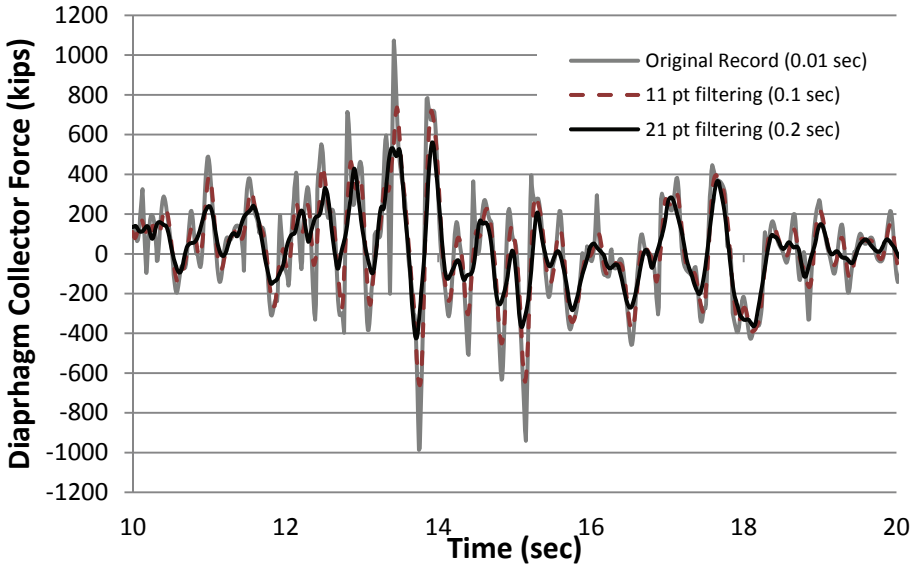

Figure C-14 Time-point averaging filter of diaphragm force time-history (second floor of 6-story special SCBF, Kobe ground motion).

The effects of these three factors on the diaphragm collector force demands for the 12-story special SCBF are shown in Figure C-15, where consideration of all three factors reduces the peak demands in the lower stories by about half. As indicated, the largest reductions come from the adjustment from MCE to DBE intensities and next by the 0.1 second averaging (10 Hz filter). However, even with these three adjustments, the maximum normalized median forces of 0.6g to 0.8g are still 3 to 4 times larger than the lower bound $F_{px,min}$ (criterion 3) of 0.2g specified values on the diaphragm forces for the 12-story special SCBF. Moreover, as the specified diaphragm forces are controlled by the lower-bound $F_{px,min}$ (criterion 3), the collector forces would not be subject to the overstrength adjustment.

Further study of the effect of various reductions in rigidity between story masses and the vertical elements of the seismic force-resisting system are needed. Elastic

flexibility, cracking, bond slip, and limited yielding are all factors that could reduce the collector forces computed here. The filtering performed in this study is an illustration that the effects could be significant.

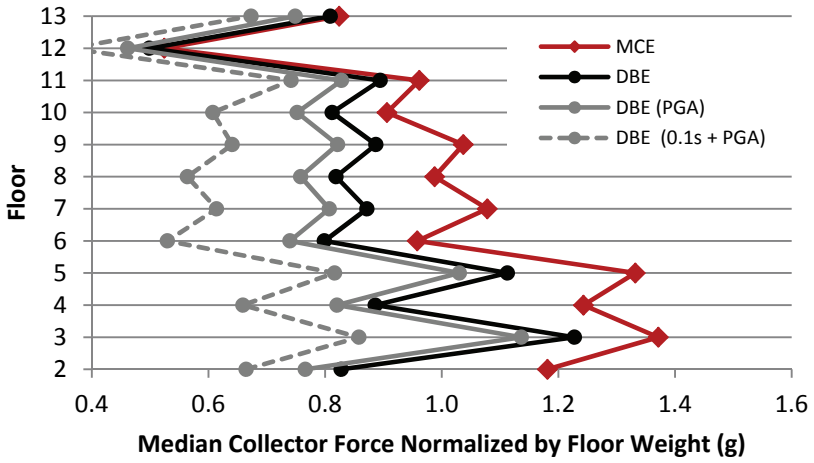

Figure C-15 Normalized diaphragm forces for 12-story special SCBF archetype with adjustments for intensity, PGA correction, frequency filtering.

C.5 Special Reinforced Concrete Moment Frame Studies

Similar to the study of SCBF systems, special RCMF systems are studied to investigate the capacity design requirements for force-controlled components. Shown in Figure C-16 are three special RCMF systems that were studied, modeled modeled after the 4-, 12-, and 20-story perimeter frame designs investigated in the FEMA P-695 report. These frames were designed in accordance with ASCE/SEI 7-10 and the related ACI 318-11 requirements. Nonlinear analyses were performed using OpenSees, where the modeling features and criteria are essentially the same as those used in the FEMA P-695 studies, except for some minor adjustments and corrections to some of the modeling parameters. Beams and columns were modeled with concentrated plastic hinges that capture strength and stiffness degradation using the model shown previously in Figure C-3. Beam-column joint elements that represent the finite joint size and account for limited panel zone deformations are used.

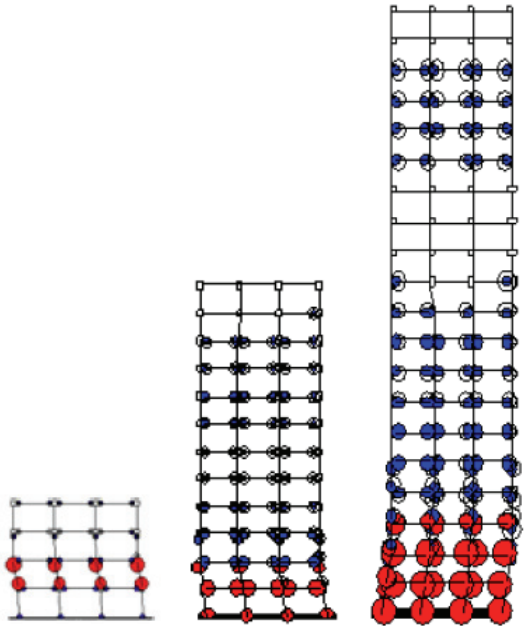

Figure C-16 Special RCMF archetypes.

C.5.1 Results from Static Pushover Analyses

Shown in Figure C-17 is a pushover curve for the 4-story special RCMF archetype, which is generally representative of the pushover results for each of the special RCMF archetypes. In the 4-story frame, deformations generally concentrate in one or two stories, leading to large drift ratios and, ultimately, loss of capacity. In the 12- and 20-story frames, the deformations concentrate in two to four stories. The static overstrength, Ω, calculated for each archetype is summarized in Table C-5, along with values calculated in the previous FEMA P-695 study. The calculated overstrength of 1.5 in this study is fairly close to the values of 1.6 and 1.7, calculated in the FEMA P-695 study. Considering the contributions to overstrength from the resistance factor ($\phi = 0.9$) and expected material strength factor ($R_y = 1.25$ for steel reinforcement), the calculated overstrength of 1.5 indicates a remaining overstrength factor of about 1.1, which reflects the combined effects of member sizing, strain hardening, and inelastic force redistribution. The overstrength ratios are about one-half of the ASCE/SEI 7-10 value of Ω_O equal to 3 for moment frames.

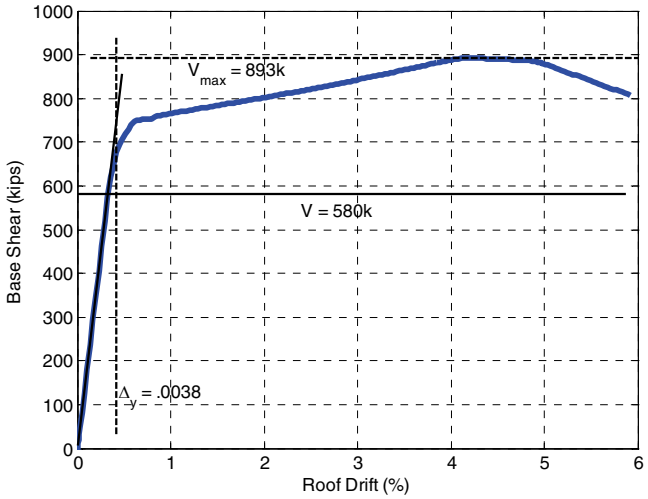

Figure C-17 Illustrative monotonic pushover curve for 4-story special RCMF archetype.

Table C-5 Summary of Special RCMF Archetype Nonlinear Analysis Results

	Design and Model Data			Static Ω		Dynamic Collapse S_{CT} (g)	
Special RCMF	T (sec)	T_1 (sec)	S_{MT} (g)	Prior Study	This Study	Prior Study	This Study
4-story	0.8	1.2	1.11	1.6	1.5	2.1	2.3
12-story	2.1	2.0	0.42	1.7	1.5	0.6	0.7
20-story	3.4	2.6	0.27	1.6	1.5	0.5	0.4

C.5.2 Results from Dynamic Analyses

Incremental nonlinear dynamic analyses were run up to collapse, and force demands were recorded for the following force-controlled component actions: shear in beams and columns, axial column force, and diaphragm/collector forces. The analyses were run using the FEMA P-695 far field ground motion set, as described previously for the special SCBF analyses.

As summarized in Table C-5, the median collapse capacity, S_{CT}, for all three special RCMFs calculated in this study are similar to those calculated previously in the FEMA P-695 study. Factors contributing to the slight increase in the collapse capacities in this study include: (1) an adjustment to the calculation of viscous damping coefficients; (2) omission of the 0.25 live load from the dynamic mass calculation, which was included in the prior FEMA P-695 study; and (3) slight adjustments to a few of the member stiffness properties.

Calculated force demands from the dynamic analyses are compared below to various types of checks to estimate the maximum demands. Some of the force demand checks are based on ones currently specified in ASCE/SEI 7-10 and ACI 318-11, whereas other general checks are intended to assess the accuracy of calculating

demands through the elastic design force demand multiplied by the pushover overstrength, Ω.

C.5.3 Evaluation of Beam Shear Force Demands

Chapter 21 of ACI 318-11 specifies the minimum required beam shear force necessary to develop the probable flexural strength of the beams, assuming reverse curvature bending with hinges at the end of each member. The probable flexural strength, M_{prb}, is calculated using an effective steel yield strength of $1.25f_y$. Beam shear force demands were monitored for both interior and exterior bays up the height of the building at varying ground motion intensities. Shown in Figure C-18, are the median beam shear demands for selected bays and stories, normalized by the probable beam strength demand, $2M_{prb}/L$, where L is the clear distance between columns. With a few exceptions of top floors in the taller buildings, the median beam shears tend to saturate at a value of about 0.8 to 0.9 times the probable strength. As summarized in Table C-6, because of the saturation at the probable beam strength, the median MCE beam shear demands have very low record-to-record variability with coefficients of variation of about 1% to 6%. As summarized in Table C-7, the median demands saturated at ground motion intensities that ranged from 0.2 to 0.8 times the MCE intensity. Finally, when compared to elastic design force demands from response spectra analyses, the median beam shear demands ranged from about 2 to 4 times the elastic design forces. These are in contrast to the pushover overstrength ratios, Ω, equal to 1.5 for the three moment frames.

Table C-6 Record-to-Record Variability in Force Demands for Special RCMF Components

	Coefficient of Variation			
	Beam Shear	Column Shear	Column Axial	Collectors
4-story	1 to 3%	5 to 12%	5 to 7%	10 to 28%
12-story	1 to 6%	5 to 17%	7 to 27%	15 to 40%
20-story	1 to 4%	6 to 19%	8 to 27%	17 to 49%

Table C-7 Normalized Ground Motion Saturation Intensity for Special RCMF Components

	$S_{a,saturation}/S_{a,MCE}$			
	Beam Shear	Column Shear	Column Axial	Collectors
4-story	0.2 to 0.4	0.7 to >1	0.2 to 0.3	0.5 to >1
12-story	0.3 to 0.8	0.5 to 1.0	0.3 to 1	0.8 to >1
20-story	0.4 to 0.8	0.4 to 0.8	0.3 to 0.8	0.8 to >1

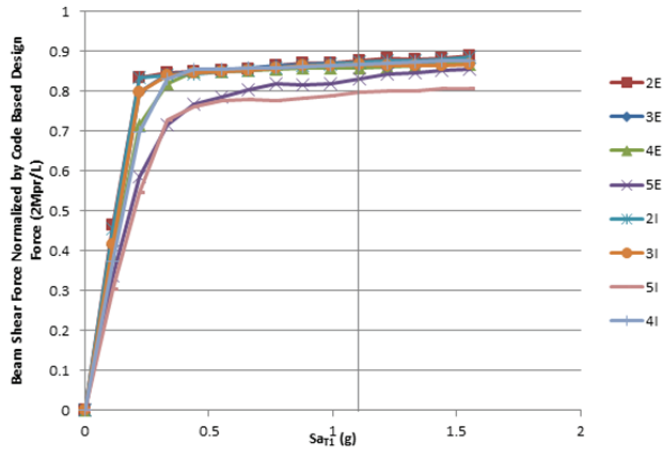

(a)

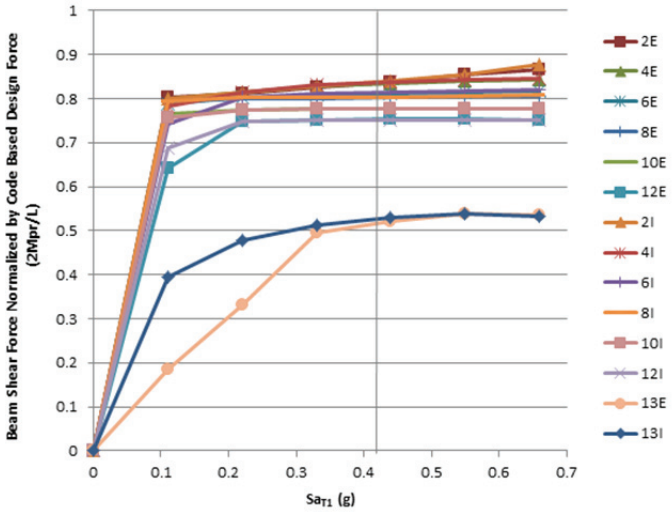

(b)

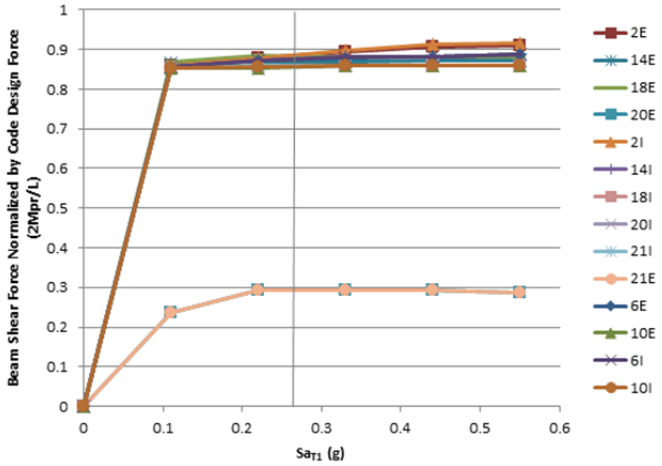

(c)

Figure C-18 Normalized beam shear force demands for special RCMF archetypes: (a) 4-story; (b) 12-story; and (c) 20-story.

C.5.4 Evaluation of Column Shear Force Demands

The required shear strengths of the columns in the special RCMF system are based on capacity design requirements outlined in ACI 318-11 and NIST GCR 8-917-1, *Seismic Design of Reinforced Concrete Special Moment Frames: A Guide for Practicing Engineers* (NIST, 2008). These requirements specify that the maximum shears should be determined based on the following:

1. The probable flexural strength, M_{prc}, of the column at the beam-column joint faces,
2. *Exception:* The shears need not exceed those determined from the probable strength M_{prb} of the beams framing into the joint.
3. NIST GCR 8-917-1 recommends only applying criterion #1 (M_{prc} demands) and not criterion #2 (M_{prb} demands) because where multiple columns frame into a joint, the distribution of the probable maximum moment from the beams is an indeterminate problem which cannot be accurately obtained from elastic analysis. Instead, an alternative methodology for limiting the column shear based on the probable beam flexural strength, M_{prb}, which involves scaling up the elastic design force in the column VE_{col} by the ratio of the maximum probable beam strength to the moment demands in the beam from elastic analysis (ME_{bm}) is recommended.

All three criteria were investigated in this study.

Median column shear force demands are shown in Figure C-19, where the demands are normalized by the shear associated with the column probable strength, M_{prc} (criterion 1). In contrast to the beam shear demands, column shear demands tend to saturate less, particularly in the 4-story building, where forces begin to saturate at a normalized demand of about 0.5 to 0.6, but then continue to increase up to and beyond the MCE intensity. On the other hand, the shear demands in the 20-story frame tend to saturate well below MCE intensities but at varied normalized force ratios, ranging from 0.7 to 0.9 for interior columns and 0.4 to 0.5 for exterior columns. As summarized in Table C-6, the record-to-record variability for the column shear (COV values of 5% to 19%) is larger than that for beam shears; and, as summarized in Table C-7, when the column shears saturate, they tend to do so at higher ground motion intensities (at 0.4 to 1.0 of the MCE).

Summarized in Table C-8 are shear force demands at selected locations in the 12-story special RCMF. Here the median demands at MCE intensities are normalized by the three capacity design criteria and the elastic design force demands. Referring to the second column of the table, and neglecting the data from the top story, the median shear demands range from 2.8 to 4.6 times the elastic design force demand. This is in contrast to the calculated pushover force ratio of Ω equal to 1.5. Data from the third to fifth columns indicate that none of the capacity design provisions provide

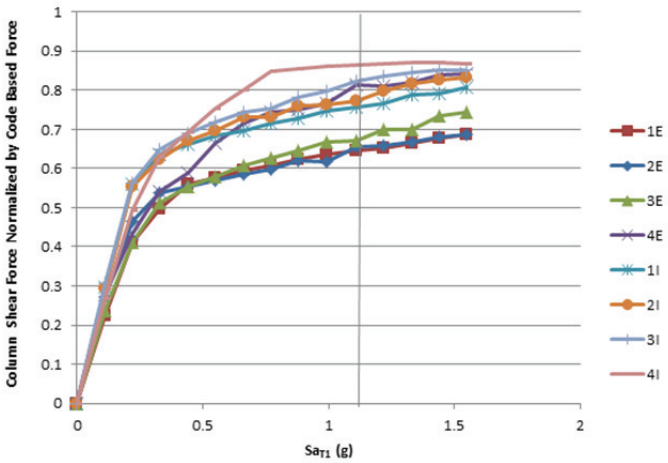

(a)

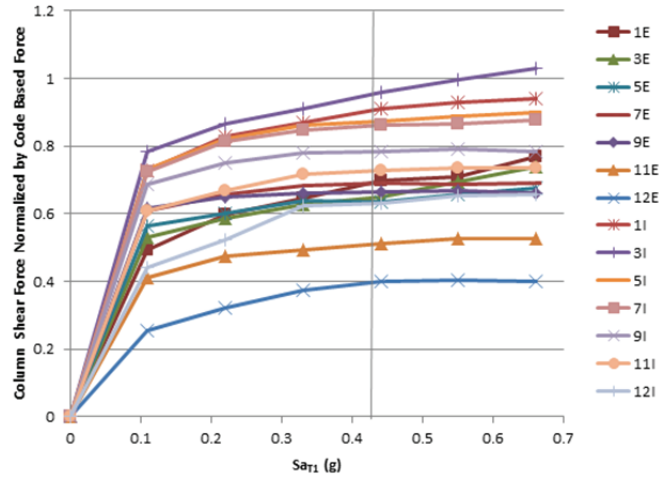

(b)

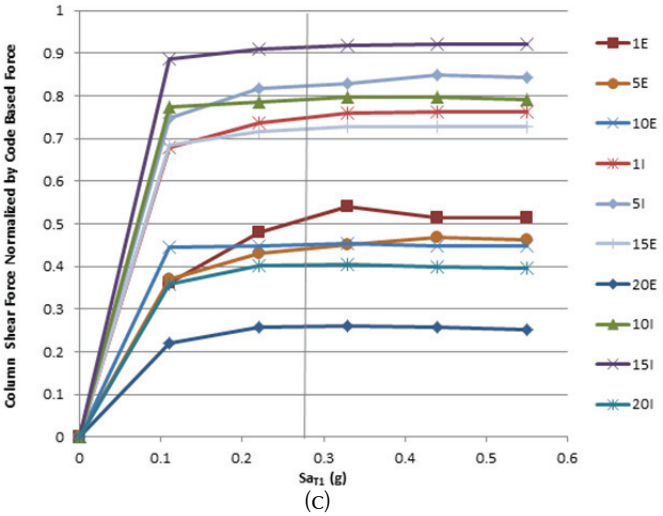

(c)

Figure C-19 Normalized column shear force demands for special RCMF archetypes: (a) 4-story; (b) 12-story; and (c) 20-story.

Table C-8 Column Shear Force Demands at MCE for 3-Bay, 12-Story Special RCMF

Column Location	$V_{MCE\ col}/V_{E\ col}$	$V_{MCE\ col}/V_{Mprc}$	$V_{MCE\ col}/V_{Mprb1}$	$V_{MCE\ col}/V_{Mprb2}$
1Exterior	3.1	0.70	1.06	0.70
3Exterior	2.8	0.65	1.47	1.29
5Exterior	2.8	0.64	1.31	1.18
7Exterior	2.8	0.69	1.30	1.12
9Exterior	3.2	0.67	0.87	1.21
11Exterior	4.6	0.51	0.68	1.41
12Exterior	7.1	0.40	0.47	1.20
1Interior	3.1	0.91	1.09	0.91
3Interior	3.0	0.96	1.28	1.12
5Interior	2.9	0.87	1.17	1.04
7Interior	3.0	0.86	1.15	0.72
9Interior	3.2	0.79	0.91	1.08
11Interior	3.8	0.73	0.77	1.12
12Interior	4.9	0.63	0.53	1.46

consistent accuracy, as compared to the calculated medians. The criterion based on the column strength (M_{prc} criterion 1 in column 3) tends to be conservative. The other two criteria based on the beam strengths (M_{prb1} and M_{prb2} in columns 4 and 5) tend to be better on average (with ranges around 1.0); but, they both reveal instances where they underestimate the median MCE demands by up to 50%.

C.5.5 Evaluation of Column Axial Force Demands

Although ACI 318-11 does not have capacity design rules for axial force demands in columns of moment frames, other specifications do. For example, ANSI/AISC 341-10 requires that frame columns be designed for the maximum load that can be transferred to the columns from connecting beams. In the interest of providing a general assessment of capacity design requirements, the implications of this axial force design requirement was assessed for the special RCMF as part of this study. Specifically, the column force demands were compared to the forces resulting from the forces imposed by the maximum shear force demands in the beams (associated with their probable flexural strengths) and by the elastic earthquake design forces multiplied by Ω equal to 1.5.

The median column axial force demands as a function of earthquake intensity and normalized by criterion #1 (beam shears based on probable moment) are plotted in Figure C-20. The forces are only plotted for exterior columns as these are most

affected by overturning effects. Similar to beam and column shears, axial forces tend to saturate at ground motion intensities on the order of 0.2 to 1.0 of the MCE intensity (Table C-7). In the 4-story frame the forces saturate at about 0.9 times the mechanism force demand, which is consistent with the saturation of beam shears. As the frames get taller, the forces saturate at lower forces: ratios of about 0.75 to 0.85 in the 12-story frame and 0.65 to 0.8 in the 20-story frame. Table C-6 shows that the record-to-record variation in median MCE column force demands are also higher (COV values of 5% to 27%) than those for shear forces in beams and columns. The variability is also larger in the taller frames.

The median MCE column axial force demands are compared to the specified values based on the probable beam shear forces (M-Capacity) and the amplified elastic design forces (W-RSA) in Figure C-21. In all cases, the M-Capacity demand is conservative (more so for the taller frames than the shorter frames). Otherwise, with the exception of the top two stories in the tall buildings, the M-Capacity demand provides a fairly consistent margin up the height of the building. The amplified elastic force demand, W-RSA, is also fairly consistent, though on the unconservative side, particularly for the taller buildings. The W-RSA underestimates the critical forces in the lower stories by about 20% to 40% in the 12- and 20-story buildings. However, the amplified elastic demands are based on the calculated Ω value of 1.5. Had the specified Ω_O value of 3 been used, the amplified values would be conservative by about 20% to 40% in the lower stories. The elastic force demands tend to be more consistent in the moment frames (Figure C-21) as compared to the braced frames (Figure C-8), because the inelastic effects of brace yielding and buckling in the special SCBFs are more dramatic than beam hinge yielding in the special RCMFs.

C.5.6 Evaluation of Diaphragm Collector Force Demands

The median collector forces are plotted for each of the special RCMF archetypes at varying earthquake intensities in Figure C-22, where they are normalized by the floor weight (mass). Median values at three intensities, 0.11g at the first-mode period, DBE, and MCE, are plotted in Figure C-23. Statistics on record-to-record variability and saturation intensities are summarized in Table C-6 and Table C-7, respectively. Comparisons between the median MCE demands and the specified diaphragm forces are plotted in Figure C-24.

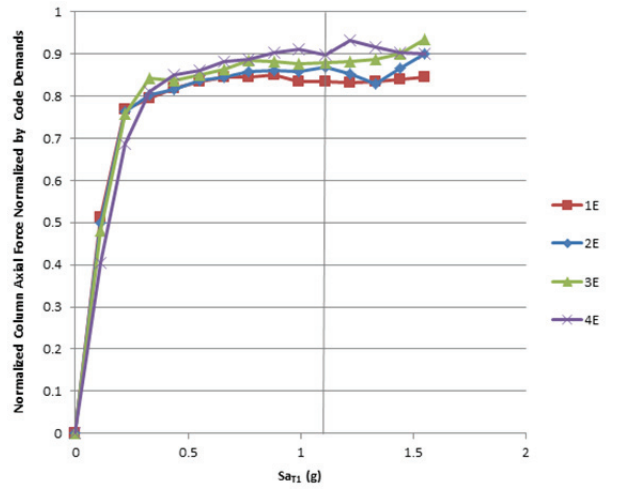

(a)

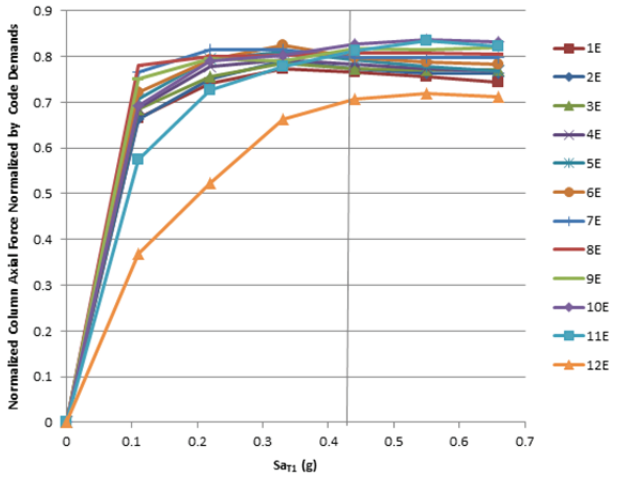

(b)

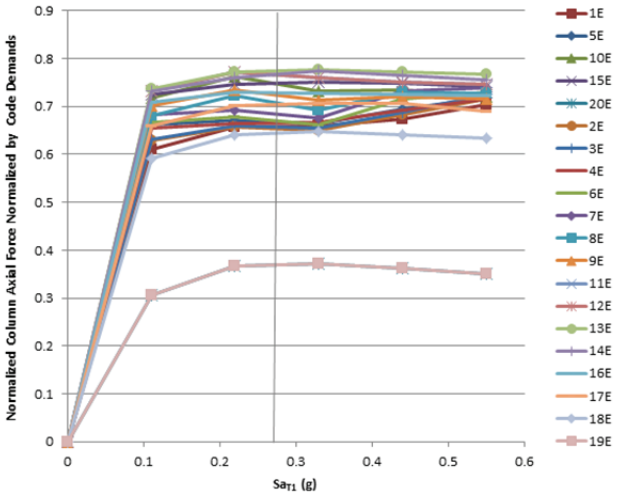

(c)

Figure C-20 Normalized column axial force demands for special RCMF archetypes: (a) 4-story; (b) 12-story; and (c) 20-story.

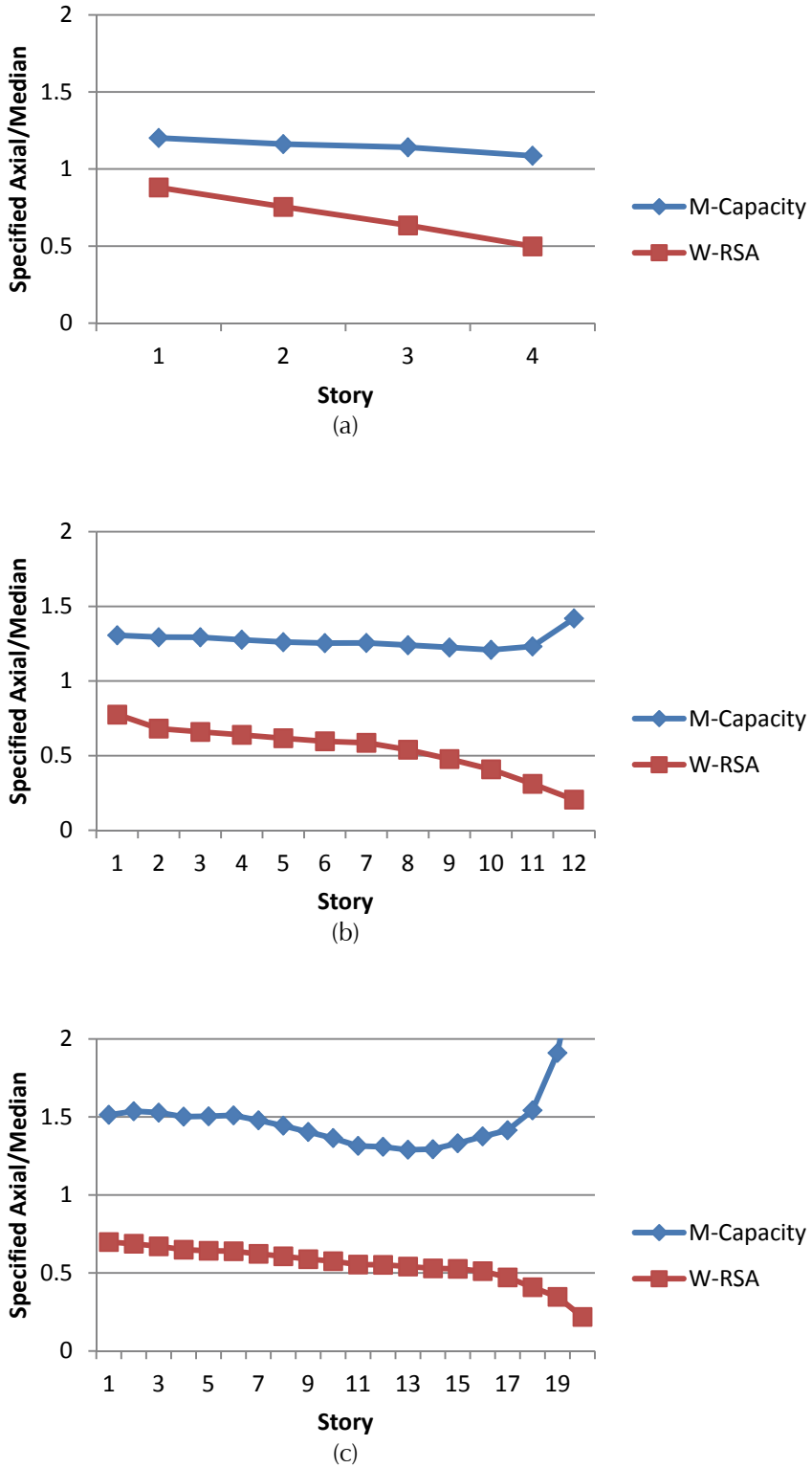

Figure C-21 Specified axial column force normalized by median demands at MCE intensity for special RCMF archetypes: (a) 4-story; (b) 12-story; and (c) 20-story.

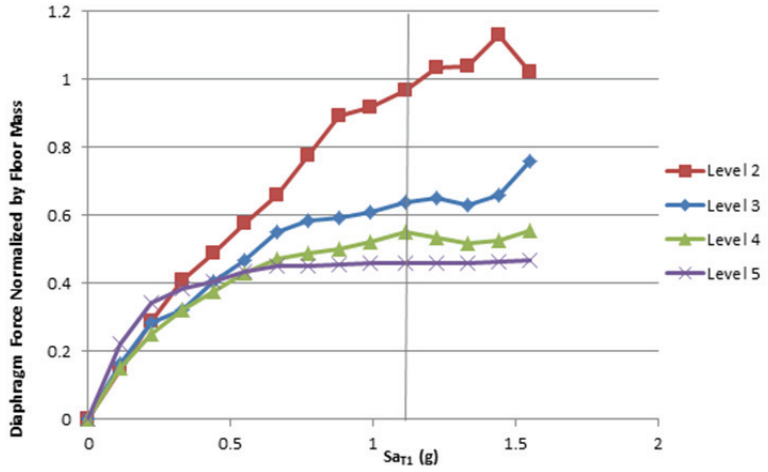

(a)

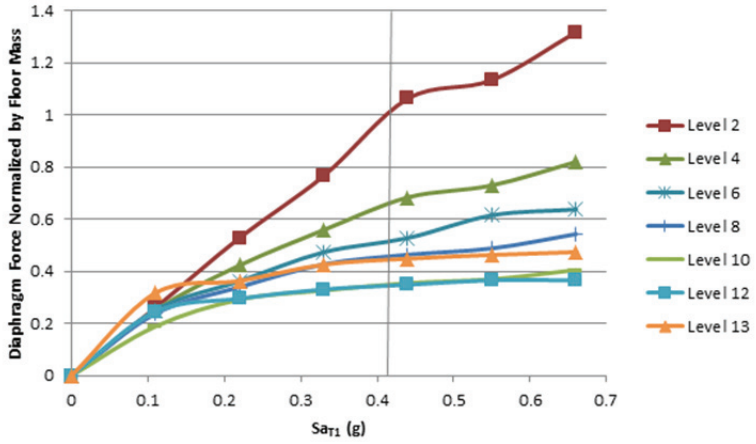

(b)

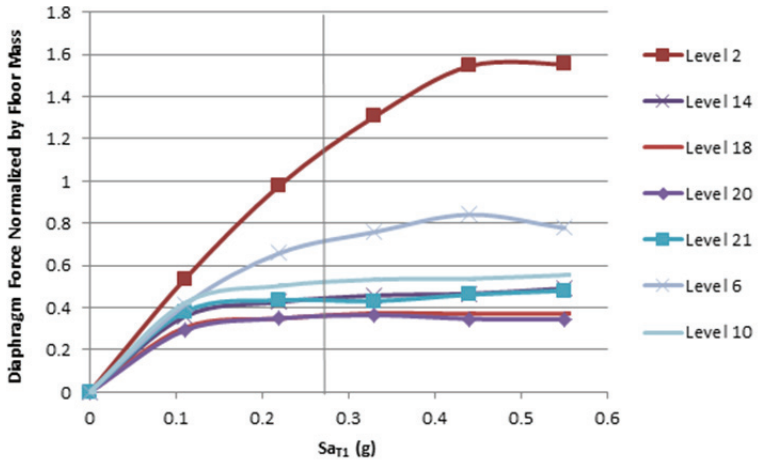

(c)

Figure C-22 Normalized collector force demands for special RCMF archetypes: (a) 4-story; (b) 12-story; and (c) 20-story.

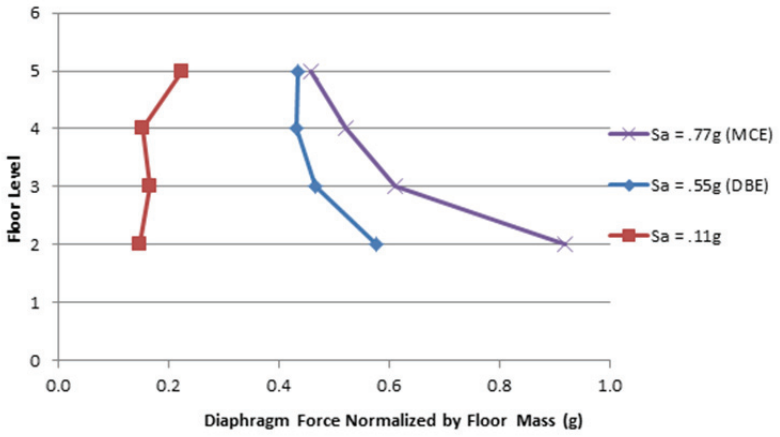

(a)

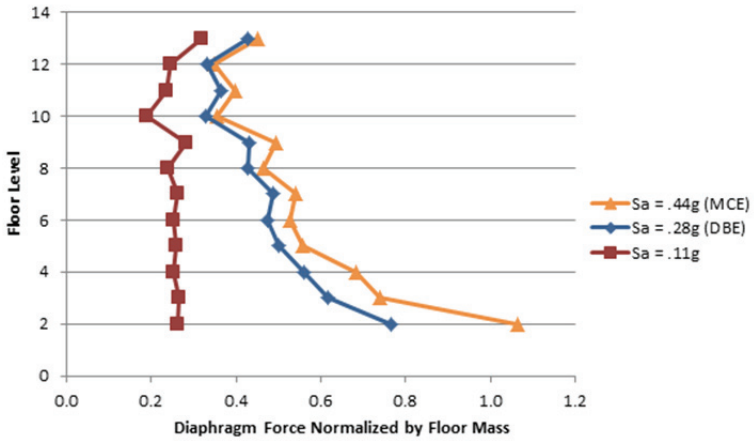

(b)

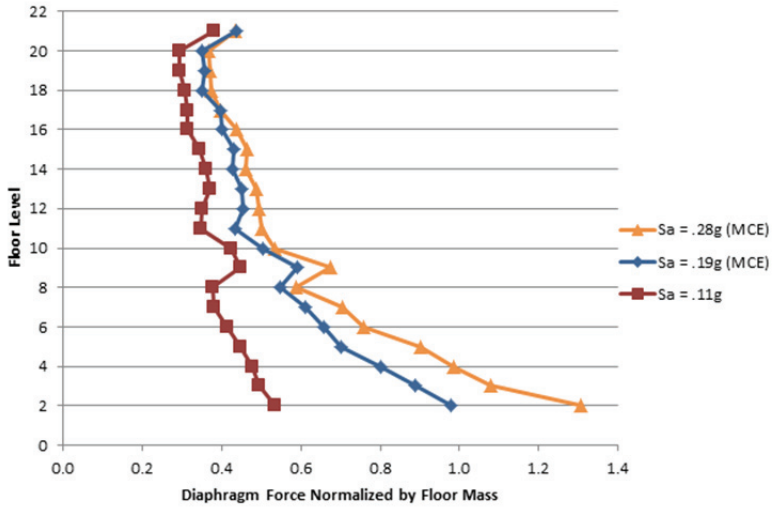

(c)

Figure C-23 Collector force demands normalized by floor weight at MCE intensity for special RCMF archetypes: (a) 4-story; (b) 12-story; and (c) 20-story.

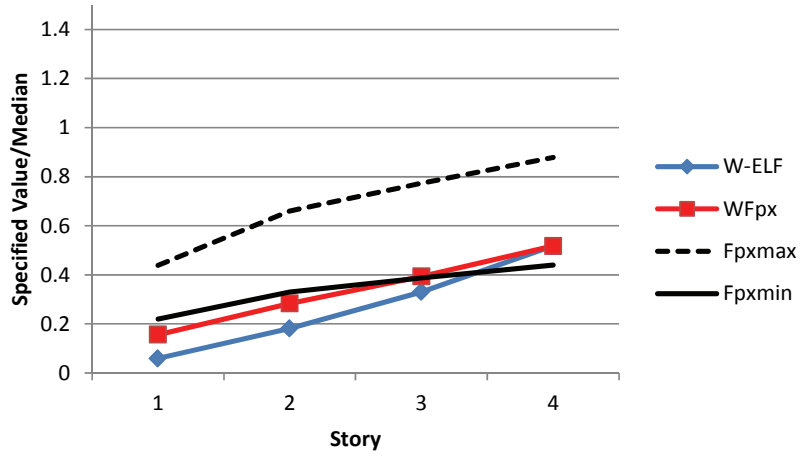

(a)

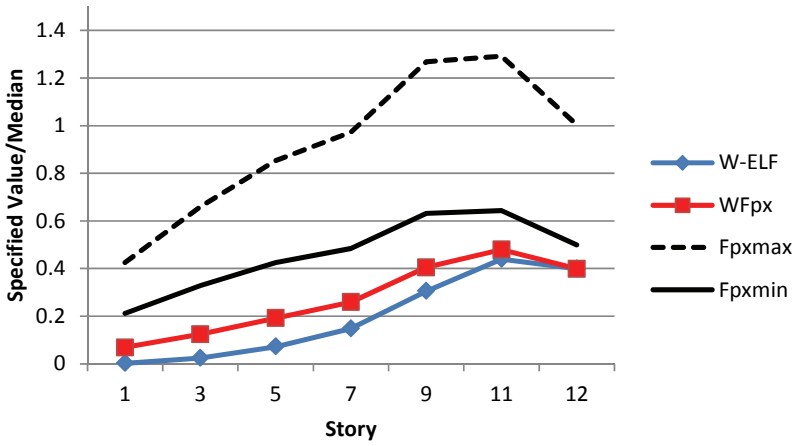

(b)

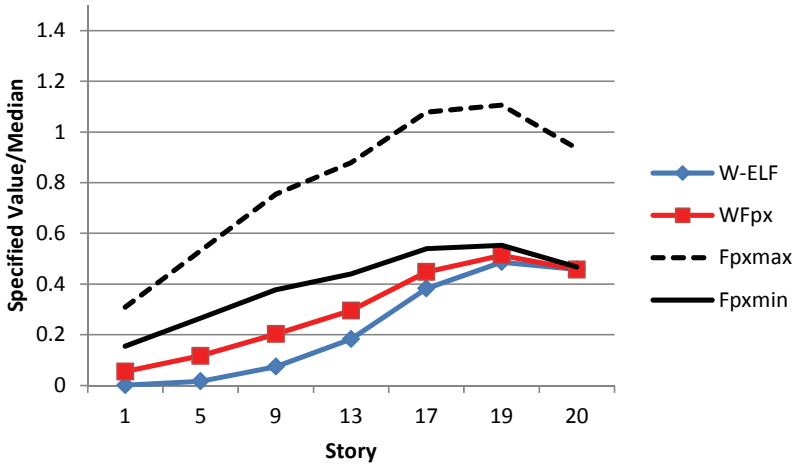

(c)

Figure C-24 Specified collector force normalized by median demands at MCE intensity for special RCMF archetypes: (a) 4-story; (b) 12-story; and (c) 20-story.

As noted for special SCBFs, when compared to the other components, the normalized collector forces have considerably more variability. The diaphragm collector forces tend to saturate in the upper floors, where accelerations are limited by inelastic yielding in the lower floors. However, there is little saturation in the lower floors, where the diaphragm forces correlate with PGA. For the 20-story special RCMF, ground motions are scaled at a period of T = 3.4 seconds, which corresponds to a PGA of about 1.7g (see Figure C-13). From this perspective, median MCE diaphragm demands of 1.3g (Figure C-23c) are not surprising. As described previously for braced frames, the peak values at the base could be adjusted to better reflect MCE or DBE PGAs and consider high frequency filtering. Assuming an adjustment to the DBE PGA of 0.6g and a 0.8 adjustment for high frequency (10 Hz) filtering, the peak value of 1.3g at the base of the 20-story special RCMF would reduce to about 0.4g (i.e., 1.3g x 0.6g/1.7g x 0.8). However, even with these adjustments, the specified diaphragm forces at the base of the 20-story frame, equal to $F_{px,min}$ of 0.2g (Figure C-24), would still be just half of the median demands.

C.6 Observations and Findings

The observations and findings from the studies in this chapter are distinguished between those that generally relate to seismic design and others that are specific to the overstrength and capacity design requirements.

C.6.1 General Findings

- Apart from the few general requirements in ASCE/SEI 7-10, current material design standards make limited use of the overstrength factor, Ω_O, resorting instead to more explicit capacity design approaches where required strengths are based on force demands calculated using the expected strengths of yielding components. In comparisons between forces calculated using system overstrength factors versus member strength-based capacity design factors, the member strength-based factors are usually more accurate – particularly where the forces of interest are governed by local behavior adjacent to yielding elements (e.g., shear in beams with flexural hinges, connections in yielding braces). Moreover, whereas the commentary to ASCE/SEI 7-10 implies that capacity design approaches can be applied to limit the required strengths to a value less than that calculated by Ω_O (implying that the Ω_O will tend to envelope the force demands), it is more typical that the Ω_O force is offered as an exception to relieve the forces that would otherwise be required by a strict capacity design requirement. Thus, the rationale given for Ω_O is somewhat inconsistent with its formulation and how it is applied.
- The designation of force-controlled components and the use of capacity-based design concepts to proportion force-controlled components are highly variable across different system types and materials. Whereas some provisions, notably

those for steel-framed structures, make fairly extensive use of capacity-based design concepts, other provisions (e.g., for wood framed structures) make relatively little use of capacity design requirements. Accordingly, the use and design relevance of Ω_O is quite varied across systems and materials.

- Nonlinear analyses conducted entailed the reanalysis of special RCMF and SCBF archetypes that were evaluated in prior FEMA P-695 studies. As such, these provided an opportunity for an independent check on the results of prior studies through independent analyses. In some cases, the nonlinear collapse analysis results in this study agreed fairly well with those of prior studies. However, in other cases the archetype analysis results were considerably different (up to a factor of about two in the calculated median collapse capacity) from those reported in prior studies. These results highlight the extent to which the FEMA P-695 evaluation of collapse safety is sensitive to model types and modeling assumptions used in the archetype analyses.
- Whereas the FEMA P-695 collapse analysis procedures were originally conceived to assess overall system collapse that is dominated by inelastic behavior associated with first-mode response, the FEMA P-695 procedures are less effective at assessing other effects, such as variability of force demands in force-controlled components and their influence on collapse safety. For example, the study of diaphragms and collectors revealed their force demands to be based on short-period response, which can be significantly overestimated using the first-mode period scaling procedures of FEMA P-695. Moreover, the use of median model parameters in the FEMA P-695 analyses precludes the direct assessment of how variability in design requirements and behavior of force-controlled components influences structural collapse.

C.6.2 Specific Findings

- The static strength is not necessarily an accurate measure of the maximum forces that can develop in the structural components. This is particularly true where higher mode or transient pulse-like effects are present. For example, where higher modes are significant, the maximum shear in concrete walls is not necessarily limited by hinging at the base of wall. Similarly, in braced frames, the localization of pushover deformations in one or two stories do not necessarily reflect the maximum forces that can develop under dynamic loading. The collector forces in the lower stories of a building are often considerably larger than inferred by first-mode pushover behavior and the associated ELF-based equations in ASCE/SEI 7-10.
- Where force demands of force-controlled components are controlled by yielding of adjacent elements, the capacity design provisions of current standards tend to work well, in that the median force demands can be reliably calculated and the

variability in the maximum force because of ground motion variability is fairly limited. On the other hand, for force-controlled components whose response depends more on overall system behavior, the medians are more difficult to calculate and the variability is higher. For example, brace connection forces and beam shear forces in optimally designed systems had well-controlled median and COV values less than about 10%. However, median values of axial column force demands were not well-predicted and had COV values of up to 30%. The discrepancies are largest for the floor diaphragm and collector forces for lower stories in tall buildings, where the demands reflect the high frequency characteristics of the ground motion input. In the 20-story frame building, the calculated median values appeared to have little relationship to the yield strength of the frame and COV values of up to 50% were observed in the collector forces.

- Although force-controlled components with well-controlled mechanisms had low variability, the forces in these components tend to increase and saturate rapidly at low ground motion intensities, sometimes reaching their full force demands at ground motion intensities of about 20% to 30% of the MCE intensity. This can be important from the standpoint of system reliability because these force-controlled components will experience their maximum demands much more frequently (smaller return periods) than the deformation-controlled components will experience their maximum deformation demands. In other words, although the MCE level force demands provide a reasonable measure of the maximum force demands on force-controlled components, the frequency of occurrence is typically much higher than implied by MCE intensity checks.
- ASCE/SEI 7-10 procedures for calculating diaphragm and collector forces tend to significantly underestimate the force demands, especially in taller structures. For example, analysis results of the 12-story special SCBF and 12- and 20-story special RCMF archetypes suggest that the current ASCE/SEI 7-10 provisions may underestimate collector forces by more than two times. These large discrepancies cannot be corrected by revising the static overstrength values because the errors have more to do with how dynamic pulse (or higher mode) behavior is represented. In this regard, the rationale for applying the overstrength factor to collector force demands has less to do with the system overstrength and more to do with simply providing an extra margin of safety in the collectors. However, there is no reliability basis to establish appropriate margins.
- Design approaches that employ nonlinear dynamic analysis (e.g., ASCE/SEI 7-10 Chapter 16) avoid the need to estimate overstrength effects through Ω_O because they allow explicit calculation of inelastic force demands in force-controlled components. Current standards and guidelines (e.g., ASCE/SEI 7-10 Chapter 16 and the PEER *Guidelines* and LATBSDC *Procedure*) generally include distinctions between deformation-controlled and force-controlled components,

and they make allowances for the variability in force demands on force-controlled components. However, there are some striking differences between these documents. Most notably, these differences are the following: (1) ASCE/SEI 7-10 calculates demands at the DBE levels, whereas PEER *Guidelines* calculate demands at MCE levels; (2) ASCE/SEI 7-10 uses a maximum of 7 ground motions to characterize the upper bound demand due to ground motion variability, whereas the PEER *Guidelines* impose a multiplier on the mean demands; and (3) the PEER *Guidelines* differ in how the component strengths are calculated, i.e., whether expected or nominal material strengths are assumed and whether or not resistance factors, ϕ, are included. Moreover, it is not clear that any of these provisions for design of force-controlled provisions have been statistically assessed for conformance with the expected collapse safety of the overall seismic force-resisting system.

C.7 Recommendations

The recommendations resulting from the studies in this appendix are as follows:

- It is recommended that given the limited and somewhat inconsistent use of Ω_O in current design standards, the inconsistency in calculated pushover strengths as compared to specified Ω_O for various systems, and the general difficulty and ambiguity in quantifying the overstrength factor, the system overstrength definition and provisions in current building codes should be replaced with alternative requirements that are tailored to the specific design situation. For example, where material design provisions, such as ANSI/AISC 341-10, make reference to Ω_O, it is suggested that the references be replaced with specific values that pertain to the specific situation. As a future study, it is recommended to develop guidelines for establishing consistent criteria for the design of force-controlled components. The intent of such guidelines is to help ensure consistency in requirements for force-controlled components that are developed in building codes and standards.
- Notwithstanding the previous suggestion to eliminate the general specification of system-specific Ω_O values (e.g., the specification of Ω_O values in Table 12.2-1 of ASCE/SEI 7-10), given that the Ω_O term is longstanding in the building code, a default value of Ω_O should be specified where other requirements do not apply. Because the stated premise in the commentary is for Ω_O to provide an upper bound on response, it is suggested to define the default value of Ω_O equal to 3.

C.8 Future Studies

Based on the preliminary studies described in this appendix and other supporting research, it is recommended to develop improved requirements for force-controlled components that provide more consistent reliability. It is further suggested that new

provisions should probably not rely as much (or at all) on the single system overstrength factor, Ω_O. Specific aspects of this work include the following:

- For force-controlled components where the imposed force demands are due to yielding of adjacent members, a reliability-based methodology should be developed that can be employed by specification committees to develop risk-consistent capacity design factors and requirements for design by elastic analysis. This could, for example, employ a methodology that is similar to the first-order second moment methods employed in the original development of load resistance factor design provisions, except that the force demands are determined based on the yielding deformation-controlled elements. The underlying reliability factors (reliability index) should be consistent with the collapse risk implied by the FEMA P-695 and Project 07 procedures (Luco et al., 2009).
- Procedures and guidelines to determine force demands in force-controlled components that result from overall system response, which may or may not be limited by the inelastic pushover strength of the structure should be developed. This procedure would take the place of the current amplified earthquake load equation that is based on overstrength system factors, Ω_O. The guidelines would likely need to differentiate between different system components and be tailored to the components of interest. As a minimum, such procedures should accurately evaluate forces in axial column forces because of overturning in moment frames and braced frames and supports under walls and discontinuous walls. The procedures should employ appropriate design factors to control the reliability index .
- Given the growing use of nonlinear dynamic (response-history) analysis for design, a reliability-based methodology should be developed to determine appropriate design requirements for force-controlled components based on the results of nonlinear dynamic analyses. The proposed provisions should be consistent with current procedures for applying nonlinear dynamic analysis in design (i.e., ASCE/SEI 7-10, Chapter 16 or the PEER *Guidelines*) and provide a reliability index that is consistent with collapse risk criteria of FEMA P-695 and Project 07.
- To the extent that proper design of collectors is essential to building safety and current building code requirements appear to significantly underestimate collector force demands, a study should be undertaken to establish more accurate criteria for determining force demands in diaphragms and collectors. Such a study should consider the way collector forces are affected by both inertia effects and inelastic force redistributions and the extent to which high frequency response can be either neglected or otherwise considered in collector design. For example, the evaluation should consider whether data-smoothing techniques are

appropriate to reflect time-averaging of force demands based on expected material response and acceptance criteria for collectors.

- To the extent that there are important design criteria that fall outside the scope of the FEMA P-695 Methodology and cannot be accurately evaluated using the existing procedures, a study should be undertaken to identify important design criteria that cannot be accurately evaluated by the current FEMA P-695 Methodology, and to develop appropriate adaptations to the FEMA P-695 Methodology to consider these criteria. For example, the evaluation of diaphragm and collector forces revealed how scaling procedures based on the first-mode response (first-mode period) can significantly overestimate force demands associated with higher mode response. More fundamentally, the current FEMA P-695 framework does not provide a rigorous basis to evaluate seismic design criteria for force-controlled components (except through the judgment-based procedures for determining the inherent variability in system response).
- To the extent that the conclusions of a FEMA P-695 assessment can be quite sensitive to the nonlinear analysis models and modeling assumptions, examining appropriate and effective ways to ensure reliability in the procedures would be useful. This may, for example, lead to more specific reporting requirements for summarizing key assumptions and modeling criteria or requirements for performing complementary archetype studies by two independent entities, including a requirement that they identify and resolve significant differences in model attributes and agree on a common set of analysis model assumptions and criteria. Associated with this, the study could examine the extent to which observed variations in the analysis results are consistent with establishing the judgment-based variability in collapse assessment and acceptance criteria. Extending the notion of two independent entities for archetype analyses to establishing the representative archetype configurations and system designs may also be worthwhile.

Appendix D
Study of Long-Period Systems

D.1 Introduction

Prior studies of the FEMA P-695 Methodology evaluating the collapse performance of a seismic-force-resisting systems (SFRS) suggest that if long-period systems (fundamental period, *T*, greater than 2 seconds) are designed using the design spectrum and the same *R* factor values as those used for systems with shorter periods, the collapse risk will be significantly higher for long-period systems. This is shown by the data in Figure 2-1. The objectives of this study are to investigate the collapse risk of long-period systems and develop recommendations for modifying the design of long-period systems to achieve an approximately uniform collapse probability across all periods.

To accomplish these objectives, the design base shear required to achieve a collapse risk of 10% under the Maximum Considered Earthquake (MCE) was computed for long-period concrete and steel frame archetypes designed and analyzed as part of the studies summarized in the FEMA P-695, *Quantification of Building Seismic Performance Factors*, (FEMA, 2009) and NIST GCR 10-917-8, *Evaluation of the FEMA P-695 Methodology for Quantification of Building Seismic Performance Factors*, (NIST, 2010) reports. Additionally, a series of long-period reinforced concrete core-wall archetypes was designed for Seismic Design Category (SDC) D, analyzed per the FEMA P-695 Methodology to determine collapse risk and the design base shear required to achieve a 10% collapse risk was computed.

The results of this investigation indicate that for long-period structures with walls, achieving an acceptable collapse risk, given the seismic loads determined according to ASCE/SEI 7-10, *Minimum Design Loads for Buildings and Other Structures* (ASCE, 2010), requires a design that exceeds the minimum requirements defined by the ACI 318-08 Code, *Building Code Requirements for Structural Concrete and Commentary* (ACI, 2008). This includes: (1) design for shear demands that are significantly larger than those determined directly from the ASCE/SEI 7-10 loads; (2) design to achieve flexural strength at the location of a second flexural hinge above the base of the wall that exceeds the demand determined from the ASCE/SEI 7-10 load distribution (this is intended to ensure that drift and deformation demands at the location of a second hinge are not excessive); and (3) inclusion of confining reinforcement at the location of the second flexural hinge to achieve flexural ductility. These additional requirements for achieving acceptable collapse risk follow

from the nonlinear response mechanism for walls and the impact of higher-mode response. The development of a flexural hinge near the base of a walled structure limits the moment at the base of the wall but does not limit the shear demand at the base of the wall or the flexural demand elsewhere up the height of the wall; instead the development of a flexural hinge near the base of a wall results in a reduced effective height for the resultant lateral load and an increase in the base shear. Higher-mode response results in the development of a second flexural hinge above the base of the wall and contributes to the drop in the effective height.

It is not known if, like walls, the nonlinear response of other SFRS results in issues in the long-period range that can significantly increase collapse risk. Assuming that this is not the case and evaluating the collapse risk of long-period walls neglecting the impact of shear demand, the results of this investigation suggest that an approximately uniform collapse probability across all periods can be achieved if long-period systems are designed using the design spectrum, the same R factor values as are used for shorter period systems, and the ASCE/SEI 7-10 minimum base shear limit.

D.2 Background

D.2.1 Design of Long-Period Systems Using ASCE/SEI 7-10

The seismic design of long-period systems using ASCE/SEI 7-10 is particularly affected by the following factors:

- **The approximate fundamental period of the structure, T_a, and the design period, $T = C_u T_a$.** The design period, T, is determined by the building height, structure type, and design spectrum and is typically less than the fundamental period of the structure computed from a modal (eigenvalue) analysis, T_1. Thus, the design period acts to increase the base shear used in design because in the long-period range, smaller periods are associated with higher spectral accelerations.
- **The minimum base shear requirement.** For most regions, the minimum base shear is defined as $0.044 S_{DS} I_e W > 0.01 W$, where S_{DS} is the spectral response acceleration parameter in the short-period range, I_e is the importance factor, and W is the seismic weight. According to ASCE/SEI 7-10, if modal response spectrum analysis (RSA) is used to determine seismic demands, the design base shear computed must exceed 0.85 of the base shear computed from the design spectral response acceleration parameter at the design period. If equivalent lateral force (ELF) analysis is used, the design base shear must exceed the minimum base shear.
- **Story drift limit.** Drift limits were introduced in the 1971 edition of the Uniform Building Code (UBC) to limit damage for service-level events and

reduce collapse risk for design-level events. For long-period systems, the requirement that story drifts not exceed the allowable story drift may result in a stiffer, stronger building and, thus, a structure that is effectively designed for a higher base shear.

- **Stability coefficient (P-delta) requirements.** For long-period systems that experience relatively large drifts under seismic loading, P-delta effects on story shears and moments can be significant. ASCE/SEI 7-10 requires that the drift-based stability coefficient for all stories not exceed a given limit. For systems with large axial loads and drifts, designing to meet this requirement may result in a stiffer, stronger building and, thus, a structure that is effectively designed for a higher base shear.

Given the impact of the above factors on the design of tall structures, the collapse risk of long-period systems could be reduced by modifying any of the above as well as by modifying the *R* factor used in design of long-period systems.

D.2.2 Response Mechanisms for Long-Period Systems That Contribute to Increased Collapse Probability

A number of previous studies have addressed the seismic response of long-period systems and the response mechanisms that can contribute to increased collapse risk for these systems. Results of these studies include the following:

- Large overturning forces may result in high compression demands at the base of the structure and, as a result, in reduced drift capacity because of buckling and crushing.
- Large drifts can amplify P-delta effects and increase base moment demands.
- In a moment frame structure, column yielding can result in a single- or multi-story mechanism for which P-delta effects exacerbate demands and cause collapse. This has been demonstrated by Haselton et al. (2011) and Krawinkler and Zareian (2007).
- In wall structures, flexural yielding may result in a reduction of the effective height of the lateral load distribution, an increase in the base shear associated with development of the flexural strength of the wall, and, thus, reduced drift capacity.

D.2.3 Results of Previous Research

In developing and evaluating the FEMA P-695 Methodology, numerous archetypes of multiple SFRS were designed and analyzed to determine collapse risk. These studies are documented in the FEMA P-695 and NIST GCR 10-917-8 reports. As discussed in Chapter 2, the results of these studies indicate that if design is

accomplished using the design spectrum, reduced R factor values are required for long-period systems to achieve a uniform collapse risk of 10% under the MCE.

However, as discussed above, seismic design of long-period systems per ASCE/SEI 7-10 is affected by a number of factors beyond the design spectrum. For a subset of the systems studied previously, Figure D-1 and Figure D-2 show the base shear coefficient, C_s, required to achieve a 10% collapse risk plotted versus the design period, T, (Figure D-1) and versus the computed fundamental period, T_1, (Figure D-2) of the structure. The systems included in Figure D-1 and Figure D-2 have ASCE/SEI 7-10 R factors of 6 (dashed blue) and 8 (solid red) and were designed for SDC D_{max}. Also shown in Figure D-1 and Figure D-2 are the SDC D_{max} design spectra reduced using $R = 6$ and $R = 8$, with a tail defined by the ASCE/SEI 7-10 minimum base shear requirement.

The data in these figures suggest that a 10% collapse risk can be achieved for long-period systems via modification of the required base shear coefficient, C_s. Specifically, the data in Figure D-1 and Figure D-2 suggest that the current minimum base shear requirement may be sufficient to achieve 10% collapse risk. However, in the long-period range, the data in these figures are extremely limited and primarily for reinforced concrete and steel moment frames. In this range, buckling-restrained braced frames show different trends than moment frames.

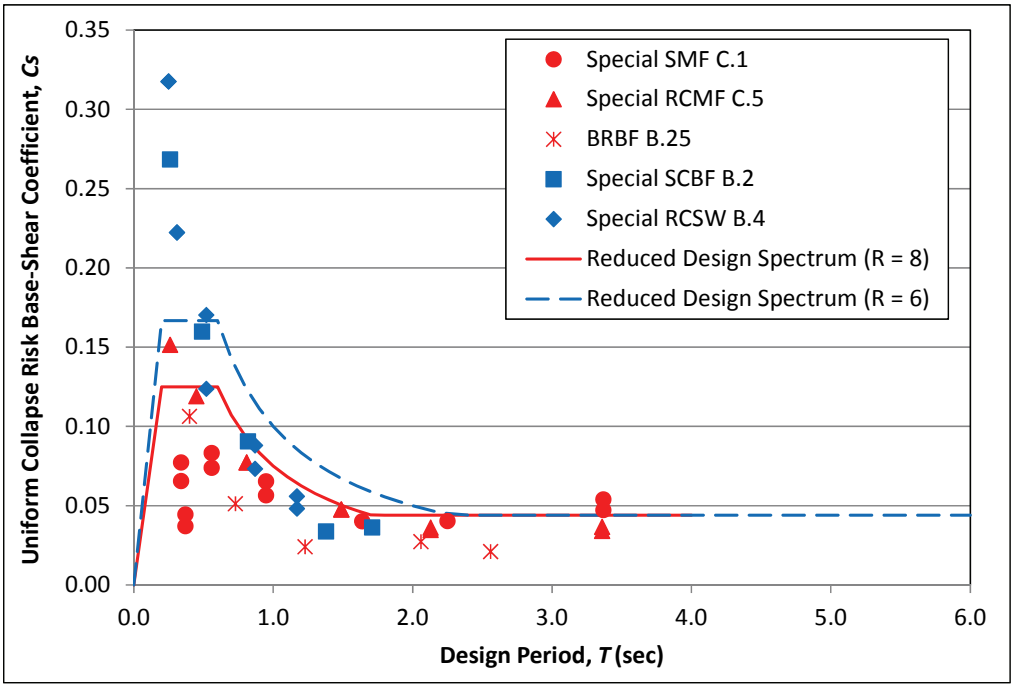

Figure D-1 Base shear coefficient, C_s, required for 10% collapse risk versus design period, T.

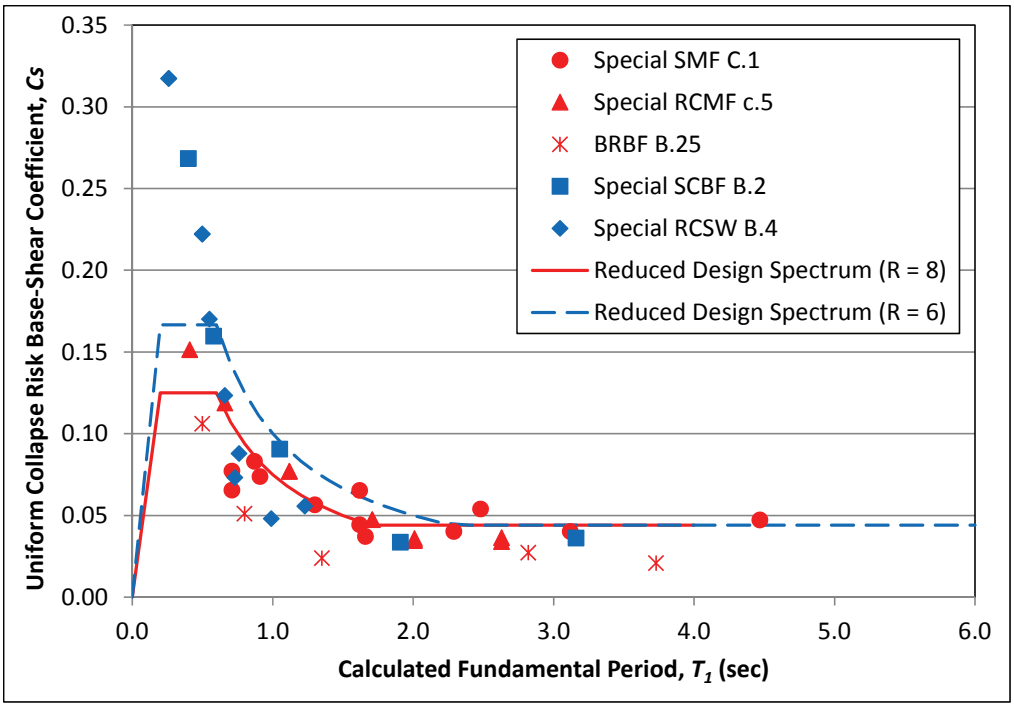

Figure D-2 Base shear coefficient, C_s, required for 10% collapse risk versus calculated fundamental period, T_1.

D.3 Approach for Developing Recommendations for Base Shear Requirements for Long-Period Systems

To develop recommendations for base shear requirements of long-period systems, the data set presented in the previous figures was extended as follows:

- In order to ensure that design recommendations are appropriate for different SFRS, the dataset was supplemented with data for concrete walls. Eight special reinforced concrete wall buildings were designed using ACI 318-08, the FEMA P-695 SDC D_{max} spectrum, and ASCE/SEI 7-10 without consideration of drift and P-delta and stability requirements. Walls were analyzed to determine collapse risk and base shear coefficient required to achieve a 10% collapse risk.
- Both ELF and RSA approaches were employed because designs according to each may result in significantly different load distributions (and thus different base moment demands associated with the same base shear demand).

D.4 Design of Long-Period Special Reinforced Concrete Core-Wall Archetypes

D.4.1 Quality Rating of Design Requirements and Test Data

Special reinforced-concrete core-wall archetypes were designed in accordance with ACI 318-08 and ASCE/SEI/SEI 7-10. The recommendations of *Guidelines for Performance-Based Seismic Design of Tall Buildings* (PEER, 2010), were used to

size walls for shear demand. Additional experimental data were used, as necessary, to support the development of nonlinear models.

D.4.1.1 Quality Rating of Design Requirements

ACI 318-08 and ASCE/SEI 7-10 do not specifically address design of long-period core-wall systems. *2006 IBC Structural/Seismic Design Manual: Code Application Examples, Volume 1* (SEAOC, 2006), PEER *Guidelines*, and NIST GCR 11-917-11, *Seismic Design of Cast-in-Place Concrete Special Structural Walls and Coupling Beams* (NIST, 2011), as well as other documents indicate potential shortcomings of the code-based design approach detailed in ACI 318-08 and ASCE/SEI 7-10.

Experimental evidence exists that walls responding in a flexural manner can lose lateral load carrying capacity at moderate to low drifts because of the effect of shear coupled with inelastic flexural action (Birely 2012; Gogus, 2010; NIST, 2010). This so called shear-flexure interaction can lead to a compressive failure in the compressive zone under lower flexural demands than might be expected. Current design requirements do not address this response mode.

Current recommendations for effective stiffness of concrete walls typically specify a single value targeting an average value of yield stiffness for the wall section ($0.5E_cI_g$, $0.4A_cE_c$). However, it has been shown in the literature (Adebar et al., 2007; Panagiotou and Restrepo, 2007) that the stiffness of wall systems can be affected by axial load demand, layout of reinforcing steel, and dynamic load effects. Also, experimental evidence (Beyer et al., 2011; Massone and Wallace, 2004) indicates shearing deformations can become much larger in wall regions that experience inelastic flexural demands.

Given the above, a quality rating of (B) Good was assigned to the design requirements for concrete core wall systems.

D.4.1.2 Quality Rating of Test Data

A detailed summary of test data for concrete wall sections is provided by Gogus (2010). For long-period (i.e., mid- to high-rise) core walls, little experimental evidence exists. Recent tests (Lowes et al., 2011; Birely et al., 2010; Turgeon, 2011) have simulated the base of mid-rise buildings subjected to expected seismic demands. These experimental programs further support the detrimental effect shear-flexure interaction can have on the drift capacity of wall systems.

For the current study, experimental data from several test programs were used to define parameters for numerical simulation of nonlinear wall response. Results reported by Thomsen and Wallace (1995), Dazio et al. (2009), Lowes et al. (2011), Vallenas et al. (1979), Liu (2004), Oh et al. (2002), Oesterle et al. (1976), and Pilakoutas and Elnashai (1995) have been used as a basis for comparison between

model simulation and experimental response. These data are used to assess the capability of the selected modeling approach to accurately predict yield stiffness, wall strength, and displacement capacity.

Existing test data provide a basis for developing a modeling approach that is capable of predicting stiffness, strength, and ductility of wall systems. However, test data are limited and do not span a wide range of wall designs. Very few tests have been performed addressing response and performance of long-period wall systems; recent tests have addressed mid-rise wall systems. Very few tests provide data characterizing degradation in lateral load carrying capacity and onset of loss of axial-load carrying capacity. This limits the accuracy of prediction of loss of axial-load carrying capacity. In consideration of these limitations regarding available experimental data, a quality rating of (B) Good was assigned.

D.4.2 Building Configuration

Designs were completed for four building heights ranging from 16 stories (192 feet) to 30 stories (360 feet); story heights were taken as 12 feet for all stories. Figure D-3 shows a plan view of the building with core walls. In all cases, the building was assumed to have a footprint of 100 feet by 100 feet, and the SFRS was assumed to comprise two C-shaped walls acting independently when loaded in the direction of the wall web and acting as a coupled system when loaded in the direction of the wall flanges. Only loading in the direction of the wall webs was considered for design. Walls were assumed to be a minimum of 25 feet long and 18 inches thick.

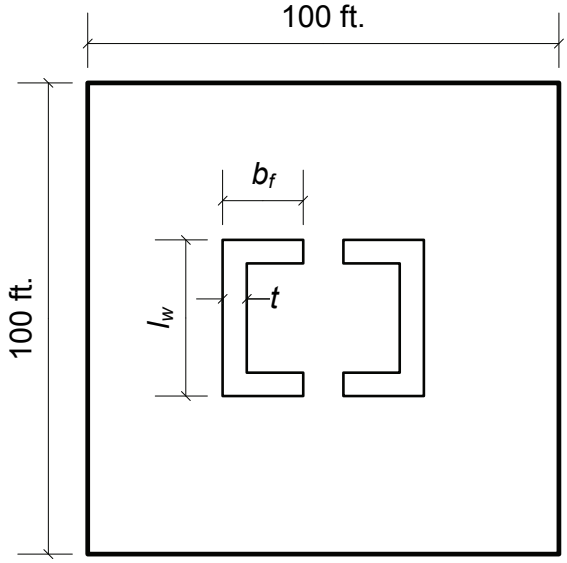

Figure D-3 Plan view of special reinforced concrete core-wall archetype.

D.4.3 Design Methodology

D.4.3.1 Determination of Seismic Demands

Walls were designed using SDC D_{max} spectrum. Designs were developed using demands determined from both the RSA and ELF procedures as defined in ASCE/SEI 7-10. Base shear demands determined using the ELF procedure employed the design period and, as necessary, the minimum base shear limit. Base shear demands determined from RSA were typically less than those determined using the ELF procedure and were scaled to 100% of the ELF base shear to be consistent with anticipated changes to ASCE/SEI 7. In computing demands using RSA, a line-element model was employed in which flexural stiffness was defined equal to 50% of the gross-section stiffness and axial and shear stiffness were taken equal to 100% of the section stiffness, as recommended in ASCE/SEI 41-06 (ASCE, 2007). A seismic dead load of 170 psf was assumed. Table D-1 and Table D-2 provide seismic design parameters for walls designed using RSA and ELF procedures, respectively. Note that entries denoted with MRSA in the ID column were archetypes designed using demands determined from RSA and entries denoted with ELF were designed using demands determined from the ELF procedure.

Table D-1 Seismic Design Parameters for Walls Designed Using RSA Demands

		Key Configuration Design Parameters					
ID	No. of Stories	SDC	*R*	*T* (sec)	T_1 (sec)	*V/W* (g)	$S_{MT}(T)$ (g)
MRSA1	16	D_{max}	6	1.44	3.52	0.069	0.63
MRSA2	20	D_{max}	6	1.71	4.57	0.059	0.53
MRSA3	24	D_{max}	6	1.96	5.74	0.051	0.46
MRSA4	30	D_{max}	6	2.31	7.58	0.044	0.39

Table D-2 Seismic Design Parameters for Walls Designed Using ELF Demands

		Seismic Design Parameters					
ID	No. of Stories	SDC	*R*	*T* (sec)	T_1 (sec)	*V/W* (g)	$S_{MT}(T)$ (g)
ELF1	16	D_{max}	6	1.44	2.13	0.069	0.63
ELF2	20	D_{max}	6	1.71	2.98	0.059	0.53
ELF3	24	D_{max}	6	1.96	3.78	0.051	0.46
ELF4	30	D_{max}	6	2.31	5.03	0.044	0.39

The FEMA P-695 Methodology recommends the use of ELF procedure for design of archetype configurations, except for cases where the ELF method is not permitted by ASCE/SEI 7-10. Table 12.6-1 of ASCE/SEI 7-10 allows the usage of the ELF

procedure for torsionally-regular reinforced concrete core-wall structures for which the period is less than 3.5 times the transition period of the earthquake design spectrum. Assuming a seismic dead load of 170 psf, for the range of building heights considered, modal analysis results yielded computed fundamental periods, T_1, long enough to disallow use of the ELF method. However, the design periods, T, calculated using FEMA P-695 Equation 5-5 (identical to the upper limit on calculated period per ASCE/SEI 7-10) in general, allowed for the use of the ELF method. Ultimately, designs were developed using both methods.

In computing demands using the RSA method, an elastic line-element model was employed with flexural, shear, and axial stiffness properties of $0.5E_cI_g$, $0.4E_cA_{cv}$, E_cA_g, respectively, where E_c is the concrete elastic modulus defined per ACI 318-08 for $f_c' = 5000$ psi, I_g is the gross-section moment of inertia, A_g is the gross area of the wall, and A_{cv} is the area of the wall carrying shear. A seismic dead load of 170 psf was assumed. Demands computed using RSA employed four modes (sufficient to meet ASCE/SEI 7-10 mass participation requirements); modes were widely enough spaced that the square root of the sum of the squares (SRSS) method was used to combine modal contributions to demand quantities. Base shear demands determined using the ELF procedure were greater than those determined using RSA. Base shear computed per RSA were scaled up to 100% of ELF level.

The data in Table D-1 and Table D-2 show a computed fundamental period, T_1, that is significantly longer than the design period, T. Given that the design period is intended to represent the median of measured building periods, it is not surprising that the computed periods of the core-wall buildings differ from this value. However, anecdotal evidence suggests that although the computed fundamental period of a core-wall building designed for construction on the West Coast is typically longer than the design period, it is also typically less than the computed periods listed in Table D-1 and Table D-2. The greater flexibility of the archetype buildings designed for this project is attributed to the fact that these buildings were not designed to meet all of the performance requirements typically considered in practice.

D.4.3.2 Wall Design

Walls were designed in accordance with ACI 318-08 using seismic demands determined from the ELF and RSA procedures defined in ASCE/SEI 7-10; the recommendations of the PEER *Guidelines* were used to size walls for shear demand. Basic assumption employed in designing the walls were the following: (1) a minimum length, l_w, of 25 feet and a minimum thickness of 18 inches; (2) concrete compressive strength, f_c, of 5000 psi and Grade 60 reinforcement; (3) an axial load at the base of the wall equal to $0.1f_cA_g$; (4) uniformly distributed longitudinal reinforcement with a target longitudinal reinforcement ratio of 1.00%; (5) fixed boundary conditions at the base of the wall with no consideration given to soil-

structure interaction; and (6) no torsional demands. For walls designed using RSA demands, wall length, l_w, and thickness, t, were determined by the shear demand and wall flange length, b_f, was determined by the flexural demand at the base of the wall. Shear stress demands were limited to $2-3\sqrt{f_c'}$ psi per the recommendations of the PEER *Guidelines* and walls were designed to achieve the maximum shear strength based on ACI 318-08. For walls designed using ELF demands, wall design was determined primarily by flexural demands at the base of the wall. Table D-3 lists configuration and design parameters for the walls.

Table D-3 Special Reinforced Concrete Core-Wall Configuration and Design Parameters

ID	No. of Stories	l_w (ft)	t (in)	b_f (ft)	Axial Load $A_g f_c$	Shear Stress Demand $\sqrt{f_c'}$ (psi)	$\varphi V_n/V_u$	$\varphi M_n/M_u$	h_{eff}/h_w
MRSA1	16	25	18	4	0.10	2.5	1.9	1.0	0.39
MRSA2	20	25	18	7	0.10	2.6	1.8	1.0	0.37
MRSA3	24	25	18	10	0.10	2.7	1.8	1.0	0.35
MRSA4	30	25	18	15	0.10	2.9	1.7	1.0	0.33
ELF1	16	32	24	5	0.10	1.4	3.4	1.0	0.73
ELF2	20	32	24	7	0.10	1.5	3.2	1.0	0.74
ELF3	24	32	24	10	0.10	1.6	3.0	1.0	0.75
ELF4	30	32	24	15	0.10	1.7	2.8	1.0	0.76

Design of the walls (length, thickness, and horizontal reinforcement ratio) for shear demand was based on the recommendation of the PEER *Guidelines*. ACI 318-08 Section 21.9.4.4 and Section 9.3.4 limit the shear stress demand on a single pier wall to $6\sqrt{f_c'}$ psi. However, nonlinear analyses of moderate to tall walled buildings have demonstrated amplification of base shear demand beyond that determined from elastic analysis, and the PEER *Guidelines* recommend that shear demand under the design-level event be limited to $2-3\sqrt{f_c'}$ psi. Thus, walls were designed per the recommendations of the PEER *Guidelines* such that $\phi V_n > V_u$ with $\phi = 0.6$ where shear is computed per ACI 318-08. The impact of the shear design procedure on collapse probability is addressed further in Pugh (2012). Shear demands as well as shear capacity-demand ratios listed in Table D-3 are for the base section of the wall.

Design of the walls (flange length, longitudinal reinforcement ratio and confinement reinforcement) for flexural demand followed directly from ACI 318-08. Flange length and longitudinal reinforcement ratio were determined such that $\phi M_n > M_u$ with $\phi = 0.9$ where flexural strength M_n is computed assuming an axial load of $0.1 f_c A_g$ per ACI 318-08. Per ACI 318-08 Section 21.9.6.2 and Section 21.9.6.3, special boundary elements were not required; however, the relatively high longitudinal reinforcement ratio did trigger stricter spacing requirements on transverse reinforcement per Section 21.9.6.5a. If the walls had been designed for loading both

parallel and perpendicular to the web, special boundary elements would have been required. It is not expected that the simulated response of the walls with special boundary elements would have been materially different than that presented below. Table D-4 provides details of the longitudinal reinforcement layout. Flexural capacity demands at the base of the wall are listed in Table D-3.

Table D-4 Longitudinal Reinforcement Layout

ID	Stories	ρ_v (%)	Reinforcing Layout
MRSA1	1-16	1.00	2 - #9 @ 11”
MRSA2	1-20	1.00	2 - #9 @ 11”
MRSA3	1-24	1.00	2 - #9 @ 11”
MRSA4	1-30	1.00	2 - #9 @ 11”
ELF1	1-16	0.75	2 -#9 @ 11”
ELF2	1-20	1.00	2- #10 @ 10.5”
ELF3	1-24	1.20	2- #11 @ 10.5”
ELF4	1-30	1.40	2-# 11 @ 9”

The wall designs defined in Table D-3 and Table D-4 show that use of ELF procedure for determination of seismic demands results in a longer, thicker wall with a larger longitudinal reinforcement ratio. The ELF distribution is dominated by the first mode; first-mode loading results in a relatively large base moment demand and a relatively low base shear demand. This is reflected in the large effective height, h_{eff}/h_w in Table D-3, at which the base shear acts for the ELF distribution. Base moment demand as determined by RSA is dominated by the contribution of the first-mode; however the spectral acceleration for the first mode is relatively low given the large first-mode period. Thus, base moment demand per RSA is significantly less than that determined by ELF for the same base shear demand. Base shear demand as determined by RSA is dominated by the contribution of higher modes, which have significantly higher spectral accelerations than does the first mode. For higher modes, the resultant base shear acts at a relatively low effective height, so these modes do not contribute as much to the base moment demand as they do to the base shear demand. This is reflected in the relatively low effective height, h_{eff}/h_w in Table D-3, at which the base shear acts for the RSA distribution. These factors result in the design for RSA demands being driven by shear demand as well as flexural demand while the design for ELF demands is driven primarily by flexural demand.

Wall configuration and design parameters listed in Table D-3 are for the base of the wall. As discussed previously, nonlinear response and higher mode effects result in moment and shear demands, up the height of the wall, that exceed those determined from the ELF procedure or RSA. To minimize inelastic flexural response and the likelihood of shear demand-capacity ratios in excess of 1.0, the base cross section design was assumed to continue up the height of the structure (Table D-4).

To assess the impact of this on the design, a suite of walls was designed assuming that a new cross-section design would be introduced approximately every four stories and that $\phi V_n > V_u$ and $\phi M_n > M_u$ at all locations; walls were designed using demand determined from ELF procedure and using RSA. This stepped-down design approach is considered to be consistent with practice. Preliminary analysis indicated that these designs would exhibit significantly higher collapse probabilities than the designs in which the cross section at the base of the wall was continued up the height of the wall; these higher collapse probabilities were due to significant inelastic flexural deformation demands and shear demands above the base of the wall. The impact on collapse probability of the flexural design envelope is addressed in Pugh (2012).

D.4.3.3 Evaluation of Wall Designs for Wind Loading

The concrete wall buildings designed for seismic lateral loading were analyzed for wind loading (85 mph exposure C). Walls were found to have adequate capacity for wind loading. Using expected material strength and stiffness, all designs, except for the 30-story RSA design, were found to meet the 1-year acceleration limit for residential construction in ISO 6897:1984 (ISO, 1984). No modifications were made to the 30-story RSA design to meet the ISO acceleration limits.

D.5 Nonlinear Analysis of Reinforced Concrete Wall Buildings Using OpenSees

Collapse risk for long-period concrete walls was determined according to the FEMA P-695 Methodology using the OpenSees platform (http://opensees.berkeley.edu/). Buildings were modeled using a series of nonlinear frame elements and linear shear springs to model the concrete walls and a P-delta column with essentially zero stiffness to simulate base moment demand due to P-delta effects from seismic gravity load. Walls were modeled using displacement-based frame elements with nonlinear fiber-type cross-section models to simulate flexural and axial response and elastic shear springs to simulate shear deformation. Multiple frame elements were used for each story at the base of the wall to provide accurate simulation of flexural response; one shear spring was used per story. Fiber-type cross-section models employed typical material response models; however, to limit mesh sensitivity, the typical stress-strain response models for concrete and steel were modified to account for the element length associated with each fiber section. A uniformly distributed gravity load was applied to the wall at each story to achieve a total axial load at the base of the wall of $0.1 f_c A_w$. The remainder of the gravity load (190 psf) was applied to the P-delta column. Hysteretic damping was supplemented by Raleigh damping of 2.5% in the first and third modes.

D.5.1 Simulation of Wall Response

Walls were modeled using displacement-based frame elements with nonlinear fiber-type cross-section models to simulate flexural and axial response and elastic shear springs to simulate shear deformation. The following sections provide a detailed description of the model.

D.5.1.1 Background on the Displacement-Based Beam-Column Element

The displacement-based beam-column element available for use in the OpenSees software platform was used to model the flexural-axial response of the core wall. This element determines flexural response based on member cross-section models distributed at Gauss-Lobotto integration points along the length of the element. Element end moments and axial forces are determined as a weighted average of the section responses. Each cross-section along the element length is described by a fiber-type section model. Nonlinear concrete and steel one-dimensional stress-strain constitutive models were used to define the response of the fibers that compose the fiber-type section model.

The displacement-based beam-column element formulation assumes a linear curvature distribution along the length of the element. Thus, in regions where inelastic deformations are concentrated, a finer mesh (i.e., more elements per story) is typically required to accurately represent the nonlinear curvature distribution. Another important aspect of the displacement-based element formulation is that equilibrium is satisfied only at the ends of the element. Thus, individual sections along the element length are often subjected to significant variations in axial load. This variation can lead to errors in predicted response due to the axial-flexural interaction. Studies performed on this element indicate that coarse meshes can lead to large variations of axial load within the element while finer meshes diminish this effect.

The displacement-based beam-column element was chosen for use over the force-based and lumped-plasticity beam-column elements that are also available in the OpenSees platform for several reasons. First, in the lumped-plasticity element formulation, nonlinearity is assumed to be constrained to sections at the ends of the element; because nonlinear flexural response can occur at any location up the height of the wall, this assumption was deemed inappropriate. Second, the displacement- and force-based distributed plasticity elements could be expected to provide similar accuracy in simulating response, assuming appropriate meshing is used. Third, the displacement-based element was considered to provide consistency with the displacement-based elements employed typically in practice and with previous studies applying the FEMA P-695 Methodology to assess the collapse risk of walled building that employed displacement-based elements (NIST, 2010; Gogus, 2010).

D.5.1.2 Meshing Walls Using the Displacement-Based Beam-Column Element

Given the characteristics and observed performance of the displacement-based beam-column element described above, walls were meshed using four elements each in the bottom four stories of the building and one element each in upper stories. Four stories was assumed to be an upper-bound on the wall region expected to undergo large inelastic flexural demands; significant inelastic response was not expected higher up the wall. Subsequent analysis results supported the assumption that significant inelastic demands at the base of the wall were limited to the bottom four stories; however, significant inelastic demands were observed near mid-height of the wall at the location of the second plastic hinge.

D.5.1.3 Nonlinear Material Model for Concrete

The stress-strain response of concrete is simulated using the modified Kent-Park model developed by Yassin (1994). This material model is designated as Concrete02 in the OpenSees program. Figure D-4 shows an idealization of the cyclic concrete stress-strain response history defined by this model.

Given the high longitudinal reinforcement ratio, ACI 318-08 requires that confining transverse reinforcement, including cross-ties, be provided over the entire cross-section; thus all concrete was assumed to be confined concrete. However, because special boundary elements are not required by the Code, the volumetric reinforcement ratio is relatively low and the effect of confinement on concrete response is moderate. The effects of the confining transverse reinforcement are calculated using the Razvi and Saatcioglu (1999) model developed for rectangular-shaped confined cores. Based on a minimum amount of required transverse reinforcement (0.25%), this confinement model yields a modest strength increase of 8% and a strain ductility (strain at crushing) increase of 5.

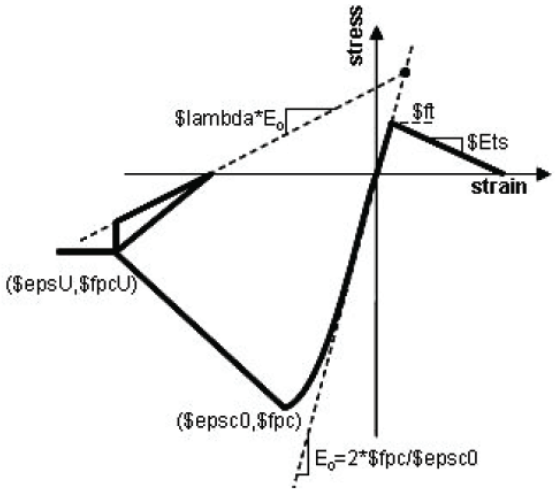

Figure D-4 Concrete stress-strain response model in OpenSees (Mazzoni et al., 2010).

For the Concrete02 model, the peak strength parameter, f_{pc}, was taken as the enhanced expected compressive strength, f'_{cce}, and the strain at peak strength, ε_{c0}, was taken to be the calculated value using the Razvi and Saatcioglu model, 0.004. The post-peak descending branch of the model was defined using values of $0.1f'_{cce}$ and 0.02 for parameters f_{pcU} and ε_U, respectively. Concrete tensile strength, f_t, was taken to be $4\sqrt{f'_c}$ and the tension softening slope, E_{ts}, was taken as 250 ksi. The unloading parameter, λ, was taken as the default value of 0.1.

D.5.1.4 Nonlinear Material Model for Reinforcing Steel

The selected uniaxial material to describe cyclic steel reinforcement response is the Giuffre-Menegotto-Pinto model with isotropic strain hardening developed by Filippou et al. (1983). This material model is designated as Steel02 in the OpenSees program. The yield stress of the reinforcement is taken as the expected yield strength of the reinforcing steel (f_{ye} = 70.2 ksi). The hardening slope is set assuming an ultimate strength of 105 ksi being reached at a strain value of 0.35. Because this material does not allow for reinforcement fracture, the material is attached to a MinMax material in OpenSees, which allows a strain limit to be applied to the model. The MinMax wrapper takes the fracture strain to be 0.35 in both tension and compression. Once the material reaches this strain level, the stress in the material is reduced to zero.

D.5.1.5 Softening Response and Material Regularization

An additional consideration in simulating the post-peak response of a structural system is the strain localization that can occur in a softening system. Once softening begins, the critical section can continue to soften while the remaining sections unload elastically and causes all further inelastic deformation to localize at a single section. This leads to a more rapid unloading response than would be experimentally observed unless the energy released because of softening at the critical section is similar to the energy released by the material during the physical softening process. In the context of a finite element model, this localization can lead to mesh dependent results, where the softening branch of the predicted response is dependent on the mesh size selected by the user. The displacement beam-column element chosen for the current study exhibits this localization effect and Figure D-5 shows the effect of mesh size on the softening response of the wall section.

To alleviate this mesh sensitivity, the technique of fracture energy regularization proposed by Coleman and Spacone (2001) was introduced into the model. This technique introduces fracture energy, G_f, as an additional material property for each material composing the fiber-type section model. The fracture energy represents the area under the stress-displacement diagram for the material and is assumed to be a property that remains constant regardless of the mesh size (element / wall length associated with the section). For model implementation, once the mesh size is

selected, the characteristic material length associated with each element integration point is known. With the characteristic length known, the post-peak material stress-strain response is modified to ensure the area under the stress-displacement diagram is equal to the selected value of fracture energy for the material. Figure D-6 shows results presented in Figure D-5 with regularization of both the concrete and the steel material response; these results show minimal mesh dependency. Material regularization for nonlinear analysis of concrete walls is discussed in Pugh (2012).

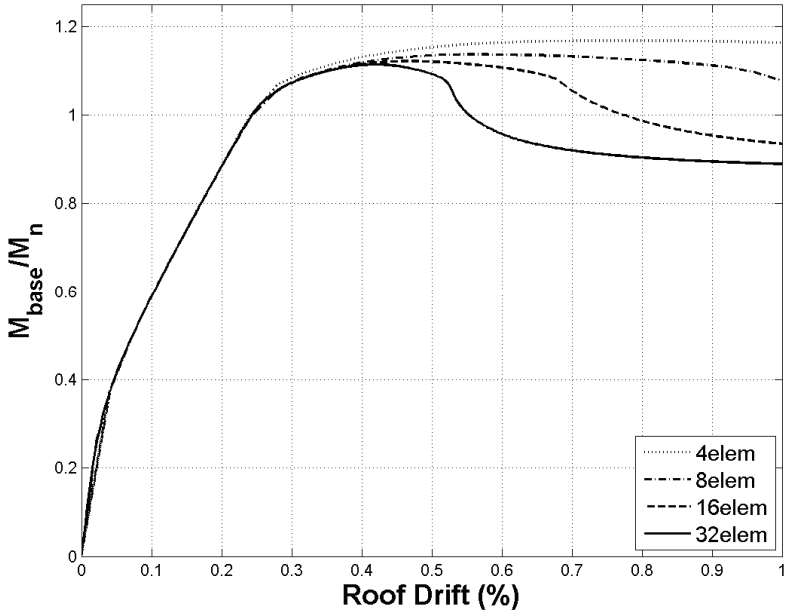

Figure D-5 Localized softening response based on mesh size.

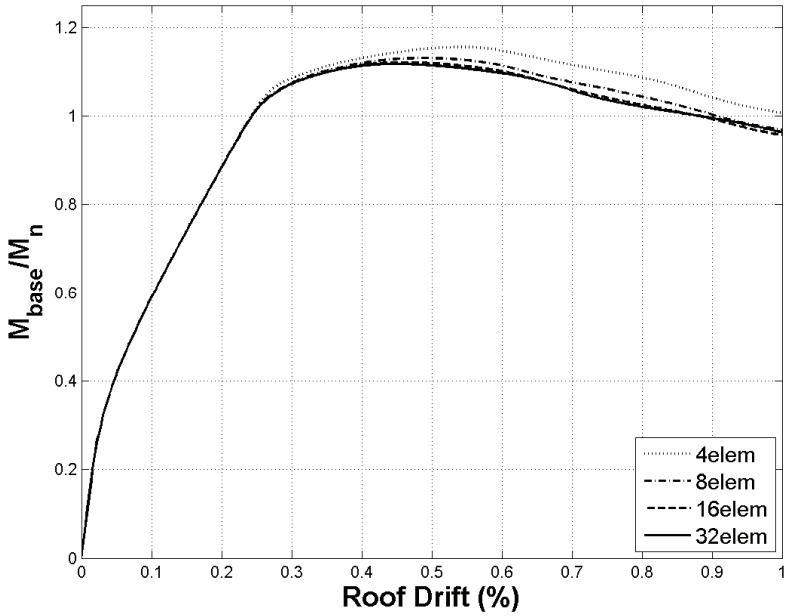

Figure D-6 Regularized softening response based on mesh size.

D.5.1.6 Shear Model

Experimental data (Lowes et al., 2011; Massone and Wallace, 2004) show that shear deformations can exceed those predicted using elastic models in regions of walls when significant inelastic flexural demands occur. In low- to mid-rise walls, the height over which inelastic flexural demands occur may be a significant portion of the total wall height. In this case, a reduced shear stiffness value can be justified to account for the additional shear deformations that would be underpredicted if elastic shear stiffness, $0.4A_cE_c$, was assumed. However, for tall walls, the height over which significant inelastic flexural action occurs is a much smaller portion of the total height. In this case, the use of a reduced shear stiffness value in the region where significant inelastic flexural response is observed and elastic shear stiffness in the remainder of the wall is considered appropriate. For wall buildings designed herein, it is assumed that the inelastic flexural zone is small enough relative to the total building height to justify a single elastic shear stiffness value over the entire wall height.

D.5.1.7 Model Validation

The modeling approach presented above was validated through comparison of measured and simulated global load-displacement response for a series of experimental test data available in the literature. The modeling approach was found to simulate wall strength to within 5% and stiffness to yield within 15%. Results of the validation study also show that the global results and local demand parameters are mesh independent and converge to unique values.

Drift capacity simulated using this approach exceeds experimentally determined drift capacity. This is attributed to the simplicity of the model, which does not simulate the impact of bond-slip and flexure-shear interaction. To enable accurate simulation of loss of lateral load-carrying capacity, use of a compressive strain limit is recommended. Using this approach, loss of lateral load-carrying capacity is defined to occur when concrete compressive strain exceeds a defined limit.

D.5.2 Non-Simulated Collapse Criteria for Special Reinforced Concrete Core-Wall Buildings

To enable accurate assessment of collapse risk, non-simulated collapse criteria were employed. Use of these criteria entailed post-processing of nonlinear analysis results to determine if any of the collapse criteria had been met. If any one of these criteria was met, the building was deemed to have collapsed. These non-simulated collapse criteria are described in the following subsections.

D.5.2.1 Flexural Compression Failure

The wall modeling approach described above overpredicts the measured drift capacity of concrete walls. Many walls have been observed to exhibit loss of lateral

load-carrying capacity due to flexural compression failure (Birely, 2012). To enable accurate simulation of collapse due to loss of lateral load carrying capacity from flexural compression failure, a concrete compressive strain limit model was developed. Using an experimental data set comprising 20 concrete walls observed to lose lateral load carrying capacity due to flexural compression failure (i.e., crushing of the toe of the wall) and the modeling approach described above, the average simulated concrete compression strain at 20% loss of lateral loading carrying capacity (deemed to be the onset of loss of lateral load carrying capacity) was determined to be negative 0.01 in/in.

D.5.2.2 Story Drift Limit

Most experimental tests of walls have not investigated wall response beyond the point of loss of lateral load carrying capacity. However, building collapse may be more closely associated with loss of axial load-carrying capacity than with loss of lateral load carrying capacity. Based on engineering judgment and other factors detailed by NIST (2010), a story drift limit of 5% is taken as a non-simulated limit on loss of axial load carrying capacity.

D.5.2.3 Shear-Flexure Interaction

Experimental data show that increasing shear demand-capacity ratio reduces drift capacity for planar walls responding in flexure. A similar model was used in NIST (2010) to assess collapse of walls as part of the FEMA P-695 evaluation effort. The drift capacity plotted in Figure D-7 is defined as the drift at the effective height of the laboratory test specimen at a 20% loss of lateral load carrying capacity. This relationship was used also as a non-simulated collapse criterion. The average effective height of the wall test specimens from which the data in Figure D-5 were collected was $2l_w$, where l_w is the in-plane length of the wall. Thus, in implementing this non-simulated collapse criterion, the drift at a height equal to twice the wall length (50 ft and 64 ft) determined from nonlinear analysis was used. The base shear demand determined from nonlinear analysis was also used.

D.5.3 Quality Rating of Analytical Models

The modeling approach employed in this investigation has been validated using an extensive experimental data set. However, the simplicity of the model requires the use of multiple non-simulated collapse models which are based on engineering judgment and limited experimental data. In light of these limitations, a quality rating of B (Good) was assigned to the analytical models used in this study.

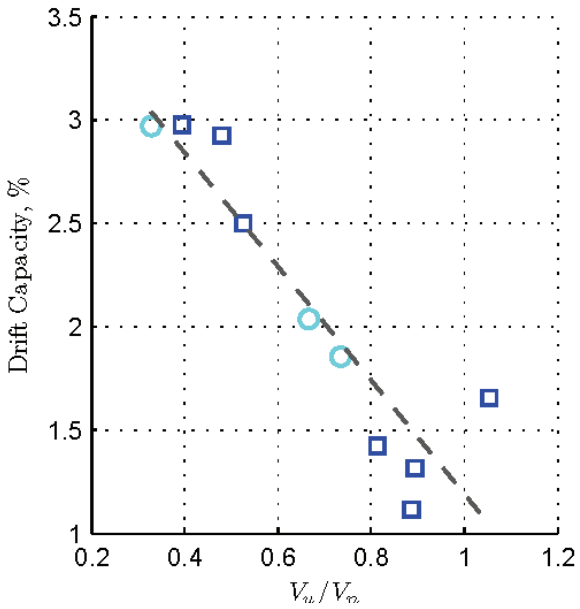

Figure D-7 Drift capacity for walls compliant with ACI 318-08 with axial load responding in flexure (Birely, 2012). Dark blue squares indicate walls for which loss of lateral strength is due to compressive failure (concrete crushing and buckling of longitudinal reinforcement); light blue circles indicate walls for which loss of lateral strength is due to buckling and subsequent tensile fracture of longitudinal reinforcement.

D.6 Collapse Risk Assessment Using FEMA P-695 Methodology

D.6.1 Nonlinear Pushover Analysis

Assessment of collapse risk using the FEMA P-695 Methodology requires results of nonlinear static (i.e., pushover) analyses. These results are used to assess system overstrength and ductility. Overstrength and system ductility factors for all wall designs are presented in Table D-5.

Pushover analyses were conducted in accordance with the FEMA P-695 Methodology. This requires application of a lateral load distribution that is consistent with the fundamental mode shape of the structural model. As Table D-5 shows, this approach leads to calculation of overstrength factors that are less than one for systems that are designed using seismic load distributions that are not first-mode dominated. Higher modes dominate the seismic load distribution for walls designed using RSA, and the effective height for the RSA load distribution is much less than that associated with the first mode. Thus, when a first mode load pattern is applied to the building model in a pushover analysis, the nominal flexural strength of the wall is reached at the base of the wall at a base shear that is significantly lower than the design base shear. Thus, the overstrength factor, which is defined to be based on base shear according the FEMA P-695 Methodology, is less than one. If the overstrength factor is based on base moment instead, values in excess of 1.0 are

computed. The same issues affect the overstrength factors for the ELF-based walls (Table D-5) but to less of an extent.

Given the issues with the overstrength factors determined from the pushover analyses, system ductility (Table D-5) was calculated using the base shear versus roof drift history determined from the pushover analysis.

Table D-5 Pushover Analysis Results

	Design Configuration		Pushover Results	
ID	No. of Stories	Seismic SDC	*Static Ω*	μT
MRSA1	16	D_{max}	0.48	12
MRSA2	20	D_{max}	0.42	10
MRSA3	24	D_{max}	0.36	8
MRSA4	30	D_{max}	0.30	7
ELF1	16	D_{max}	1.05	21
ELF2	20	D_{max}	0.97	16
ELF3	24	D_{max}	0.95	14
ELF4	30	D_{max}	0.89	11

D.6.2 Incremental Dynamic Analysis Results and Calculation of Collapse Margin Ratio

According to the FEMA P-695 Methodology, collapse risk is assessed using the results of incremental dynamic analyses (IDA) with the specified far-field ground motion data set. Data from the IDA are post-processed using the non-simulated collapse criteria discussed above to determine the spectral acceleration at the design period of the structure, $T = C_u T_a$, at which collapse is predicted to occur. These data are then used to compute the median spectral acceleration at the design period of the structure at collapse, S_{CT}. The collapse margin ratio, *CMR*, is calculated as the ratio of the median collapse intensity, S_{CT}, to the spectral intensity for the MCE, S_{MT}.

Table D-6 and Table D-7 summarize the IDA results without and with consideration of the shear-based non-simulated collapse criterion because it is not known if results determined with the criterion are respresentative of long-period buildings or long-period walled buildings. Results include the median spectral acceleration at collapse, S_{CT}, and the *CMR*. The collapse criteria columns indicate the percentage of ground motion records for which "collapse" was determined by that particular criterion. The criteria are: (1) simulated collapse (Sim.); (2) concrete crushing as determined by a concrete compressive strain in excess of negative 0.01 in/in (Concrete Strain); (3) story drift in excess of 5% (Story Drift); and (4) the shear-based drift capacity model (Shear-Based). The latter two are non-simulated collapse criteria. The average base shear demand-capacity ratio at the collapse intensity level is also indicated.

Table D-6 IDA Results without Shear-Based Collapse Criterion

ID	No. of Stories	$S_{MT}(T)$ (g)	$S_{CT}(T)$ (g)	*CMR*	Collapse Criteria			Mean Base Shear D/C Ratio at Collapse
					Sim.	*Conc. Strain*	*Story Drift*	
MRSA1	16	0.63	1.12	1.81	0%	35%	65%	1.40
MRSA2	20	0.53	0.84	1.58	0%	0%	100%	1.56
MRSA3	24	0.46	0.74	1.61	0%	0%	100%	1.69
MRSA4	30	0.39	0.62	1.59	0%	0%	100%	1.98
ELF1	16	0.63	1.25	2.02	0%	47%	53%	1.21
ELF2	20	0.53	1.05	1.98	0%	7%	93%	1.47
ELF3	24	0.46	0.87	1.89	0%	0%	100%	1.63
ELF4	30	0.39	0.86	2.21	4%	0%	96%	2.17

Table D-7 IDA Results with Shear-Based Collapse Criterion

ID	No. of Stories	$S_{MT}(T)$ (g)	$S_{CT}(T)$ (g)	*CMR*	Collapse Criteria				Mean Base Shear D/C Ratio at Collapse
					Sim.	*Conc. Strain*	*Story Drift*	*Shear Based*	
MRSA1	16	0.63	0.62	1.00	0%	0%	0%	100%	1.03
MRSA2	20	0.53	0.32	0.60	0%	0%	0%	100%	1.00
MRSA3	24	0.46	0.28	0.61	0%	0%	0%	100%	1.12
MRSA4	30	0.39	0.23	0.59	0%	0%	0%	100%	1.23
ELF1	16	0.63	0.62	1.00	0%	0%	0%	100%	0.98
ELF2	20	0.53	0.42	0.79	0%	0%	0%	100%	0.98
ELF3	24	0.46	0.37	0.80	0%	0%	0%	100%	1.10
ELF4	30	0.39	0.23	0.59	0%	0%	0%	100%	1.31

The data in Table D-6 summarize results without consideration of the shear-based collapse criterion. These data show that for the 16-story buildings, there were no simulated collapses, 35% of the collapses were due to concrete crushing, and 65% due to exceeding 5% story drift. Taller buildings all collapsed under the non-simulated criterion of exceeding the 5% story drift. *CMR* values range from 1.6 to 2.2, suggesting acceptable collapse risk. However, the data in Table D-6 also show that if the shear-based collapse criterion is not considered, the average shear demand-capacity ratio at the base of the wall at collapse ranges from 1.40 to 2.17; such high shear demands cannot be sustained reliably and typically result in non-ductile failure.

The data in Table D-7 show that if the shear-based collapse criterion is considered, this criterion determines collapse for all ground motion records. *CMR* values range from 0.6 to 1.0 suggesting unacceptably high collapse risk. The data in Table D-7 show also that the shear demand-capacity ratios at the base of the wall at the collapse intensity are approximately 1.0. This suggests that low *CMR* values (and high collapse probabilities) similar to those listed in Table D-7 would be computed if the

shear-based non-simulated collapse criterion was simplified from the linear model by Birely (2012) that links drift capacity with shear demand-capacity ratio to a pure strength-based model in which collapse is defined to occur when the shear demand-capacity ratio exceeds 1.0.

The data in Table D-6 and Table D-7 show that under earthquake loading, concrete wall buildings develop base shear demands that greatly exceed the design demands determined using ASCE/SEI 7-10 linear analysis procedures. These excessive shear demands are due to a drop in the effective height at which the seismic lateral loads act because of the following: (1) the development of a flexural hinge at the base of the wall (which limits the moment at the base of the wall but not the shear demand at the base of the wall or the demands elsewhere up the height of the wall); (2) the concentration of nonlinearity at the base of the wall; and (3) higher-mode response. This amplification of base shear demand in walls has been observed by a number of researchers (Krawinkler, 2006; Panneton et al., 2006; Panagiotou and Restrepo, 2009). Although a few studies suggest that the amplification of base shear demands is not unique to walls (Haselton et al., 2011), it is not known if amplification of base shear occurs in all SFRS. Additionally, the collapse risk posed by high shear demands in walls is considered to be somewhat unique, because walls are a SFRS in which a single element resists seismic shear and moment demand and in which these response modes interact to reduce deformation capacity even in code compliant elements. Moment frames could be considered to be somewhat similar to walls in that seismic demands are transferred to the foundation through columns. However, with columns, seismic demands are resisted through moment, shear, and axial load, and experimental data show that drift capacity of code-compliant columns is less sensitive to shear demand. Given the unique seismic force-resisting characteristics of walls and the potential that the collapse risk determined for walls using the shear-based collapse criterion is not representative of long-period buildings in general, collapse risk was computed without and with consideration of the shear-based criterion.

D.6.3 Performance Evaluation

Performance was evaluated by determining the probability of collapse for each building design. The probability of collapse was determined from the adjusted collapse margin ratio, *ACMR*, and the total system collapse uncertainty, β_{TOT}. The *ACMR* is found by multiplying the *CMR* by the system spectral shape factor, *SSF*, which is a function of the system ductility determined using the results of the static pushover analysis. The total system collapse uncertainty is a function of the quality ratings allocated to the design requirements, test data, and nonlinear model development. Table D-8 lists the collapse probability for each building configuration without consideration of the shear-based non-simulated collapse criterion and Table D-9 lists the collapse probability for each building including the shear-based non-

simulated collapse criterion. The collapse probabilities listed in the tables are consistent with *CMR* values listed in Table D-6 and Table D-7.

Table D-8 Performance Evaluation without Shear-Based Collapse Criterion

	Design Configuration		Computer Collapse Margin Parameters				
ID	No. of Stories	SDC	*CMR*	μ_T	*SSF*	*ACMR*	Collapse Prob.
MRSA1	16	D_{max}	1.81	12	1.6	2.87	2%
MRSA2	20	D_{max}	1.58	10	1.6	2.55	4%
MRSA3	24	D_{max}	1.61	8	1.6	2.59	4%
MRSA4	30	D_{max}	1.59	7	1.6	2.48	4%
ELF1	16	D_{max}	2.02	21	1.6	3.21	1%
ELF2	20	D_{max}	1.98	16	1.6	3.19	1%
ELF3	24	D_{max}	1.89	14	1.6	3.05	2%
ELF4	30	D_{max}	2.21	11	1.6	3.55	1%

Table D-9 Performance Evaluation with Shear-Based Collapse Criterion

	Design Configuration		Computer Collapse Margin Parameters				
ID	No. of Stories	SDC	*CMR*	μ_T	*SSF*	*ACMR*	Collapse Prob.
MRSA1	16	D_{max}	1.00	12	1.6	1.59	19%
MRSA2	20	D_{max}	0.60	10	1.6	0.97	52%
MRSA3	24	D_{max}	0.61	8	1.6	0.98	52%
MRSA4	30	D_{max}	0.59	7	1.6	0.92	56%
ELF1	16	D_{max}	1.00	21	1.6	1.59	19%
ELF2	20	D_{max}	0.79	16	1.6	1.28	32%
ELF3	24	D_{max}	0.80	14	1.6	1.30	31%
ELF4	30	D_{max}	0.59	11	1.6	0.95	54%

D.6.4 Calculation of the Base Shear Coefficient Required to Achieve Uniform Collapse Risk

Using the data in Table D-1, Table D-2, Table D-8, and Table D-9 and Equation 2-1 (repeated below), the base shear coefficient required to achieve a 10% uniform collapse probability under the MCE, $Cs_{10\%}$, may be estimated as follows:

$$R_{UR10\%} = \left(\frac{S_{MT}/1.5}{V/W}\right)\left(\frac{ACMR}{ACMR_{10\%}}\right)$$

$$Cs_{10\%} = \frac{S_{MT}}{1.5R_{UR_{10\%}}} \qquad \text{(D-1)}$$

By combining the two equations above, the definition for $Cs_{10\%}$ is identical to Equation 3-6 which was used for buildings designed for the previous studies.

This approach was used to add the collapse risk data generated for tall walls to the data from previous studies (Figure D-1 and Figure D-2). Figure D-8 through Figure D-11 show the complete data set; long-period wall data are identified as "Special RCSW Long Period" and shown in the figures using blue x's. Note that Figure D-8 and Figure D-9 show $C_{s10\%}$ plotted versus design period and fundamental period from RSA, respectively, for the case of collapse probability determined without use of the shear-based collapse criterion. Figure D-10 and Figure D-11 show similar data for the case of collapse probability determined with use of the shear-based collapse criterion.

As discussed in Chapter 3, the approach used to estimate the R and C_s factors required to achieve 10% probability of collapse under the MCE assumes a linear relationship between design base shear and collapse probability; this approximation has been shown to be good when $ACMR$ is approximately equal to $ACMR_{10\%}$. For walled building collapse determined without use of the shear-based collapse criterion, $ACMR$ is not significantly different from $ACMR_{10\%}$, thus the approximation of $C_{s10\%}$ is considered to be good. For walled building collapse determined with use of the shear-based collapse criterion, $ACMR$ is significantly different from $ACMR_{10\%}$,and the approximation of $C_{s10\%}$ is considered to be poor.

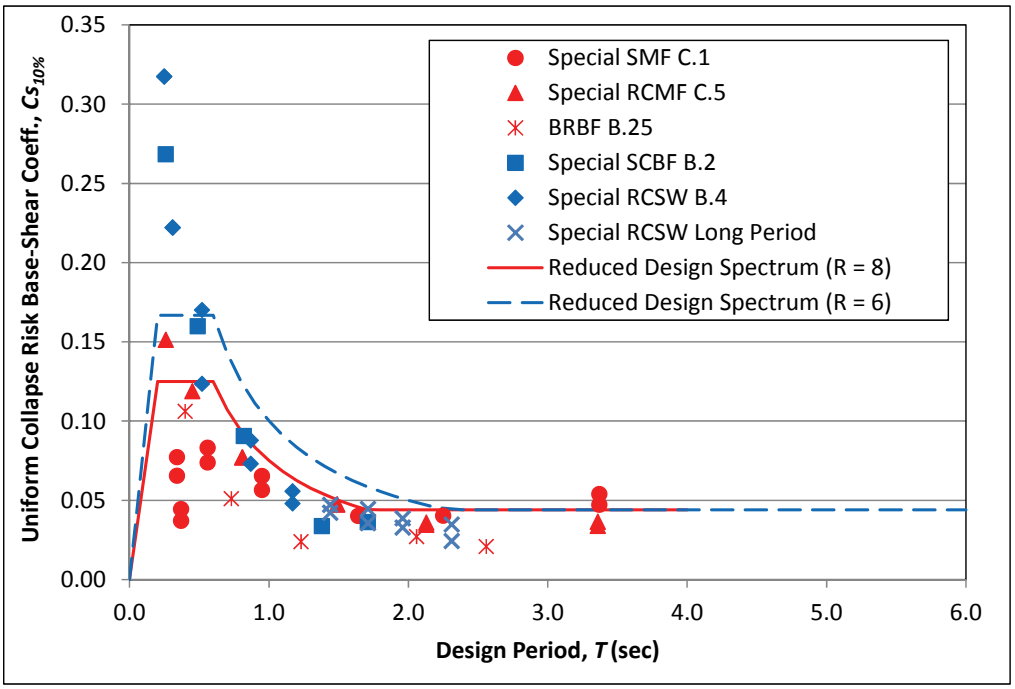

Figure D-8 Base shear coefficient required to achieve uniform collapse risk of 10%, $C_{s10\%}$, versus design period, T, without shear-based collapse criterion used for determination of wall collapse.

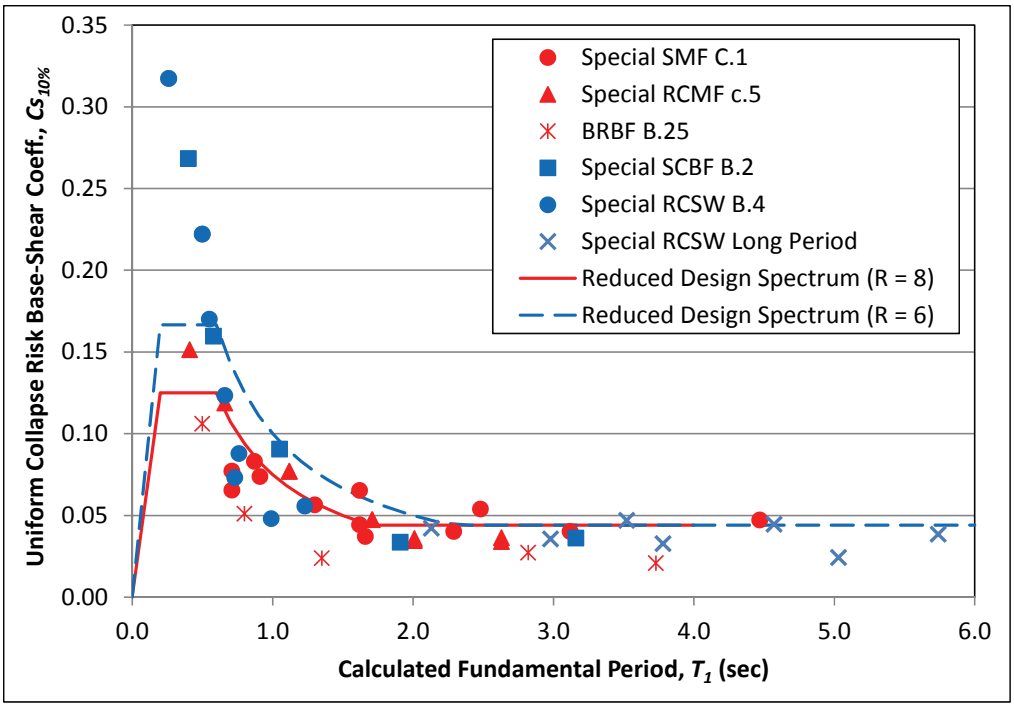

Figure D-9 Base shear coefficient required to achieve uniform collapse risk of 10%, $C_{s10\%}$, versus calculated fundamental period from RSA, T_1, without shear-based collapse criterion used for determination of wall collapse.

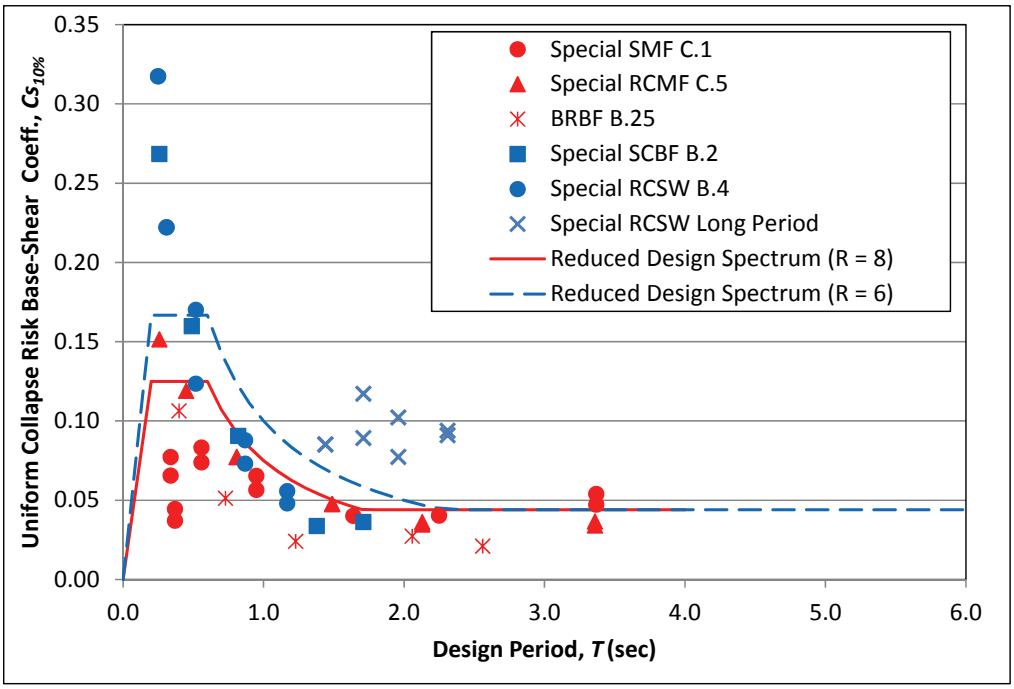

Figure D-10 Base shear coefficient required to achieve uniform collapse risk of 10%, $C_{s10\%}$, versus design period, T, with shear-based collapse criterion used for determination of wall collapse.

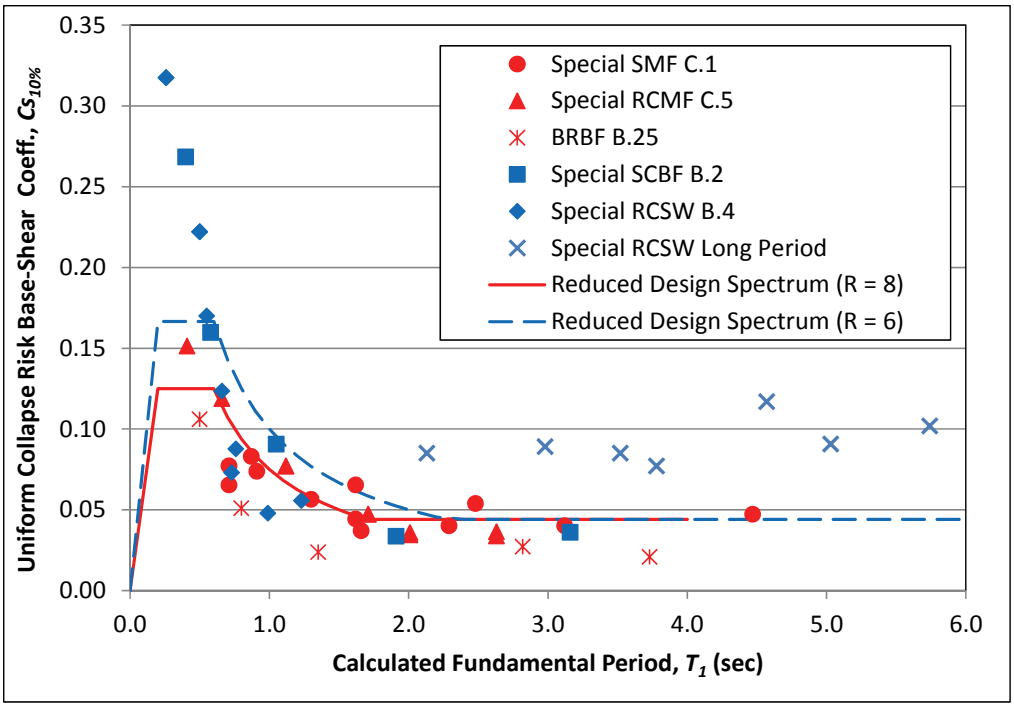

Figure D-11 Base shear coefficient required to achieve uniform collapse risk of 10%, $C_{s10\%}$, versus calculated fundamental period from RSA, T_1, with shear-based collapse criterion used for determination of wall collapse.

D.6.5 Impact of Ground Motion Scaling and Higher Mode Effects on Collapse Risk

For long-period concrete wall buildings, earthquake response was found to be dominated by contributions from modes other than the first (primarily the second and third). However, the FEMA P-695 Methodology assumes building response is dominated by the first mode, with ground motions scaled such that the median value of the spectral acceleration for the suite of motions used for assessment is anchored to the MCE spectrum at a period value of $C_u T_a$. To investigate the impact on the computed collapse risk of ground motion scaling and higher-mode effects, collapse risk was estimated using spectral acceleration values for the second mode. Collapse risks computed using second-mode spectral acceleration values were found to be significantly less than those computed using first-mode spectral accelerations.

The FEMA P-695 Methodology assumes that building response is dominated by the contribution of the first mode. To assess collapse risk, the median spectral acceleration of the suite of ground motions used to assess collapse risk is anchored to the MCE at the design period, $C_u T_a$. Specifically, *CMR* is defined as the ratio of the median spectral acceleration at the design period, $C_u T_a$ that results in collapse for half of the ground motions to the spectral ordinate of the MCE spectrum at the design period. The *CMR* computed with spectral values for design period could be very different from the *CMR* using spectral values for higher modes. Additionally, to

determine collapse risk, the *CMR* is adjusted to account for spectral shape. Again building response is assumed to be first-mode dominated. The *ACMR* could be different if response is determined primarily by higher modes.

To assess the impact of ground motion scaling and higher mode contributions, collapse risk was determined using an alternative definition of the *CMR*. The alternative *CMR* is taken as the ratio of the median of the spectral acceleration at the second period, T_2, to the spectral acceleration of the MCE at T_2. In determining this alternate *CMR*, no new analyses were conducted. Instead, the *CMR* was computed in the following manner, where all spectral accelerations are computed at T_2: (1) for each (normalized) ground motion, the spectral acceleration corresponding to collapse was determined; (2) the median spectral acceleration at collapse was determined for the suite of motions; and (3) *CMR* was defined as the ratio of this median spectral acceleration to the MCE spectral acceleration. For any individual motion, there is uncertainty in determining the spectral acceleration corresponding to collapse as analyses were conducted for incrementally increasing spectral acceleration values; and while the increment was constant with respect to the design period, it was not constant with respect to T_2.

Table D-10 provides collapse probabilities predicted using the standard FEMA P-695 Methodology (first mode scaling) and using the FEMA P-695 Methodology with *CMR* computed on the basis of second-mode scaling. Results are provided for both the RSA and ELF wall designs with collapse determined using the shear-based collapse criterion. These results show that for long-period concrete wall building, ground motion scaling on the basis of T_2 results in reduced collapse risk. These results suggest that additional research should be done to assess the impact of ground motion scaling on collapse risk for all structures and, in particular, for long-period systems in which higher modes determine response.

Table D-10 Performance Evaluation with the Shear-Based Collapse Criterion

				First Mode Scaling			Second Mode Scaling		
ID	No. of Stories	μ_T	*SSF*	*CMR*	*ACMR*	*Collapse Probability*	*CMR*	*ACMR*	Collapse Probability
MRSA1	16	12	1.6	1.00	1.59	19%	1.08	1.72	15%
MRSA2	20	10	1.6	0.60	0.97	52%	0.92	1.47	23%
MRSA3	24	8	1.6	0.61	0.98	52%	0.71	1.13	35%
MRSA4	30	7	1.6	0.59	0.92	56%	0.72	1.15	35%
ELF1	16	21	1.6	1.00	1.59	19%	1.48	2.37	5%
ELF2	20	16	1.6	0.79	1.28	32%	1.26	2.01	9%
ELF3	24	14	1.6	0.80	1.30	31%	0.89	1.42	25%
ELF4	30	11	1.6	0.59	0.95	54%	0.83	1.33	28%

D.7 Observations and Findings

D.7.1 General Findings on Reinforced Concrete Wall Buildings

The study of the collapse risk of long-period reinforced concrete wall buildings found that significant revisions in design codes and the design process are required for these systems. Following are key findings and observations addressing seismic design and performance of long-period reinforced concrete wall buildings.

- The results of nonlinear analyses indicate that under design level earthquake loading, base shear demands will greatly exceed those computed using either the ELF or RSA method and the design spectrum. This amplification of the base shear demand is attributed to development of a flexural "hinge" at the base of the wall and higher-mode response; both of these mechanisms result in the base shear acting at a lower effective height. Although the base moment is limited by flexural yielding of the wall, reduction of the effective height at which the base shear acts results in an increased base shear demand.
- The results of nonlinear analyses indicate that walls in tall buildings typically develop a second flexural hinge above the base of the wall. If the vertical moment demand distribution determined by either the ELF or RSA methods is used to reduce the wall flexural capacity up the height of the wall, deformation demands at the location of this section hinge may be excessive and result in unacceptable performance.
- The data in Figure D-7 through Figure D-10 and Table D-7 and Table D-8 indicate that if the impact of shear stress demand on drift capacity is considered, long-period walls designed using the results of linear analysis to achieve low shear stress demand at the base in order to develop the maximum allowable (per ACI 318-08) cross-sectional shear strength at the base in order to minimize flexural yielding and shear demand-capacity above the base have unacceptably high collapse probabilities under the MCE.

On the basis of these general findings, the following needs are determined: (1) additional research to assess amplification of shear demand in walls with shorter heights and in coupled walls; (2) additional research to determine strength and detailing requirements to ensure acceptable performance of flexural hinges located above the base of the wall; and (3) design recommendations for reduced shear stress demand in walls.

D.7.2 General Findings on FEMA P-695 Methodology

This investigation of the collapse risk of long-period concrete wall buildings resulted also in the following observation on the FEMA P-695 Methodology: Scaling of earthquake ground motions based on the spectral acceleration at the design period of the structure resulted in essentially arbitrary scaling of the motions, with respect to

the design spectrum, at shorter periods. Higher modes contributing significantly to the base shear demand (more than 60% for long-period walls) likely introduces significant uncertainty and bias in the computed collapse risk.

D.7.3 Specific Findings

If collapse probabilities for long-period concrete wall buildings computed without consideration of reduced drift capacity because of shear demand are considered to be representative of long-period buildings in general, then these data in combination with collapse risk data from previous studies of concrete and steel frames suggest that acceptable collapse risk can be achieved for long-period systems of any height using a minimum base shear requirement.

As discussed in Section D.6.2, the shear-based collapse criterion for walls, in which the drift capacity of the wall is reduced as the shear demand-capacity ratio increases, is considered to be system specific. It is not known if issues similar to the amplification of shear demands and interaction of flexure-shear mechanisms for walls exist for other SFRS in the long-period range and could result in increased collapse probability for these systems. As such, in considering R factors and seismic demands for long-period systems in general, it is deemed appropriate to employ wall collapse probability data determined without consideration of the shear-based collapse criterion. These data, combined with similar data for a few concrete and steel frames, suggest that the current ASCE/SEI 7-10 requirements for determination of seismic demands, including the minimum base shear requirement but excluding limits on building height, result in acceptable collapse risks of less than 10% for long-period buildings.

Although the above data suggest that the desired collapse risk can be achieved using a minimum base shear demand in the long-period range and ignoring building height limits, the data are quite limited. The data in Table D-7 and Figure D-7 and Figure D-8 are for structures designed for the maximum spectral acceleration intensity associated with Seismic Design Category D; other design categories have not been considered. Additionally, the data in Figure D-7 and Figure D-8 include relatively few data points for concrete and steel frame buildings.

D.8 Recommendations

The data presented in Table D-7, Figure D-7, and Figure D-8 suggest that acceptable collapse risk can be achieved for long-period systems using a minimum base shear requirement. However, given the relatively small number of data points available for long-period systems, a minimum base shear equation cannot be developed at this time. It is expected that a minimum base shear equation would depend on either the spectral acceleration intensity in the short period range, as defined by S_{MS}, or in the long-period range, as defined by S_{M1}, and, possibly, the strength reduction factor, R_M.

Thus, the equation defining the minimum base shear coefficient, $C_{sM} = V/W$, could take one of the following forms:

$$\begin{aligned} C_{sM} &\geq \alpha S_{MS} I_e \\ C_{sM} &\geq \alpha S_{M1} I_e \\ C_{sM} &\geq \alpha S_{M1} / (R_M / I_e) \\ C_{sM} &\geq \alpha S_{MS} / (R_M / I_e) \end{aligned} \tag{D-2}$$

D.9 Future Studies

The results of this and previous studies suggest that an acceptable collapse risk can be achieved for long-period systems if seismic demands are determined using a minimum base shear requirement. However, a more extensive data set is required to verify this. Thus, studies such as the one described above for concrete walls must be conducted for several additional commonly employed SFRS (concrete and steel moment frames as well as steel braced frames) and for SFRS designed for construction in SDC B and SDC C.

In designing structures as part of the additional study, efforts should be made to introduce a similar level of conservatism, and clearly establish the design methodology employed. The results of this study suggest that to achieve acceptable collapse risk, long-period concrete wall buildings must be designed to achieve extremely low shear stress demands under design-level loading. It is expected that similar requirements may exist for other SFRS; for example, design of concrete and steel moment frames to achieve acceptable collapse risk may require column-to-beam strength ratios that exceed current code requirements.

Appendix E

Overview of Toolkit for Automated Implementation of FEMA P-695 Methodology

E.1 Introduction

The Methodology described in FEMA P-695 report, *Quantification of Building Seismic Performance Factors* (FEMA, 2009), is straightforward, but is computationally extensive. For example, the evaluation of a single performance group consisting of three archetype models may involve thousands of nonlinear dynamic response-history analyses, and a full implementation of the Methodology may require the evaluation of several such performance groups. Associated with the analyses are several gigabytes of computational results. When all of this information is processed, the Methodology produces only two values (the adjusted collapse margin ratio (*ACMR*) and overstrength) for each model in the performance group, as well as an average of these values for the performance group.

Individuals wishing to perform a FEMA P-695 evaluation on a structural system must be experts in nonlinear dynamic analysis of structures and highly proficient in data processing and management. Such analysis requires the development of custom procedures in Matlab (or similar programs) and analysis models for OpenSees (or similar programs), the execution of analyses in some methodical fashion, and the collection and post-processing of data. The development and testing of such procedures alone can consume hundreds of hours before even one performance group is evaluated.

In recognition of this complexity and the volume of analysis required by the problem-focused undertaken in this project, a "Toolkit" was created to minimize the need for analysts to develop custom procedures and thereby to produce FEMA P-695 system evaluations in a fraction of the time that would otherwise be required. Although the Toolkit saves time, it does not reduce the complexity of the analysis, nor does it diminish the need for the individual performing the system evaluation to be an expert in structural analysis and data management.

All files necessary to run the Toolkit, except OpenSees and TCL files are provided on the "P-695 Toolkit" pages of a website maintained at Virginia Tech. Persons wishing to obtain access to this site must provide a written request to the developer

(fcharney@vt.edu). After approval, the user will be provided with the appropriate login information and passwords.

The Toolkit has been developed entirely in Matlab and is based on the OpenSees (http://opensees.berkeley.edu/) structural analysis program. The user may execute the program within the Matlab environment, or use the version of the program, which runs outside of Matlab. Users of the latter version of the program need not be proficient in Matlab, and need not have the full Matlab program installed on their system. However, all users of the Toolkit must be experts in OpenSees. Because OpenSees operates within the TCL scripting environment, users of the Toolkit must be familiar with TCL. However, use of the Toolkit will greatly reduce the level of proficiency required in developing TCL script.

The Toolkit is consists of six main modules (or tools) each of which is operated through the use of a Graphical User Interface (GUI). The GUI for the ground motion (GM) tool, shown in Figure E-1, is typical of the interfaces used for each of the modules.

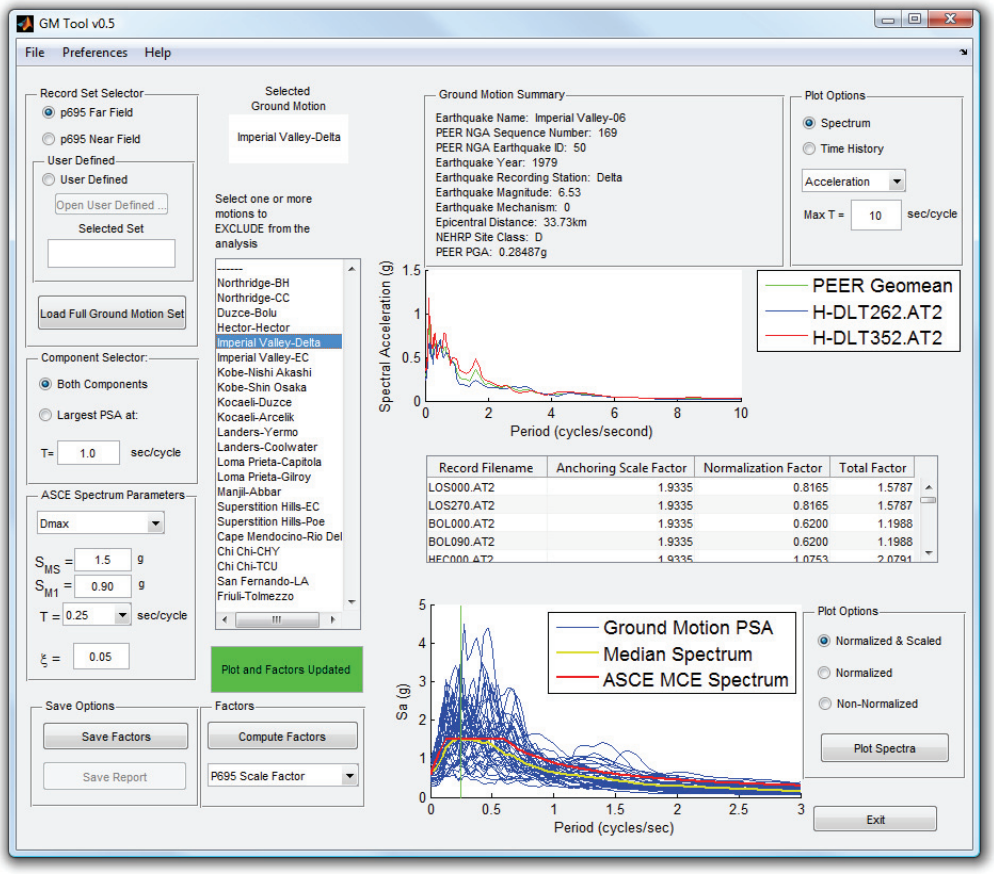

Figure E-1 Graphical user interface for the GM tool.

The basic flow control between modules is illustrated in Figure E-2.

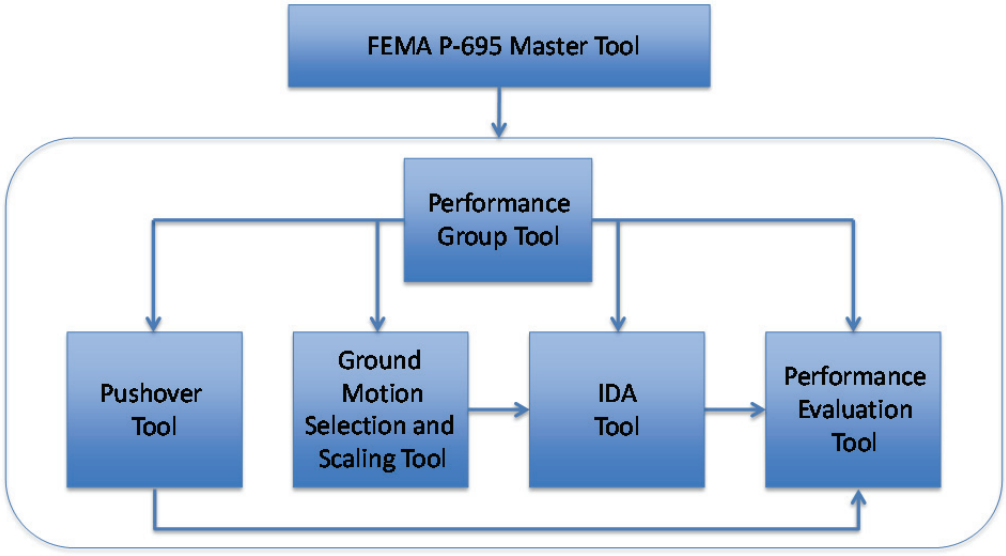

Figure E-2 Basic layout of Toolkit.

The purpose of each tool is briefly described below. More detailed explanations of each of the tools are provided later in this document.

E.1.1 FEMA P-695 Master Tool

This tool is used to access the other five tools and provides information on how far the analysis has progressed. However, use of the Master tool is not required because each tool may be executed on a stand-alone basis. Use of the Master tool is recommended, however, as it minimizes the likelihood that the analyst will attempt to operate a given tool before all of the data are ready for that tool.

E.1.2 Performance Group Tool

This tool provides all of the information that is required to create a performance group and to enter or access information for each index archetype model that is associated with the performance group. No computations are performed within this tool.

E.1.3 Pushover Tool

This module performs a modal analysis for each index archetype model; this analysis provides the period of vibration and mode shape for the first mode of the model. The module also performs a gravity load analysis and pushover analysis for each index archetype model; these archetypes provide the model's strength and period-based ductility. The TCL script required for performing the modal and pushover analysis is automatically created from four basic TCL files that are provided by the user for each index archetype model.

E.1.4 Ground Motion Selection and Scaling (GM) Tool

This tool allows the analyst to select the Far-Field or Near-Field ground motion record sets defined in FEMA P-695 and then to normalize and scale the ground motions as will be required by the Incremental Dynamic Analysis tool. Users may also provide custom ground motions sets or define ground motion subsets from any predefined set.

E.1.5 Incremental Dynamic Analysis (IDA) Tool

This tool sets up and performs Incremental Dynamic Analysis (IDA) for each index archetype model subjected to each normalized and scaled ground motion and reports ground motion intensity multipliers at which a simulated collapse or several non-simulated collapses occur. These multipliers are used to compute collapse margin ratios, *CMR*, and other related parameters in the Performance Evaluation tool. The TCL script required for performing the nonlinear dynamic analysis is automatically created from four basic TCL files that are provided by the user for each index archetype model. The user is also responsible for defining information (in a simple text format) for the OpenSees recorders that are used to report collapse data back to the tool but need not develop TCL script for the recorders because the Toolkit develops this automatically.

The IDA analysis may be executed on the user's local computer or may be ported to an external computer on which the parallel version of OpenSees has been installed. The use of the parallel version of OpenSees has been tested on the Ithaca Cluster at Virginia Tech and has been shown to be extremely efficient with reductions in run times of a factor of ten or better.

After the IDA analysis is performed, the Performance Evaluation tool may be run in a post-processing mode to determine the influence of certain parameters to the computed results. Parameters that may be queried include uncertainty assignments for design, testing, and analysis, exclusion or inclusion of various selected non-simulated collapse parameters, and exclusion or inclusion of selected index archetype models.

The IDA module has not (yet) been fully optimized for FEMA P-695 analysis. Each index archetype model is subjected to each ground motion, with the ground motion intensity being systematically incremented by a scale factor. The user has the option to stop the analysis when any given non-simulated collapse occurs or to continue the analysis up to simulated collapse. In the latter case, the program records when each non-simulated collapse measure has been exceeded. This brute force methodology generally results in longer overall execution times but has the advantage of allowing maximum versatility in the post-processing of results. Section E.3 describes in detail

how collapse information is recorded, and also describes how the program handles analyses that fail to converge.

E.1.6 Performance Evaluation Tool

This tool collects and processes all of the information produced by the other tools to produce *ACMR* values for each index archetype model, and then compares these values with the acceptable *ACMR* values related to a target probability of collapse of 20% for individual index archetype models or 10% for the mean *ACMR* for the performance group. Overstrength parameters are also provided for each index archetype model and for the performance group as a whole. A summary of the full FEMA P-695 evaluation is provided in a report that is produced as a Microsoft Excel spreadsheet.

E.2 Information Needed to Perform FEMA P-695 Analysis

Prior to running any module, the user must have on hand a variety of information for the performance group being evaluated and for each index archetype model within the performance group.

The following information is necessary for each performance group:

- Name,
- Performance group description,
- System description,
- Design *R* value,
- Seismic Design Category,
- Uncertainties for design rules, testing information, and modeling uncertainties,
- Gravity load domain,
- Period domain,
- Number of index archetype models in performance group,
- Method of analysis used in system design, and
- Ground motion record set to be used in analysis.

The following information is necessary for each index archetype model:

- Model name,
- Model description,
- Number of stories,

- Number of similar elements in structure (typically only one such element is analyzed),
- Empirical period of vibration, T,
- Period adjustment factor, C_u,
- Seismic weight, W (for entire structure),
- Design base shear (for entire structure),
- R effective (will be less than R design when governed by minimum base shear),
- Table of story nodal tags and story masses for entire structure (to determine the coefficient C_o (Equation 6-8 in FEMA P-695), and to identify the story levels at which the pushover loading is applied),
- Number of non-simulated collapse indicators,
- Non-simulated collapse limits and control parameters,
- Basic OpenSees TCL files (four for each index archetype model), and
- OpenSees recorder definition files (one for each index archetype model).

All of the above information, with the exception of the basic TCL files, the recorder definition files, and the non-simulated collapse information, are typically entered directly into the Performance Group tool using the GUI. The data that are entered into the GUI may be saved to a text file for future use and may then be recalled, edited, and saved for future use. Additionally, the data may be entered into a text file directly, and then imported into the GUI.

E.2.1 Interaction with OpenSees

The Toolkit has been written to minimize the level of proficiency needed for developing TCL script for OpenSees. Thus, only four basic TCL files need to be developed by the user. These files must be entered by hand and are as follows:

- SetUpModel.tcl
- GravityLoad.tcl
- ModelGeometry.tcl
- SectionAndMaterials.tcl

The files contain structural and gravity loading information only. OpenSees TCL script that is necessary for running the gravity, modal, pushover, and IDA analyses is automatically written to separate files by the Toolkit. See Section E.6 provides a detailed description of each of the OpenSees files used by the Toolkit.

OpenSees recorder descriptions are provided by the user in text files, and this information is automatically translated by the Toolkit into TCL script. However, not all possible recorders have been included in the Toolkit. Thus, the TCL script created by the Toolkit must be altered to incorporate new recorders. Section E.7 provides detailed information on setting up OpenSees recorders.

After all of the appropriate TCL files have been developed by the Toolkit, OpenSees is automatically executed within the Toolkit. Thus, the user need not execute OpenSees directly.

E.2.2 Simulated and Non-Simulated Collapses and Convergence

The Toolkit has considerable flexibility in how various collapse measures may be included in a system evaluation. There are two kinds of "collapse" that can be monitored by the program:

- **Simulated collapse.** This kind of collapse occurs when the lateral displacement at the roof level of the structure changes dramatically over a small change in ground motion intensity. This is generally associated with a "flattening" of the Incremental Dynamic Analysis (IDA) roof displacement curve for the model, as shown in Figure E-3 for Ground Motions (GM) 1, 2, and 3. A simulated collapse did not occur for GM 4 in Figure E-3. Note that the simulated collapse mode is automatically monitored by the Toolkit, and does not require the definition of an OpenSees recorder.
- **Non-simulated collapse.** This kind of collapse occurs when some damage measure is exceeded prior to the occurrence of a simulated collapse. Damage measures associated with non-simulated collapses may include strain, stress, deformation, acceleration, force, or loss of strength (as associated with fatigue failures of braces, for example). The occurrence of several non-simulated collapses (prior to a simulated collapse) is shown in Figure E-3. Note that Nonsimulated Collapse 1 did not occur prior to Simulated Collapse for GM 1.

An OpenSees recorder must be defined for each non-simulated collapse parameter, and the numerical value associated with collapse must be specified. Additionally, the user must assign a "Stop Analysis" flag for each non-simulated collapse parameter. A value of "1" (the default) will terminate the analysis and record the IDA information when the collapse parameter is exceeded and a value of "0" will allow the analysis to proceed up to the occurrence of a simulated collapse.

As an example, assume an analysis has three non-simulated collapse measures as follows:

1. Maximum compressive extreme fiber strain in concrete,
2. Maximum strain in steel reinforcement in boundary element, and

3. Maximum base shear.

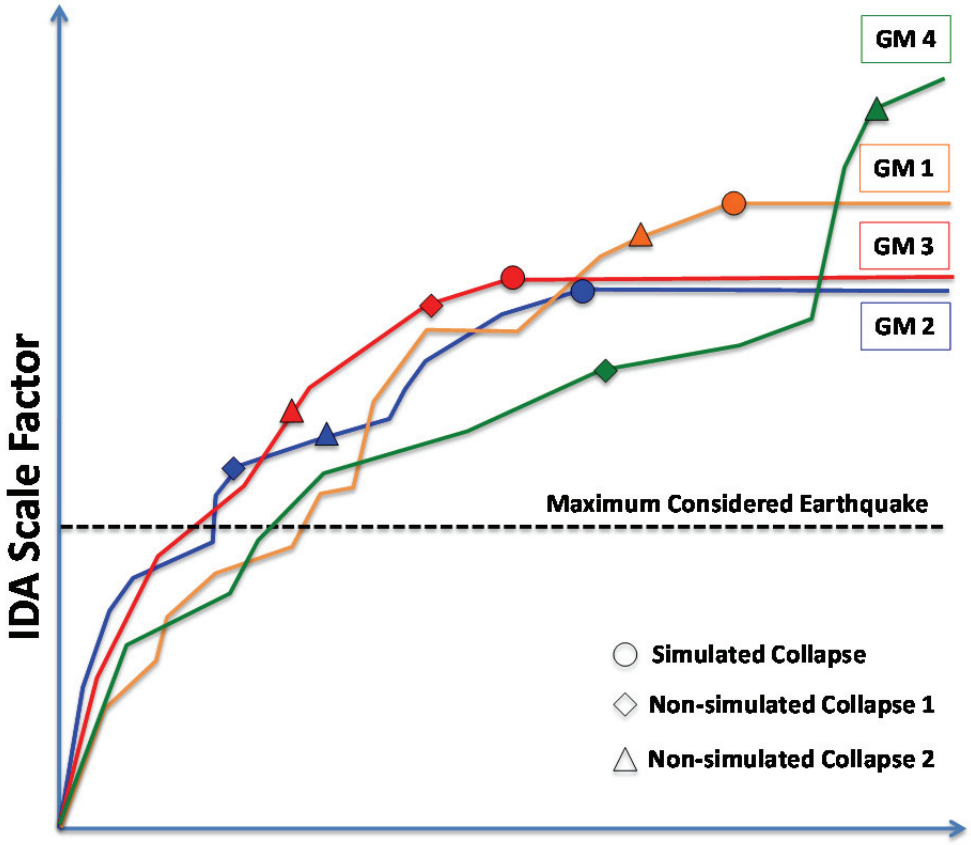

Figure E-3 Demonstration of simulated and non-simulated collapses.

Table E-1 below shows the (hypothetical) information recorded by the Toolkit for the first ten ground motions and the last ground motion in the analysis of a given index archetype model, Model A. The full table would be composed of one row for each ground motion in the complete analysis, 44 rows for the full FEMA P-695 Far Field record set. The first column of the table is the ground motion designation. The second column indicates the ground motion scale factor at which a simulated collapse occurred. Columns three, four, and five provide the ground motion scale factor at which each of the non-simulated collapse is reached. A blank cell in columns three through five indicates that a collapse did not occur. Column six contains the minimum scale factor among all collapses, and column seven is a numeric indicator of what type of collapse the minimum scale factor was associated with.

A table similar to Table E-1 would be provided for each index archetype model in the performance group. The *CMR* for each index archetype model would be taken as the median value in column six of each table. Alternate assessments of collapse could be obtained by eliminating any of the collapse measures from the analysis.

Table E-1 Example Collapse Information for Index Archetype Model

Ground Motion	Simulated Collapse	Non-simulated Collapse			Minimum Collapse	Collapse Type
		1	*2*	*3*		
1A	5.32	3.27	3.54	1.54	1.54	3
1B	6.01	3.88	5.32	3.43	3.43	3
2A	4.35	3.65			3.65	1
2B	3.17				3.17	0
3A	5.03	3.11	3.65	2.76	2.76	3
3B	6.02	2.99	5.43	4.12	2.99	1
4A	5.90	5.03	2.98	3.54	2.98	2
4B	6.01	1.66	5.43		1.66	1
5A	6.88		3.77	2.98	2.98	3
5B	5.99	5.43	5.85	4.32	4.32	3
…	…	…	…	…	…	…
22B	4.97		3.76	2.95	2.95	3

Tables that summarize the data in Table E-1 are provided in the Performance Evaluation Tool. These summary tables can be saved for both the index models and the performance group.

E.3 Basic Program Directory and File Structure

Before installing and operating the Toolkit, the user must be familiar with the basic directory and file structure, shown in Figure E-4, to understand the installation procedures for the program. This directory structure is automatically created when the Toolkit is installed on the system. In this illustration, the main folder is named **ATC 84 Toolkit**. A brief description of each folder follows:

The **Program Files** folder contains all of the Matlab code, either in native Matlab form (.m files and .fig files) or compiled (.exe) versions of these files. The native code is used and executed within the Matlab program while the compiled code executes outside of Matlab, using a runtime compiler. Section E.5 provides additional detail on these two versions of the program.

Three ground motion folders are part of the file structure: **P695_Far_Field**, **P695_Near_Field**, and **User Defined**. The P695_Far_Field and P695_Near_Field folders both contain flat files associated with the ground motion record sets. The User Defined folder contains subfolders with user defined ground motion sets.

The **Documentation** folder contains all of the documentation for the Toolkit.

The **Performance_Group** folder contains a series of subfolders, each used to contain all of the information related to a FEMA P-695 evaluation. Because a typical FEMA P-695 analysis consists of the evaluation of several performance groups, there will be

one subfolder for each performance group. Similarly, each performance group will contain several index models; thus, there will be one folder for each index archetype model within each performance group.

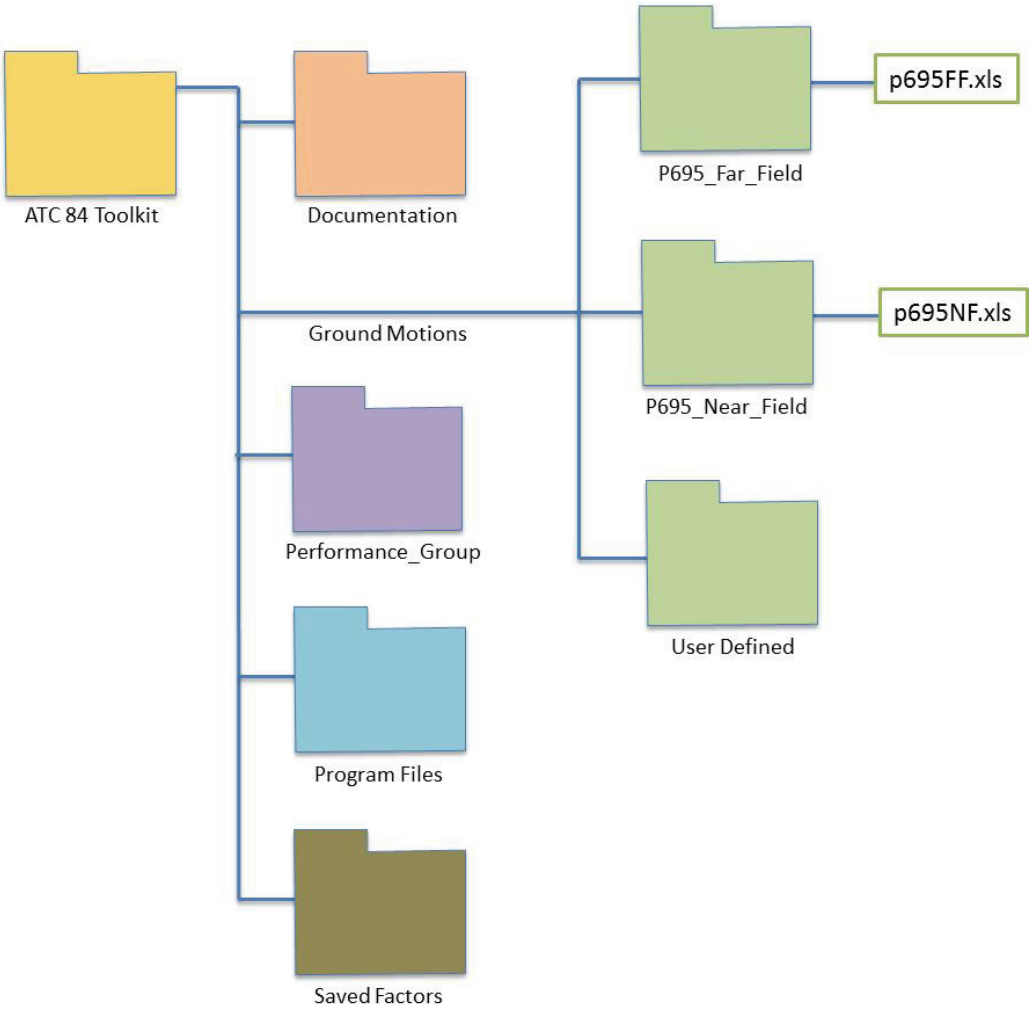

Figure E-4 Basic directory and file structure for the Toolkit.

E.4 Program Installation and Set-Up

The Toolkit is provided in both compiled and non-compiled versions. The compiled (stand alone) version runs outside of the Matlab environment, and Matlab need not be installed. However, the Matlab runtime environment is required. The non-compiled version of the Toolkit operates within Matlab, thus, the user must have full implementation of Matlab on his or her computer.

The user of either version of the program must have the TCL interpereter and OpenSees installed on the local computer. Complete instructions for installing both versions of the program, as well as OpenSees and TCL are provided below.

The Toolkit has been developed and tested on Microsoft Windows-based computers up through Version 7. It is expected that versions compatible with other operating systems, such as MAC OS and UNIX/LINUX, will be provided in the future.

E.4.1 Installing OpenSees and TCL

OpenSees and TCL are available from the OpenSees website, http://opensees.berkeley.edu/index.php. The user must register as an OpenSees user before they can download the programs. During the installation of TCL, "c:\program files\tcl" should be specified as the location for the program and the executable file "opensees.exe" should be placed in "c:\program files\tcl\bin."

E.4.2 Installing Program Files for the Non-Compiled Version of the Toolkit

In the non-compiled version of the Toolkit, all program operations are performed within the Matlab environment. Thus, the user must have the full version of Matlab installed on their computer.

All of the required directories and files for executing the toolkit are automatically created when the non-compiled version of the Toolkit is downloaded to the user's system. Typically, this download will be in the form of a .zip file. The Matlab script for running the program is provided in the Program Files directory. The content of this directory is explained in Section E.5.

E.4.3 Installing Matlab Files and the Runtime Environment for the Compiled Version of the Toolkit

In the compiled version of the program, all program operations are performed by use of an executable file. Prior to running the Toolkit, the user must download and install the Matlab Runtime Compiler (MCR) version 7.13 (provided with the Toolkit program files), even if Matlab is already installed on the user's computer.

All of the required directories and files for executing the Toolkit are automatically created when the compiled version of the Toolkit is downloaded to the user's system. Typically, this download will be in the form of a .zip file. The Matlab executables for running the program are provided in the Program Files directory. The content of this directory is explained in Section E.5.

E.5 Detailed Program File Structure

All files for running the Toolkit are contained within the folder **ATC 84 Toolkit**, as presented in Figure E-4. The main toolkit folder contains the files required for running the Toolkit. For the non-compiled version, the Toolkit files are as follows:

GM_Tool.fig
GM_Tool.m
IDA_Tool.fig

IDA_Tool.m
Master_Tool.fig
Master_Tool.m
PE_Tool.fig
PE_Tool.m
PG_Tool.fig
PG_Tool.m
Pushover_Tool.fig
Pushover_Tool.m

For the compiled version, the Toolkit files are as follows:

GM_Tool.exe
IDA_Tool.exe
Master_Tool.exe
PE_Tool.exe
PG_Tool.exe
Pushover_Tool.exe

Detailed descriptions of the subfolders are presented in the following sections.

E.5.1 Program Files

The **Program Files** folder contains the files used by each module in the toolkit. All versions of the Toolkit contain the following TCL and Microsoft Excel files:

NGA_Flatfile.xls
RunDynamic.tcl
RunDynamicMP.tcl
RunPushover.tcl
RunPushoverCycle.tcl
test.tcl

The non-compiled version of the Toolkit also contains the following Matlab (.m) files:

evaluateIM.m
getuserdir.m
LinSpec.m
NGA_Motion.m
p695_norm.m
Rspec.m
showinfowindow.m
write_damping_tcl.m
write_dyn_analysis.m
write_gm_tcl.m
write_push_analysis.m

write_recorder_dyn.m
write_recorder_push.m
write_tcl_header.m

The files contained within the **Program Files** folder should never be modified.

E.5.2 Ground Motions

The **Ground Motions** folder contains three subfolders:

The **Far Field** folder contains the PEER NGA files associated with the FEMA P-695 Far-Field ground motion record set and a Microsoft Excel flat file for the record set. The files contained within this folder are as follows:

ABBAR—L.AT2
ABBAR—T.AT2
ARC000.AT2
ARC090.AT2
A-TMZ000.AT2
A-TMZ270.AT2
B-ICC000.AT2
B-ICC090.AT2
BOL000.AT2
BOL090.AT2
B-POE270.AT2
B-POE360.AT2
CAP000.AT2
CAP090.AT2
CHY101-E.AT2
CHY101-N.AT2
CLW-LN.AT2
CLW-TR.AT2
DZC180.AT2
DZC270.AT2
G03000.AT2
G03090.AT2
H-DLT262.AT2
H-DLT352.AT2
HEC000.AT2
HEC090.AT2
LOS000.AT2
LOS270.AT2
MUL009.AT2
MUL279.AT2
NIS000.AT2
NIS090.AT2
P-695FF.xls
PEL090.AT2
PEL180.AT2
RIO270.AT2
RIO360.AT2
SHI000.AT2
SHI090.AT2
TCU045-E.AT2
TCU045-N.AT2
YER270.AT2
YER360.AT2

The **Near Field** folder contains the PEER NGA files associated with the FEMA P-695 Near-Field record set and a Microsoft Excel flat file for the record set. The files contained within this folder are as follows:

0637-270.AT2
0637-360.AT2
A-STU000.AT2
A-STU270.AT2
B-PTS225.AT2
B-PTS315.AT2
BRN000.AT2
BRN090.AT2
CLS000.AT2
CLS090.AT2
CPM000.AT2
CPM090.AT2
DZC180.AT2
DZC270.AT2
ERZ-EW.AT2
ERZ-NS.AT2
GAZ000.AT2
GAZ090.AT2
H-BCR140.AT2
H-BCR230.AT2
H-CHI012.AT2
H-CHI282.AT2
H-E06140.AT2
H-E06230.AT2
H-E07140.AT2
H-E07230.AT2
IZT090.AT2
IZT180.AT2
LCN260.AT2
LCN345.AT2

P-695NF.xls	*S2240.AT2*	*TCU065-N.AT2*
PET000.AT2	*S2330.AT2*	*TCU067-E.AT2*
PET090.AT2	*STC090.AT2*	*TCU067-N.AT2*
PSI0047.AT2	*STC180.AT2*	*TCU084-E.AT2*
PSI0317.AT2	*STG000.AT2*	*TCU084-N.AT2*
RRS228.AT2	*STC090.AT2*	*TCU102-E.AT2*
RRS318.AT2	*SYL090.AT2*	*TCU102-N.AT2*
S1010.AT2	*SYL360.AT2*	*YPT060.AT2*
S1280.AT2	*TCU065-E.AT2*	*YPT330.AT2*

The **User Defined** folder contains the Microsoft Excel flat file and ground motion recorders for a user-defined ground motion set.

Note that all ground motions must be stored in the PEER NGA format, consisting of five header lines followed by the acceleration data, written in units of g, five terms per line.

E.5.3 Documentation

The **Documentation** folder contains the documentation associated with the Toolkit. The following files are contained within this folder:

0 Read Me First!.docx
1 Master Tool Overview.docx
2 Performance Group Tool Overview.docx
3 Pushover Tool Overview.docx
4 Ground Motion Tool Overview.docx
5 IDA Tool Overview.docx
6 Performance Evaluation Tool Overview.docx
7 Parallel OpenSEES on Ithaca.docx
8 Examples Manual
9 App A File Structure Overview.docx
10 App B Pushover Recorder Input File Format.docx
11 App C IDA Recorder Input File Format.docx

E.5.4 Performance_Group

The **Performance_Group** folder contains the files associated with the models and the results files. The hierarchy of folders presented in Figure E-5 is expected. According to this, each performance group contains both a **Models** and **Results** directory. Within both of these directories is a folder for each index model. Each index model folder in the **Models** directory contains the files *GravityLoad.tcl*, *ModelGeometry.tcl*, *RecorderDynamic.txt*, *RecorderStatic.txt,* *SectionAndMaterial.tcl*, and *SetUpModel.tcl*.

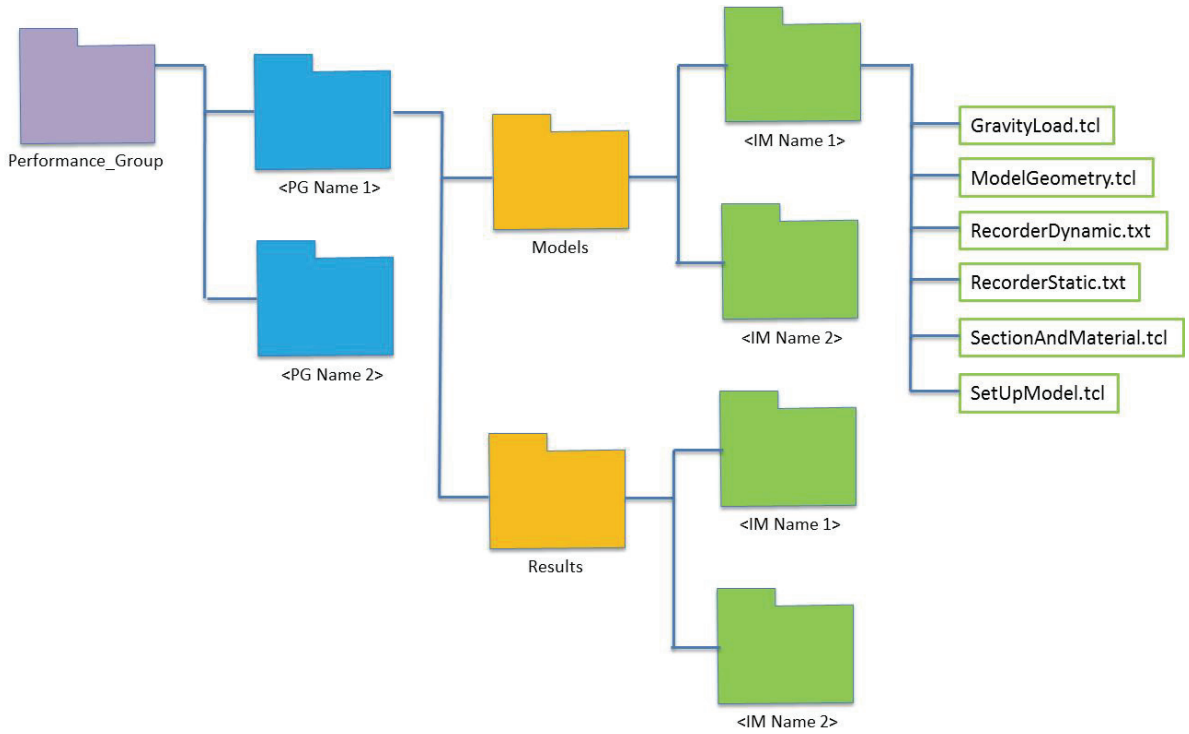

Figure E-5 File structure for the Performance_Group folder.

E.6 Detailed Descriptions of Basic OpenSees Input Files

Use of the Toolkit requires that the user prepare four TCL files. These files are used as the basis for developing more detailed TCL files for gravity load, modal, pushover, and dynamic analyses. During the IDA, the script *SetUpModel.tcl* is called once at the beginning of the analysis, but the scripts *GravityLoad.tcl*, *ModelGeometry.tcl*, and *SectionAndMaterial.tcl* are called at the beginning of each analysis because the model information is erased at the end of each analysis. The simplified model in Figure E-6 is used to help illustrate the use of the TCL files.

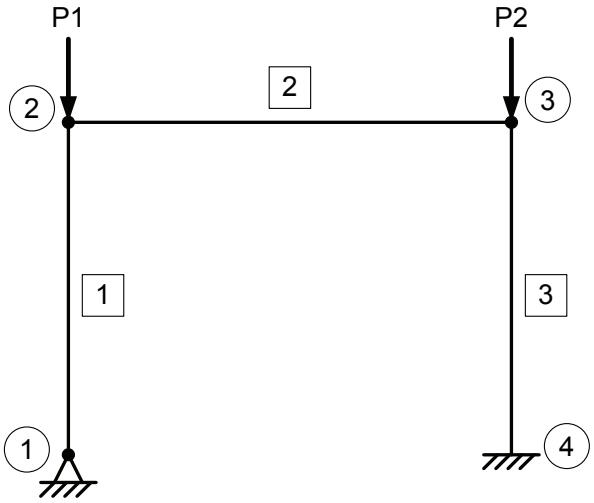

Figure E-6 Example simple portal frame.

E.6.1 SetUpModel.tcl

The script *SetUpModel.tcl* defines variables that are common to all analyses for the index model. These variables include units and flags for controlling analysis parameters, such as turning on and off P-delta effects. This script is also used for defining procedures that are pertinent to the model. Commands for defining geometry and loads (e.g., elements, nodes, or load patterns) must be defined in the other scripts as this script is called only once for an IDA. For example, the magnitude of gravity point loads "P1" and "P2" for the example in Figure E-4 can be defined in this script and saved in variables "P1" and "P2."

E.6.2 GravityLoad.tcl

The script *GravityLoad.tcl* defines the magnitude and location of concentrated and distributed gravity loads on the entire model. The gravity load is any load applied to the model before the static pushover or dynamic analysis and is sustained throughout the analysis. The gravity load is defined in a load pattern with a tag of 1. This script does not contain the syntax to run the gravity load portion of the analysis. For example, variables "P1" and "P2" defined in the script *SetUpModel.tcl* can be positioned on nodes 2 and 3 on the structure in Figure E-4 using a load pattern in this script.

E.6.3 ModelGeometry.tcl

The script *ModelGeometry.tcl* defines the nodal locations and element connectivity of the entire model. The boundary conditions, masses, and geometric transformations are also defined in this script. For example, the nodal locations of nodes 1, 2, 3, and 4, the connectivity of elements 1, 2, and 3, and the boundary conditions at nodes 1 and 4 are defined in this script.

E.6.4 SectionAndMaterial.tcl

The script *SectionAndMaterial.tcl* defines the sections and materials for all elements in the model. For example, the section and material properties for elements 1, 2, and 3 are defined in this script.

E.7 Setting up OpenSees Recorders

Recorder information is defined using a keyword format in the file *RecorderStatic.txt* for the static analyses and *RecorderDynamic.txt* for the dynamic analyses in the model file directory for each index model. The Toolkit is compatible with six different recorders in OpenSees, including node, truss element, drift, element section, element beam-column, and element fiber recorder. The general format of each recorder definition in the file *Recorder.txt* is as follows:

- Line 1: Keyword, unique type, IDA information, and stop limit

- Lines 2 through Line N – 1: Model component information
- Line N: Results file prefix

E.8 Detailed Toolkit Documentation

The Toolkit documentation contains a User's Manual for each tool, which provides detailed information and explains interaction with other tools. The files contained within the **Documentation** folder and descriptions of the files are presented below:

Read Me First! provides important information that needs to be reviewed by the user before using the Toolkit for the first time.

Master Tool Overview provides a detailed description of the Master tool and describes the capabilities of the tool and its interface with the other tools.

Performance Group Tool Overview provides a detailed description of the Performance Group tool and describes the capabilities of the tool.

Pushover Tool Overview provides a detailed description of the Pushover tool and describes the capabilities of the tool.

Ground Motion Tool Overview provides a detailed description of the Ground Motion tool and describes the capabilities of the tool.

IDA Tool Overview provides a detailed description of the IDA tool and describes the capabilities of the tool.

Performance Evaluation Tool Overview provides a detailed description of the Performance Evaluation tool and describes the capabilities of the tool.

Parallel OpenSEES on Ithaca describes the procedure for running analysis scripts created by the IDA tool on parallel machines using the Ithaca Cluster at Virginia Tech as an example.

Examples Manual provides examples for using the Toolkit.

File Structure Overview presents a detailed overview of the file structure for the Toolkit. It also discusses the files within each folder and the files that must be created by the user before using the Toolkit.

Pushover Recorder Input File Format outlines the format required for defining additional recorders for the static pushover analysis besides the roof displacement recorder.

IDA Recorder Input File Format outlines the format required for defining recorders for the dynamic analysis. IDA parameters, such as non-simulated collapse limits, are also described in this document.

E.9 Procedure for Running FEMA P-695 Analyses

The procedure for running the Toolkit consists of preparing the OpenSees TCL files listed in Section E.6, preparing the recorder files described in Section E.7, and then executing the modules in the sequence illustrated in Figure E-2.

E.10 Preparing Analysis Results

The analysis results are reported using worksheets that contain summarized data from the Performance Evaluation tool. The three tables that are generated summarize the design parameters, summary of collapse results, and summary of collapse performance evaluation. Examples of these tables are provided in Tables E-3, E-4, and E-5.

E.11 Future Toolkit Additions

The current release of the Toolkit has many capabilities and reduces the work required to run a FEMA P-695 analysis. However, future additions are planned for the Toolkit to improve its capabilities. The additions are described as follows:

E.11.1 Optimized FEMA P-695 Incremental Dynamic Analyses

The current IDA tool runs a set of IDA scale factors defined by the user before the analysis begins. Therefore, the user must have insight into the approximate IDA scale factor associated with 50% of the models collapsing or run many more analyses than is necessary to calculate the *CMR*. The user may also iterate on analyses to find the *CMR*. The optimized IDA option would use an algorithm to quickly find the *CMR* while running the minimum number of analyses.

E.11.2 Spectrum-Matched Ground Motions

The current release of the Ground Motion tool is only capable of scaling original ground motion records either by the methodology described in FEMA P-695 report or to the MCE spectrum at a specified period. Adding the ability to use spectrum-matched ground motions will allow the user to investigate the benefits (and problems) of using spectrum-matched ground motions in collapse analysis of structures.

If this tool is added, the user would only need to identify the spectrum-matching algorithm to be used (these would not be developed separately but would use existing code) as well as the matching parameters, such as target spectrum and frequency range.

E.11.3 Restart Option for Incremental Dynamic Analyses

An IDA may need to be stopped on a personal computer or one of the analyses may fail and cause the analysis process to start. The current release of the Toolkit only

allows analyses to be run only in their entirety. If an analysis crashes, the entire analysis must be rerun and the previous results are overwritten. Incorporating the ability to restart the analysis would enable the user to run the analysis from the point where it failed. It would also allow a user to stop the analysis and restart the analysis when the computer resources can again be dedicated to the analysis. The ability to restart an analysis would also enable a user to perform additional analyses to refine the accuracy of the IDA scale factors without clearing the previous results.

E.11.4 Analysis Report

An analysis report would further summarize the results of the analysis process beyond the tables provided in the Performance Evaluation tool. The analysis report would be a collection of Microsoft Excel files that are written by the individual tools.

The Performance Group tool would produce one file (*problemname_PG.xls*), containing one tab for the performance group and one tab for each index archetype model. All of the information entered into the Performance Group tool would be "echoed" in this file.

Additionally, the tab for the Performance Group would be updated by the other modules to log the progress of the FEMA P-695 analysis, providing the date and time that each module was last executed in association with the performance group being analyzed.

The Pushover tool would produce one file (*problemname_MP.xls*) containing one tab for each index archetype model. Information written to the report would include the first mode period of vibration, T, the first mode shape, and the pushover curve force-displacement coordinates, V_{max}, δ_u, $\delta_{y,eff}$, C_o, μ_T, and Ω.

The Ground Motion tool would produce one file (*problemname_GM.xls*) containing one tab for each index archetype model. Results provided for each model would include the full list of ground motions in the record set and computed normalization and scale factors for the set. Normalization and scale factors would be shown as zero if the individual ground motion was not included in the analysis. Also included in the file would be the target spectrum ordinates, the target period of vibration, the target damping, and the basis for scaling.

The report for the IDA tool (*problemname_ID.xls*) would contain one tab for each index archetype model. The data written would be similar to that shown in Table E-1. Also available is a separate file (*problemname_PG_raw.xls*) containing the raw IDA data for each index archetype model.

The Performance Evaluation tool would produce one file (*problemname_PE.xls*), with one tab containing a summary table in addition to the summary tables that are already saved.

E.12 Toolkit Demonstration on Special Reinforced Masonry Shear Wall Systems

This example analyzes a performance group of special reinforced concrete masonry shear wall systems. Three shear walls are included in this performance group with varying heights. Figure E-7 and Table E-2 summarize the properties of the performance group. Although the tools can be accessed individually, this example outlines the use of the Master tool to perform the analyses and final evaluation.

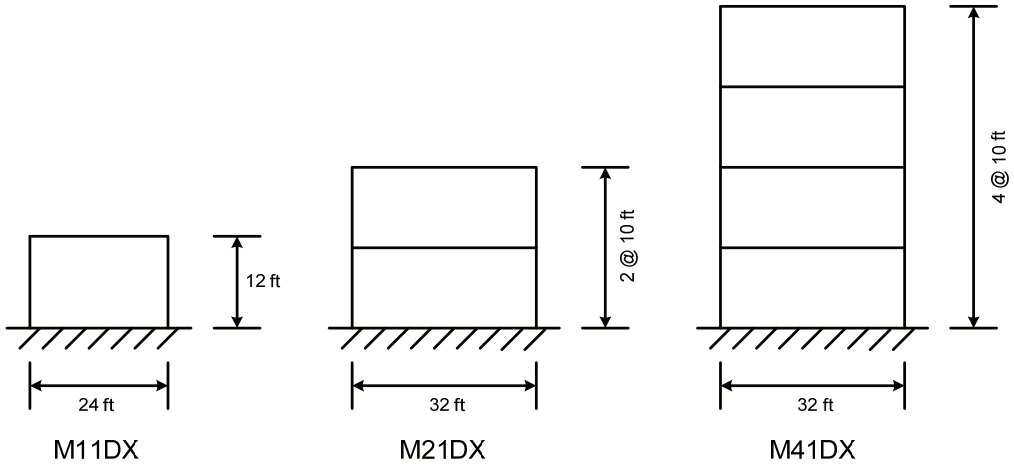

Figure E-7 Dimensions of the special reinforced concrete masonry shear wall system.

Table E-2 Properties of the Special Reinforced Concrete Masonry Shear Wall System

Archetype Design ID Number	No of Stories	Gravity Loads	Period Domain	SDC	*R*	$C_u T_a$ (sec)	V_{des}/W (g)	$S_{MT}(T)$ (g)
M11DX	1	High	Low	D_{max}	1	0.25	0.478	1.50
M21DX	2	High	Low	D_{max}	1	0.26	0.274	1.50
M41DX	4	High	Low	D_{max}	1	0.45	0.125	1.50

E.12.1 Master Tool

The analysis process begins by opening the Master tool. The Master tool is comprised of six segments, five corresponding to the five modules and one displaying the performance group directory name, as shown in Figure E-8. The color behind each component indicates the status of that component, red for not completed and green for completed.

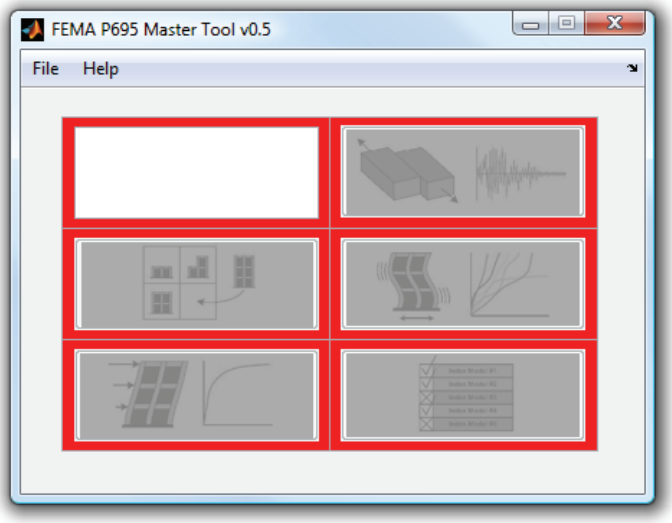

Figure E-8 Initialized Master tool.

Select *File -> New* to create a new performance group. After selecting the performance group directory, the Performance Group tool automatically opens. Closing any open tool returns control of the process to the Master tool where other tools are accessed. The Master tool aids the user in following the FEMA P-695 procedure by allowing access only to the tools that apply to the next step in the process.

E.12.2 Performance Group Tool

To begin the analysis process, the performance group and index model information is input into the Performance Group tool, as shown in Figure E-9. The performance group information is entered into the *Performance Group* panel of the tool and the index archetype model information is input into the *Index Model* panel. Information for the different index archetype models is input by selecting the archetype design ID number from the popup menu at the top of the *Index Model* panel.

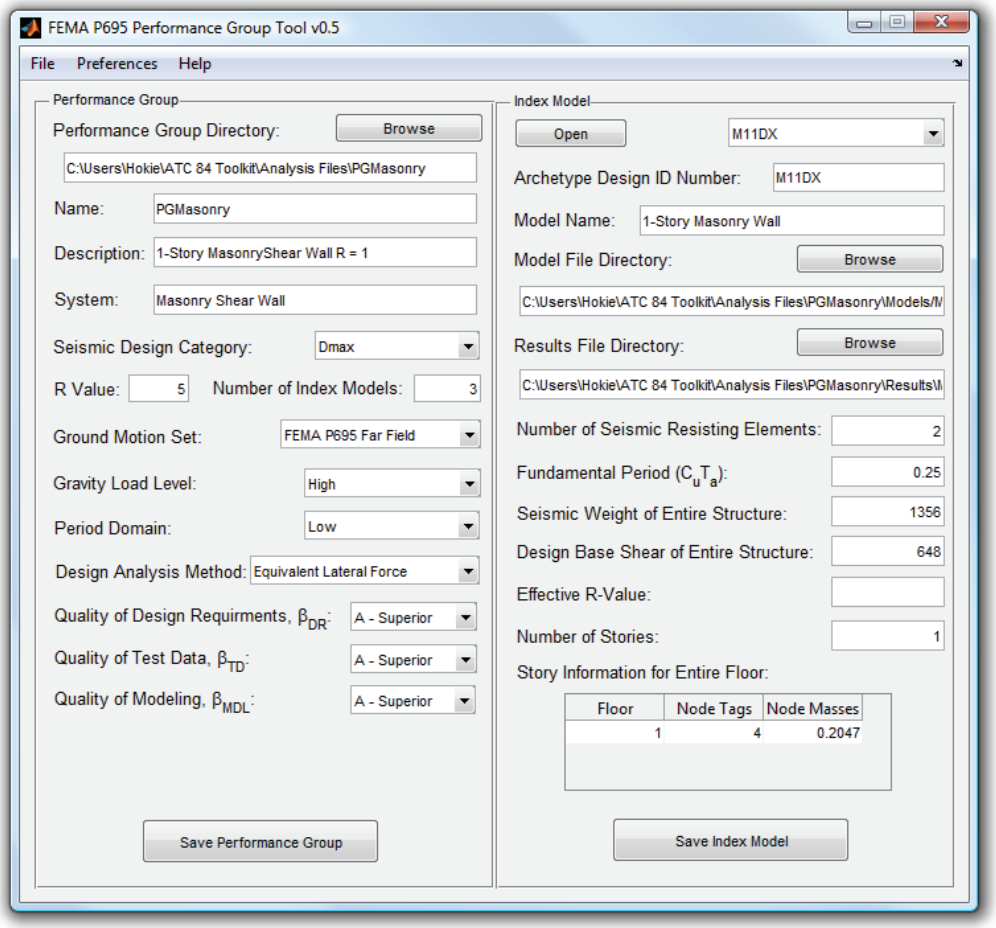

Figure E-9 Performance Group tool.

After saving the performance group, close the Performance Group tool. The Master tool reappears, now with the performance group directory displayed and both the Performance Group directory and the Performance Group tool highlighted in green, as shown in Figure E-10. Moving the cursor over the different buttons indicates the corresponding tool. The Pushover tool, Ground Motion tool, and IDA tool are now accessible by the Master tool, but the analyses must be completed before the Performance Evaluation tool is accessible.

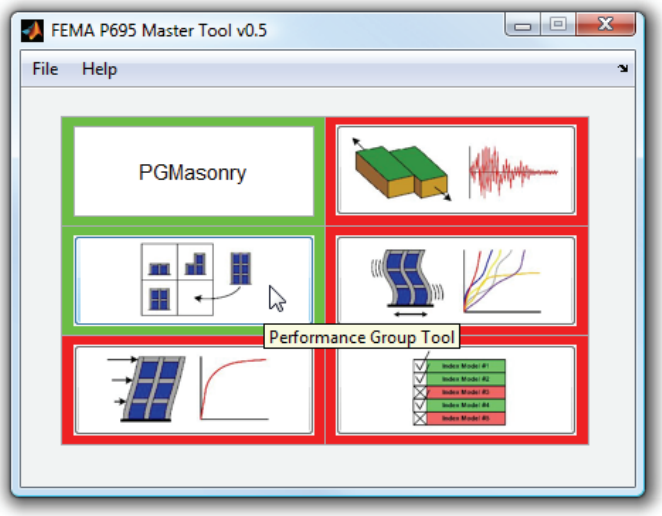

Figure E-10 Performance group defined in Master tool.

E.12.3 Pushover Tool

The pushover analysis is performed using the Pushover tool. The user selects the Pushover tool button from the Master tool, and the initialized tool opens, as shown in Figure E-11.

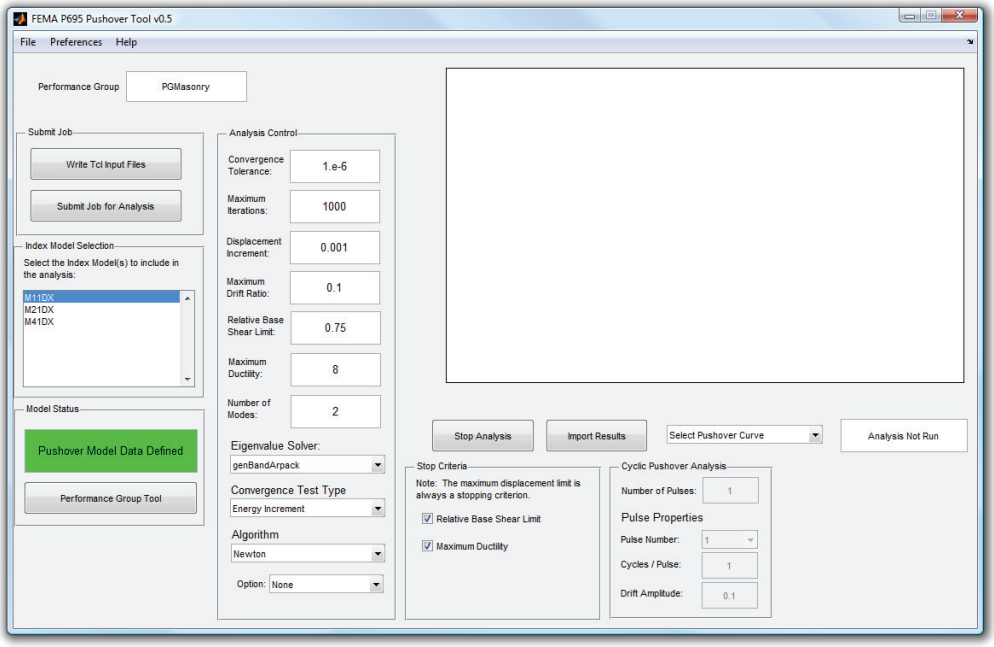

Figure E-11 Initialized Pushover tool.

This tool offers the flexibility of performing either a monotonic pushover curve or a cyclic pushover curve. For a monotonic pushover curve, the pushover analysis can stop based on FEMA P-695 criteria, such as relative base shear or maximum ductility, or the pushover analysis can be performed up to a prescribed maximum

roof drift ratio. When performing a cyclic pushover analysis, the number of pulses, cycles per pulse, and roof drift ratio amplitude per pulse are specified. The user can also select either a lateral load distribution based on the mass-normalized first mode shape, a uniform distribution, or a triangular distribution. Either analysis TCL files can be written, or the analysis can be performed within the tool. After selecting *Submit Job for Analysis* from the *Submit Job* panel, pushover curves are displayed in the plot on the right side of the tool, as shown in Figure E-12. To view an individual pushover curve, as shown in Figure E-13, the user selects *Individual Pushover Curve* from the popup menu under the plot.

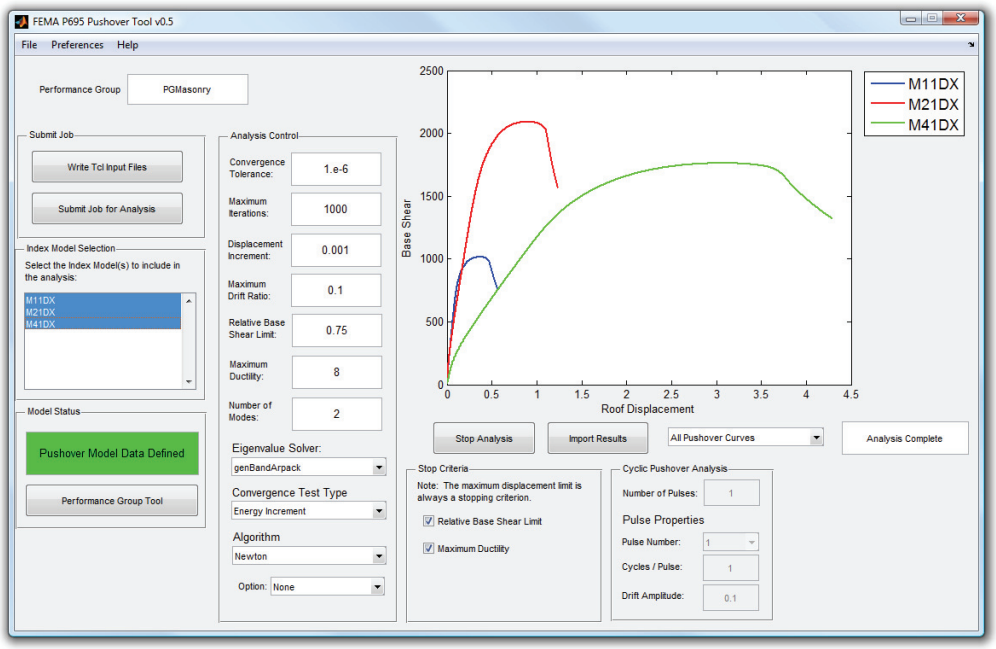

Figure E-12 Pushover tool with analysis results.

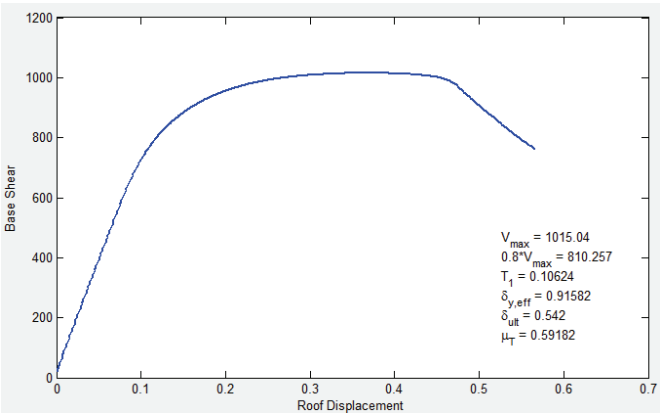

Figure E-13 Individual pushover curve.

E.12.4 Ground Motion Tool

Ground motion normalization and scaling is performed by opening the performance group in the Ground Motion (GM) tool by selecting it from the Master tool. In the example shown in Figure E-14, the Ground Motion tool automatically imports the FEMA P-695 Far-Field ground motion set because that was the set specified in the Performance Group tool, as shown in Figure E-14.

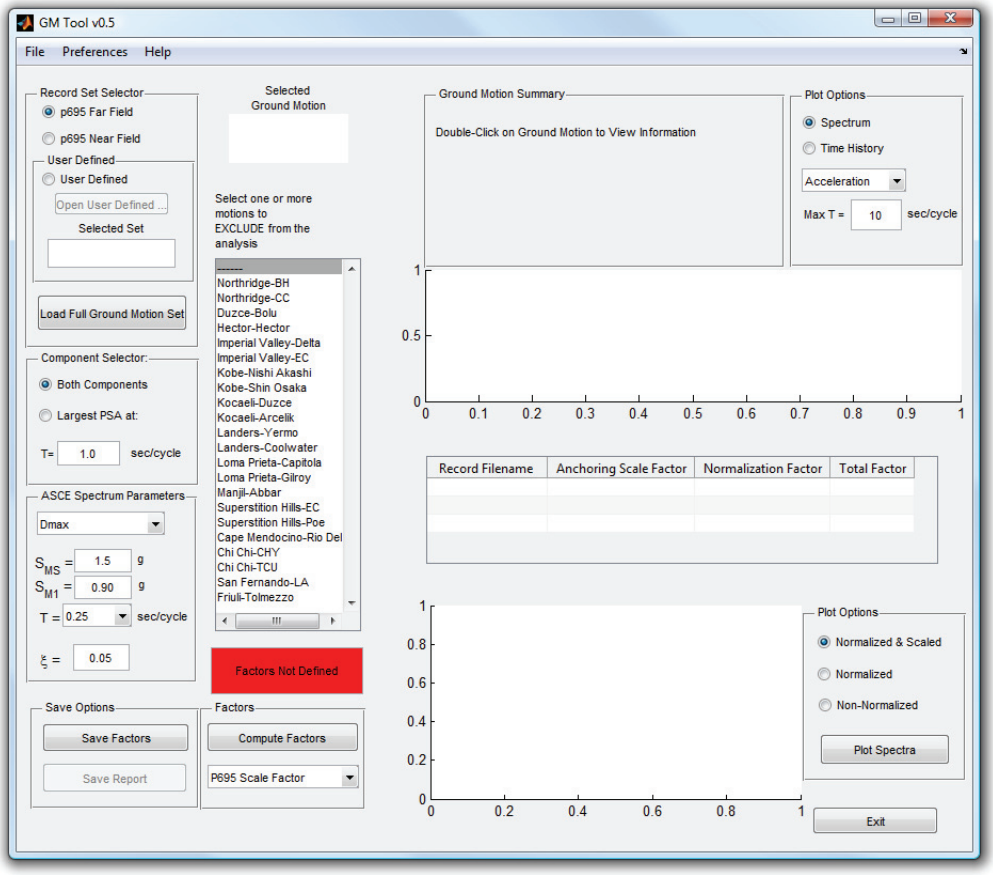

Figure E-14 Initialized GM tool.

Information about the different ground motions is viewed by double-clicking on the ground motion name in the list. The information appears in the upper right corner of the tool, as shown in Figure E-15, point A. To calculate the normalization and scaling factors, select *Compute Factors* in the *Factors* panel, shown in point B. The normalization and scaling factors for all models in the performance group are calculated and displayed in the table. To display the normalized and scaled ground motion spectra, select *Plot Spectra* in the *Plot Options* panel, shown in point C. The scaled and normalized, normalized, or non-normalized spectra can be plotted here. The factors are saved by selecting *Save Factors* from the *Save Options* panel.

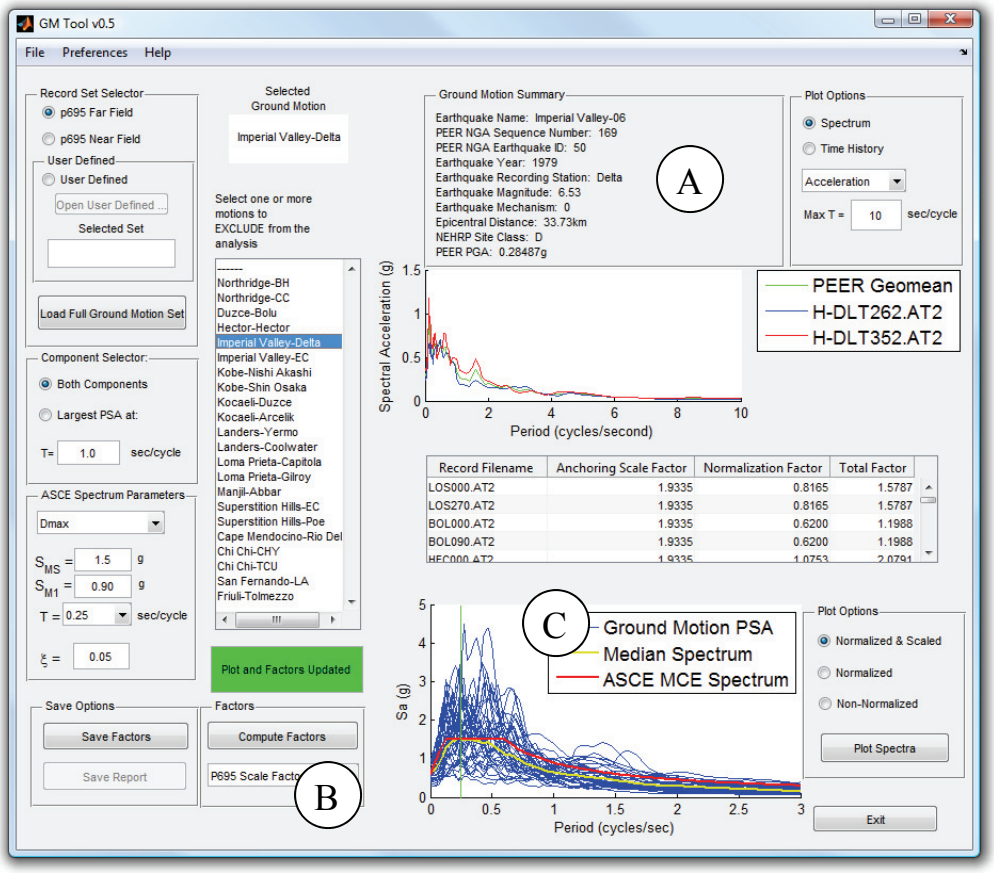

Figure E-15 GM tool with factors computed.

E.12.5 Incremental Dynamic Analysis Tool

The Incremental Dynamic Analysis is set up and performed using the IDA tool. The IDA tool is initialized by selecting the IDA tool button from the Master tool. The IDA scale factors are set from 0.2 to 2.0 with 10 increments in the *IDA Scaling Factors* panel. Damping is assigned in the *Damping Properties* panel as a damping ratio of 0.035 in the first mode and 0.0125 in the second mode for all elements. Stiffness proportional damping is also set to be proportional to the initial stiffness matrix. The default settings for the analysis in the *Analysis Control* panel are used. The IDA tool with all settings prepared for the analysis is presented in Figure E-16. The recorded output and non-simulated collapse parameters are specified in a separate text file, *RecorderDynamic.txt*, which is placed in the same directory as the model analysis files.

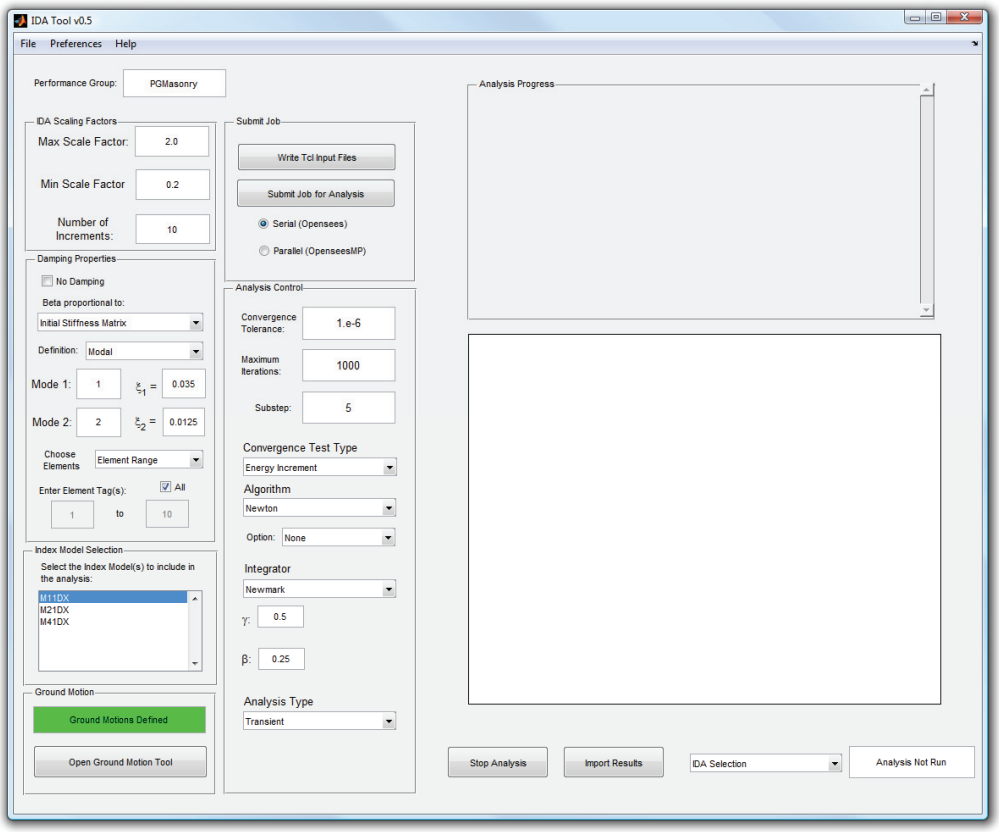

Figure E-16 IDA tool prepared for analysis.

The analysis can either be run on the local machine (serial only) or a parallel machine. The TCL analysis files are created by selecting *Write Tcl Input* Files in the *Submit Job* panel. Selecting the local machine and *Submit Job for Analysis* will run the analysis in the tool and update the IDA spaghetti curve and progress bars during the analysis. If the parallel option is selected, either button will write the input files only. After running an analysis outside of the tool, the results are imported into the tool using the *Import Results* button. Importing the results requires the user to specify the results directory and the index model Matlab data structure file. Figure E-17 presents the results from importing the results for the 4-story model.

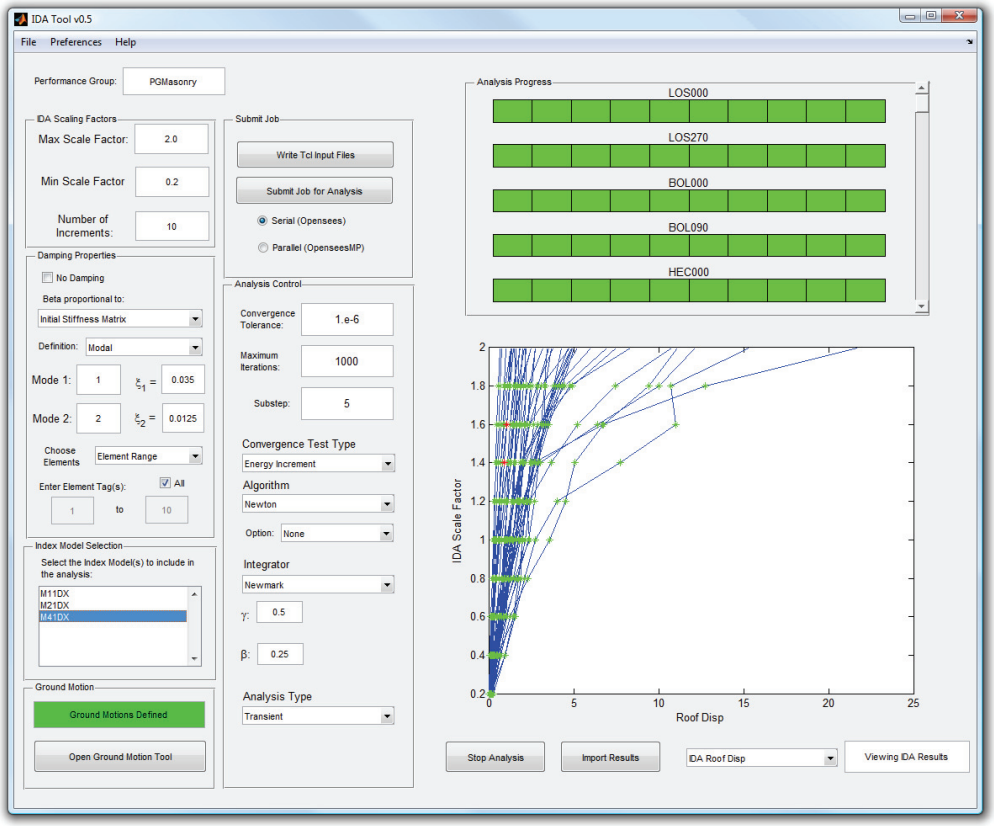

Figure E-17 IDA tool with analysis results.

E.12.6 Performance Evaluation Tool

After all analyses are finished, the Master tool will indicate that all modules are complete except the Performance Evaluation tool, as shown in Figure B-18. The Master tool will now allow the user to access the Performance Evaluation tool.

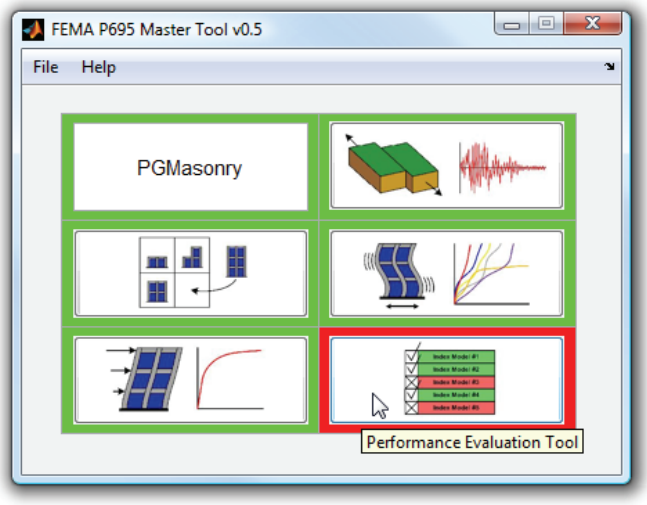

Figure E-18 Accessing Performance Evaluation tool in Master tool.

After all analyses are finished, the results are analyzed using the Performance Evaluation tool. While initializing the tool, the performance group for the masonry models is selected. The initialized Performance Evaluation tool appears as in Figure E-19. Information about the performance group and the index model selected from the list are presented in the panels on the right side of the tool. The nonsimulated collapse parameters can be verified or changed using the *Evaluation Parameters* panel. The simulated collapse parameters are also specified in this panel. The user has the option of changing uncertainty factors, collapse limits, and the index models and ground motions that are included in the performance group evaluation using the panels on the left half of the tool.

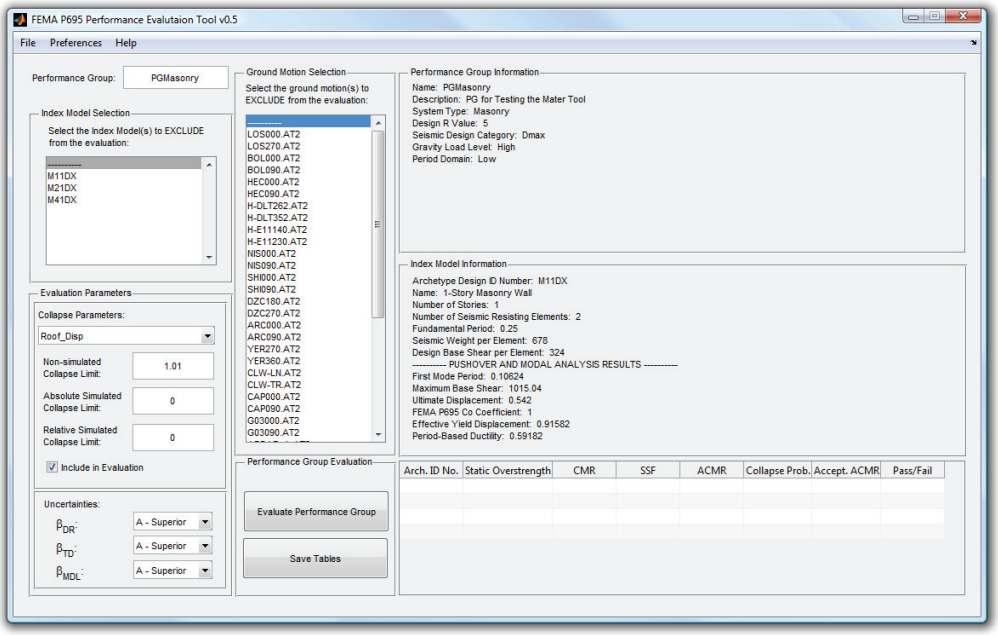

Figure E-19 Initialized Performance Evaluation tool.

The performance group is evaluated by selecting the *Evaluate Performance Group* button. The results of the evaluation are displayed in the table in the lower right corner of the tool, as shown in Figure E-20. Additional tables of information are saved to Microsoft Excel spreadsheets by selecting the *Save Tables* button. Additional tables containing results for the special reinforced concrete masonry shear wall models are shown in Tables E-3, E-4, and E-5.

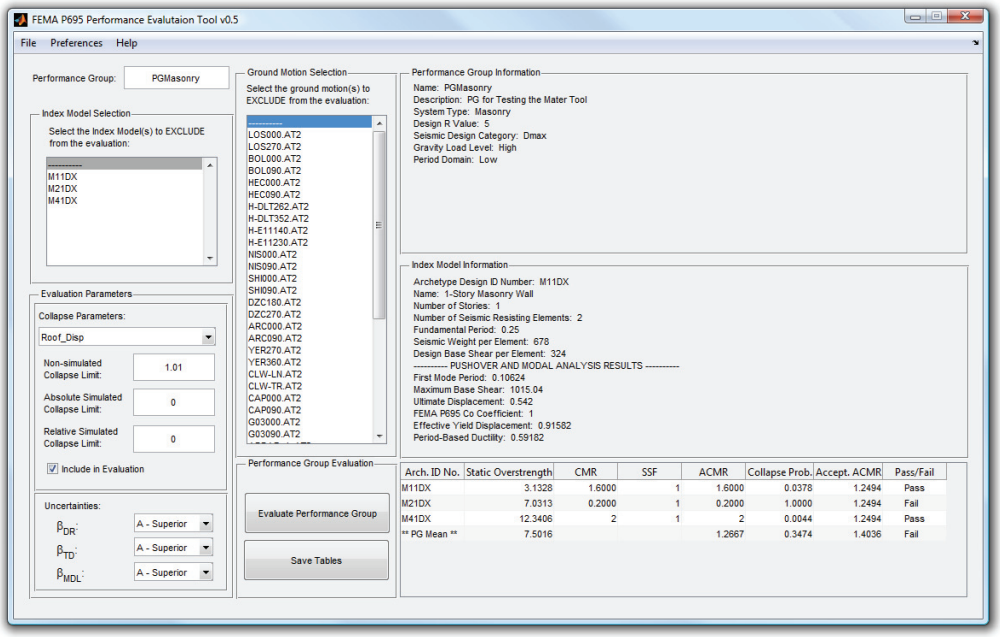

Figure E-20 Performance Evaluation tool.

Table E-3 Design Properties for Special Reinforced Concrete Masonry Shear Wall Archetypes

Archetype Design ID Number	No. of Stories	Gravity Loads	SDC	*R*	*T*(sec)	T_1(sec)	V_{des}/W (g)	$S_{MT}(T)$ (g)
M11DX	1	High	D_{max}	1	0.25	0.106	0.478	1.50
M21DX	2	High	D_{max}	1	0.26	0.097	0.274	1.50
M41DX	4	High	D_{max}	1	0.45	0.153	0.125	1.50

Table E-4 Summary of Collapse Results

Archetype Design ID Number	No. of Stories	Gravity Loads	SDC	Static Overstrength	$S_{MT}(T)$ (g)	$S_{CT}(T)$ (g)	CMR
M11DX	1	High	D_{max}	3.13	1.50	2.39	1.6
M21DX	2	High	D_{max}	7.03	1.50	3.89	2.6
M41DX	4	High	D_{max}	12.34	1.50	4.49	3

Table E-5 Summary of Collapse Performance Evaluation

Archetype Design ID Number	No. of Stories	Gravity Loads	SDC	Static Overstrength	*CMR*	Period-Based Ductility	*SSF*	*ACMR*	Collapse Probability	*Acceptable ACMR*	Pass/Fail
M11DX	1	High	D_{max}	3.13	1.6	0.59	1	1.6	3.78E-02	1.249	Pass
M21DX	2	High	D_{max}	7.03	2.6	0.76	1	2.6	1.52E-04	1.249	Pass
M41DX	4	High	D_{max}	12.34	3	0.97	1	3	1.65E-05	1.249	Pass
	PG Mean			**7.50**				**2.4**	**1.27E-02**	**1.404**	**Pass**

E.13 Running Incremental Dynamic Analyses Outside of the Toolkit on a Multiple Processor Machine

Because of the large number of dynamic analyses and the nontrivial duration of each analysis, running an IDA can take hours, days, or weeks. To reduce the total duration of the analyses, IDAs are run outside of the Toolkit on large, multiple processor machines. The following example demonstrates the procedure for creating the analysis files, transferring them to another machine, running the analysis files, and importing them into the IDA tool.

E.13.1 Create Analysis Files

Creating the analysis files begins with the same procedure as running the dynamic analyses through the IDA tool. Open the IDA tool and input the preferences for IDA scale factors, damping, and analysis parameters. However, select the *Parallel (OpenseesMP)* radio button instead of the *Serial (Opensees)* radio button, as shown in Figure E-21. Select the "Write Tcl Input Files" button to create the analysis files. The IDA tool creates analysis files that are compatible with OpenseesMP.

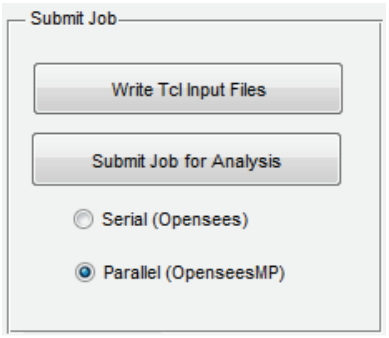

Figure E-21 Options for writing analysis files.

E.13.2 Set Up Analysis on Multiprocessor Machine

To run the analysis on a separate multiprocessor machine, the analysis files and ground motion files must be transferred to the machine. Ithaca, a supercomputer at Virginia Tech (http://www.arc.vt.edu/arc/Ithaca/index.php), is used to demonstrate this process. For additional detail on using the Toolkit with other clusters, refer to 7 *Parallel OpenSEES on Ithaca.docx* in the **Documentation** folder. Ithaca is a UNIX system, so a shell software is required to interface with it from a Windows machine. SSH Secure Shell Client is the shell software used in this example. Ithaca requires a username and password to access the system.

The ground motion record files must be transferred to the multiprocessor machine. In this example, the FEMA P-695 Far-Field record set is used. After logging onto Ithaca, the folder *P695_Far_Field* is copied to the computer using the shell software. The folder structure associated with the performance group must be recreated on the multiprocessor machine exactly as it is on the local machine, preferably close to the

ground motion record files. The files *DefineVariablesDynamic.tcl*, *GravityLoad.tcl*, *ModelGeometry.tcl*, *RunDynamicMP.tcl*, *SectionAndMaterial.tcl*, and *SetUpModel.tcl* must all be transferred to Ithaca. Before transferring the file *DefineVariablesDynamic.tcl* to Ithaca, the path to the ground motion records and results directory must be modified. Open the file and change the ground motion record path next to the variable *eqpath*, as shown below.

```
# Ground Motion Files
set eqpath "/home/hokie/P695_Far_Field/"  ;  # Ground Motion Directory
```

Change the results file directory by changing the path next to the variable *resDir*, as shown below.

```
# Results Directory
set resDir "/home/hokie/PGMasonry/Results/M11DX"
```

In this example, damping depends on the natural frequencies of the first two modes. The file *Natural_Frequency.out* is transferred to the results directories for each of the index models. After transferring the files to Ithaca, querying the contents of the model folder returns the result shown in Figure E-22.

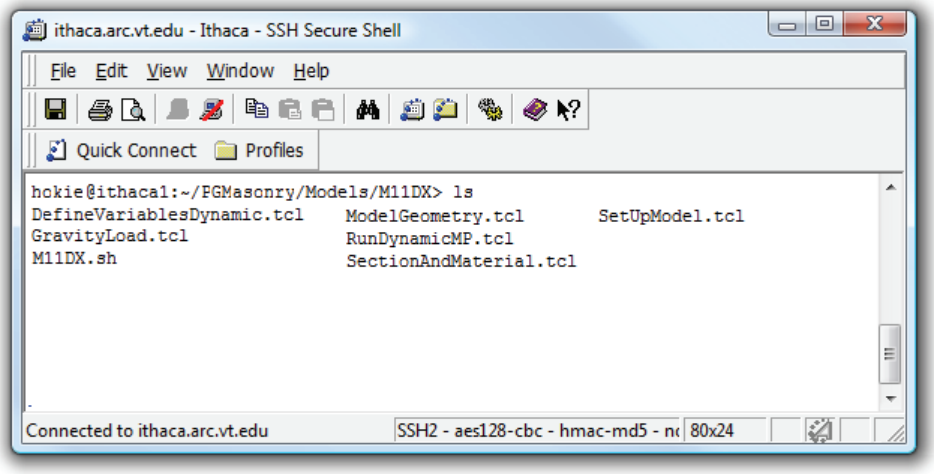

Figure E-22 File transfer on multiprocessor machine.

E.13.3 Run Analysis on Multiprocessor Machine

Ithaca uses a queuing system to schedule jobs. The queuing system requires a text file that indicates the number of processors requested and the duration of the job. In this example, this information is stored in *M11DX.sh*. After submitting the job to the queue, the user periodically checks the progress of the job. If the requested time for the analysis was inadequate to complete the job, the job may be restarted with more time requested or analysis parameters may need to be adjusted.

E.13.4 Import Results into IDA Tool

After the analyses have completed successfully, the shell software is used to transfer the results files to the local computer. Only the results file *Convergence.out* and the files with the form *IDA_<Prefix>_<GM File Name>.out* need to be transferred. The results files must be transferred to the correct corresponding index model results folder on the local machine. After the files are transferred, the IDA tool is used to view the results. The IDA tool is opened with the performance group and the *Import Results* button is used to view the results. After selecting this button, select the performance group. The results appear as in Figure E-17.

References

ACI, 2008, *Building Code Requirements for Structural Concrete and Commentary*, ACI 318-08, American Concrete Institute, Farmington Hills, Michigan.

ACI, 2011, *Building Code Requirements for Structural Concrete and Commentary*, ACI 318-11, American Concrete Institute, Farmington Hills, Michigan.

Adebar, P., Ibrahim, A.M.M., and Bryson, M., 2007, "Test of high-rise core wall: Effective stiffness for seismic analysis," *Structural Journal*, Vol. 104, No. 5, pp. 549-559.

AISC, 2010, *Seismic Provisions for Structural Steel Buildings*, ANSI/AISC 341-10, American Institute of Steel Construction, Chicago, Illinois.

ASCE, 2006, *Minimum Design Loads for Buildings and Other Structures*, ASCE/SEI 7-05, including Supplement No. 1, American Society of Civil Engineers, Reston, Virginia.

ASCE, 2007, *Seismic Rehabilitation of Existing Buildings*, ASCE/SEI 41-06, American Society of Civil Engineers, Reston, Virginia.

ASCE, 2010, *Minimum Design Loads for Buildings and Other Structures*, ASCE/SEI 7-10, American Society of Civil Engineers, Reston, Virginia.

ATC, 1978, *Tentative Provisions for the Development of Seismic Regulations for Buildings*, ATC-3-06 Report, Applied Technology Council, Redwood City, California.

ATC, 1995, *Structural Response Modification Factors*, ATC-19 Report, Applied Technology Council, Redwood City, California.

Beyer, K., Dazio, A., and Priestley, M.J., 2011, "Shear deformations of slender reinforced concrete walls under seismic loading," *Structural Journal*, Vol. 108, No 2, pp. 167-177.

Birely, A., 2012, *Seismic Performance of Slender RC Walls*, Ph.D Dissertation, Department of Civil and Environmental Engineering, University of Washington, Seattle, Washington.

Birely, A., Lowes, L.N., Lehman, D.E., Marley, K., Hart, C., and Kuchma, D.A., 2010, "Investigation of the seismic response of slender planar concrete walls," *9th U.S. National and 10th Canadian Conference on Earthquake Engineering 2010*, Earthquake Engineering Research Institute, Oakland, California.

Calvi, G.M., Priestly, M.J.N., and Kowalsky, M.J., 2008, *Displacement-Based Seismic Design of Structures*, IUSS Press, Italy, http://www.iusspress.it.

CEN, 2004, *Eurocode 8: Design of Structures for Earthquake Resistance*, Comite Europeen de Normalisation, Brussels, Belgium.

Charney, F.A., Talwalkar, R., Bowland, A., and Barngrover, B., 2010, "NONLIN-EQT: A computer program for earthquake engineering education," *9th U.S. National and 10th Canadian Conference on Earthquake Engineering 2010*, Earthquake Engineering Research Institute, Oakland, California.

Chopra, A.K., Goel, R.K., and De la Llera, J.C., 1998, "Seismic code improvements based on recorded motions of buildings during earthquakes," *SMIP98 Seminar Proceedings*, California Department of Conservation, Division of Mines and Geology, Office of Strong Motion Studies, Sacramento, California.

Chopra, A.K., and Chintanapakdee, C., 2004, "Inelastic deformation ratios for design and evaluation of structures: Single-degree-of-freedom bilinear systems," *Journal of Structural Engineering*, Vol. 130, No. 9, pp. 1309-1319.

Coleman, J., and Spacone, E., 2001, "Localization issues in force-based frame elements," *Journal of Structural Engineering*, ASCE, Vol. 127, No. 11, pp 1257-1265.

Dazio, A., Beyer, K., and Bachmann, H., 2009, "Quasi-static cyclic tests and plastic hinge analysis of RC structural walls," *Engineering Structures*, Vol. 31, No. 7, pp 1556-1571.

FEMA, 1985, *NEHRP Recommended Seismic Provisions for the Development of Seismic Regulations for New Buildings*, Federal Emergency Management Agency, Washington, D.C.

FEMA, 2003, *Hazard Loss Estimation Methodology Earthquake Model HAZUS-MH MR1 Advanced Engineering Building Module Technical and User's Manual*, developed by the Department of Homeland Security Emergency Preparedness and Response Directorate, Federal Emergency Management Agency, Mitigation Division, Washington, D.C.

FEMA, 2005, *Improvement of Nonlinear Static Seismic Analysis Procedures*, FEMA 440 Report, prepared by the Applied Technology Council for the Federal Emergency Management Agency, Washington, D.C.

FEMA, 2009, *Quantification of Building Seismic Performance Factors*, FEMA P-695 Report, prepared by the Applied Technology Council for the Federal Emergency Management Agency, Washington, D.C.

FEMA, 2012a, *HAZUS The Federal Emergency Management Agency's Methodology for Estimating Potential Losses from Disasters*, Federal Emergency Management Agency, Washington, D.C. Available at http://www.fema.gov/hazus.

FEMA, 2012b, *Seismic Performance Assessment of Buildings, Methodology and Implementation*, FEMA P-58, prepared by the Applied Technology Council for the Federal Emergency Management Agency, Washington, D.C.

Filippou, F.C., Popov, E.P., and Bertero, V.V., 1983, *Effects of Bond Deterioration on Hysteretic Behavior of Reinforced Concrete Joints*, EERC 83-19 Report, Earthquake Engineering Research Center, University of California, Berkeley, California.

Franklin, S., Lynch, J., and Adams, A., 2001, *Performance of Rehabilitated URM Shear Walls Flexural Behavior of Piers*, Department of Civil Engineering, University of Illinois at Urbana-Champaign, Urbana, Illinois.

Gardener, D.R., Bull, D.K., and Carr, A.J., 2008, "Internal forces of concrete floor diaphragms in multi-storey buildings," *Proceedings*, 2008 New Zealand Society of Earthquake Engineering Conference, Paper No. 21, 8 pp.

Goel, R.K., and Chopra, A.K., 1997a, "Period formulas for moment resisting frame buildings," *Journal of Structural Engineering*, Vol. 123, No. 11, pp. 1454-1461.

Goel, R.K., and Chopra, A.K., 1997b, *Vibration Properties of Buildings Determined from Recorded Earthquake Motions*, Report No. UCB/EERC-97/14, Earthquake Engineering Research Center, University of California, Berkeley, California.

Goel, R.K., and Chopra, A.K., 1998, "Period formulas for concrete shear wall buildings," *Journal of Structural Engineering*, Vol. 124, No. 4, pp. 426-433.

Gogus, A., 2010, *Structural Wall Systems – Nonlinear Modeling and Collapse Assessment of Shear Walls and Slab-Column Frames*, Ph.D. Dissertation, Department of Civil and Environmental Engineering, University of California, Los Angeles, California.

Haselton, C.B., and Deierlein, G.G., 2007, *Assessing Seismic Collapse Safety of Modern Reinforced Concrete Frame Buildings*, John A. Blume Earthquake Engineering Center Technical Report No. 156, Stanford University, Stanford, California.

Haselton, C.B., Liel, A.B., Deierlein, G.G., Dean, B.S., and Chou, J.H., 2011, "Seismic collapse safety of reinforced concrete buildings. I: Assessment of

ductile moment frames," *Journal of Structural Engineering*, Vol. 137, No. 4, pp. 481-491.

ISO, 1984, *Guidelines for the Evaluation of the Response of Occupants of Fixed Structures, Especially Buildings and Off-Shore Structures, to Low-Frequency Horizontal Motion (0,063 To 1 Hz)*, ISO 6897:194, International Standards Organization, Geneva, Switzerland.

Jennings, P., 1963, *Response of Simple Yielding Structures to Earthquake Excitation*, Ph.D. Dissertation, California Institute of Technology, Pasadena, California.

Krawinkler, H., 2006, "Importance of good nonlinear analysis," *The Structural Design of Tall and Special Buildings*, Vol. 15, No. 5, pp. 515-531.

Krawinkler, H., and Nasser, A., 1992, "Seismic design based on ductility and cumulative damage demands and capacities," *Nonlinear Seismic Analysis and Design of Reinforced Concrete Buildings*, Elsevier Applied Science, New York, New York.

Krawinkler, H., and Zareian, F., 2007, "Prediction of collapse – How realistic and practical is it, and what can we learn from it?," *The Structural Design of Tall and Special Buildings*, Vol. 16, No. 5, pp. 633-653.

LATBSDC, 2011, *An Alternative Procedure for Seismic Analysis and Design of Tall Buildings Located in the Los Angeles Region*, Los Angeles Tall Buildings Structural Design Council, Los Angeles, California.

Lignos, D.G., and Krawinkler, H., 2011, "Deterioration modeling of steel components in support of collapse prediction of steel moment frames under earthquake loading," *Journal of Structural Engineering*, Vol. 137, No. 11, pp. 1291-1302.

Liu, H., 2004, *Effect of Concrete Strength on the Response of Ductile Shear Walls*, MSCE Thesis, Department of Civil Engineering and Applied Mechanics, McGill University, Montreal, Quebec, Canada.

Lopez, W., and Sabelli, R., 2004, "Seismic design of buckling-restrained braced frames," *Steel TIPS Report*, Structural Steel Educational Council, Moraga, California.

Lowes, L.N., Lehman, D.E., Birely, A.C., Kuchma, D.A., Marley, K., and Hart, C.R., 2011, *Behavior, Analysis, and Design of Complex Wall Systems: Planar Wall Test Program Summary Document*. Available at http://nees.org/resources/3677.

Luco, N., Ellingwood, B.R., Hamburger, R.O., Hooper, J.D., Kimball, J.K., and Kircher, C.A., 2009, "Risk-targeted versus current seismic design maps for the conterminous United States," *Proceedings*, SEAOC Convention.

Massone, L.M., and Wallace, J.W., 2004, "Load-deformation responses of slender reinforced concrete walls," *Structural Journal*, Vol. 101, No. 1, pp. 103-113.

Mazzoni, S., McKenna, F., Fenves, G., and et al., 2010, *Open System for Earthquake Engineering Simulation (OpenSees) Command Language Manual.* Available at http://opensees.berkeley.edu.

Miranda, E., 2000, "Inelastic displacement ratios for structures on firm sites," *Journal of Structural Engineering*, Vol. 126, No. 10, pp 1150-1159.

Miranda, E., and Bertero, V.V., 1994, "Evaluation of strength reduction factors for earthquake resistant design," *Earthquake Spectra*, Vol. 2, No. 10, Earthquake Engineering Research Institute, Oakland, California.

Mitchell, D., Tremblay, R., Karacebeyli, E., Paultre, P., Saatcioglu, M., and Anderson, D.L., 2003, "Seismic force modification factors for the proposed 2005 edition of the National Building Code of Canada," *Canadian Journal of Civil Engineering*, Vol. 30, pp. 308-327.

Newmark, N., and Hall, W.J., 1982, *Earthquake Spectra and Design*, EERI Monograph Series, Earthquake Engineering Research Institute, Oakland, California.

NIST, 2008, *Seismic Design of Reinforced Concrete Special Moment Frames: A Guide for Practicing Engineers*, NIST GCR 8-917-1, NEHRP Seismic Design Technical Brief No. 1, prepared by the NEHRP Consultants Joint Venture, a partnership of the Applied Technology Council and the Consortium of Universities for Research in Earthquake Engineering for the National Institute of Standards and Technology, Gaithersburg, Maryland.

NIST, 2010, *Evaluation of the FEMA P-695 Methodology for Quantification of Building Seismic Performance Factors*, NIST GCR 10-917-8, prepared by the NEHRP Consultants Joint Venture, a partnership of the Applied Technology Council and the Consortium of Universities for Research in Earthquake Engineering for the National Institute of Standards and Technology, Gaithersburg, Maryland.

NIST, 2011, *Seismic Design of Cast-in-Place Concrete Special Structural Walls and Coupling Beams: A Guide for Practicing Engineers*, NIST GCR 11-917-11, NEHRP Seismic Design Technical Brief No. 6, prepared by the NEHRP Consultants Joint Venture, a partnership of the Applied Technology Council and the Consortium of Universities for Research in Earthquake Engineering for the National Institute of Standards and Technology, Gaithersburg, Maryland.

NRC, 2005, *National Building Code of Canada 2005*, National Research Council Canada, Ontario, Canada.

Oesterle, R.G., Aristizabal-Ochoa, A.E., Carpenter, J.E., Russell, H.G., and Corley, W.G., 1976, *Earthquake Resistant Structural Walls – Tests of Isolated Walls*, Report No. NSF/RA-760815, prepared by the Portland Cement Association for the National Science Foundation, Washington, D.C.

Oh, Y.H., Han, S.W., and Lee, L.H., 2002, "Effect of boundary element details on the seismic deformation capacity of structural walls," *Earthquake Engineering & Structural Dynamics*, Vol. 31, No. 8, pp. 1583-1602.

Panagiotou, M., and Restrepo, J.I., 2007, "Lessons learnt from the UCSD full-scale shake table testing on a 7-story residential building slice," *Proceedings of the 2007 Structural Engineers Association of California Convention*, pp. 57-74, Squaw Creek, California.

Panagiotou, M., and Restrepo, J., 2009, "Dual-plastic hinge design concept for reducing higher-mode effects on high-rise cantilever wall buildings," *Earthquake Engineering & Structural Dynamics*, Vol. 38, No. 12, pp. 1359-1380.

Panneton, M., Leger, P., and Tremblay, R., 2006, "Inelastic analysis of a reinforced concrete shear wall building according to the national building code of Canada 2005," *Canadian Journal of Civil Engineering*, Vol. 33, No. 7, pp. 854-871.

PEER/ATC, 2010, *Modeling and Acceptance Criteria for Seismic Design and Analysis of Tall Buildings*, PEER/ATC-72-1 Report, prepared by the Applied Technology Council in cooperation with the Pacific Earthquake Engineering Research Center, Redwood City, California.

PEER, 2010, *Guidelines for Performance-Based Seismic Design of Tall Buildings*, Report No. 2010/05, developed by the Pacific Earthquake Engineering Research Center as part of the Tall Buildings Initiative, University of California, Berkeley, California.

Pilakoutas, K., and Elnashai, A., 1995, "Cyclic behavior of reinforced concrete cantilever walls, part II: Discussion and theoretical comparisons," *Structural Journal*, Vol. 92, No. 4, pp. 425-433.

Pugh, J.S., 2012, *Numerical Simulation of Walls and Seismic Design Recommendations for Walled Buildings*, PhD. Dissertation, Department of Civil and Environmental Engineering, University of Washington, Seattle, Washington.

Qi, X., and Moehle, J., 1991, *Displacement Design Approach for Reinforced Concrete Structures Subjected to Earthquakes*, Report No. UCB/EERC-91/02, University of California, Berkeley, California.

Razvi, S., and Saatcioglu, M., 1999, "Confinement model for high-strength concrete," *Journal of Structural Engineering*, Vol. 125, No. 3, pp. 281-289.

Richards, P.W., 2009, "Seismic column demands in ductile braced frames," *Journal of Structural Engineering*, Vol. 135, No. 1, pp. 33-41.

Rodriguez, M.E., Restrepo, J.I., and Carr, A.J., 2002, "Earthquake-induced floor accelerations in buildings," *Earthquake Engineering & Structural Dynamics*, Vol. 31, pp. 693-718.

Ruiz-Garcia, J., and Miranda, E., 2003, "Inelastic displacement ratios for evaluation of existing structures," *Earthquake Engineering & Structural Dynamics*, Vol. 32, No. 8, pp. 1237-1258.

Ruiz-Garcia, J., and Miranda, E., 2004, "Inelastic displacement ratios for design of structures on soft soil sites," *Journal of Structural Engineering*, Vol. 130, No. 12, pp 2051-2061.

SEAOC, 1999, *SEAOC Blue Book: Seismic Design Recommendations of the SEAOC Seismology Committee*, Structural Engineers Association of California, Sacramento, California.

SEAOC, 2006, *2006 IBC Structural/Seismic Design Manual: Code Application Examples Volume 1*, Structural Engineers Association of California, Sacramento, California.

Thomsen IV, J.H., and Wallace, J.W., 1995, *Displacement-based Design of RC Structural Walls: An Experimental Investigation of Walls with Rectangular and T-shaped Cross Sections*, Report No. CU/CEE-95/06, Department of Civil Engineering, Clarkson University, Potsdam, New York.

TMS, 2005, *Building Code Requirements for Masonry Structures*, TMS 402-05/ACI 530-05/ASCE 5-05, the Masonry Society, Boulder, Colorado.

TMS, 2008, *Building Code Requirements for Masonry Structures*, TMS 402-08/ACI 530-08/ASCE 5-08, the Masonry Society, Boulder, Colorado.

TMS, 2011, *2011 Masonry Standard Joint Committee's Book - Building Code Requirements and Specification for Masonry Structures*, *Containing TMS 402-11/ACI 530-11/ASCE 5-11, TMS 602-11/ACI 530.1-11/ASCE 6-11, and Companion Commentaries*, the Masonry Society, Boulder, Colorado.

Turgeon, J., 2011, *The Seismic Performance of Coupled Reinforced Concrete Walls*, MSCE Thesis, Department of Civil and Environmental Engineering, University of Washington, Seattle, Washington.

Uang, C.M., and Smith, M.D., 2011, *Proposed Metal Building Moment Frame Systems*, presentation to the Building Seismic Safety Council Provisions Update Committee, September 15, 2011, San Francisco, California.

Uriz, P., and Mahin S.A., 2008, *Toward Earthquake-Resistant Design of Concentrically Braced Steel-Frame Structures*, PEER Report 2008/08, University of California, Berkeley, California.

Vallenas, J.M., Bertero, V.V., and Popov, E.P., 1979, *Hysteretic Behavior of Reinforced Concrete Structural Walls*, Report No. UCB/EERC-79/20, Earthquake Engineering Research Center, University of California, Berkeley, California.

Veletsos, A., Newmark, N., and Chelapati, C., 1965, "Deformation spectra for elastic and inelastoplastic systems subjected to ground shock and earthquake motions," *Proceedings of the Third World Congress on Earthquake Engineering*, Auckland and Wellington, New Zealand.

Victorsson, V.K., Baker, J.W., Krawinkler, H., and Deierlein, G.G., 2011, *The Reliability of Capacity-Designed Components in Seismic Resistant Systems*, John A. Blume Engineering Center Technical Report No. 177, Stanford University, Stanford, California.

Vidic, T, Fajar, P., and Fischinger, M., 1994, "Consistent inelastic design spectra: strength and displacement," *Earthquake Engineering and Structural Dynamics*, Vol. 23, pp. 507-521.

Yassin, M.H.M., 1994, *Nonlinear Analysis of Prestressed Concrete Structures Under Monotonic and Cyclic Loads*, Ph.D. Dissertation, Department of Civil and Environmental Engineering, University of California, Berkeley, California.

Project Participants

National Institute of Standards and Technology

John (Jack) R. Hayes, Jr.
Engineering Laboratory (MS8604)
National Institute of Standards and Technology
100 Bureau Drive
Gaithersburg, Maryland 20899
www.NEHRP.gov

Steven L. McCabe
Engineering Laboratory (MS8604)
National Institute of Standards and Technology
100 Bureau Drive
Gaithersburg, Maryland 20899
www.NEHRP.gov

John (Jay) L. Harris III
Engineering Laboratory (MS8604)
National Institute of Standards and Technology
100 Bureau Drive
Gaithersburg, Maryland 20899
www.NEHRP.gov

NEHRP Consultants Joint Venture

APPLIED TECHNOLOGY COUNCIL
201 Redwood Shores Parkway, Suite 240
Redwood City, California 94065
www.ATCouncil.org

CONSORTIUM OF UNIVERSITIES FOR
RESEARCH IN EARTHQUAKE ENGINEERING
1301 S. 46th Street, Building 420
Richmond, California 94804
www.CUREE.org

Joint Venture Management Committee

James R. Harris
J.R. Harris & Company
1775 Sherman Street, Suite 2000
Denver, Colorado 80203

Christopher Rojahn
Applied Technology Council
201 Redwood Shores Parkway, Suite 240
Redwood City, California 94065

Robert Reitherman
Consortium of Universities for Research in
Earthquake Engineering
1301 S. 46th Street, Building 420
Richmond, California 94804

Andrew Whittaker
University at Buffalo
Dept. of Civil, Structural, and Environ. Engin.
230 Ketter Hall
Buffalo, New York 14260

Joint Venture Program Committee

Jon A. Heintz (Program Manager)
Applied Technology Council
201 Redwood Shores Parkway, Suite 240
Redwood City, California 94065

Michael Constantinou
University at Buffalo
Dept. of Civil, Structural, and Environ. Engin.
132 Ketter Hall
Buffalo, New York 14260

C.B. Crouse
URS Corporation
1501 4th Avenue, Suite 1400
Seattle, Washington 98101

William T. Holmes
Rutherford & Chekene
55 Second Street, Suite 600
San Francisco, California 94105

Jack P. Moehle
University of California, Berkeley
Dept. of Civil and Environmental Engineering
325 Davis Hall MC 1792
Berkeley, California 94720

James R. Harris (ex-officio)
Andrew Whittaker (ex-officio)

Project Manager

Ayse Hortacsu
Applied Technology Council
201 Redwood Shores Parkway, Suite 240
Redwood City, California 94065

Project Technical Committee

Charles A. Kircher (Technical Director)
Kircher & Associates
1121 San Antonio Road, Suite D-202
Palo Alto, California 94303

FinleyA. Charney
Virginia Polytechnic Institute
Dept. of Civil and Environmental Engineering
200 Patton Hall MS 0105
Blacksburg, Virginia 24060

Gregory G. Deierlein
Stanford University
Dept. of Civil and Environmental Engineering
Blume Earthquake Engineering Center M3037
Stanford, California 94305

James R. Harris
J.R. Harris & Company
1775 Sherman Street, Suite 2000
Denver, Colorado 80203

William T. Holmes
Rutherford & Chekene
55 Second Street, Suite 600
San Francisco, California 94105

John D. Hooper
Magnusson Klemencic Associates
1301 Fifth Avenue Suite 3200
Seattle, Washington 98101

Laura N. Lowes
University of Washington
Dept. of Civil and Environmental Engineering
Box 352700
Seattle, Washington 98103

Working Group Members

Henry Burton
Stanford University
Dept. of Civil and Environmental Engineering
Blume Earthquake Engineering Center M3037
Stanford, California 94305

Scott Darling
Virginia Polytechnic Institute
Dept. of Civil and Environmental Engineering
200 Patton Hall MS 0105
Blacksburg, Virginia 24060

Matthew R. Eatherton
Virginia Polytechnic Institute
Dept. of Civil and Environmental Engineering
200 Patton Hall MS 0105
Blacksburg, Virginia 24060

Jennifer Foschaar
Stanford University
Dept. of Civil and Environmental Engineering
Blume Earthquake Engineering Center M3037
Stanford, California 94305

Andrew Hardyniec
Virginia Polytechnic Institute
Dept. of Civil and Environmental Engineering
200 Patton Hall MS 0105
Blacksburg, Virginia 24060

Curt B. Haselton
California State University, Chico
Dept. of Civil Engineering
475 East 10th Avenue
Chico, California 95926

Joshua Pugh
University of Washington
Dept. of Civil and Environmental Engineering
Box 352700
Seattle, Washington 98103

Project Review Panel

Robert E. Bachman
R.E. Bachman Consulting Structural Engineers
25152 La Estrada Drive
Laguna Niguel, California 92677

David R. Bonneville
Degenkolb Engineers
235 Montgomery Street Suite 500
San Francisco, California 94104

Kelly E. Cobeen
Wiss Janney Elstner Associates, Inc.
2200 Powell Street Suite 925
Emeryville, California 94608

Ronald O. Hamburger
Simpson Gumpertz and Heger
One Market Street Suite 600
San Francisco, California 94105

Greg Kingsley
KL&A Inc. Structural Engineers and Builders
3457 Ringsby Court, Unit 212
Denver, Colorado 80216

Richard E. Klingner
University of Texas at Austin
Dept. of Civil Engineering
One University Station C1748
Austin, Texas 78712

Philip Line
American Wood Council
803 Sycolin Road, Suite 201
Leesburg, Virginia 20175

James O. Malley
Degenkolb Engineers
235 Montgomery Street Suite 500
San Francisco, California 94104

Bonnie E. Manley
American Iron and Steel Institute
41 Tucker Road
Norfolk, Massachusetts 02056

Jack P. Moehle
University of California Berkeley
325 Davis Hall MC1792
Berkeley, California 94720

Laurence Novak
Portland Cement Association
5420 Old Orchard Road
Skokie, Illinois 60077

Charles W. Roeder
University of Washington
Dept. of Civil and Environmental Engineering
233-B More Hall Box 2700
Seattle, Washington 98195

Kurt Stochlia
International Code Council
5360 Workman Mill Road
Whittier, California 90601

FEMA Representative

Robert D. Hanson
Federal Emergency Management Agency
2926 Saklan Drive
Walnut Creek, California 94595

Workshop Participants

James Daniel Dolan
Dept. of Civil and Environmental Engineering
Washington State University
P.O. Box 642910
Pullman, Washington 99164

Satyendra K. Ghosh
S.K. Ghosh and Associates, Inc.
334 E. Colfax Street #E
Palatine, Illinois 60067

John Gillengerten
5155 Holly Drive
Shingle Springs, California 95682

Rakesh Goel
Dept. of Civil and Environmental Engineering
California Polytechnic State University
San Luis Obispo, California 93407

Henry Huang
City of Tustin
300 Centennial Way
Tustin, California 92780

Sara Jalali
Santa Clara University
Dept. of Civil Engineering
1326 Hoover Street Apt. 2
Menlo Park, California 94025

Martin Johnson
ABS Consulting, Inc.
300 Commerce Suite 200
Irvine, California 92602

Gyimah Kasali
Rutherford & Chekene
55 Second Street, Suite 600
San Francisco, California 94105

John Kiland
KPW Structural Engineers, Inc.
130 Webster Street Suite 200
Oakland, California 94607

Nico Luco
U.S. Geological Survey
P.O. Box 25046, MS 966
Denver, Colorado 80225

Michael Mahoney
Federal Emergency Management Agency
500 C Street, SW
Washington, D.C. 20472

Rafael Sabelli
Walter P. Moore
595 Market Street Suite 2130
San Francisco, California 94105

John Silva
Hilti Inc.
84 Mt. Rainier Drive
San Rafael, California 94903

Harold Sprague
Black & Veatch
6601 College Blvd.
Overland Park, Kansas 66211

Chris Tokas
Office of Statewide Health
Planning and Development
Sacramento, California 95814

Chia-Ming Uang
Dept. of Structural Engineering
University of California, San Diego
La Jolla, California 92093